

Syndromic scalp defects: Genotype-phenotype studies in Johanson-Blizzard syndrome and Adams-Oliver syndrome.

Dissertation

zur Erlangung des akademischen Grades

doctor rerum naturalium

(Dr. rer. nat.)

genehmigt durch die Fakultät für Naturwissenschaften
der Otto-von-Guericke-Universität Magdeburg

von Diplom-Biologin Maja Sukalo
geboren am 13. Juli 1985 in Oldenburg (Oldb.)

Gutachter: Prof. Dr. med. Martin Zenker
Prof. Dr. rer. nat. Andreas Winterpacht

eingereicht am: 22. April 2016
verteidigt am: 30. September 2016

TABLE OF CONTENTS

Table of Contents.....	I
List of Figures	IV
List of Tables	V
Summary.....	VIII
Zusammenfassung.....	IX
List of Abbreviations.....	XI
1 Introduction.....	1
1.1 Syndromic scalp defects	2
1.2 Johanson-Blizzard syndrome (JBS).....	3
1.2.1 The E3 ubiquitin ligase UBR1	4
1.2.2 Exocrine pancreatic insufficiency (EPI)	7
1.2.3 Hypoplasia of alae nasi	9
1.2.4 Oligodontia.....	10
1.3 Adams-Oliver syndrome (AOS)	11
1.3.1 Terminal transverse limb defects (TTLD).....	12
1.3.2 Cutis marmorata telangiectatica congenita (CMTC).....	14
1.3.3 Autosomal dominant types of AOS	15
1.3.4 Autosomal recessive types of AOS.....	17
1.4 Aims.....	19
2 Material and Methods.....	20
2.1 Patients.....	20
2.2 Material	21
2.3 Methods	22
2.3.1 DNA extraction	22
2.3.2 RNA extraction	23
2.3.3 Determination of DNA quality and quantity.....	23
2.3.4 Primer design.....	24
2.3.5 Polymerase chain reaction (PCR).....	24
2.3.6 Reverse transcription PCR (RT-PCR)	26
2.3.7 PCR amplification of GC-rich targets.....	27

2.3.8	Multiplex PCR.....	28
2.3.9	Long-range PCR.....	29
2.3.10	Gel electrophoresis	30
2.3.11	PCR product purification	30
2.3.12	Cycle sequencing reaction	31
2.3.13	Sequencing reaction clean-up.....	32
2.3.14	Sequence analysis	32
2.3.15	Western blot.....	32
2.3.16	Whole genome amplification	35
2.3.17	Multiplex ligation-dependent probe amplification (MLPA)	35
2.3.18	Microsatellites	39
2.3.19	Evaluation of sequence variants and nomenclature.....	40
2.3.20	Leiden Open Variation Database (LOVD)	41
3	Results.....	42
3.1	<i>UBR1</i> and Johanson-Blizzard syndrome.....	42
3.1.1	Sanger sequencing of the <i>UBR1</i> gene.....	42
3.1.2	Splice site mutations of the <i>UBR1</i> gene.....	46
3.1.3	Missense mutations of the <i>UBR1</i> gene	49
3.1.4	Larger genomic deletions and duplications of the <i>UBR1</i> gene	49
3.1.5	SNPs and unclassified variants of the <i>UBR1</i> gene	53
3.1.6	Distribution of mutations along the <i>UBR1</i> protein.....	54
3.1.7	JBS patients lacking <i>UBR1</i> mutations	55
3.1.8	Functional analysis of selected <i>UBR1</i> missense mutations.....	58
3.1.9	Phenotypic spectrum associated with <i>UBR1</i> deficiency	60
3.2	Adams-Oliver syndrome.....	67
3.2.1	<i>DOCK6</i>	67
3.2.2	<i>ARHGAP31</i>	77
3.2.3	<i>RBPJ</i>	77
3.2.4	<i>EOGT</i>	78
3.2.5	<i>NOTCH1</i>	79
3.2.6	<i>DLL4</i>	87
4	Discussion.....	88
4.1	Johanson-Blizzard syndrome	88

4.1.1	Phenotype associated with <i>UBR1</i> deficiency.....	90
4.1.2	Genotype-phenotype correlations.....	92
4.1.3	Pathophysiology of JBS.....	95
4.1.4	Molecular genetic analysis of the <i>UBR1</i> gene in diagnostics.....	96
4.1.5	Critical reappraisal of the literature.....	97
4.2	Adams-Oliver syndrome.....	99
4.2.1	Genetic basis of AOS.....	99
4.2.2	AOS mutation detection frequency.....	100
4.2.3	Mutation spectrum and genotype-phenotype correlations.....	101
4.2.4	AOS pathways.....	106
4.2.5	Common mechanisms underlying syndromic scalp defects.....	109
5	Conclusions.....	112
	References.....	113
	Appendix A: Material.....	121
	Appendix B: Oligonucleotides.....	127
	Appendix C: Mutation analysis.....	137
	Appendix D: Other tables.....	148
	Danksagung.....	XV
	Curriculum Vitae.....	XVII
	Publications.....	XVIII
	Erklärung.....	XX

LIST OF FIGURES

Figure 1.1: Variability of midline scalp defects.....	3
Figure 1.2: UBR1 overview.	4
Figure 1.3: The mammalian N-end rule pathway.	5
Figure 1.4: The ubiquitin-proteasome system in eukaryotes.....	6
Figure 1.5: Endocrine and exocrine function of the human pancreas.	7
Figure 1.6: Underdeveloped alae nasi in three JBS patients from our cohort.	9
Figure 1.7: Oligodontia of permanent teeth in a patient from our JBS cohort.	10
Figure 1.8: Phenotypic spectrum of limb defects in AOS patients.....	13
Figure 1.9: CMTC in AOS patients from literature.	14
Figure 1.10: ARHGAP31 = Rho GTPase-activating protein 31.	15
Figure 1.11: RBPJ = recombination signal binding protein for immunoglobulin kappa J.....	16
Figure 1.12: NOTCH1 = homolog of <i>Drosophila</i> Notch 1.....	17
Figure 1.13: DLL4 = delta-like 4.	17
Figure 1.14: DOCK6 = dedicator of cytokinesis 6.....	18
Figure 1.15: EOGT = EGF domain-specific O-linked N-acetylglucosamine transferase.....	18
Figure 2.1: Flowchart of major methods.....	22
Figure 2.2: MLPA procedure.	37
Figure 3.1: LOVD entries for <i>UBR1</i> mutations.....	46
Figure 3.2: Electropherograms of <i>UBR1</i> splice site mutations.....	48
Figure 3.3: MLPA results of probemix UBR1-E.....	50
Figure 3.4: Analysis of the index patient from family JBS-50.	51
Figure 3.5: Analysis of family JBS-52.....	52
Figure 3.6: UBR1 protein with its conserved domains and distribution of mutations.....	55
Figure 3.7: Electropherograms showing the mutation c.1688C>A (p.Ala563Asp).....	56
Figure 3.8: UBR1 immunoblotting (1).....	56
Figure 3.9: Protein degradation assay.	59
Figure 3.10: UBR1 immunoblotting (2).....	59
Figure 3.11: Oblique facial clefts in patients with JBS.....	63
Figure 3.12: LOVD entries for <i>DOCK6</i> variants.....	68
Figure 3.13: Electropherogram of a <i>DOCK6</i> splice site mutation.....	71

Figure 3.14: DOCK6 protein with known functional domains and distribution of mutations.....	71
Figure 3.15: ACC of the scalp and TTLD of the hands.....	74
Figure 3.16: Brain imaging of AOS patients with <i>DOCK6</i> mutations.....	75
Figure 3.17: Clinical pictures of a patient with <i>EOGT</i> -associated AOS.....	78
Figure 3.18: NOTCH1 protein with functional domains and distribution of mutations. ..	81
Figure 3.19: Analysis of a splice site mutation in <i>NOTCH1</i> . ..	82
Figure 3.20: Clinical features of AOS patients with <i>NOTCH1</i> mutations.	83
Figure 3.21: Pedigrees of AOS families with <i>NOTCH1</i> mutations.....	86
Figure 4.1: Mutational spectrum in the <i>UBR1</i> gene.....	88
Figure 4.2: Broad range of underdeveloped alae nasi in JBS patients.	90
Figure 4.3: Genotype-phenotype correlation in JBS patients.	94
Figure 4.4: Timeline of publications of genes associated with AOS.....	99
Figure 4.5: AOS mutation detection frequency in our Magdeburg cohort.	100
Figure 4.6: Regulatory circle of ARHGAP31 and DOCK6.....	107
Figure 4.7: Simplified schematic of the canonical Notch signalling pathway.....	108
Figure 4.8: Hypothetical connection between Notch signalling and the N-end rule pathway.....	111

LIST OF TABLES

Table 1.1: Classification of aplasia cutis congenita (ACC).	1
Table 1.2: Proposed classification for aplasia cutis congenita of the scalp.	2
Table 1.3: Features for clinical diagnosis of AOS.....	11
Table 1.4: Subtypes of terminal transverse limb defects.....	12
Table 2.1: Standard PCR reagents.....	25
Table 2.2: Standard PCR conditions (touchdown).	25
Table 2.3: Reagents for reverse transcription PCR.	26
Table 2.4: Temperature protocol for reverse transcription PCR.	26
Table 2.5: Reagents for GC-rich PCR amplification.	27

Table 2.6: Cycling conditions for GC-rich PCR amplification.	27
Table 2.7: Reagents for multiplex PCR.....	28
Table 2.8: Cycling conditions for multiplex PCR.....	28
Table 2.9: Reagents for long-range PCR.....	29
Table 2.10: Cycling conditions long-range PCR.....	29
Table 2.11: Cycle sequencing reagents.....	31
Table 2.12: Standard cycle sequencing conditions.....	31
Table 2.13: Standard protein dilution series.....	33
Table 2.14: Dilution series Bradford micro assay.....	34
Table 2.15: SDS gel ingredients.....	34
Table 2.16: <i>UBR1</i> synthetic probemixes.....	36
Table 3.1: <i>UBR1</i> mutations identified in patients with JBS.....	43
Table 3.2: <i>UBR1</i> splice site mutations that were investigated in cDNA.....	47
Table 3.3: Larger deletions and duplications in the <i>UBR1</i> gene.....	50
Table 3.4: SNPs and unclassified variants of the <i>UBR1</i> gene.....	54
Table 3.5: Phenotypic spectrum in JBS with different missense mutations.....	58
Table 3.6: Overview of mutations and clinical data of all JBS patients.....	64
Table 3.7: Mutations in the <i>DOCK6</i> gene that are related to AOS.....	69
Table 3.8: Unclassified variants of the <i>DOCK6</i> gene.....	73
Table 3.9: AOS patients with <i>DOCK6</i> mutations.....	76
Table 3.10: Unclassified variants in <i>ARHGAP31</i>	77
Table 3.11: Mutations in the <i>NOTCH1</i> gene that are related to AOS.....	80
Table 3.12: AOS patients from the Magdeburg cohort with <i>NOTCH1</i> mutations.....	84
Table 4.1: Appearance of typical symptoms in AOS subtypes.....	105
Table 4.2: List of NICDAC species generated in the cell-free assay.....	109
Table A.1: Chemicals and reagents.....	121
Table A.2: Antibodies.....	122
Table A.3: Kits.....	122
Table A.4: Commercial buffers and solutions.....	122
Table A.5: Preparation of customised buffers and solutions.....	123
Table A.6: Consumables.....	124
Table A.7: Laboratory equipment.....	125

Table A.8: Software	126
Table A.9: Online tools	126
Table B.1.1: <i>UBR1</i> standard primer.....	127
Table B.1.2: <i>DOCK6</i> standard primer.....	128
Table B.1.3: <i>ARHGAP31</i> standard primer.....	130
Table B.1.4: <i>RBPJ</i> standard primer.....	131
Table B.1.5: <i>EOGT</i> standard primer.....	131
Table B.1.6: <i>NOTCH1</i> standard primer.....	132
Table B.1.7: <i>DLL4</i> standard primer.....	133
Table B.2.1: <i>UBR1</i> primer for splice site analysis.....	134
Table B.2.2: <i>UBR1</i> primer for analysis of family JBS-52.....	134
Table B.2.3: <i>DOCK6</i> RT-Primer.....	134
Table B.2.4: <i>NOTCH1</i> RT primer.....	134
Table B.2.5: <i>GAPDH</i> RT primer.....	134
Table B.3.1: <i>UBR1</i> MLPA probes.....	135
Table C.1.1: <i>UBR1</i> missense mutations.....	137
Table C.1.2: <i>UBR1</i> unclassified missense variants.....	140
Table C.1.3: <i>DOCK6</i> missense mutations.....	141
Table C.1.4: <i>DOCK6</i> unclassified missense variants.....	141
Table C.1.5: <i>ARHGAP31</i> unclassified missense variant.....	143
Table C.1.6: <i>NOTCH1</i> missense mutations.....	143
Table C.2.1: <i>UBR1</i> splice site mutation analysis.....	145
Table C.2.2: <i>UBR1</i> splice site analysis of unclassified variants.....	146
Table C.2.3: <i>DOCK6</i> splice site mutation analysis.....	146
Table C.2.4: <i>DOCK6</i> splice site analysis of unclassified variants.....	146
Table C.2.5: <i>ARHGAP31</i> splice site analysis of unclassified variants.....	147
Table C.2.6: <i>EOGT</i> splice site mutation analysis.....	147
Table C.2.7: <i>NOTCH1</i> splice site mutation analysis.....	147
Table D.1: Complete AOS cohort from Magdeburg.....	148
Table D.2: Classification of intellectual disability (ID).....	148
Table D.3: Critical review of 91 JBS literature cases from 78 publications.....	149

SUMMARY

This PhD thesis work was aimed towards a better understanding of the clinical spectrum, and the genetic and molecular basis of Johanson-Blizzard syndrome (JBS, MIM #243800) and Adams-Oliver syndrome (AOS, MIM #100300), two distinct congenital malformation syndromes that are linked by the occurrence of scalp defects as part of both disorders. By investigating 71 patients with variable phenotypes, this study could further delineate JBS as a genetically homogeneous disease caused by mutations of the *UBR1* gene (MIM *605981), encoding for a ubiquitin ligase of the N-end rule pathway. By utilising Sanger sequencing and a self-designed multiplex ligation-dependent probe amplification analysis, the mutation detection rate reached 97.5% in patients with this recognisable phenotype. The mutations are distributed among the whole *UBR1* protein, with clustering of missense mutations in domains of known and unknown function. In patients with a molecularly proven *UBR1* defect, the symptoms exocrine pancreatic insufficiency, hypo-/aplasia of alae nasi, and oligodontia of permanent teeth emerged as the major clinical criteria. Assessment of genotype-phenotype correlations revealed that biallelic truncating mutations were statistically associated with a more severe phenotype when compared to patients with at least one non-truncating allele, but intra- and interfamilial variability prohibits a precise prediction of severity of symptoms on the basis of the mutation type.

For AOS, which is characterised by congenital scalp and terminal transverse limb defects and variably associated with cardiovascular and neurological anomalies, no gene was known at the start of this thesis, but research efforts by different groups have meanwhile revealed a wide genetic heterogeneity: the genes *DOCK6* (MIM *614194) and *EOGT* (MIM *614789) have been associated to autosomal recessive AOS, while mutations of *ARHGAP31* (MIM *610911), *RBPJ* (MIM *147183), *NOTCH1* (MIM *190198), and *DLL4* (MIM *605185) have been discovered in patients with autosomal dominant AOS. Molecular genetic investigations performed in our AOS patient cohort as part of a joint effort with two European partners could contribute to the identification of two novel genes for autosomal dominant AOS by this consortium, namely *NOTCH1* and *DLL4*. *NOTCH1* mutations emerged as the most frequent underlying genetic cause for AOS in our cohort (30% of cases). Studies that were part of this thesis could particularly expand the mutational spectrum and delineate specific phenotype associations of *NOTCH1*-related AOS. Frequent cardiovascular involvement and reduced penetrance of the phenotype were evident in affected families. Resequencing of the *DOCK6* gene, for which mutations had previously been described in only five families, identified ten new families with mutations in this gene. Evaluating the clinical data disclosed a highly penetrant association of this genetic subtype of AOS with neurodevelopmental and ocular anomalies. Nevertheless, a mutation detection rate of 45% in our AOS cohort when sequencing the six known AOS-associated genes suggests further genetic heterogeneity.

The known functional roles of AOS genes in *NOTCH1* signalling and cytoskeleton regulation support disturbed angiogenesis as the underlying pathomechanism in AOS. A hypothesis how impaired protein degradation underlying JBS might be linked to *NOTCH1* signalling is presented and provides a hint to a possible common mechanism for the development of scalp defects in both syndromes.

ZUSAMMENFASSUNG

Das Ziel der vorliegenden Arbeit war es, ein besseres Verständnis der klinischen, genetischen und molekularen Grundlagen des Johanson-Blizzard-Syndroms (JBS, MIM #243800) und des Adams-Oliver-Syndroms (AOS, MIM #100300) zu erlangen. Diese beiden seltenen, genetisch bedingten Fehlbildungssyndrome verbindet das Auftreten von angeborenen Skalpdefekten. Die Annäherung über die beiden klinisch distinkten Erkrankungen stellte in Aussicht, mögliche gemeinsame molekulare Pathomechanismen zu identifizieren. Durch die Untersuchungen an 71 Patienten mit variablen Phänotypen im Rahmen dieser Studie konnte das JBS als genetisch homogene Krankheit bestätigt werden, wobei ausschließlich Mutationen des *UBR1*-Gens (MIM *605981), welches eine Ubiquitin-Ligase des N-end rule Signalweges codiert, als ursächlicher Defekt gefunden wurden. Unter der Verwendung von Sanger-Sequenzierung und einer selbst entworfenen „multiplex ligation-dependent probe amplification“ (MLPA)-Analyse konnte eine Mutationsdetektionsrate von 97,5% bei Patienten mit dem typischen Bild des JBS erreicht werden. Die mit JBS assoziierten *UBR1*-Mutationen sind über das gesamte *UBR1*-Protein verteilt, wobei sich einige der Missense-Mutationen in Domänen mit bekannter und unbekannter Funktion gruppieren. In Patienten mit molekulargenetisch nachgewiesenem *UBR1*-Defekt konnten die Symptome exokrine Pankreasinsuffizienz, Hypo- oder Aplasie der Nasenflügel, sowie Oligodontie des bleibenden Gebisses als klinische Hauptmerkmale und obligatorische Kriterien für das JBS herausgearbeitet werden. Auswertung von Genotyp-Phänotyp-Korrelationen ergab, dass biallelisch trunkierende Mutationen statistisch gesehen häufiger mit einem schwerer ausgeprägten Phänotypen assoziiert sind als Patienten mit wenigstens einem nicht-trunkierten Allel; jedoch verbietet die beobachtete intra- und interfamiliäre Variabilität eine präzise Vorhersage des Schweregrades der Symptome allein auf Basis des Mutationstyps.

Für das AOS, welches durch angeborene Skalpdefekte und terminale transversale Extremitätendefekte, sowie durch variabel auftretende kardiovaskuläre und neurologische Anomalien charakterisiert ist, waren zu Beginn dieser Arbeit noch keine Gene bekannt. Forschungsanstrengungen verschiedener Arbeitsgruppen haben mittlerweile eine breite genetische Heterogenität gezeigt: die Gene *DOCK6* (MIM *614194) und *EOGT* (MIM *614789) wurden mit autosomal-rezessivem AOS in Verbindung gebracht, während Mutationen von *ARHGAP31* (MIM *610911), *RBPJ* (MIM *147183), *NOTCH1* (MIM *190198) und *DLL4* (MIM *605185) in Patienten mit autosomal-dominantem AOS gefunden wurden. Molekulargenetische Untersuchungen unserer AOS-Patientenkohorte im Rahmen einer Kollaboration mit zwei europäischen Partnern konnten zur Identifizierung zwei neuer Gene für autosomal-dominantes AOS beitragen, genauer *NOTCH1* und *DLL4*. Mutationen im *NOTCH1*-Gen wurden in 30% der Patienten unserer Kohorte nachgewiesen und stellten sich hier als die häufigste genetische Ursache für AOS heraus. Die genetischen Untersuchungen im Rahmen dieser Doktorarbeit konnten bei *NOTCH1*-assoziiertem AOS das Mutationsspektrum erweitern und den spezifischen Phänotyp weiter abgrenzen. In den betroffenen Fällen wurde häufig eine kardiovaskuläre Beteiligung, sowie reduzierte Penetranz des Phänotyps festgestellt. Eine Resequenzierung des *DOCK6*-Gens, in welchem vorhergehend nur in

fünf Familien eine Mutation gefunden wurde, konnte in zehn weiteren Familien Mutationen dieses Gens identifizieren. Auswertung der klinischen Daten zeigte bei diesem genetischen Subtyp des AOS eine hochpenetrante Assoziation mit neurologischen und okulären Entwicklungsstörungen. Dennoch konnten nur 45% der Fälle aus unserer AOS-Patientenkohorte durch die Sequenzierung der sechs bekannten, AOS-assoziierten Gene gelöst werden; dieses spricht für eine weitere genetische Heterogenität des Syndroms.

Die AOS-Gene haben bekannte funktionelle Rollen im NOTCH1 Signalweg und in der Regulierung des Zytoskelettes, was zu der Annahme passt, dass eine gestörte Angiogenese der zugrundeliegende Pathomechanismus beim AOS ist. Tatsächlich handelt es sich bei den typischen klinischen Defekten beim AOS um Läsionen, die vaskulären Disruptionen entsprechen. Die vaskuläre Pathogenese gilt vermutlich auch für die Skalpdefekte beim JBS. Vorgestellt wird eine neue Hypothese über einen möglichen Zusammenhang zwischen gestörter Proteindegradation, welche beim JBS ursächlich ist, und dem NOTCH1-Signalweg als gemeinsamer Mechanismus bei der Entstehung von Skalpdefekten in beiden Syndromen.

LIST OF ABBREVIATIONS

ACC	aplasia cutis congenita
AOS	Adams-Oliver syndrome
ARHGAP31	Rho GTPase-activating protein 31
ASD	atrial septal defect
BDGP	Berkeley Drosophila Genome Project; online tool
BLAST	Basic Local Alignment Search Tool
BRCA1	breast cancer 1
C-	carboxyl / COOH
Ca ²⁺	calcium ion
CDC42	cell division cycle 42
cDNA	complementary DNA
CHD	congenital heart defect(s)
CMTC	cutis marmorata telangiectatica congenita
CT	computed tomography
dbSNP	Single Nucleotide Polymorphism database
ddH ₂ O	ultra-pure water
ddNTP	dideoxynucleotide
DLL1	delta-like 1
DLL3	delta-like 3
DLL4	delta-like 4
DMSO	dimethyl sulfoxide
DNA	deoxyribonucleic acid
dNTP	deoxynucleotide
DOCK6	dedicator of cytokinesis 6
EDTA	ethylenediaminetetraacetic acid
EGF	epidermal growth factor
EOGT	EGF domain specific O-linked N-acetylglucosamine transferase
EPI	exocrine pancreatic insufficiency
et al.	et alii/aliae/alia (and others)
EUROCAT	European surveillance of congenital anomalies
ExAC	Exome Aggregation Consortium
F, FP	forward primer
G protein	GTPase; guanine nucleotide binding protein
GAP	GTPase-activating protein
GAPDH	glyceraldehyde-3-phosphate dehydrogenase
GDP	guanosine diphosphate
GEF	guanine nucleotide exchange factor
GERP	Genomic Evolutionary Rate Profiling; online tool
GNAQ	G protein subunit alpha q
GTP	guanosine triphosphate
GTPase	guanine nucleotide binding protein
H ₂ O	water
HES1	Hes family bHLH (basic helix-loop-helix) transcription factor 1
HEY1	Hes-related family bHLH (basic helix-loop-helix) transcription factor with YRPW motif 1
HRP	horseradish peroxidase

IgG	immunoglobulin G
IUGR	intrauterine growth restriction
IQ	intelligence quotient
JAG1	jagged 1
JAG2	jagged 2
JBS	Johanson-Blizzard syndrome
LCL	lymphoblastoid cell line
LOVD	Leiden Open (source) Variation Database
LPO	left probe oligonucleotide
MAF	minor allele frequency
MD	Medicinae Doctor (Doctor of Medicine)
MgCl ₂	magnesium chloride
MIM	(Online) Mendelian Inheritance in Men
MLPA	multiplex ligation-dependent probe amplification
MRI	magnetic resonance imaging
mRNA	messenger RNA
MutPred	Mutation Prediction; online tool
n	size of statistical sample
N-	amino- / NH ₂ -
NCBI	National Center for Biotechnology Information
NICD	Notch intracellular domain
NOTCH1	homolog of Drosophila Notch 1
O-GlcNAc	O-linked N-acetylglucosamine
p.?	protein was not analysed but supposed to be affected
PARK2	parkin RBR E3 ubiquitin protein ligase
PBS	phosphate-buffered saline
PCR	polymerase chain reaction
PDX1	pancreatic and duodenal homeobox 1
PolyPhen-2	Polymorphism Phenotyping v2; online tool
PROVEAN	Protein Variation Effect Analyzer; online tool
R, RP	reverse primer
r.spl.?	RNA was not analysed but the change is expected to affect splicing
RAC1	Ras-related C3 botulinum toxin substrate 1
RBPJ	recombination signal binding protein for immunoglobulin kappa J region
RIPA	radioimmunoprecipitation assay
RNA	ribonucleic acid
RPO	right probe oligonucleotide
RT-PCR	reverse transcription PCR
SBDS	Shwachman-Bodian-Diamond syndrome ribosome assembly guanine nucleotide exchange factor
SDS-PAGE	sodium dodecyl sulphate polyacrylamide gel electrophoresis
SIFT	Sorting Intolerant From Tolerant; online tool
siRNA	small interfering RNA
SNP	single nucleotide polymorphism
SPINK1	serine peptidase inhibitor, Kazal type 1
SPRI	solid phase reversible immobilisation
Taq	<i>Thermus aquaticus</i>
TBE	Tris/borate/EDTA
TBST	Tris-buffered saline/Tween20
TE	Tris/EDTA

TGP	1000 Genomes Project
tRNA	transfer RNA
TTLD	terminal transverse limb defects
Ub	ubiquitin
UBE3A	ubiquitin protein ligase E3A
UBR box	zinc finger-like domain
UBR1	ubiquitin protein ligase E3 component N-recognin 1
UBR2	ubiquitin protein ligase E3 component N-recognin 2
UBR4	ubiquitin protein ligase E3 component N-recognin 4
UBR5	ubiquitin protein ligase E3 component N-recognin 5
UCSC	University of California, Santa Cruz
UV	ultraviolet
VHL	von Hippel-Lindau tumor suppressor
VSD	ventricular septal defect
WNT10A	Wnt family member 10A

UNITS

°C	degree Celsius
∞	infinity
bp	base pair(s)
cm	centimetre(s)
cm ²	square centimetre(s)
g	gravity force
kb	kilo base pair(s)
kDa	kilodalton(s)
M	molar
mA	milliampere(s)
Mb	mega base pair(s)
mg	milligram(s)
min	minute(s)
ml	millilitre(s)
mM	millimolar
µg	microgram(s)
µl	microlitre(s)
nm	nanometre(s)
ng	nanogram(s)
nt	nucleotide(s)
pH	negative of the logarithm to base 10 of the concentration
pmol	picomole(s)
rpm	revolutions per minute
sec	second(s)
U	unit(s)
V	volt(s)
w/v	weight/volume concentration
x	fold

AMINO ACIDS

A	Ala	Alanine
C	Cys	Cysteine
D	Asp	Aspartic acid
E	Glu	Glutamic acid
F	Phe	Phenylalanine
G	Gly	Glycine
H	His	Histidine
I	Ile	Isoleucine
K	Lys	Lysine
L	Leu	Leucine
M	Met	Methionine
N	Asn	Asparagine
P	Pro	Proline
Q	Gln	Glutamine
R	Arg	Arginine
S	Ser	Serine
T	Thr	Threonine
V	Val	Valine
W	Trp	Tryptophan
Y	Tyr	Tyrosine

NUCLEOBASES

A	Adenine/Adenosine
C	Cytosine/Cytidine
G	Guanine/Guanosine
T	Thymine/5-Methyluridine

1 INTRODUCTION

Aplasia cutis congenita (ACC) comprises a clinically and etiologically heterogeneous group of inborn skin defects. The congenital absence of skin is most commonly restricted to the scalp vertex; underlying structures, such as skull and dura, may also be affected. Classification of ACC was attempted by several authors. The classification by Frieden [1986] is the most frequently applied one; he classified ACC into nine groups characterised by the localisation and pattern of ACC, associated anomalies, and mode of inheritance (Table 1.1). The causes underlying ACC are heterogeneous, including several exogenous factors, such as prescribed drugs like methimazole and carbimazole [Dutertre et al., 1991], fetus papyraceus [Lemke et al., 1993] and/or placental infarcts/anomalies [Levin et al., 1980], amniotic band disruptions [Higginbottom et al., 1979], or congenital infections with Herpes simplex [Harris et al., 1986] or varicella [Baillie, 1983]. Scalp defects are assumed to be the result of incomplete vascularisation and ectodermal growth defects. Genetic causes may vary from chromosomal aberrations, such as trisomy 13 (Patau syndrome) and deletion 4p- (Wolf-Hirschhorn syndrome) to monogenic point mutations that were detected in Johanson-Blizzard syndrome (JBS, MIM #243800) or Adams-Oliver syndrome (AOS, MIM #100300). The majority of ACC cases represent sporadic occurrence without involvement of other anomalies [Demmel, 1975; Frieden, 1986]. In familial cases, autosomal dominant inheritance is more common, but autosomal recessive inheritance has also been documented in families with scalp defects. This work was focused on two monogenic syndromic types of scalp defects, namely AOS and JBS.

Table 1.1: Classification of aplasia cutis congenita (ACC).

Adapted from [Frieden, 1986].

Group	Description
1	Scalp ACC without multiple anomalies
2	Scalp ACC with associated limb anomalies
3	Scalp ACC with associated epidermal and organoid nevi
4	ACC overlying embryologic malformations
5	ACC with associated fetus papyraceus or placental infarcts
6	ACC associated with epidermolysis bullosa
7	ACC localised to extremities without blistering
8	ACC caused by specific teratogens
9	ACC associated with malformation syndromes

A classification exclusively for ACC of the scalp is shown in Table 1.2. It was established by Silberstein et al. in 2014 and is based on size of the defect, affected layers, and involvement of veins.

Table 1.2: Proposed classification for aplasia cutis congenita of the scalp.

Adapted from [Silberstein et al., 2014]

Type	Size of defect	Layers involved	Involvement of veins
0	Any	Intact epidermis without skin appendages (scarred, hairless area on the scalp)	No
I	<15 cm ²	Skin defect, no skull bone defect	No
II	>15 cm ²	Skull bone defect, exposed dura	No
III	Any, usually large	Skin and skull defect with exposed dura and sagittal sinus	Enlarged exposed veins
IV	Any, usually large	Skin, skull, and dura defect with brain exposure	Any, usually with enlarged exposed veins

1.1 SYNDROMIC SCALP DEFECTS

Aplasia cutis congenita of the scalp can occur as a non-syndromic single defect or in a syndromic context. Inborn syndromic scalp defects were described in a small proportion of inherited diseases. In **Johanson-Blizzard syndrome**, the congenital scalp defects can usually be classified as group 9, according to Frieden [1986], and as types 0 and I, according to Silberstein et al. [2014]. They are associated with exocrine pancreatic insufficiency (EPI), oligodontia of permanent teeth, and hypoplasia of alae nasi. About two thirds of the JBS patients present with ACC of the scalp [Zenker, 2008]. **Adams-Oliver syndrome** is characterised by ACC of the scalp and terminal transverse limb defects (TTLD); therefore, it is classified as group 2 (Table 1.1). Severity of the skin defect can vary from type 0 to IV intensity (Table 1.2). In both, JBS and AOS, midline scalp defects presumably caused by incomplete vascularisation were described (Figure 1.1). When associated with anomalies of the breast and external ear, aplasia cutis congenita of the scalp is an indication of **scalp-ear-nipple syndrome** (MIM #181270), which is also called Finlay-Marks syndrome. Another entity including ACC together with skull defects and eye abnormalities is called **Knobloch syndrome** (MIM #267750). In **oculoectodermal syndrome** (MIM #600268), a combination of ACC and epibulbar dermoids is described. **Encephalocraniocutaneous lipomatosis** (MIM #613001) is a related disorder characterised by ocular and central nervous system anomalies in combination with skin lesions that can include scalp defects. **Focal dermal hypoplasia** (MIM #305600), which is also called Goltz syndrome or Goltz-Gorlin syndrome, is a

syndromic form of ectodermal dysplasia that also can include scalp lesions. The skin defects in this syndrome are characterised by missing dermis with intact epidermis. Together with other symptoms, scalp defects can also be seen in **Patau syndrome**.

Congenital scalp defects are an occasional symptom in several other genetic syndromes such as **Wolf-Hirschhorn syndrome** (MIM #194190), **Fryns syndrome** (MIM %229850), and **Opitz syndrome type II** (MIM #145410).

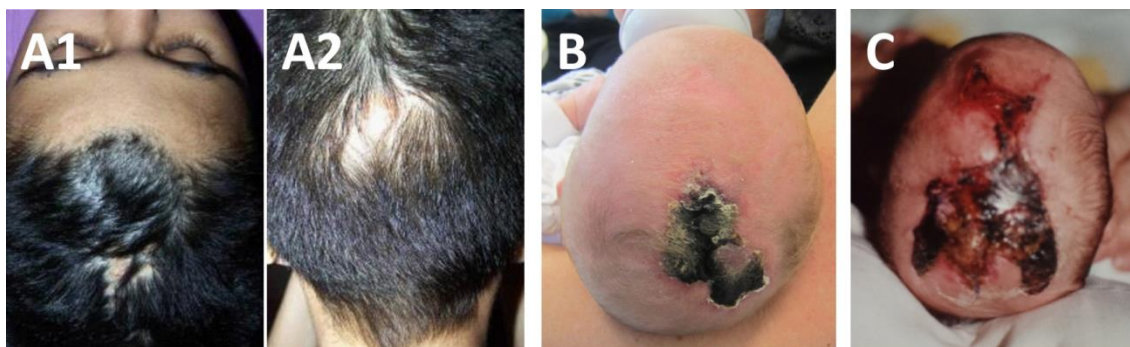


Figure 1.1: Variability of midline scalp defects.

(A) 13-year-old girl with JBS. (A1) Healed scalp defect at the border between frontal and vertex region. (A2) Additional hairless spot in same patient located at parietal-occipital region. (B) 1-month-old female AOS patient with aplasia cutis of the occiput. (C) Baby boy with AOS showing large scalp defect and underlying bony defect spanning from parietal to vertex region.

1.2 JOHANSON-BLIZZARD SYNDROME (JBS)

Johanson-Blizzard syndrome is a clinically distinct, autosomal recessively inherited congenital malformation syndrome. The clinical hallmarks of this multisystem disorder are nasal wing hypo-/aplasia and EPI, the later one being typically present at birth or manifesting in early infancy. Hearing impairment, ACC of the scalp, dental defects, hypothyroidism, cognitive impairment of variable degree, short stature, and urogenital and anorectal malformations are additional common features of the syndrome [Zenker, 2008]. The eponymic name of this condition goes back to Ann Johanson and Robert Blizzard, who in 1971 described three unrelated girls affected by congenital aplasia of the alae nasi, deafness, hypothyroidism, dwarfism, absent permanent teeth, and malabsorption. Since then, more than 60 cases of this entity have been reported. The birth prevalence of JBS in Europe has been estimated to be approximately 1:250,000 [Zenker et al., 2005].

Autosomal recessive inheritance was suggested by Schussheim et al. [1976] due to parental consanguinity in their case. Further cases with parental consanguinity, affected siblings born to unaffected parents, and gender independent occurrence strengthened this assumption. The molecular basis of JBS was discovered by Zenker et al. [2005], who reported homozygous and compound-heterozygous mutations of the *UBR1* gene (MIM *605981) as the underlying cause in JBS patients.

1.2.1 THE E3 UBIQUITIN LIGASE UBR1

The human *UBR1* gene is located on chromosome 15q15.2. It spans 163 kb and contains 47 exons (Figure 1.2A) that encode for a protein called ubiquitin protein ligase E3 component N-recognin 1 with a total length of 1749 amino acids. No functional protein isoform variants are known. The UBR1 protein contains two zinc finger motifs, a UBR box and a cysteine- and histidine-rich RING-H2 domain (Figure 1.2B) [Kwak et al., 2004; Kwon et al., 1998; Xie and Varshavsky, 1999].

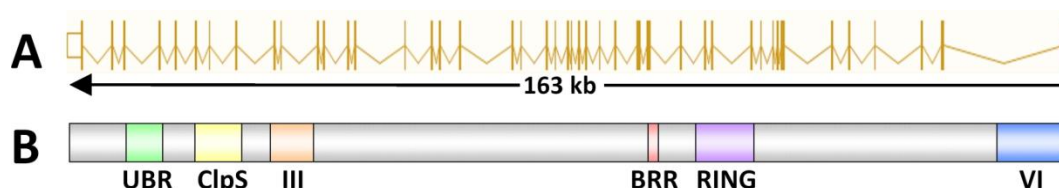


Figure 1.2: UBR1 overview.

(A) Exon-intron structure of the *UBR1* gene spanning about 163 kb including 47 exons [Ensembl GRCh38.p2]. (B) UBR1 protein with its conserved domains. The protein contains several distinct regions, such as the UBR box (green), a highly conserved substrate-binding domain. The ClpS region (yellow) shows sequence similarity to prokaryotic ClpS which is an accessory subunit for recognition of degrons by the ATP-dependent protease ClpAP [Zeth et al., 2002]. Region III (orange) denotes a sequence that is highly conserved among UBR1 and UBR2 in different species but the function of which is unclear. The conserved region VI (blue) largely overlaps with a domain that is believed to function in regulation of protein activity by covering or exposing protein binding domains (autoinhibitory domain) [Tasaki et al., 2012]. The basic residue-rich region (BRR, pink) has been found in yeast *ubr1* for binding to *rad6* [Kwon et al., 1998; Xie and Varshavsky, 1999]. The RING domain (purple) is a cysteine- and histidine-rich region that is present in several E3 Ub ligases [Kwon et al., 2001; Kwon et al., 2003; Xie and Varshavsky, 1999].

UBR1 represents one of at least four E3 ubiquitin (Ub) ligases of the N-end rule pathway, an evolutionary conserved and ubiquitously expressed intracellular proteolytic pathway involved in ubiquitin-mediated degradation of many proteins (Figure 1.3). Specifically, this N-end rule relates the stability of a protein to the identity of its N-terminal amino acid [Bachmair et al., 1986; Varshavsky, 1996]. Degrons (primary degradation signals) have destabilising N-terminal residues that are

recognised by N-recognins (E3 Ub ligases) in the N-end rule pathway. Those destabilising N-terminal residues can be divided into three distinct subsets: primary, secondary, and tertiary (Figure 1.3). Tertiary and secondary destabilising residues require modifications prior to degradation. The tertiary destabilising residues Cys, Asn, and Gln are oxidised or deamidated (by specific N-terminal amidases) to become secondary destabilising residues, namely oxidised Cys, Asp, and Glu. Those secondary destabilising residues are then arginylated by the Arg-tRNA protein transferase ATE1. The three arginylated residues, plus Arg, Lys, and His (basic residues) form the group of type 1 primary destabilising residues, which are recognised by the UBR box of all N-recognins (UBR1/2/4/5). On the other hand, the bulky hydrophobic residues Leu, Phe, Trp, Tyr, and Ile are type 2 primary destabilising residues and are recognised by the N-terminal domain that is only existent in UBR1 and UBR2 [Tasaki et al., 2005].

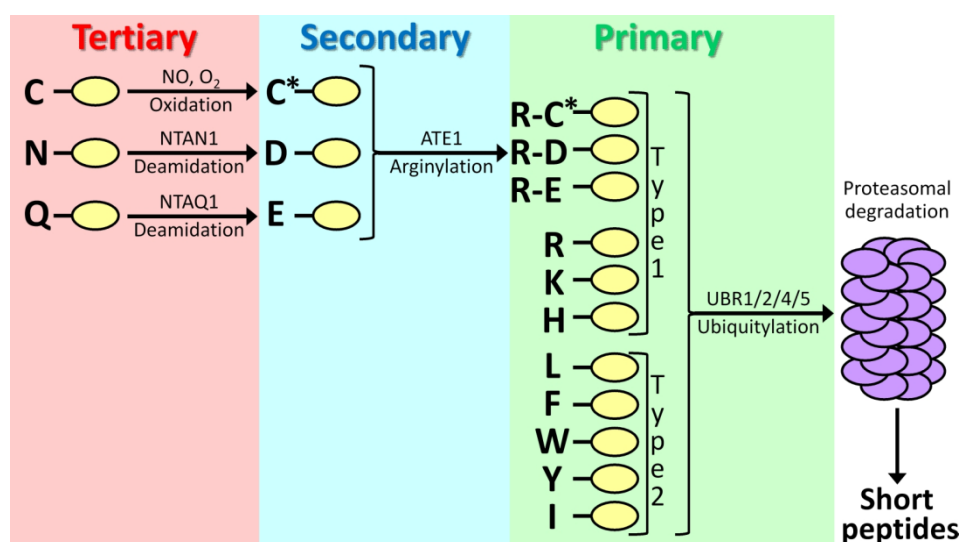


Figure 1.3: The mammalian N-end rule pathway.

N-terminal residues are indicated by single-letter abbreviations for amino acids. Yellow ovals denote the remaining portion of a protein substrate. “Primary”, “secondary”, and “tertiary” denote mechanistically distinct subsets of destabilizing N-terminal residues. NO, nitric oxide; O₂, oxygen; NTAN1, Asn-specific N-terminal amidase; NTAQ1, Gln-specific N-terminal amidase; C*, oxidised Cys; ATE1, Arg-tRNA protein transferase. Adapted from [Tasaki et al., 2005] and [Zenker, 2008].

In a next step, the proteins carrying N-terminal primary destabilising residues are ubiquitinated by the E3 Ub ligases UBR1/2/4/5. The ubiquitin-proteasome system regulates degradation of intracellular proteins. Ubiquitin mediates selective proteolysis through its enzymatic conjugation to proteins that contain degrons. Thereby, those proteins are marked for degradation of the 26S proteasome [Varshavsky, 2012]. Figure 1.4 schematically shows this process in eukaryotes.

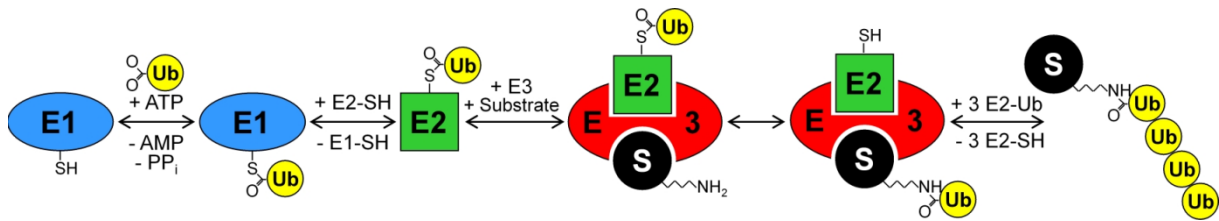


Figure 1.4: The ubiquitin-proteasome system in eukaryotes.

Initially, ubiquitin (Ub) is bound to E1 (Ub activating enzyme) in an ATP-requiring step. Subsequently, this Ub can be transferred to E2 (Ub conjugating enzyme). E2 then complexes with E3 (Ub ligating enzyme) and a substrate (S); in this conformation the Ub can be transferred to the substrate. By repeating this process, poly-Ub chains can be formed adjacent to the substrate. The specific length of those chains determines degradation of the substrate by the 26S proteasome.

The regulated degradation of specific proteins through the N-end rule pathway is involved in selective elimination of misfolded proteins, regulation of DNA repair, segregation of chromosomes, G protein signalling, regulation of meiosis and apoptosis, and many more (summaries by [Hwang et al., 2011; Tasaki et al., 2012; Varshavsky, 2011, 2012]). However, the full spectrum of its complex biological functions is still not well understood.

Today, over 400 Ub ligases are known and only a minority is involved in the N-end rule pathway. As they regulate many processes, there are, besides JBS, further diseases that are related to defective Ub ligases. For example, mutations in *UBE3A* (MIM *601623), which also functions as a transcriptional corepressor, account for approximately 25% of patients with **Angelman syndrome** (MIM #105830); the remaining 75% are caused by three other mutational mechanisms [Kishino et al., 1997]. The gene *VHL* (MIM *608537) encodes two protein products. Mutations in this gene can cause **von Hippel-Lindau syndrome** (MIM #193300) and several other inherited cancer forms [Nordstrom-O'Brien et al., 2010]. An autosomal recessive form of **Parkinson disease** (juvenile type 2, MIM #600116) is caused by mutations in the parkin gene (*PARK2*, MIM *602544) [Yoshii et al., 2011]. Another well-known gene, namely *BRCA1* (MIM *113705), also encodes for an E3 ubiquitin ligase. Mutations in this gene were associated to **familial breast-ovarian cancer** (MIM #604370) and a form of **pancreatic cancer** (MIM #614320) [Miki et al., 1994].

1.2.2 EXOCRINE PANCREATIC INSUFFICIENCY (EPI)

The pancreas is a gland with dual functions, both in the endocrine and exocrine system (Figure 1.5). The endocrine part consists of the Islets of Langerhans producing several hormones, including insulin, glucagon and somatostatin that play a role in glucose metabolism. The exocrine portion of the pancreas is composed of duct cells and acinar cells, forming acini. The acinar cells produce secretory granules containing zymogenes that are released into the pancreatic duct system. In the duodenum these precursor proteins are subsequently activated to digestive enzymes classified as protease (trypsinogen, chymotrypsinogen), lipase and amylase. They play an essential role in digesting proteins, fat and starch.

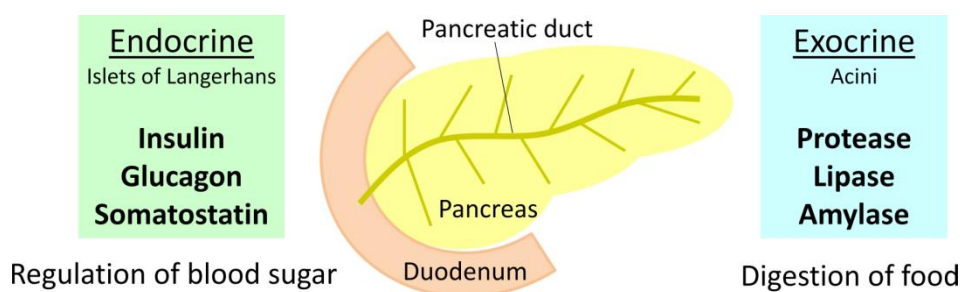


Figure 1.5: Endocrine and exocrine function of the human pancreas.

In EPI, a lack of the above mentioned exocrine digestive enzymes causes malabsorption of nutrients leading to diarrhea, malnutrition, and vitamin deficiencies. Further consequences include generalised edema and anemia. Patients require a lifetime treatment with supplements replacing the lacking enzymes.

Patients with JBS present with insufficiency of the exocrine pancreas as a consistent feature with neonatal or infantile onset [Zenker et al., 2005]. As *UBR1* is the gene mutated in JBS, one has to suggest a critical role of the UBR1 protein in either development or maintenance of acinar cells [Zenker et al., 2006]. Autopsy findings in JBS cases revealed a selective defect of acinar tissue, whereas islets of Langerhans and ducts are quite well preserved [Daentl et al., 1979; Moeschler et al., 1987; Vanlieferinghen et al., 2001], but the precise pathogenesis of the acinar cell loss remains elusive [Zenker et al., 2006]. There is evidence that the destruction of pancreatic tissue in JBS is caused by inflammatory acinar cell damage, which resembles a severe destructive pancreatitis of intrauterine onset; this may implicate UBR1 in the defence of acinar cells against noxious stimuli [Zenker et al., 2006]. Compared to patients with cystic fibrosis (MIM

#219700), the bicarbonate secretion in patients with JBS is much less impaired [Jones et al., 1994]. Diabetes is an occasional finding in JBS and seems to develop during the teenage years which might be due to a progressive course of the pancreatic destruction [Zenker et al., 2006].

Pancreatic insufficiency can be acute or chronic and may be seen sporadically or in a familial background. Several diseases with congenital or early childhood onset EPI have been reported. Acquired EPI can be caused by malnutrition, juvenile tropical pancreatitis (additionally associated with *SPINK1* mutations), congenital viral infections, chronic enteropathy, surgical excision, or chronic pancreatitis [Durie, 1997]. EPI is a frequent symptom in **Johanson-Blizzard syndrome**. It can also be seen in other genetically determined diseases and without any genetic background. **Pancreatic agenesis** is a rare malformation and leads to congenital endocrine and exocrine pancreatic insufficiency [Winter et al., 1986]; this disease can be caused by mutations in the *PDX1* gene [Schwitzgebel et al., 2003] and has an incidence of less than 1:1,000,000 live births. **Pancreatic agenesis and congenital heart defects** (MIM #600001) is a very rare syndrome in which endocrine and exocrine pancreatic insufficiency is a consistent feature caused by complete absence or marked hypoplasia of the pancreas [Lango Allen et al., 2012]. In 86% of patients with **Shwachman-Bodian-Diamond syndrome** (MIM #260400) steatorrhea caused by pancreatic insufficiency is present [Ginzberg et al., 1999]. The insufficiency is induced by extensive fatty replacement of pancreatic acinar tissue. It was reported that 50% of the patients can become pancreatic-sufficient with normal fat absorption later in life [Dror and Freedman, 2002]. Another inherited disease with a high frequency of EPI (approximately 85%, [Kerem et al., 1989]) is **cystic fibrosis**, where the symptoms are caused by mutations in the genes of an ion channel. Frequency is estimated to be between 1:8,000 and 1:10,000. In patients with **nephropathic cystinosis** (MIM #219800), pancreatic endocrine and exocrine insufficiency develops later in life; the disease has an incidence of 1:100,000 to 1:200,000 live births. In **Pearson marrow-pancreas syndrome** (MIM #557000) the exocrine pancreatic dysfunction is caused by fibrosis of the pancreas. Generalised pancreatic insufficiency was also documented in patients with **enterokinase deficiency** (MIM #226200). Hereditary syndromes with a rare frequency of EPI are **Alagille syndrome** (MIM #118450), **hereditary pancreatitis**, and **maturity-onset diabetes of the young, type VIII** (MIM #609812).

1.2.3 HYPOPLASIA OF ALAE NASI

The formation of a human nose starts during the fourth week of gestation, when several swellings appear on the fetal face [Castillo, 1994]. Hypo- or aplasia of the nasal wings is another consistent feature in JBS. The manifestation ranges from subtle, near to normal hypoplasia of the nasal wings to complete aplasia or even facial clefting involving the nose. Figure 1.6 exemplarily shows three patients with a-/hypoplasia of alae nasi.



Figure 1.6: Underdeveloped alae nasi in three JBS patients from our cohort.

(A) Male patient aged 5 months with aplasia of alae nasi [Almashraki et al., 2011]. (B) Propositus aged 22 years with hypoplastic nasal wings [Sukalo et al., 2014a]. (C) Girl aged 3 years presenting with subtle hypoplasia of alae nasi [Atik et al., 2015]. Reprinted with permissions from Baishideng Publishing Group, John Wiley and Sons, and Elsevier.

There are only a few syndromes that show a nasal phenotype that may be reminiscent of the one seen in JBS patients. **Oculodentodigital dysplasia** is associated with hypoplasia of alae nasi, besides of variable involvement of the eyes, dentition, and fingers; the nasal phenotype in this syndrome has also been described as prominent columella with thin anteverted nares. Cases of **tricho-rhino-phalangeal syndrome type 1** (MIM #190350) were described to have narrow alae nasi, prominent nasal tip, and pear-shaped nose with high philtrum [Giedion, 1966] that can look like the nasal wing hypoplasia described in JBS. Da-Silva [1991] described 73 individuals from two large multigenerational clans with **Waardenburg syndrome type 1** (MIM #193500) and associated hypoplasia of the nasal wings.

1.2.4 OLIGODONTIA

Selective tooth agenesis (MIM # 106600) without associated systemic disorders can be divided into two types: oligodontia, defined as agenesis of six or more permanent teeth, and hypodontia, defined as agenesis of less than six teeth [Pirinen et al., 2001]. The amount of missing teeth in both cases does not include absence of third molars. Absence of all permanent teeth is termed anodontia. There are many syndromes associated with the partial absence of teeth. The agenesis may affect the deciduous dentition, permanent dentition, or both. In JBS, oligodontia of permanent teeth is a constant observation (Figure 1.7), but often not diagnosed until primary school age.



Figure 1.7: Oligodontia of permanent teeth in a patient from our JBS cohort.

A female JBS patient aged 13 years had well documented oligodontia. Pictures show dental status in frontal view, upper jaw, lower jaw, and x-ray imaging of jaw and teeth. The patient has complete absence of permanent teeth and is also missing several deciduous teeth. Dental reconstruction is planned.

Several forms of **selective tooth agenesis** include oligodontia and hypodontia of permanent teeth. Also in many forms of **ectodermal dysplasia**, abnormal or missing teeth were reported [Cluzeau et al., 2011]. By examining the dentition of seven patients with **Wolf-Hirschhorn syndrome**, it was suggested that oligodontia may be a common symptom, although previously not well-documented in this disease [Nieminen et al., 2003]. In **Weyers acrofacial dysostosis** (MIM #193530) and an allelic disorder called **Ellis-van Creveld syndrome** (MIM #225500), missing teeth have been documented. It was postulated that mutations of the *WNT10A* gene are responsible for hypo-/oligodontia of permanent teeth in **Schöpf-Schulz-Passarge syndrome** (MIM #224750) and **odontoonychodermal dysplasia** (MIM #257980) [Bohring et al., 2009]. The **Coffin-Lowry syndrome** (MIM #303600), an X-linked mental retardation syndrome, can also be associated with hypodontia. Further very rare inherited diseases with oligodontia or hypodontia of permanent teeth are **Hay-Wells syndrome** (MIM #106260), **dominant deafness-onychodystrophy syndrome** (MIM #124480), **Axenfeld-Rieger syndrome type 1** (MIM #180500), **frontometaphyseal dysplasia** (MIM #305620), **trichodontal dysplasia** (MIM #601453), and several forms of **hypomyelinating leukodystrophy**.

1.3 ADAMS-OLIVER SYNDROME (AOS)

The Adams-Oliver syndrome, first described by Adams and Oliver in 1945, is a clinically and genetically heterogeneous disorder characterised by the association of ACC and TTLD. The congenital skin defects are mostly restricted to the scalp, predominantly to the scalp vertex, with or without underlying bony defect. They may range from small, hairless patches on the head to massive skin defects spanning the whole scalp. Limb defects can be very subtle, such as brachydactyly or hypoplastic nails, but also include amputation defects of fingers, toes, hands, feet, or even parts of the arms and legs. These anomalies have to be distinguished from such limb defects that can be caused by exogenous factors (including amniotic band disruptions, medication or drug intake, and prenatal infections).

Several further symptoms have been described, such as congenital heart defects (CHD; 20%), cutis marmorata telangiectatica congenita (CMTC; 20%), and vascular and neurological abnormalities [Snape et al., 2009]. The incidence of AOS was estimated to 1 in 225,000 live births [Adams and Oliver, 1945]. According to Snape et al. [2009], the presence of two major features is considered sufficient for a diagnosis of AOS (Table 1.3). Autosomal dominant, as well as autosomal recessive inheritance has been documented, the later one with a more complex phenotype frequently including ocular and neurological anomalies. Many sporadic cases have been recorded. Variable expression even within the same family has been described in literature [Kuster et al., 1988; Lin et al., 1998; Verdyck et al., 2003].

Table 1.3: Features for clinical diagnosis of AOS.

[Snape et al., 2009]

Major features	Minor features
Terminal transverse limb defects	Cutis marmorata telangiectatica congenita
Aplasia cutis congenita	Congenital cardiac defect
Family history of AOS	Vascular anomaly

Limb defects and CMTC are discussed in detail below (chapters 1.3.1 and 1.3.2). There is a wide variation in cardiac anomalies described in AOS, including tetralogy of Fallot, atrial septal defect (ASD), ventricular septal defect (VSD), aortic coarctation, valve abnormalities, hypoplastic left and right ventricles, double outlet right ventricle, and patent ductus arteriosus (summary by [Snape et al., 2009]). In AOS patients, also a wide range of vascular defects was described, but the majority of these findings were CMTC or

pulmonary hypertension. Also the neurological abnormalities were variable, including developmental delay and mental retardation, microcephaly, epilepsy, cortical dysplasia, and intracranial calcifications (summary by [Snape et al., 2009]). Taking all mentioned symptoms into consideration, Snape et al. [2009] hypothesised that defects of vasculogenesis may underlie this disorder.

1.3.1 TERMINAL TRANSVERSE LIMB DEFECTS (TTLD)

Congenital limb abnormalities can be uni- or bilateral, restricted to the upper or lower limbs, or affect all four limbs. The prevalence is estimated to less than 6:10,000 live births [Froster-Iskenius and Baird, 1989]. The etiology of these defects is very complex, involving chromosomal abnormalities, single gene disorders, intrauterine factors, vascular events, maternal diseases and exposures, but many cases remain unsolved (summary by [Ermito et al., 2009]). Terminal transverse limb defects describe the absence of a distal structure of the limb with proximal structures being more or less normal [EUROCAT, 2004]. They may be isolated or associated with other anomalies. A classification of subtypes was established by EUROCAT, the European surveillance of congenital anomalies (Table 1.4).

Table 1.4: Subtypes of terminal transverse limb defects.
Adopted from [EUROCAT, 2004].

Subtype	Description
1. Amelia	Total absence of the extremities
2. Hemimelia	Total absence of the forearm and hand or of foreleg and foot
3. Acheiria	Absence of hand
4. Apodia	Absence of foot
5. Adactyly	Absence of digits
6. Ectrodactyly	Total or partial absence of phalanx

In AOS, limb defects include amputations, syndactyly, brachydactyly, and oligodactyly [Stittrich et al., 2014]; Figure 1.8 shows varying degrees of TTLD in AOS patients. Hemimelia (TTLD Subtype 2, see Table 1.4) is the most severe subtype of TTLD documented so far [Adams and Oliver, 1945]. Disturbance of vascular genesis is supposed to be the underlying reason for TTLD in AOS [Swartz et al., 1999].



Figure 1.8: Phenotypic spectrum of limb defects in AOS patients.

(A) Patient from literature [McGoey and Lacassie, 2008]. (A1) Upper limbs with bilaterally short forearms, four rudimentary digits on the right, and five on the left. (A2) Lower limbs with near to total adactyly. (B) Patient 3.1 in Sukalo et al. [2015]. (B1) Amputation defects of fingers (right hand clenched). (B2) Shortened toes of left foot, amputation defects of right toes and missing nails. (C) Patient 2.1 in Sukalo et al. [2015]. (C1) Short fingers with narrowing tips, clinodactyly of 5th digit. (C2) Stubby toes with partial syndactyly 2-3. Reprinted with the permission from John Wiley and Sons.

Similar distal limb defects were reported in two further congenital diseases that are also presumed to result from vascular defects. **Poland syndrome** (MIM %173800) comprises unilateral absence or hypoplasia of the pectoralis muscle and a variable degree of ipsilateral hand and digit anomalies. This can also be a part of another syndrome, such as **Moebius syndrome** (MIM %157900), which is characterised by congenital facial palsy with impairment of ocular abduction and orofacial dysmorphism. In about one third of the patients with Moebius syndrome, limb deformities, including the full picture of Poland syndrome, are observed. Many other genetic entities with limb defects are known, but terminal location of these defects is typically seen in the three syndromes mentioned above.

A frequent non-genetic reason of TTLD is the **amniotic band disruption complex** (MIM %217100). Early amniotic ruptures are supposed to mainly cause stillbirths, whereas later ruptures result primarily in limb malformation [Higginbottom et al., 1979]. The effects of amniotic banding can vary from circumferential grooves to whole-limb amputation defects, predominantly asymmetrical.

1.3.2 CUTIS MARMORATA TELANGIECTATICA CONGENITA (CMTC)

The term **livedo reticularis** describes a condition of dilated capillary blood vessels where stagnation of blood causes mottled skin colouration. **Cutis marmorata** refers to temporary livedo caused by a normal physiological response after exposure to cold and is common in infants and also often seen in adults. In contrast, **cutis marmorata telangiectatica congenita** is a rare inborn vascular disorder characterised by persistent mottling of the skin. It can occur as an isolated finding (MIM 219250) or in the context of inherited syndromes, often together with other (cardio-) vascular defects. Associated anomalies – particularly minor defects – were noted in 80% of the patients [Devillers et al., 1999]. Figure 1.9 shows the appearance of CMTC in three AOS patients.



Figure 1.9: CMTC in AOS patients from literature.

(A) 4-year-old female [Maniscalco et al., 2005]. (B) 7-month-old propositus (patient 1 from [Patel et al., 2004]). (C) 1-month-old baby boy (patient 2 from [Patel et al., 2004]). Reprinted with the permission from John Wiley and Sons.

In the proper meaning of the word, CMTC was only documented in two syndromic contexts. In **Adams-Oliver syndrome**, the CMTC is a minor feature and seen in around 20% of the patients [Snape et al., 2009]. Additionally, the patients often suffer from CHD which can also be caused by abnormal vascularisation. The **megalencephaly-capillary malformation-polymicrogyria syndrome** (MIM #602501) is a syndromic entity that, besides other characteristics, frequently includes vascular malformations. It has a prevalence of less than 1 in 1,000,000 and is also called macrocephaly-cutis marmorata telangiectatica congenita.

Vascular cutaneous anomalies that may resemble CMTC were reported in some other hereditary diseases. The **Sturge-Weber syndrome** (MIM #185300) commonly presents with facial cutaneous vascular malformations, also called port-wine stains. This syndrome can be caused by somatic mosaic mutations in the *GNAQ* gene; the same gene is mutated in **congenital capillary malformations** (MIM #163000) which has similar

symptoms. Patients with **Klippel-Trenaunay-Weber syndrome** (MIM #149000) show vascular malformation in limbs also described as large cutaneous hemangiomas, which are associated with overgrowth of the affected limb. The **Bockenheimer's syndrome** is characterised by venous malformation on the extremities. Congenital malformations of the capillary blood vessels can occasionally be seen in **Cornelia de Lange syndrome** (type 1, 4, 5), **Coffin-Siris syndrome** (MIM #135900), and **Coffin-Lowry syndrome** (MIM #303600).

1.3.3 AUTOSOMAL DOMINANT TYPES OF AOS

At the beginning of this study, in 2010, no genes related to AOS were known. Since then, identification of AOS-associated genes had a rapid progress. This study was involved in detection of new AOS genes. Due to systematic reasons, the six genes that are known today are already included in this introduction to describe the fundamental principles of the related proteins and pathways.

The first mutations associated with AOS were described in **ARHGAP31** (MIM #610911) [Southgate et al., 2011]. This gene is located at 3q13.32-q13.33. It contains 12 exons and is translated into a protein of 1,444 amino acids in length (Figure 1.10). **ARHGAP31** encodes a protein called Rho GTPase-activating protein 31. Rho GTPases can cycle between inactive GDP-bound and active GTP-bound forms which is used to regulate a variety of cellular functions, such as proliferation and cytoskeletal dynamics. The cycling is regulated by guanine nucleotide exchange factors and GTPase-activating proteins (GAPs). **ARHGAP31** is a GAP for the Rho GTPases **CDC42** (MIM #116952) and **RAC1** (MIM #602048), which have an established role in the organisation of the actin cytoskeleton [Tcherkezian et al., 2006]. The genetic subtype is determined as **AOS1** (MIM #100300).

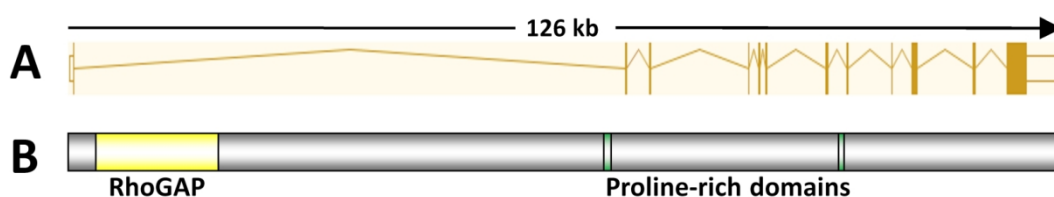


Figure 1.10: ARHGAP31 = Rho GTPase-activating protein 31.

(A) Exon-intron structure showing 12 exons [Ensembl, GRCh38.p2]. (B) Domains of the ARHGAP31 protein; adapted from [Southgate et al., 2011]. The RhoGAP domain is essential for GTPase-activation, whereas the proline-rich domains are sites of phosphorylation.

Hassed et al. [2012] identified mutations in **RBPJ** (MIM *147183) to cause another form of autosomal dominant AOS (AOS3, MIM #614814). The **RBPJ** gene is located at 4p15.2 and has several protein coding transcript variants (Figure 1.11A). It encodes the recombination signal binding protein for immunoglobulin kappa J which acts as the primary transcriptional regulator for Notch receptors, and thus plays a role in the Notch signalling pathway which regulates gene expression for specification of cell fate in diverse tissues during development. Two different missense mutations were found to segregate with autosomal dominant AOS in two kindreds [Hassed et al., 2012].

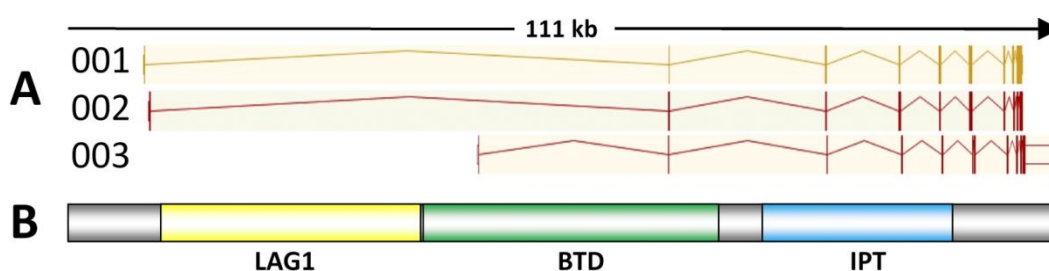


Figure 1.11: RBPJ = recombination signal binding protein for immunoglobulin kappa J.

(A) Exon-intron structure of the transcripts RBPJ-001, -002, and -003. [Ensembl, GRCh38.p2]. (B) Domains of the RBPJ protein (isoform 1, NP_005340.2), adapted from NCBI. LAG1 (DNA binding domain): 47-178 [Kovall and Hendrickson, 2004]; BTD (Beta-trefoil DNA-binding domain): 179-328 [Kovall and Hendrickson, 2004]; IPT (Ig-like, plexins, transcription factors): 350-446 [Iso et al., 2003].

Another autosomal dominant genetic subtype, AOS5 (MIM #616028), is related to heterozygous mutations of **NOTCH1** (MIM *190198). This gene is located at 9q34.3. Intron-exon structure and protein domains are displayed in Figure 1.12. **NOTCH1** encodes a single-pass transmembrane receptor that plays a key role in the Notch signalling pathway. The extracellular domain contains 36 EGF (epidermal growth factor)-like repeats and three Lin-12 NOTCH repeats (LNRs). A transmembrane domain separates this part from the intracellular domain, which consists of an RBP-J κ -associated molecule (RAM), several ankyrin repeats (ANK), a transactivation domain (TAD), and a PEST motif that is rich in proline, glutamic acid, serine, and threonine. In 2005, Garg et al. identified **NOTCH1** mutations as the underlying reason for aortic valve disease-1 (MIM #109730). Nearly 10 years later this gene was also found to cause AOS with congenital cardiac defects when Stittrich et al. [2014] detected five different **NOTCH1** mutations in five unrelated AOS families. A connection between **NOTCH1** and AOS with cardiac defects has already been postulated in 2008 [Digilio et al., 2008].

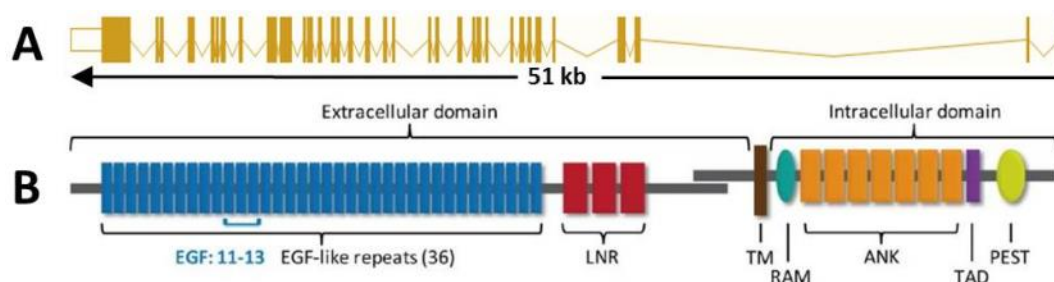


Figure 1.12: NOTCH1 = homolog of *Drosophila* Notch 1.

(A) Exon-intron structure showing 34 exons [Ensembl, GRCh38.p2]. (B) Domains of the NOTCH1 protein, adopted from [Southgate et al., 2015]. EGF, epidermal growth factor; LNR, Lin-12/Notch repeats; TM, transmembrane domain; RAM, RBP-J κ -associated molecule; ANK, ankyrin repeats; TAD, transactivation domain; PEST, peptide sequence that is rich in proline, glutamic acid, serine, and threonine.

The latest discovery in this field is the *DLL4* gene (MIM *605185), that was reported by Meester et al. in 2015. AOS6 (MIM #616589) has been assigned to this genetic subtype. This gene is located at 15q15.1 and contains 11 coding exons (Figure 1.13). The delta-like 4 protein is known to be a transmembrane ligand for Notch receptors and plays an essential role in vascular development and angiogenesis. The expression is restricted to endothelial cells, to arteries and capillaries in particular [Suchting et al., 2007].

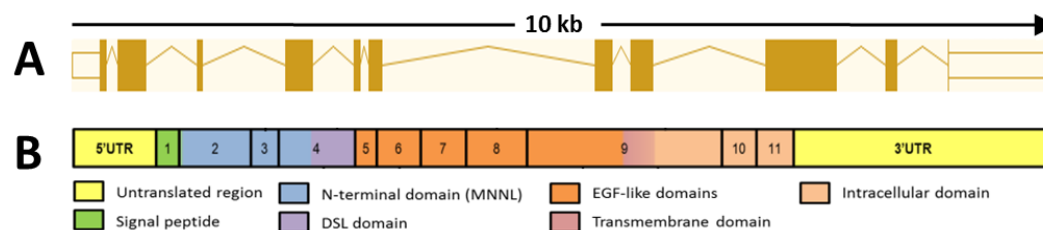


Figure 1.13: DLL4 = delta-like 4.

(A) Exon-intron structure showing 11 exons [Ensembl, GRCh38.p2]. (B) Exons and domains of the DLL4 protein, adopted from [Meester et al., 2015].

1.3.4 AUTOSOMAL RECESSIVE TYPES OF AOS

Patients with AOS from families suggesting autosomal recessive inheritance were frequently found to have a more complex phenotype compared to sporadic patients or those with autosomal dominant inheritance. In a large scale literature review, Snape et al. [2009] summarised that 32% of the patients with a supposed autosomal recessive mode of inheritance had neurological involvement, and 22% presented with developmental delay. Additionally, a significant proportion of these patients were noted to have ocular anomalies.

Shaheen et al. [2011] identified mutations in **DOCK6** (MIM *614194) to cause autosomal recessive AOS (AOS2, MIM #614219). **DOCK6** is located at 19p13.2 and encodes a protein called dedicator of cytokinesis 6, an atypical guanine nucleotide exchange factor (GEF) that functions as a GEF for CDC42 and RAC1 [Miyamoto et al., 2007]. Therefore, **DOCK6** has a role in remodelling of the actin cytoskeleton. Chromosomal location, exon-intron structure and protein domains of **DOCK6** are displayed in Figure 1.14.

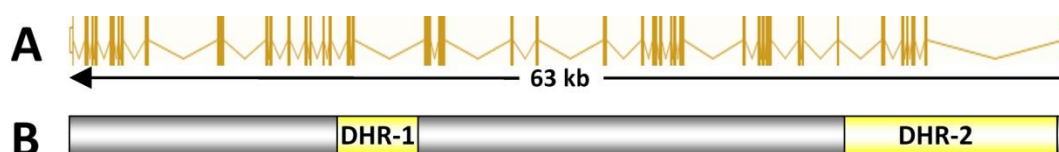


Figure 1.14: DOCK6 = dedicator of cytokinesis 6.

(A) Exon-intron structure showing 48 exons [Ensembl, GRCh38.p2]. (B) Domains of the **DOCK6** protein, adapted from [Sukalo et al., 2015]. DHR, DOCK-homology region.

Mutations of **EOGT** (MIM *614789), which is located at 3p14.1, were also associated to autosomal recessive AOS (AOS4, MIM #615297) [Shaheen et al., 2013]. The EGF domain specific O-linked N-acetylglucosamine transferase **EOGT** is essential for posttranslational modification of specific molecules, including NOTCH1 [Sakaidani et al., 2012]. By glycosylating a subset of extracellular EGF-domain-containing proteins, it plays a role in regulation of intracellular signalling, endocytosis, transcription, and protein stability [Sakaidani et al., 2012]. Impaired O-GlcNAc transferase function of the **EOGT** protein leads to a lack of O-glycosylated NOTCH1 and thus impairs the canonical Notch signalling pathway. Figure 1.15 shows exon-intron structure of the **EOGT** gene and known functional domains of the encoded protein.

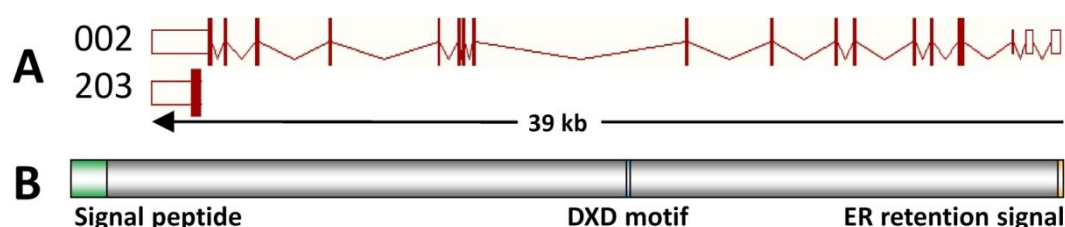


Figure 1.15: EOGT = EGF domain-specific O-linked N-acetylglucosamine transferase.

(A) Exon-intron structure showing 15 coding exons of isoform **EOGT-002**. An alternative last exon is included in **EOGT-203**. (B) Domains of the **EOGT** protein, adapted from [Ogawa et al., 2015]. ER, endoplasmic reticulum; DXD, amino acid sequence that is invariant among glycosyltransferases (D, aspartate; X, any residue; D, aspartate).

1.4 AIMS

The aim of this study was to further elucidate the genetic and molecular basis of two syndromic conditions with congenital scalp defects as a clinical feature, JBS and AOS.

In a prospectively recruited cohort of patients with JBS, the known gene *UBR1* was analysed to expand the mutational spectrum and to establish possible genotype-phenotype correlations. Furthermore, functional characterisation of *UBR1* mutations should be investigated. Identification of new candidate genes for JBS was a secondary goal, provided that *UBR1* mutation-negative patients with this phenotype were observed.

Another major aim was regarding the genetic basis of AOS, which was completely unknown at the start of this project. Genetic heterogeneity of AOS was assumed because of different inheritance patterns and the known clinical variability. Our large cohort of AOS cases should serve for identification of novel genes as well as confirmation of the significance of newly published genes, including also the evaluation of mutational spectrum, functional consequences of mutations, and genotype-phenotype correlations.

Based on a more detailed understanding of the molecular pathogenesis of both investigated hereditary syndromes, JBS and AOS, we expected to gain more insights into the complex pathophysiology of congenital scalp defects, the clinical symptom that is shared by these otherwise distinct syndromes. This knowledge was supposed provide a possible clue for other hereditary syndromes with scalp defects.

2 MATERIAL AND METHODS

2.1 PATIENTS

Patients with a suspected diagnosis of **JBS** were evaluated with a standardised clinical checklist submitted by the referring clinician. Moreover, clinical photographs were reviewed by an experienced clinical geneticist (M.Z.). Inclusion criteria were relatively soft to possibly discover *UBR1*-related phenotypes beyond the previously known phenotypic spectrum of JBS and/or delineate new clinical entities or subtypes. Patients with at least one of the following symptoms were included in the expanded JBS cohort: syndromic scalp defects, and/or pancreatic insufficiency, and/or facial anomalies that were recognised as JBS-like. According to the clinical phenotype, this heterogeneous study population included 71 individuals that were classified into three major categories:

- patients with a phenotype typical or suggestive of JBS (n=24)
- patients with nosologically undefined phenotypes only partially overlapping with JBS (n=33), and
- patients with isolated EPI (n=14).

Prior to this study, 88 index patients were genetically analysed in the Zenker lab within the JBS project. A mutation of the *UBR1* gene was detected in 35 of those families, including 13 families that were initially published by Zenker et al. [2005]. In addition to the 71 novel patients that were investigated within this PhD study, the 35 previously identified *UBR1*-positive families were included in analyses that were performed within the scope of this PhD study (functional analyses, systematic *in silico* evaluation, analyses of genotype-phenotype correlation).

The study was approved by the Ethics Board of the Medical Faculty of the University of Erlangen (processing number 2417). Informed consent was obtained from all patients or parents.

The large heterogeneous **AOS** study cohort from Magdeburg consisted of 53 patients from 43 unrelated families, including 33 index patients with clinically determined AOS, nine index patients with only ACC and one case that has been previously published as a variant of AOS with cognitive impairment, but without scalp defect [Brancati et al., 2008]

(Table D.1). Additionally, patient cohorts from our collaboration partners in London and Antwerp were included in this project. Parental consanguinity and/or the presence of multiple affected children of clinically unaffected parents were regarded as possible indicators of autosomal-recessive inheritance. Parent-child transmission of the phenotype within a family suggested autosomal-dominant inheritance. The study was approved by the institutional review boards of the participating centres, University of Magdeburg/Erlangen, Guy's and St Thomas' Hospitals London, and University of Antwerp. Written informed consent was obtained from the patients and/or the parents.

2.2 MATERIAL

All chemicals and reagents, antibodies, commercially available kits and buffers and solutions, instructions for preparation of buffers and solutions, consumables, laboratory equipment, software, online tools, and oligonucleotides used in this study are listed in Appendix A (material) and Appendix B (oligonucleotides).

2.3 METHODS

Figure 2.1 diagrams a flowchart of the major methods used in this study.

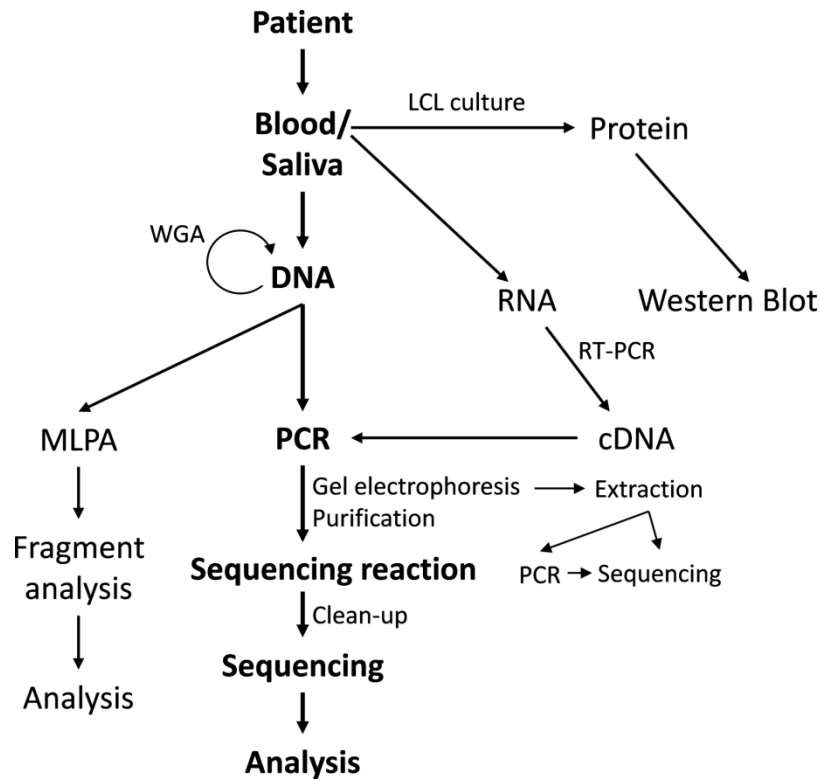


Figure 2.1: Flowchart of major methods.

LCL, lymphoblastoid cell line; WGA, whole genome amplification; PCR, polymerase chain reaction; RT-PCR, reverse transcription PCR.

2.3.1 DNA EXTRACTION

Several methods were applied to extract DNA from human EDTA blood. The chemagic DNA Blood Kit special was used on the chemagic Magnetic Separation Module I with blood volumes of 3 ml or 7 ml. DNA extraction with the help of magnetic beads was carried out in accordance with the manufacturer's instructions; the resulting DNA pellets were dissolved in elution buffer. The second automated method to extract DNA from whole blood samples applied in our lab was performed on the QIAcube robotic workstation in combination with the QIAamp DNA Blood mini Kit; the DNA collected from blood was dissolved in appropriate elution buffer. For manual column-based purification and/or to improve concentration and pureness of externally extracted DNA samples, we applied the QIAamp DNA mini Kit; final volume was dependent on the aim of this procedure.

In some patients collection of saliva samples was performed as an alternative source of genomic DNA. These samples were collected and shipped with the help of oragene·DNA collection kits (OG-250 and OG-500; OG-575 for assisted collection). DNA was extracted from the saliva-buffer mixture with the help of prepIT·L2P following the manufacturer's protocol. These procedures were routinely performed by the technical staff.

2.3.2 RNA EXTRACTION

RNA from whole blood samples was collected with the help of the PAXgene Blood RNA system. The PAXgene Blood RNA Tubes contain a buffer that stabilises RNA in whole blood samples at room temperature for a period of 3 days, which is enough to ship the samples within Germany. Shipping from abroad is also possible, but the samples have to be cooled or frozen (RNA stability: 3 days at 18-25°C, 5 days at 2-8°C, >1 year at -20°C). Nucleic acid purification was performed with the PAXgene Blood RNA Kit according to the manufacturer's instructions. RNA samples were stored at -20°C.

For extracting total RNA from human lymphoblastoid cell lines (LCLs), the RNeasy Mini Kit was used. This column based spin technology was applied according to the manufacturer's instructions. RNA samples were stored at -20°C.

2.3.3 DETERMINATION OF DNA QUALITY AND QUANTITY

DNA quality was tested on an agarose gel (1% w/v) by applying 2 µl of the DNA sample mixed with 3 µl loading dye (see also chapter 2.3.11 Gel electrophoresis). The 1 kb Plus DNA Ladder was used as a size standard. The electrophoresis system was set at 100 V – 125 V and ran for 30 min to separate DNA fragments of different lengths. A long smear of bands represents the desired product of differently sized DNA fragments.

The NanoDrop 2000/2000c UV-Vis spectrophotometer and associated software was used for measuring the concentration of nucleic acid solutions. Blank values were adapted to the solvent of each sample (ddH₂O (ultra-pure), TE buffer, elution buffer) and compared to 2 µl of the DNA sample. Baseline correction was adjusted to 340 nm.

2.3.4 PRIMER DESIGN

Oligonucleotides to prime the PCR and sequencing reactions were designed with the help of Primer3 version 4.0.0. The DNA sequences of the gene of interest were extracted from RefSeq sequences from UCSC Genome Browser, assembly GRCh37/hg19 for whole genomic sequence and Ensembl to determine the position of exons. In the UCSC Genome Browser, common SNPs (dbSNP built 138 or 142) were displayed to avoid placing a primer over a common SNP. NCBI transcript numbers and specifications are listed in the Appendix B, together with the sequences of all oligonucleotides used in this study. Optimal amplicon length was ≤ 550 bp, primers were desirably located 50 bp from the interesting region (relevant in Sanger sequencing). These rules did not apply for special applications, such as long-range PCR, cDNA sequencing and others. Primer length was set at 18-25 bases, melting temperature was 57-61°C and GC content was 40-60%. When the software was unable to design primers, the settings and desired locations were softened. The resulting oligonucleotide sequences were blasted on the UCSC Genome Browser and checked with the UCSC *in silico* PCR tool to verify specificity. Primers were ordered from Thermo Fisher Scientific (Ulm, Germany) and diluted to 100 pmol/ μ l (stock solution) or 2.5 pmol/ μ l (working solution for standard PCR and sequencing).

2.3.5 POLYMERASE CHAIN REACTION (PCR)

The PCR, a technique for targeted DNA amplification, was invented by Kary Mullis in 1983. The principle is based on cyclic changes of different temperatures to promote enzymatic amplification of specific DNA fragments; this specificity is determined by the applied primers.

Amplification of defined DNA fragments was realised by using the recombinant *Taq* DNA Polymerase kit and several further ingredients, as listed in Table 2.1. For DNA samples of low concentration or degraded DNA, Platinum *Taq* DNA polymerase was utilised with the same conditions. The reactions were either performed in 96-well PCR plates, 8 well strips, or in 0.2 ml single tubes.

Table 2.1: Standard PCR reagents.

Reagents	Volume
ddH ₂ O	5.6 μ l
Rxn Buffer (10x)	2.0 μ l
dNTPs (2 mM)	2.0 μ l
Forward primer (2.5 pmol)	2.0 μ l
Reverse primer (2.5 pmol)	2.0 μ l
MgCl ₂ (50 mM)	0.6 μ l
DMSO (100%)	1.0 μ l
Betaine (5 M)	4.0 μ l
<i>Taq</i> DNA polymerase (5 U/ μ l)	0.1 μ l
DNA (50 ng/ μ l)	0.7 μ l
Final volume	20 μl

For standard PCR reactions, a touchdown program was used (Table 2.2) on either the Applied Biosystems 2720 Thermal Cycler or the VWR DuoCycler. Annealing temperatures ranged from 65°C in the beginning to 55°C for the 33 final cycles in order to cover a wide span of different melting temperatures. For amplicons with a suspected length of >750 bp, the elongation duration was adjusted (~ 01:00 min per 1 kb).

Table 2.2: Standard PCR conditions (touchdown).

Temperature	min:sec	Step	Cycles
94°C	03:00	Initial denaturation	1
94°C	00:30	Denaturation	2
65°C	00:45	Annealing	
72°C	00:45	Elongation	
94°C	00:30	Denaturation	2
63°C	00:45	Annealing	
72°C	00:45	Elongation	
94°C	00:30	Denaturation	2
61°C	00:45	Annealing	
72°C	00:45	Elongation	
94°C	00:30	Denaturation	2
59°C	00:45	Annealing	
72°C	00:45	Elongation	
94°C	00:30	Denaturation	2
57°C	00:45	Annealing	
72°C	00:45	Elongation	
94°C	00:30	Denaturation	33
55°C	00:45	Annealing	
72°C	00:45	Elongation	
72°C	10:00	Final elongation	1
10°C	∞	Final hold	1

2.3.6 REVERSE TRANSCRIPTION PCR (RT-PCR)

Synthesis of first-strand cDNA from purified RNA was performed with the SuperScript III Reverse Transcriptase kit, with the addition of Oligo(dT)₁₂₋₁₈ Primer and pd(N)₆ Sodium Salt (random hexamers). All steps were performed on ice (if not indicated differently) and only nuclease free plastic ware and RNase free ddH₂O were used. Reagents and volumes are listed in Table 2.3, reaction conditions in Table 2.4.

Table 2.3: Reagents for reverse transcription PCR.

Reagents	Volume
Oligo(dT) ₁₈₋₂₀ Primer (0.5 µg/µl)	0.5 µl
pd(N) ₆ Sodium Salt (0.2 µg/µl)	1.0 µl
dNTPs (10 mM)	1.0 µl
RNA (1 µg)	10.5 µl
ddH ₂ O, RNase free	
5 min at 65°C incubate on ice for ≥1 min	
First-Strand Buffer (5x)	4.0 µl
Dithiothreitol DTT (0.1 M)	1.0 µl
1 µl RNase out (40 U/µl)	1.0 µl
1 µl Superscript III (200 U/µl)	1.0 µl
Final Volume	20 µl

Table 2.4: Temperature protocol for reverse transcription PCR.

Temperature	min:sec	Step
25°C	05:00	Random primer incubation
50°C	60:00	Incubation
70°C	15:00	Heat inactivation
4°C	∞	Final hold

The quality of resulting cDNA was evaluated in a standard PCR approach (see chapter 2.3.5) using *GAPDH* control primers (Table B.2.5) and gel electrophoresis (see chapter 2.3.10). As positive control, RNA gained from human placenta was utilised. The cDNAs were stored at -20°C only in post PCR surroundings to prevent contamination of other reactions.

For cDNA amplification, the same ingredients and programs as for regular PCR (chapter 2.3.5) were used, but the primers were preferably designed to span exon-exon boundaries to prevent amplification of genomic DNA (Appendix B.2).

2.3.7 PCR AMPLIFICATION OF GC-RICH TARGETS

For amplification of difficult DNA templates with high GC content and/or repetitive sequences, the GC-RICH PCR System (Table 2.5) was used according to the manufacturer's instructions (Table 2.6). Volume of each reaction was reduced to half of the recommended value. This PCR system contains a mixture of *Taq* DNA polymerase and a proofreading polymerase for high quality performance.

Table 2.5: Reagents for GC-rich PCR amplification.

Reagents	Mix 1	Mix 2
ddH ₂ O	9 µl	2 µl
dNTPs (10 mM)	1 µl	-
GC-RICH Reaction Buffer (5x)	-	5 µl
Betaine (5 M)	2.5 µl	-
Forward primer (5 pmol/µl)	2 µl	-
Reverse primer (5 pmol/µl)	2 µl	-
DNA (50 ng/µl)	1 µl	-
GC-RICH Enzyme Mix	-	0.5 µl
Final volume	17.5 µl	7.5 µl

Table 2.6: Cycling conditions for GC-rich PCR amplification.

Temperature	min:sec	Step	Cycles
94°C	05:00	Initial denaturation	1
94°C	00:30	Denaturation	2
60°C	00:30	Annealing	
72°C	01:00	Elongation	
94°C	00:30	Denaturation	2
59°C	00:30	Annealing	
72°C	01:00	Elongation	
94°C	00:30	Denaturation	2
58°C	00:30	Annealing	
72°C	01:00	Elongation	
94°C	00:30	Denaturation	2
57°C	00:30	Annealing	
72°C	01:00	Elongation	
94°C	00:30	Denaturation	32
56°C	00:30	Annealing	
72°C	01:00*	Elongation	
72°C	10:00	Final elongation	1
10°C	∞	Final hold	1

* (+ 5 sec per cycle)

2.3.8 MULTIPLEX PCR

To prove the presence – or absence – of specific DNA segments, multiplex PCR is adequate, because one can compare various amplicons within the same reaction. The Multiplex PCR Kit contains a ready-to-use mix of HotStarTaq DNA Polymerase, Multiplex PCR Buffer with MgCl₂ and dNTP mix. Apart from the DNA, a 10x primer mix has to be added (Table 2.7). This mix contains 1 µl of each forward and reverse primer (100 pmol/µl), filled to 50 µl with TE buffer. Touchdown PCR is recommended (Table 2.8), as different primer pairs are used in a single reaction. The final volume indicated by the supplier is 50 µl, but using half of this reaction volume was enough for all applications within this study.

Table 2.7: Reagents for multiplex PCR.

Reagents	Volume	½
QIAGEN Multiplex PCR Master Mix (2x)	25 µl	12.5 µl
Primer Mix (10x)	5 µl	2.5 µl
ddH ₂ O	18 µl	9 µl
DNA (50 ng/µl)	2 µl	1 µl
Final volume	50 µl	25 µl

Table 2.8: Cycling conditions for multiplex PCR.

Temperature	min:sec	Step	Cycles
95°C	15:00	Initial denaturation	1
94°C	00:30	Denaturation	2
65°C	01:00	Annealing	
72°C	01:00	Elongation	
94°C	00:30	Denaturation	2
63°C	01:00	Annealing	
72°C	01:00	Elongation	
94°C	00:30	Denaturation	2
61°C	01:00	Annealing	
72°C	01:00	Elongation	
94°C	00:30	Denaturation	2
59°C	01:00	Annealing	
72°C	01:00	Elongation	
94°C	00:30	Denaturation	2
57°C	01:00	Annealing	
72°C	01:00	Elongation	
94°C	00:30	Denaturation	31
55°C	01:00	Annealing	
72°C	01:00	Elongation	
72°C	10:00	Final elongation	1
10°C	∞	Final hold	1

2.3.9 LONG-RANGE PCR

For amplifying DNA fragments from 5 kb to 25 kb, the Expand Long Range dNTPack was used (Table 2.9). The buffer with MgCl₂ and the dimethyl sulfoxide (DMSO) were incubated at 37°C for 10 min to dissolve precipitates that might have formed during storage. To protect the polymerase that is included in the Expand Long Range Enzyme mix, denaturation should be as short and as low tempered as possible (Table 2.10), which recommends low GC-contents of the primer target sequence (45-65%). Again, half of the recommended reaction volume was sufficient for my experiments.

Table 2.9: Reagents for long-range PCR.

Reagents	Volume	½
ddH ₂ O	14.3 µl	7.15 µl
Buffer with MgCl ₂ (5x)	10.0 µl	5.0 µl
dNTP-Mix (10 mM)	2.5 µl	1.25 µl
FP (2.5 pmol)	5.0 µl	2.5 µl
RP (2.5 pmol)	5.0 µl	2.5 µl
DMSO	2.5 µl	1.25 µl
Enzyme-Mix	0.7 µl	0.35 µl
DNA (50 ng/µl)	10.0 µl	5.0 µl
Final volume	50 µl	25 µl

Table 2.10: Cycling conditions long-range PCR.

Temperature	min:sec	Step	Cycles
92°C	02:00	Initial denaturation	1
92°C	00:10	Denaturation	2
65°C	00:15	Annealing	
68°C	#	Elongation	
92°C	00:10	Denaturation	2
63°C	00:15	Annealing	
68°C	#	Elongation	
92°C	00:10	Denaturation	2
61°C	00:15	Annealing	
68°C	#	Elongation	
92°C	00:10	Denaturation	2
59°C	00:15	Annealing	
68°C	#	Elongation	
92°C	00:10	Denaturation	2
57°C	00:15	Annealing	
68°C	#	Elongation	
92°C	00:10	Denaturation	25
55°C	00:15	Annealing	
68°C	#*	Elongation	
68°C	17:00	Final elongation	1
10°C	∞	Final hold	1

(1 min per 1 kb), * (+20 sec per cycle)

2.3.10 GEL ELECTROPHORESIS

Separation of DNA fragments was accomplished using one-dimensional agarose gel electrophoresis. Analytic agarose gels (2% w/v) were prepared in 1x TBE buffer in an Erlenmeyer flask. The solution was heated in a microwave oven for 2-3 min; a magnetic swirl bar prevented over boiling. Ethidium bromide was added to a final concentration of 0.1 µg/ml and the mixture was cooled down to <60°C on a magnetic stirrer. Afterwards, the agarose solution was poured in a sealed gel tray (7x8 cm or 12x14 cm) with combs (6-12 teeth for small gel, 12-24 teeth for large gel). Solidification at room temperature took about 10-20 min. The gel was covered with 1x TBE buffer in a PerfectBlue Gel System chamber. PCR product (5 µl) was mixed with loading dye (3 µl) and pipetted into the wells of the gel. A 100 bp DNA Ladder was used as length standard. For analysing multiplex PCR approaches, 2% w/v agarose gels, 10 µl PCR product, 5µl loading dye and 100 bp DNA Ladder were used. For analysing long-range PCR products, 1% w/v agarose gels, 5-10 µl PCR product, 3-5 µl loading dye and 1 kb Plus DNA Ladder were used.

The gels were run at ~100 V (special approaches: 80-150 V) for 15-30 min (special approaches up to 150 min). Visualisation was realised with a UV transilluminator, a DevisionDBox system, and DeVision G software.

2.3.11 PCR PRODUCT PURIFICATION

For performing further steps, the PCR products were purified in two different ways. When samples were designated for regular Sanger sequencing, AMPure purification was used. The samples were processed with magnetic bead-based technology with the help of Agencourt AMPure and the Biomek NX^P Laboratory Automation Workstation. Per 1 µl PCR product, 1.8 µl magnetic beads solution was added. Pipetting up and down helps to bind the DNA strands to the beads, then the mixture was transferred to a 96-well PCR plate that was located on a SPRIPlate 96R ring magnetic plate. The beads with DNA fragments were attached to the well by magnetism and washed with 70% ethanol. The DNA fragments were separated from the beads by eluting in ddH₂O and transferred to another 96-well PCR plate. The underlying principle of this technique is called solid phase reversible immobilisation (SPRI).

When aiming for only a fraction of a mixed PCR product (e.g. multiplex PCR), a single band can be sliced off the agarose gel and extracted separately. For this purification procedure, the DNA Gel Extraction Kit or the MinElute Gel Extraction Kit was used as indicated by the manufacturers.

2.3.12 CYCLE SEQUENCING REACTION

In 1977, Frederick Sanger developed a method of DNA sequencing that is based on the selective inclusion of labelled ddNTPs during *in vitro* DNA replication that causes termination of the chains. This Sanger sequencing approach needs a DNA template, selected primers, a DNA polymerase and the fluorescently labelled ddNTPs, the two latter ones are included in the BigDye Terminator v3.1 Cycle Sequencing Kit. Of the purified PCR product, 0.5 µl were used by default. If the bands showed a very high or low concentration of PCR products, 0.25 µl to 1.0 µl of the purified PCR product were appropriate. Thermal cycling was performed on the Veriti 96-Well Fast Thermal Cycler in semi-skirted MicroAmp Fast 96-Well Reaction Plates or MicroAmp Fast Reaction Tubes. Volumes of ingredients and cycling conditions are displayed in Table 2.11 and Table 2.12. Routinely, unidirectional sequencing was performed to save time and money. When specific amplicons did not result in an unambiguously non-pathogenic sequence, or when mutations were detected, the complimentary strand was also sequenced. In Appendix B.1, the primers used for this special application are indicated with asterisks.

Table 2.11: Cycle sequencing reagents.

Reagents	Volume
ddH ₂ O	2.7 µl
Sequencing Buffer (5x)	1.0 µl
BigDye Terminator	0.2 µl
Primer (2.5 pmol)	0.6 µl
PCR product (purified)	0.5 µl
Final volume	5.0 µl

Table 2.12: Standard cycle sequencing conditions.

Temperature	min:sec	Step	Cycles
96°C*	00:10	Denaturation	26
55°C	00:10	Annealing	
60°C	01:00	Elongation	
10°C	∞	Final hold	1

*98°C if high melting temperatures were expected

2.3.13 SEQUENCING REACTION CLEAN-UP

Dye terminators (ddNTPs) were removed with the help of SPRI technology using the Agencourt CleanSEQ system on the Biomek NX^P Laboratory Automation Workstation. The sequencing reaction product was mixed with CleanSEQ solution and 85% ethanol, incubated for 7 min and transferred to a 96-well optical plate that was located on the SPRIPlate 96R ring magnetic plate. This magnet binds the beads and the attached DNA fragments to the wall of each well. All other ingredients were washed off with 85% ethanol. The remaining fluorescently labelled fragments were air dried and eluted in ddH₂O.

2.3.14 SEQUENCE ANALYSIS

Separation and base-calling of the purified Sanger sequences was performed on an ABI3500xL capillary sequencer. The ddNTP labelled fragments were electrophoretically separated in a capillary filled with a POP-7 Performance Optimised Polymer. Lasers within the sequencing machine detect the four fluorochromes that resemble the four ddNTPs and 3500 Data Collection Software records this data in an electropherogram. For fragments smaller than 500 bp, the run module "RapidSeq50_POP7" was used, for larger fragments the run module "FastSeq50_POP7" was used.

Subsequent computational sequence analysis was carried out with the help of the Sequence Pilot software (v4.2.1, built 506). This software aligns the reference sequences (uploaded from Ensembl) to the generated sequences and highlights differences. For viewing and editing the raw data, Sequencing Analysis software v5.4 was used. Chromas Lite (2.01) was the program of choice to display a neat electropherogram without automated edits or comparisons.

2.3.15 WESTERN BLOT

CELL PREPARATION AND PROTEIN ISOLATION: LCLs were established by in vitro transformation of human lymphocytes from heparin blood samples via Epstein Barr Virus according to established protocols [Neitzel, 1986]. This procedure was performed by the cytogenetic division of the Institute of Human Genetics Magdeburg (Dr. M. Volleth and colleagues).

The non-adherent LCLs were cultivated in a 50 ml cell culture flask and when enough cell material was grown, they were decanted into a lidded centrifuge tube. To separate cells from medium, the tube was centrifuged for 7 min at 1.000 rpm. Then the supernatant was removed and the cells were washed with 1x PBS. After swirling gently, the tube was again centrifuged for 7 min at 1.000 rpm with subsequent removal of the supernatant. These cell pellets can either be directly processed or stored at -20°C (short term) or -80°C (long term).

The first step of protein isolation from the pelleted LCLs is to add 100-300 µl RIPA buffer with protease inhibitor. By careful pipetting, the mixture was homogenised and subsequently put on a rocker for 30 min while chilled on ice. Centrifugation at 12.000 x g for 1 hour at 4°C forced the lysed cell compartments to form a pellet, whereas the proteins stayed solved in the supernatant and were carefully removed into another tube.

BRADFORD MICRO ASSAY: To prepare the Bradford micro assay, a Protein Standard I Bovine Plasma Gamma Globulin solution was diluted to 1 mg/ml and used to prepare a dilution series (Table 2.13).

Table 2.13: Standard protein dilution series.

#	Protein solution [1mg/µl]	H ₂ O	Concentration
1	-	1000 µl	0 ng/µl
2	1 µl	999 µl	1 ng/µl
3	2 µl	998 µl	2 ng/µl
4	5 µl	998 µl	5 ng/µl
5	10 µl	990 µl	10 ng/µl
6	15 µl	985 µl	15 ng/µl
7	20 µl	980 µl	20 ng/µl
8	25 µl	975 µl	25 ng/µl

Of the patients' protein solutions, dilutions to 1:100, 1:200 and 1:500 were made. In a 96-well flat bottom transparent microplate, 50 µl Bradford reagent was mixed with 200 µl of the diluted protein samples and incubated at room temperature for 10 min. Triplicates of protein standard and patients' protein solutions were made (Table 2.14) and measured in a M200 microplate reader with the help of TECAN Magelan Software (equipment of the Institute of Biochemistry Magdeburg). The values of the standard protein were then used to generate a calibration curve that helped to determine the protein concentrations of the patients' samples.

Table 2.14: Dilution series Bradford micro assay.

	1	2	3	4	5	6	7	8	9	10	11	12
A	1	1	1	S ₁ (1:100)	S ₁ (1:100)	S ₁ (1:100)	S ₁ (1:200)	S ₁ (1:200)	S ₁ (1:200)	S ₁ (1:500)	S ₁ (1:500)	S ₁ (1:500)
B	2	2	2	S ₂ (1:100)	S ₂ (1:100)	S ₂ (1:100)	S ₂ (1:200)	S ₂ (1:200)	S ₂ (1:200)	S ₂ (1:500)	S ₂ (1:500)	S ₂ (1:500)
C	3	3	3	S ₃ (1:100)	S ₃ (1:100)	S ₃ (1:100)	S ₃ (1:200)	S ₃ (1:200)	S ₃ (1:200)	S ₃ (1:500)	S ₃ (1:500)	S ₃ (1:500)
D	4	4	4	S ₄ (1:100)	S ₄ (1:100)	S ₄ (1:100)	S ₄ (1:200)	S ₄ (1:200)	S ₄ (1:200)	S ₄ (1:500)	S ₄ (1:500)	S ₄ (1:500)
E	5	5	5	S ₅ (1:100)	S ₅ (1:100)	S ₅ (1:100)	S ₅ (1:200)	S ₅ (1:200)	S ₅ (1:200)	S ₅ (1:500)	S ₅ (1:500)	S ₅ (1:500)
F	6	6	6	S ₆ (1:100)	S ₆ (1:100)	S ₆ (1:100)	S ₆ (1:200)	S ₆ (1:200)	S ₆ (1:200)	S ₆ (1:500)	S ₆ (1:500)	S ₆ (1:500)
G	7	7	7									
H	8	8	8									

PROTEIN SEPARATION (SDS-PAGE): To produce comparable protein bands, the same amount of proteins of each patient and control has to be used. All samples were diluted to a concentration of 50 µg in 15 µl. The protein solutions were mixed with the same amount of 2x Laemmli buffer with β-mercaptoethanol and heated to 95°C for 5 min. For separating the proteins, either a self-made SDS-PAGE (sodium dodecyl sulphate polyacrylamide gel electrophoresis) gel, or a commercially available gel (see Table 2.15 and Appendix A) was used with appropriate running buffer (Table A.5). The samples were pipetted into the stacking gel slots, 10 µl protein marker were used as a size standard. When running one gel in the Tetra Cell, 150-200 V was supplied for 25-45 min. Then the gel was equilibrated in transfer buffer for approximately 30 min.

Table 2.15: SDS gel ingredients.

Reagent	Running gel (10%)	Stacking gel (5%)
H ₂ O	3.4 ml	3.4 ml
Acrylamide	3.3 ml	830 µl
Tris buffer	2.5 ml ^a	630 µl ^b
10% SDS	100 µl	50 µl
10% APS	100 µl	50 µl
TEMED	10 µl	5 µl
Final volume	10 ml	5 ml

^aTris 1.5 M, pH 8.8; ^bTris 1 M, pH 6.8

SDS, sodium dodecyl sulphate; APS, ammonium persulfate; TEMED, tetramethylethylenediamine

PROTEIN TRANSFER (WESTERN BLOTTING): Tank blotting was performed for 3 hours at 100 mA to a nitrocellulose membrane. Afterwards, the membrane was cleansed in washing buffer. Blocking was performed with the appropriate buffer for 30 min on a rocker.

The primary antibody UBR1-1 (rabbit polyclonal antibody to mouse Ubr1) was dissolved 1:250 in the 4% blocking buffer and incubated overnight on a rocker. The membrane was then washed three times with TBST 0.1% and incubated for 1 hour with

the secondary antibody (Goat Anti-Rabbit IgG, HRP conjugate) diluted 1:5,000 in blocking buffer. Immunoblotting for β -actin served as a loading control.

CHEMILUMINESCENT PROTEIN VISUALISATION: The Visualizer Western Blot Detection Kit was used for fluorescent visualisation of the desired proteins. Working solution was prepared according to manufacturer's instructions and incubated with the membrane for 5 min while protected from light. The membrane was then adhered to a glass slide, wrapped in cling and fixed on a radiographic film in the darkroom. After 10 min exposure, the film was developed for 4 min, fixed for 10 min and washed with distilled H₂O for 30 min. Alternatively, the film was developed with the help of an AGFA x-ray developing machine (equipment of the Institute of Biochemistry Magdeburg).

2.3.16 WHOLE GENOME AMPLIFICATION

For replication of DNA samples with low volume and/or concentration, the GenomiPhi V2 DNA Amplification Kit was used, according to the manufacturer's instructions. The products were tested in a regular PCR with a reliable primer pair.

2.3.17 MULTIPLEX LIGATION-DEPENDENT PROBE AMPLIFICATION (MLPA)

MLPA is a method for relative quantification of nucleic acid fragments and can help to detect copy number differences caused by duplications and deletions of whole chromosomes, complete genes, or even a single exon. The underlying mechanism is the quantification of PCR amplification products from variably-sized oligonucleotides (optimum between 100 and 140 nt) that were generated by ligation of pairs of specific probes after binding to complementary DNA targets. Unique probes (Appendix B.3) were designed for every single exon of the *UBR1* gene, pooled into five probemixes (Table 2.16) and utilised with the DNA of clinically unambiguously identified JBS patients that lacked at least a mutation on one allele.

The original probe design had been carried out by S. Bauhuber (Erlangen), but application and further improvement was part of this work. Support was given by MRC-Holland who provide a tutorial for synthetic probe design on their homepage (<https://www.mlpa.com> and [Schouten et al., 2002]).

PROBEMIX PREPARATION: The *UBR1* gene contains a total of 47 exons, creating the need of 47 MLPA probes to cover all exons. In the SALSA MLPA P200 Human DNA reference-1 probemix, the Q-fragments (DNA quantity control) are located at ≤ 82 nt; the reference probes have a size of 173 nt and longer. So theoretically, the self-designed synthetic probes can have a size from 88-169 nt (the minimum probe length is 88 nt and the distance to another peak has to be at least 4 nt). The manufacturer gives a limit of 11 synthetic probes per probemix. Additionally, longer probes tend to create weaker signals and the price of a single oligonucleotide increases with its length. Therefore the 47 *UBR1* probes were divided into five probemixes named UBR1-A, UBR1-B, UBR1-C, UBR1-D, and UBR1-E (Table 2.16). The size ranges between 88 nt and 128 nt. Each left/right probe oligonucleotide (LPO/RPO) contains a primer binding site (PBS) and left/right hybridising sequence (LHS/RHS). After several tests, some probes were re-designed and concentration of each probe was adjusted, aiming for a more homogeneous distribution of the peaks; the final composition of the probemixes can be seen in Table 2.16.

The oligonucleotides were ordered at metabion GmbH (Planegg-Martinsried, Germany), diluted to 100 pmol/ μ l in ddH₂O and stored at -20°C. Working solution of each oligonucleotide was prepared with a final concentration of 1 pmol/ μ l. Of each LPO and RPO, the volume listed in Table 2.16 was filled up with TE to obtain a final volume of 200 μ l of each probemix.

Table 2.16: *UBR1* synthetic probemixes.
Distribution of exons and pipetting scheme.

nt	Probemix A		Probemix B		Probemix C		Probemix D		Probemix E	
	Exon	μ l								
88	-	-	-	-	23	0.8	39	0.8	-	-
96	10	0.8	27	0.8	29	0.8	30	0.8	41	0.8
100	03	0.8	21	0.8	31	0.8	36	0.8	42	0.8
104	07	1.0	16	0.8	24	0.8	33	0.8	34	0.8
108	17	0.6	25	2.4	32	0.8	40	0.8	47	0.8
112	01	0.6	26	0.8	28	0.8	35	1.6	43	0.8
116	02	2.4	05	1.0	19	0.8	22	0.8	46	0.8
120	06	0.6	08	1.0	11	0.8	37	0.8	44	0.8
124	04	2.0	09	1.0	12	0.8	14	1.0	45	1.0
128	13	0.8	15	1.6	38	0.8	18	0.6	20	0.8
TE	-	180.8	-	179.6	-	184.0	-	182.4	-	185.2

DNA SAMPLE PREPARATION: When performing an MLPA approach, at least three control DNAs have to be included for every probemix. Those reference samples were tested negative for copy number abnormalities in a CytoScan HD Array. All DNA samples (patients and controls) were diluted in ddH₂O to a final concentration of 20 ng/μl; this equals a total amount of 100 ng DNA in each reaction with a volume of 5 μl.

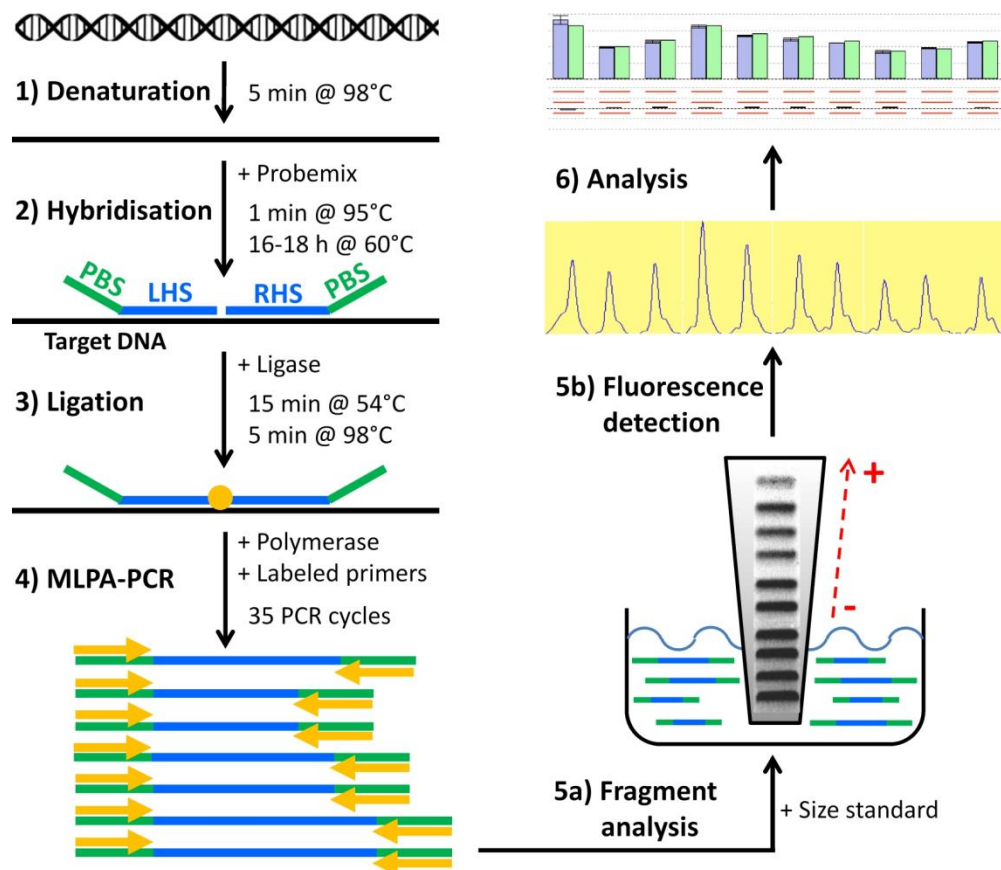


Figure 2.2: MLPA procedure.

PBS, primer binding sequence; LHS, left hybridising sequence; RHS, right hybridising sequence.

DENATURATION: In 200 μl reaction tubes, 5 μl DNA (20 ng/μl) was heated for 5 min at 98°C in the iCycler. This initial denaturation procedure separates the DNA double stranded helix to single strands that are accessible for the probes (Figure 2.2). After this heating step, the thermocycler pauses at 25°C for performing the next step.

HYBRIDISATION: While heating the DNA samples, a hybridisation mastermix was prepared for each of the probemixes, containing 1 μl reference probemix P200, 0.5 μl UBR1 self-designed probemix (either A, B, C, D, or E), and 1.5 μl SALSA MLPA buffer per sample. This mastermix was vortexed thoroughly before dispensing 3 μl to each tube. When re-starting, the thermocycler heated to 95°C for 1 min followed by cooling to 60°C.

This hybridisation step was performed overnight because the LPOs and RPOs need 16-18 hours for efficient hybridising to their target sequence.

LIGATION: The next morning, a ligase mastermix was prepared on ice containing 3 µl Ligase buffer A, 3 µl Ligase buffer B, and 25 µl ddH₂O per sample. After thoroughly vortexing these ingredients, 1 µl ligase per sample was added and the mastermix was carefully mixed by pipetting up and down. The thermocycler paused at 54°C, and 32 µl of the ligase mastermix were added to each tube. At 54°C for duration of 15 min, the LPO and RPO that have already hybridised to the DNA targets and are adjacent to each other, were ligated to form a probe of the desired length (Figure 2.2 and Appendix B.3). Afterwards, the ligase was inactivated for 5 min at 98°C, followed by cooling the samples down to 20°C. During this period, PCR mastermix was already prepared on ice.

MLPA-PCR: The PCR mastermix contained 2 µl SALSA PCR primer mix (fluorescently labelled primers that bind to the primer binding sequences of the probes), 7.5 µl ddH₂O, and 0.5 µl SALSA polymerase per sample and was distributed to new 200 µl tubes with the amount of 10 µl per tube. The samples that underwent the ligation before can be further processed when the cycler reaches 20°C; 20 µl of those samples were added to the PCR mastermixes in the new tubes at room temperature. The following PCR reaction included 35 cycles (denaturation: 95°C for 30 sec, annealing: 60°C for 30 sec, elongation: 72°C for 60 sec) followed by a final elongation (72°C for 20 min) and was cooled down afterwards to 20°C. During this reaction, the probes were exponentially amplified; their amount depended on the availability/quantity of the target sequence during the hybridisation step.

FRAGMENT ANALYSIS: The PCR products were diluted 1:3 with ddH₂O, then 0.5 µl of the dilution was mixed with 10 µl Hi-Di Formamide and 0.1 µl GeneScan 500 LIZ dye Size Standard. This mixture was heated to 98°C for 2 min and chilled on ice. The samples were injected to a 3500xL Genetic AnalyZer using the standard program MLPA_POP7xl. Gel electrophoresis within the capillaries of the sequencer separated the probes by length and detection was possible due to the fluorescently labelled primers that were included in the PCR. Analysis of the obtained electropherograms was performed with JSI Sequence Pilot software.

EVALUATION OF RESULTS: When using the JSI Sequence Pilot software, specific exons can be assigned to the peaks in the electropherogram that was generated during fragment analysis on the 3500xL Genetic AnalyZer. By comparing the peak area of each patient to those of the controls, one can detect deletion or duplication of exons, which is displayed in a bar chart.

2.3.18 MICROSATELLITES

Genotyping of polymorphic microsatellites with the help of PCR fragment length analysis is a helpful tool to determine (I) zygosity around a genetic locus, (II) maternal contamination of fetal DNA samples, and (III) for paternal testing that can be relevant for the possibility of *de novo* mutations.

The technique includes a standard PCR amplification of 250-500 bp fragments encompassing the microsatellite with specific primers. One of the primers is marked by a fluorescent dye allowing the analysis of fragment length by capillary gel electrophoresis after denaturation of the diluted amplification product with Hi-Di Formamide. A GeneScan 600 LIZ dye Size Standard v2.0 was added for calibration. Analysis was performed on the 3500xL Genetic AnalyZer (Fragment Analysis 50_POPxl_1). Interpretation of results was done with the GeneMapper software.

The AmpF ℓ STR Identifiler Plus PCR Amplification Kit is a commercial multiplex kit for simultaneous amplification and analysis of 16 polymorphic microsatellites. Within this work, it was used for verification of relationships in the evaluation of *de novo* mutations; it was used according to the manufacturer's instructions.

2.3.19 EVALUATION OF SEQUENCE VARIANTS AND NOMENCLATURE

In order to evaluate the possible pathogenicity of observed sequence variants we used databases and various online prediction tools. For **splice site prediction** the following bioinformatics tools were utilised:

- BDGP (Berkeley Drosophila Genome Project), [Reese et al., 1997]
version 0.9, last updated 28 July 2014
Human or other, minimum scores for splice sites: 0.1
- NetGene2 [Brunak et al., 1991]
version 2.42, Human

Missense mutations were rated using the following tools:

- PolyPhen-2 (Polymorphism Phenotyping v2), [Adzhubei et al., 2010]
version 2.2.2
- SIFT Human Protein (Sorting Intolerant From Tolerant), [Kumar et al., 2009]
via PROVEAN (Protein Variation Effect Analyzer v1.1.3)
- MutPred (Mutation Prediction), [Li et al., 2009]
last modified 02 Feb 2014
- GERP (Genomic Evolutionary Rate Profiling), [Cooper et al., 2005]
hg19

Variants of interest were checked regarding their appearance/frequency in ExAC Browser version 0.3 beta (Exome Aggregation Consortium) [Lek et al., 2016], dbSNP build 142 (Single Nucleotide Polymorphism database) [Sherry et al., 2001], and TGP (1000 Genomes Project) [Abecasis et al., 2012]. The ExAC Genome Browser aggregates genotype data of 60,706 unrelated individuals, independent of the phenotypes. Therefore pathogenic mutations for rare recessive disorders such as JBS may occur in this database at a low frequency for a heterozygous allele, but even a single homozygous annotation would not completely exclude a variant as disease-causing mutation. The dbSNP database also comprises polymorphisms and pathogenic variants, but the effects of the variants are displayed, if known. Protein conservation across species was checked by Standard Protein BLAST (Basic Local Alignment Search Tool, Database: Reference proteins (refseq_protein), Algorithm: blastp (protein-protein BLAST)) [Altschul et al.,

1990] and/or ClustalW2 version 2.0.12 [Larkin et al., 2007]. Segregation of the variants across family members was checked if appropriate material was available. Designation of mutations follows the guidelines of the Human Genome Variation Society (last modified March 2014) [den Dunnen and Antonarakis, 2000] and was verified by Mutalyzer Version 2.0 beta-24 [Wildeman et al., 2008]. Designation of protein coding genes was verified by using the HGNC homepage (HUGO (Human Genome Organisation) Gene Nomenclature Committee) [Gray et al., 2016]. Links to all utilised tools are tabulated in Table A.9 (see Appendix A) and the predicted results are listed in Appendix C.

2.3.20 LEIDEN OPEN VARIATION DATABASE (LOVD)

An online database was set up for all mutations in the *UBR1* gene (<http://databases.lovd.nl/shared/variants/UBR1>), as well as all available phenotype data of patients that were clinically and molecularly ascertained to have JBS (<http://databases.lovd.nl/shared/individuals/UBR1>) [Sukalo et al., 2014a]. The database was created on the Leiden Open Variation Database system, LOVD 3.0 build 08 [Fokkema et al., 2005; Fokkema et al., 2011]. The columns for JBS phenotype data were customised with the help of Ivo Fokkema.

Another database was established for mutations and unclassified variants detected in *DOCK6* (<http://databases.lovd.nl/shared/variants/DOCK6>) and the corresponding phenotype datasets (<http://databases.lovd.nl/shared/individuals/DOCK6>) [Sukalo et al., 2015].

3 RESULTS

3.1 *UBR1* AND JOHANSON-BLIZZARD SYNDROME

A total of 71 index patients from unrelated families participated in this part of the study (see chapter 2.1). In the following, 24 newly ascertained families (by applying Sanger sequencing and MLPA analysis) with phenotypes classified as typical or suggestive JBS are referred to as families JBS-36 to JBS-59. Thirty-five previously published families with JBS and *UBR1* mutations (ascertained in the Zenker lab) are referred to as JBS-1 to JBS-35 and their data are included in the analysis of the *UBR1* mutation spectrum and genotype phenotype correlations.

3.1.1 SANGER SEQUENCING OF THE *UBR1* GENE

Within this thesis, Sanger sequencing of the entire coding region and adjacent intronic sections of the *UBR1* gene was carried out in a total of 71 samples from index patients with a phenotype typical or suggestive of JBS (n=24), nosologically undefined phenotypes only partially overlapping with JBS (n=33), and isolated EPI (n=14). In 22 families, all with a phenotype classified as typical or suggestive JBS, likely causative *UBR1* mutations could be confirmed by applying a conventional Sanger sequencing approach. No mutations of the *UBR1* gene were detected in patients with atypical phenotypes or isolated EPI.

The *UBR1* mutations detected by conventional sequencing within the 22 families comprised 20 novel ones. Further experimental analyses performed for mutation detection or more in-depth examination are described below (MLPA, Western Blot, cDNA analysis). Mutation and phenotype data from *UBR1*-positive JBS families identified in the Zenker lab prior to (JBS-1 to JBS-35) and during (JBS-36 to JBS-49) my work were published as a Mutation Review comprising 61 affected individuals from 50 families [Sukalo et al., 2014a]. All patients included in this publication plus new 10 patients (JBS-50 to JBS-59) with JBS identified since then will be evaluated in the following chapters.

Sequence changes that were detected by conventional Sanger sequencing of all coding exons and flanking intronic regions (+/- 20 bp) and classified as disease-causing mutations are listed in Table 3.1. Sequence changes were generally classified as

causative mutations, if they (I) produce a premature stop codon, (II) affect the highly conserved nucleotides -1, -2, +1, +2, near splice site junctions or if they (III) delete/substitute a conserved amino acid and were observed in combination with the presence of a mutation on the second allele (see also Table 3.6). As an exception to this rule we classified nine intronic changes as pathogenic mutations that do not affect the invariant positions of the splice sites (for further evaluation of splicing effects see chapter 3.1.2). Pathogenicity of all variants was checked with MutationTaster. Missense Mutations were additionally rated using PolyPhen-2, SIFT, GERP, and MutPred; protein alignment was created using Clustal W2 and BLOSUM62-Matrix (Appendix C.1). For *in silico* prediction of hypothesized splice site mutations, NetGene2 and BDGP were used (Appendix C.2).

Table 3.1: *UBR1* mutations identified in patients with JBS.

Location	Nucleotide alteration	Predicted effect ^a	Family (JBS-)	Initial publication
Intron 01	c.81+1G>A	r.spl.? p.?	58	[Corona-Rivera et al., 2016]
Intron 01	c.81+2dupT	r.spl.? p.?	34	[Sukalo et al., 2014a]
Intron 01	c.81+5G>C	r.spl.? p.?	23	[Alkhoury et al., 2008]
Exon 03	c.364G>C	p.V122L	18	[Hwang et al., 2011]
Exon 03	c.380G>T	p.C127F	40	[Sukalo et al., 2014a]
Exon 03	c.407A>G	p.H136R	6	[Zenker et al., 2005]
Exon 04	c.477delT	p.G160Afs*5 ^b	10	[Zenker et al., 2005]
Exon 04	c.497A>G	p.H166R	31, 53	[Sukalo et al., 2014a]
Intron 04	c.529-13G>A	<i>p.N177Lfs*10</i>	20, 47	[Godbole et al., 2013]
Exon 05	c.650T>G	p.L217R	39	[Sukalo et al., 2014a]
Intron 05	c.660-2_660-1delAG	r.spl.? p.?	8, 41	[Zenker et al., 2005]
Exon 06	c.753_754delTG	p.C251*	11	[Zenker et al., 2005]
Exon 07	c.857T>G	p.I286R	17	[Sukalo et al., 2014a]
Exon 08	c.950T>C	p.L317P	33	[Liu et al., 2011]
Intron 09	c.1094-13A>G	<i>p.G365Efs*2^c</i>	14	[Sukalo et al., 2014a]
Intron 09	c.1094-12A>G	r.spl.? p.?	13	[Zenker et al., 2005]
Exon 10	c.1166_1177del12	p.A389_F392del	36	[Sukalo et al., 2014a]
Exon 11	c.1258C>A	p.Q420K	51	-
Exon 11	c.1280T>G	p.L427R	54	[Atik et al., 2015]
Exon 13	c.1507C>T	p.R503*	15, 32	[Hwang et al., 2011]
Exon 13	c.1537C>T	p.Q513*	1, 2, 43	[Zenker et al., 2005]
Exon 14	c.1648C>T	p.Q550*	3	[Zenker et al., 2005]
Exon 15	c.1688C>A	p.A563D	22, 24	[Sukalo et al., 2014a]
Exon 15	c.1759C>T	p.Q587*	4	[Zenker et al., 2005]
Exon 16	c.1886C>G	p.S629*	28	[Sukalo et al., 2014a]
Intron 16	c.1911+14C>G	<i>p.E638Vfs*29</i>	9	[Sukalo et al., 2014a]
Exon 17	c.1979_1981delTTG	p.V660del	23	[Alkhoury et al., 2008]
Exon 17	c.1993C>T	p.R665*	17	[Sukalo et al., 2014a]
Exon 18	c.2034C>A	p.Y678*	31	[Sukalo et al., 2014a]
Exon 19	c.2098T>C	p.S700P	38	[Almashraki et al., 2011]
Intron 20	c.2254+2T>C	r.spl.? p.?	6	[Zenker et al., 2005]
Exon 21	c.2260C>T	p.R754C	36	[Sukalo et al., 2014a]
Exon 21	c.2261G>A	p.R754H	45	[Sukalo et al., 2014a]

Location	Nucleotide alteration	Predicted effect ^a	Family (JBS-)	Initial publication
Exon 21	c.2294_2296delAAG	p.E766del	21	[Sukalo et al., 2014a]
Exon 21	c.2311_2312delGA	p.E771Nfs*8	57	-
Exon 21	c.2319dupT	p.H774Sfs*6	18	[Hwang et al., 2011]
Intron 21	c.2379+1G>C	r.spl.? p.?	5	[Zenker et al., 2005]
Intron 21	c.2380-1G>A	r.spl.? p.?	44	[Sukalo et al., 2014a]
Intron 22	c.2432+5G>C	r.spl.? p.?	54	[Atik et al., 2015]
Exon 24	c.2546_2547insA	p.M849Ifs*13 ^d	9	[Zenker et al., 2005]
Exon 25	c.2598delA	p.P867Hfs*12 ^e	12	[Zenker et al., 2005]
Exon 25	c.2608G>T	p.E870*	41	[Sukalo et al., 2014a]
Intron 26	c.2839+5G>A	<i>p.R914Dfs*7^f</i>	19, 25, 55	[Elting et al., 2008]
Exon 29	c.3055C>T	p.R1019*	56, 58, 59	[Corona-Rivera et al., 2016]
Exon 30	c.3304C>G	p.Q1102E	15	[Hwang et al., 2011]
Exon 30	c.3328G>T	p.E1110*	49	[Sukalo et al., 2014a]
Exon 33	c.3682C>T	p.Q1228*	30	[Sukalo et al., 2014a]
Exon 33	c.3694delC	p.L1232Wfs*17	27	[Sukalo et al., 2014a]
Exon 33	c.3724A>G	p.R1242G	21	[Sukalo et al., 2014a]
Exon 33	c.3745dupA	p.R1249Kfs*4	48	[Sukalo et al., 2014a]
Exon 34	c.3835G>A	p.G1279S	8	[Zenker et al., 2005]
Intron 35	c.3998-1G>C	<i>p.E1333_G1337del</i>	16	[Sukalo et al., 2014a]
Exon 37	c.4093C>T	p.Q1365*	39	[Sukalo et al., 2014a]
Exon 38	c.4188C>A	p.C1396*	35	[Fallahi et al., 2011]
Exon 38	c.4193delT	p.L1398Rfs*3	42	[Sukalo et al., 2014a]
Exon 39	c.4277C>T	p.P1426L	33	[Liu et al., 2011]
Exon 39	c.4280C>T	p.S1427F	27	[Sukalo et al., 2014a]
Exon 39	c.4291T>C	p.S1431P	29	[Sukalo et al., 2014a]
Exon 41	c.4524T>A	p.Y1508*	26	[Sukalo et al., 2014a]
Exon 45	c.4927G>T	p.E1643*	7	[Zenker et al., 2005]
Exon 45	c.4942delG	p.E1648Kfs*21	16	[Sukalo et al., 2014a]
Exon 45	c.4981G>A	p.G1661R	46	[Singh et al., 2014]
Exon 46	c.5080G>T	p.E1694*	34	[Sukalo et al., 2014a]
Intron 46	c.5109-3A>G	<i>p.R1704Gfs*26</i>	28	[Sukalo et al., 2014a]
Exon 47	c.5135_5144del10	p.R1712Lfs*14	37	[Sukalo et al., 2014a]

^aItalic letters indicate that the effect of splicing mutations was demonstrated on mRNA level. ^{b-d}Denominations of these previously published mutations were corrected according to current guidelines [den Dunnen and Antonarakis, 2000] (Human Genome Variation Society homepage last modified March 2014): ^bpreviously published as T159fsX164; ^cpreviously published as p.V365Efs*2; ^dpreviously published as M849fsX861; ^epreviously published as P866fsX878; ^fpreviously published as p.R947Dfs*7. Mutation nomenclature refers to GenBank reference sequence NM_174916.2. Nucleotide numbering reflects cDNA numbering with +1 corresponding to the A of the ATG translation initiation codon in the reference sequence, according to journal guidelines (www.hgvs.org/mutnomen). The initiation codon is codon 1.

The mutations listed in Table 3.1 were detected in patients with an unambiguous JBS phenotype as either homozygous or compound-heterozygous sequence changes with two exceptions where only one disease-causing allele could be identified (families JBS-24 and JBS-26). A total of 65 different mutations were detected by Sanger sequencing in 60 independent JBS families (Table 3.1). In the 120 disease-associated alleles, 35 harboured nonsense mutations (29.2%), 30 missense mutations (25.0%), 28 splice site mutations (23.3%), 16 frameshift mutations (13.3%), and three small in-frame deletions (2.5%). On eight alleles (6.7%) of this joint cohort no mutation could be

detected by applying Sanger sequencing. This was regarding five families, two with heterozygous *UBR1* mutations only detected by Sanger sequencing (JBS-24, JBS-26) and three where no mutation could be detected at all (JBS-50, JBS-52, JBS-60). These samples were subsequently analysed by MLPA analysis and, if appropriate material was available, RNA and/or the *UBR1* protein were analysed (see below).

All sequence changes listed in Table 3.1 were not found in over 200 control alleles from a multi-ethnic cohort sequenced for *UBR1* in our lab, who did not have a clinical diagnosis of JBS. In 36 families from which multiple affected individuals or unaffected siblings were available for testing, segregation of the mutations with the phenotype could be confirmed.

Table 3.1 contains eight recurrent mutations that were observed in more than one family. For some of them, the origin of the affected families suggested a common ethnic background, but other families with the same mutation did not obviously share a common background making it possible that the same changes had emerged independently. The mutation p.Gln513* was detected in four patients from three families of Costa Rican origin (JBS-1, JBS-2, JBS-43), suggesting a common ancestry / founder mutation in this population [Corona-Rivera et al., 2016; Sukalo et al., 2014a]. The missense mutation p.Ala563Asp was detected in a patient from England (family JBS-24) and in family JBS-22 (case report by [Reichart et al., 1979]) from Germany. The German family originated from Lower Saxony, giving hint to a possible common ancestor. The splice site mutation c.2839+5G>A was initially described in two families (JBS-19, JBS-25) from Turkey and Iran [Elting et al., 2008]. The authors speculate that this might be a founder mutation in that region. Since then, the mutation was again detected in homozygous state in a family of Turkish origin (JBS-55). The missense mutation p.His166Arg was detected in compound-heterozygosity with a nonsense mutation in patient from family JBS-31, and homozygous in a patient from family JBS-53. The patients' families had a Brazilian/Ukrainian and a Turkish background, respectively. Another mutation (c.529-13G>A) was detected in families from Guatemala (JBS-20) and India (JBS-47). Both index girls were homozygous carriers of this splice site mutation. A further mutation affecting the acceptor splice site, namely c.660-2_660-1delAG, was also detected in two independent families with no obvious common background. The patient from family JBS-8 from Germany was compound-heterozygous for the mentioned splice site mutation and a missense mutation; a patient of Mexican origin (family JBS-41) had a

nonsense mutation on the second allele. The truncating mutation p.Arg503* was detected in compound-heterozygosity with a missense mutation in a Portuguese patient (family JBS-15) and homozygous in three siblings from an Arab family (JBS-32). For each of these mutations there is no clear evidence for a common ethnic background of the carriers. Therefore, independent development of the same mutation in different traits cannot be excluded. The last recurrent mutation (p.Arg1019*) was detected in three unrelated families. Two patients from Turkey were homozygous carriers of this mutation (families JBS-56 and JBS-59) and a Mexican patient (family JBS-58) was compound-heterozygous for the mentioned mutation together with a splice site mutation on the other allele. The families from Turkey might have a common ancestor, whereas the mutation in the Mexican patient supposedly has developed independently.

The mutations detected in this study and before (<http://databases.lovd.nl/shared/variants/UBR1>, see also Figure 3.1) plus the clinical data of the molecularly verified JBS cases (<http://databases.lovd.nl/shared/individuals/UBR1>) were entered to LOVD.

Effect	Exon	DNA change (cDNA)	Published as	RNA change	Protein
+?/+?	01i	c.81+2dup	-	r.spl?	p.?
+?/+?	01i	c.81+5G>C	IVS1+5G>C	r.spl?	p.?
+?/+?	03	c.364G>C	-	r.(?)	p.(Val122Leu)
+?/+?	03	c.380G>T	-	r.(?)	p.(Cys127Phe)
+?/+?	03	c.407A>G	-	r.(?)	p.(His136Arg)
+?/+?	04	c.477delT	-	r.(?)	p.(Gly160Alafs*5)
+?/+?	04	c.497A>G	-	r.(?)	p.(His166Arg)

Figure 3.1: LOVD entries for *UBR1* mutations.

3.1.2 SPLICE SITE MUTATIONS OF THE *UBR1* GENE

Altered RNA splicing can usually be assumed for mutations affecting the highly conserved intronic nucleotides -1, -2, +1, +2, near the exon junction sites. This only applies to six of the 15 splice site mutations that were detected in the *UBR1* gene. Consequently, nine intronic changes that do not affect the invariant positions of the splice site were classified as pathogenic mutations. Eight of these variants were predicted *in silico* to abrogate the authentic splice site or create an ectopic splice site that reaches higher scores than the authentic site (BDGP and NetGene2, see Table C.2.1).

The effect of five of these mutations on RNA splicing could be confirmed by studies on the patients' mRNA in all cases, including that one without pathogenic prediction by BDGP (Figure 3.2). Additionally, a splice site mutation affecting the highly conserved nucleotide at position -1 in intron 35 (c.3998-1G>C) was analysed on RNA level and a deletion of five amino acid residues without frameshift was demonstrated. The predicted effects of splice site mutations are displayed in Table 3.1 in italic letters. Table 3.2 summarises nomenclature for the splice site mutations that could be investigated on RNA level.

Table 3.2: *UBR1* splice site mutations that were investigated in cDNA.

DNA	RNA	Protein (predicted)	Family
c.529-13G>A	r.528_529insCTTTTTTATAG	p.N177Lfs*10	JBS-20 JBS-47
c.1094-13A>G	r.1093_1094insAATAATCTATAG	p.G365Efs*2	JBS-14
c.1911+14C>G	r.1912_1913insTAAGTGATTCTAG	p.E638Vfs*29	JBS-09
c.2839+5G>A	r.2740_2839del	p.A914Dfs*7	JBS-19 JBS-25
c.3998-1G>C	r.3999_4013del	p.E1333_G1337del	JBS-16
c.5109-3A>G	r.5108_5109insAG	p.R1704Gfs*26	JBS-28

An overview of all detected splice site mutations, RNA analysis results, and *in silico* prediction of their pathogenicity (BDGP and NetGene2) is listed in Appendix C, Table C.2.1. Furthermore, Figure 3.2 shows electropherograms of splice site mutations generated from cDNA samples to illustrate the effects of those mutations on mRNA level; utilised primers are listed in Table B.2.1.

Continued legend to Figure 3.2: Electropherograms of *UBR1* splice site mutations.

(A) Wild type shows correct junction of exon 4 (blue box) and 5 (green box). In the cDNA the patient from family JBS-20, an intronic part of 11 nucleotides (pink box) remained in-between those exons causing a frameshift and premature stop codon (p.Asn177Leufs*10). (B) Regular junction of exons 9 (blue box) and 10 (green box) compared to cDNA sequence of the patient from family JBS-14. Twelve nucleotides of intron 9 (pink box) remain in the sequence due to incorrect splicing and cause a premature stop codon resulting in a truncated protein. (C) Frameshift mutation p.Glu638Valfs*29 was demonstrated in cDNA derived from RNA of the patient from family JBS-9. The splice site mutation causes an intronic part of 13 nucleotides (pink box, intron 16) to remain in-between exon 16 (blue box) and 17 (green box) which leads to frameshift and premature stop codon. (D) A premature stop codon is also caused by the c.2839+5G>A splice site mutation in family JBS-19. The blue box indicates exon 25, the green box exon 26, which is completely missing in the mutated cDNA, and the yellow box represents exon 27. Although the mutation is homozygous, residual wild type allele due to functioning of the original splice site can be seen. Elting et al. [2008] speculate that the nearly even level of peaks is caused by rapid degradation of the mutated mRNA. Both families (JBS-19 and JBS-25) with this mutation show a relatively mild JBS phenotype. (E) The wild type sequence shows correct junction of exon 35 (blue box) and exon 36 (green box). Red letters indicate the five amino acid residues that are missing at the beginning of exon 36 in the mutated sequence derived from the patient from family JBS-16. (F) The splice site mutation in the patient from family JBS-28 causes two intronic nucleotides of intron 46 (pink box) to remain in-between exon 46 (blue box) and exon 47 (green box) and subsequently causes the frameshift mutation p.Arg1704Glyfs*26. #allele specific RT-PCR; wt, wild type; mut, mutated.

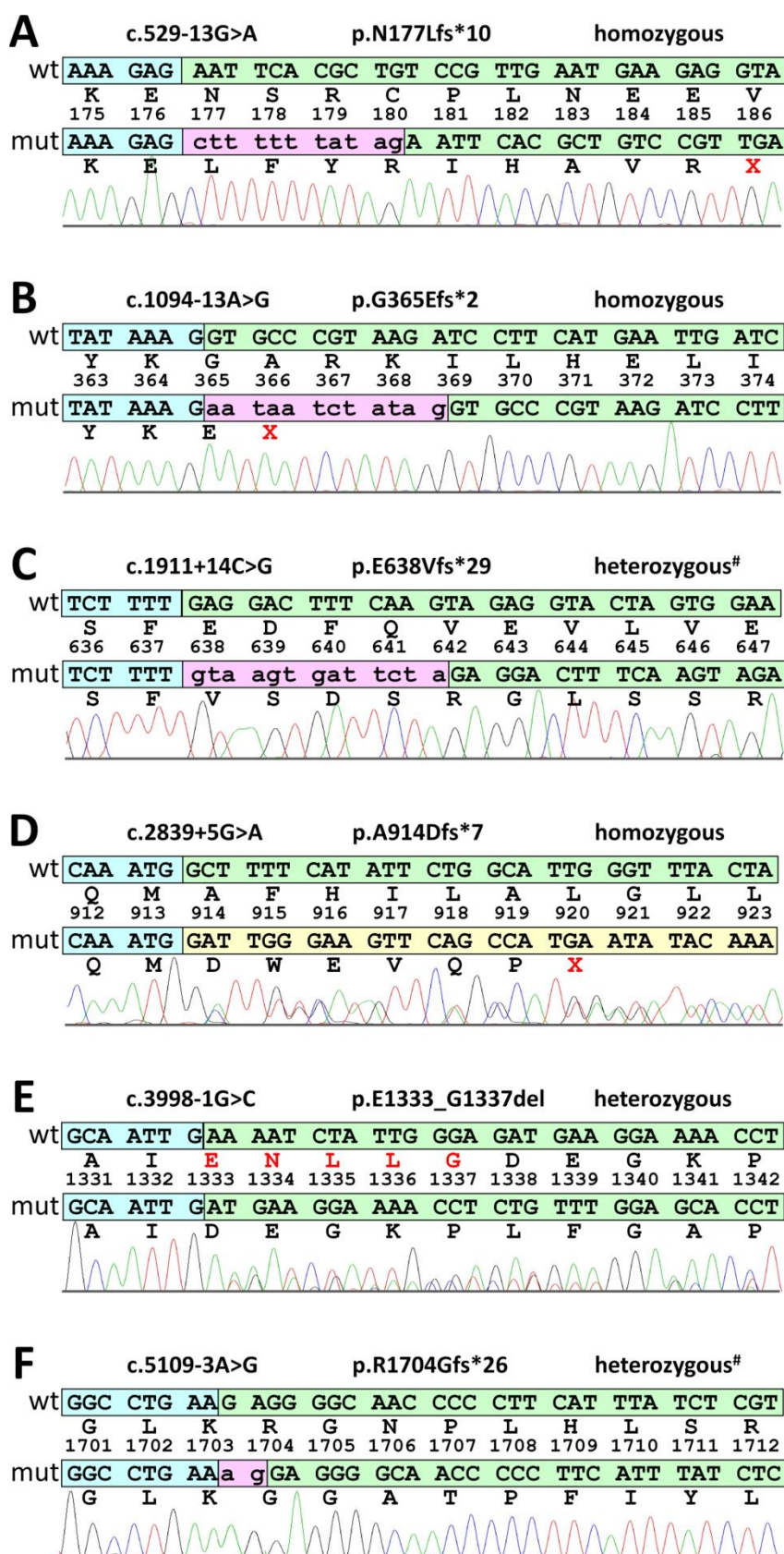


Figure 3.2: Electropherograms of *UBR1* splice site mutations.

Patients' cDNA was gained from RT-PCR that was performed with RNA extracted from lymphoblastoid cells. Capital letters indicate exonic regions, intronic regions are written in lower case letters. Wild type cDNA sequence (wt) and amino acid residues are compared to the mutated cDNA sequences (mut) and subsequent amino acid residues. *Legend continued on previous page.*

3.1.3 MISSENSE MUTATIONS OF THE *UBR1* GENE

While in the initial publication most JBS-associated alleles were carrying nonsense, frameshift and splice site mutations, a total of 20 different missense mutations were detected in our extended JBS cohort. All variations predicting missense changes were carefully and systematically evaluated in order to collect arguments supporting or challenging their pathogenic significance. Pathogenicity of missense variants was evaluated with the help of various online *in silico* prediction tools (MutationTaster, PolyPhen-2, SIFT, GERP, and MutPred). The evolutionary conservation of the affected amino acid residues and *in silico* prediction scores are shown in Appendix C.1.1.

All missense alleles were observed in a single family only, except for the mutations p.His166Arg (JBS-31 and JBS-53) and p.Ala563Asp (JBS-22 and JBS-24). In nine cases the missense change was in compound heterozygosity with a *bona fide* mutation on the second allele (JBS-6, -8, -15, -17, -18, -27, -31, -39, -54), in eight families (JBS-22, -29, -38, -40, -45, -46, -51, -53) the missense mutation was homozygous in the patients, and one patient (family JBS-33) had two different missense mutations. In family JBS-24, only a heterozygous missense mutation was detected, but the same mutation was found homozygous in another family (JBS-22).

All 20 missense mutations were checked regarding their occurrence and frequency in the online databases ExAC Genome Browser and dbSNP. Seventeen of the 20 missense changes rated as pathogenic mutations detected in the *UBR1* gene were not listed in either of the databases and none of those missense mutations was detected in a homozygous state, according to ExAC. Of the three missense variants that were existent in dbSNP, none was classified as benign. Two of those variants were additionally included in the ExAC database, both with an allele frequency below 0.002%.

Unfortunately, there is no general test available to analyse functional defects of mutant *UBR1* proteins. Only three missense mutations could be further investigated functionally in a yeast model (see chapter 3.1.8)

3.1.4 LARGER GENOMIC DELETIONS AND DUPLICATIONS OF THE *UBR1* GENE

In three patients with a clinically obvious JBS phenotype, we were not able to detect mutations of the *UBR1* gene by Sanger sequencing (families JBS-50, JBS-52, JBS-60), and in another two families, we were only able to detect one heterozygous mutation (JBS-24

and JBS-26). Those patients were additionally analysed by self-designed MLPA of the *UBR1* gene to detect deletions or duplications of one or more exons. All larger deletions/duplications of the *UBR1* gene that were detected through MLPA analysis are listed in Table 3.3.

Table 3.3: Larger deletions and duplications in the *UBR1* gene.

Location	Nucleotide alteration	Predicted effect	Family
Exon 12	c.1282-?_1439+?del	p.A428Vfs*20	JBS-50
Exon 26-29	c.2740-?_3209+?del	p.A914Hfs*6	JBS-52
Exon 30	c.3210-?_3415+?dup	p.E1139Afs*27	JBS-52
Exon 45-47	c.4836-?_5250+?del	p.?	JBS-26

Figure 3.3 shows the result of MLPA analysis in the probanda from family JBS-26, demonstrating a heterozygous deletion of exons 45-47. By Sanger sequencing, a p.Tyr1508* nonsense mutation had been detected heterozygous in this patient and her mother. The heterozygous deletion of exons 45-47 was not detected in the maternal sample. A paternal DNA sample was not available to confirm the presumed inheritance of the deletion from the father.

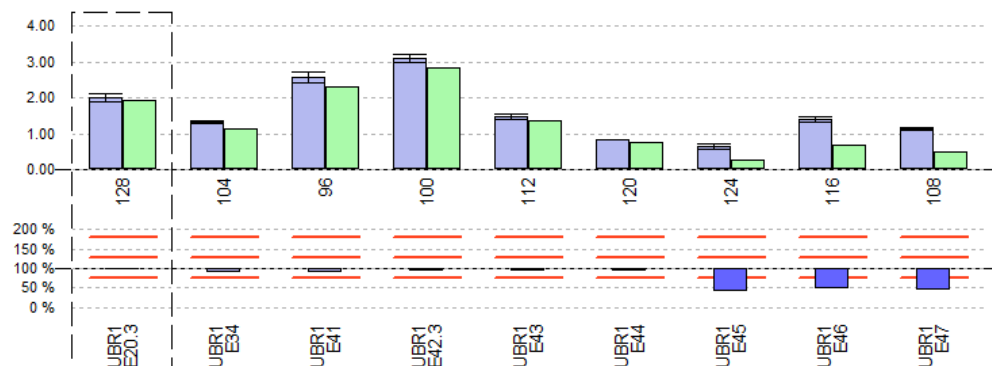


Figure 3.3: MLPA results of probemix UBR1-E.

Probemix UBR1-E contains probes for exons 20 (128 nt), 34 (104 nt), 41 (96 nt), 42 (100 nt), 43 (112 nt), 44 (120 nt), 45 (124 nt), 46 (116 nt), and 47 (108 nt). Purple bars represent the mean probe signal for three control DNAs, green bars represent the probe signal of the patient (family JBS-26). The blue bars indicate a heterozygous loss of exons 45-47 in the patient; the signal of the patient is about 50% lower compared to the control probe signal. The patient was previously detected to harbour a p.Tyr1508* nonsense mutation on the maternal allele.

The index patient from family **JBS-50** was included in this study with an unambiguous clinical diagnosis of JBS. Sequencing revealed no mutations but amplification of exon 12 was extremely difficult and a weak amplification could only be achieved in one of several attempts (retrospectively, this could be a DNA contamination). A specific MLPA probemix containing exons 10, 11, 12, and 13 (UBR1-F)

was designed for analysis of this patient, indicating a homozygous deletion of exon 12 (Figure 3.4A and B). To demonstrate the deletion of exon 12 with an independent method, multiplex PCR was performed (Figure 3.4C), where the patient consistently showed no band at the expected size for exon 12 (547 bp). Long-range PCR with the forward primer for exon 11 and reverse primer for exon 13 (expected product size 8,366 bp), with the forward primer for exon 12 and reverse for exon 13 (expected product size 6,910 bp), and regular PCR with the forward primer for exon 11 and reverse for exon 12 (expected product size 2,003 bp) did not result in a PCR product for JBS-50.1 (data not shown). Unfortunately, verification of the heterozygous exon 12 deletion by MLPA on parental samples was not possible.

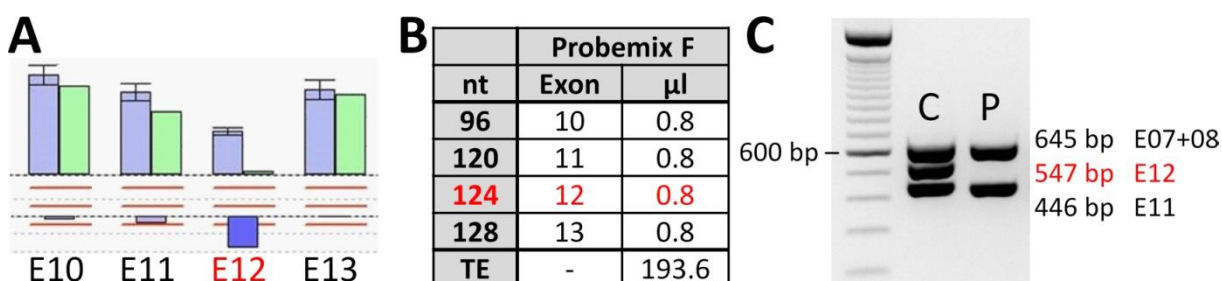


Figure 3.4: Analysis of the index patient from family JBS-50.

(A) MLPA result Probemix UBR1-F containing probes for exons 10-13. Patient shows homozygous deletion of exon 12. (B) Composition of probemix UBR1-F. (C) Multiplex PCR: no band at 547 bp for the patient, equalling no adequate binding sites for the utilised primers for exon 12; control shows expected PCR products. E, exon(s); TE, Tris/EDTA buffer; C, control; P, patient.

In a patient from family **JBS-52** Sanger sequencing also did not detect any mutation. By MLPA analysis, a heterozygous deletion of exons 26-29 of paternal origin was found, while the probe for exon 30 indicated an increased dosage in the patient and in the mother (Figure 3.5A). A PCR approach using a primer combination spanning exons 26-29 with cDNA as a template (forward primer located in exon 25 and reverse primer located at the exon-exon boundary between exon 30 and 31, see Table B.2.2 in Appendix B) showed a shorter fragment resulting from the exon 26-29 deletion in the patient and the father as well as an elongated fragment at ~1.000 bp in the patient and his mother (Figure 3.5B). Gel extraction of this band and subsequent Sanger sequencing failed in several attempts for unexplained reason. Next, an allele specific PCR where only the maternally inherited allele is amplified was performed (Figure 3.5C). This was accomplished by placing the forward primer directly into the region that is deleted on the paternal allele (Figure 3.5D). Sequencing of this fragment finally confirmed the

duplication of exon 30 in the patient and his mother. Figure 3.5E displays the constellation of alleles in family JBS-52.

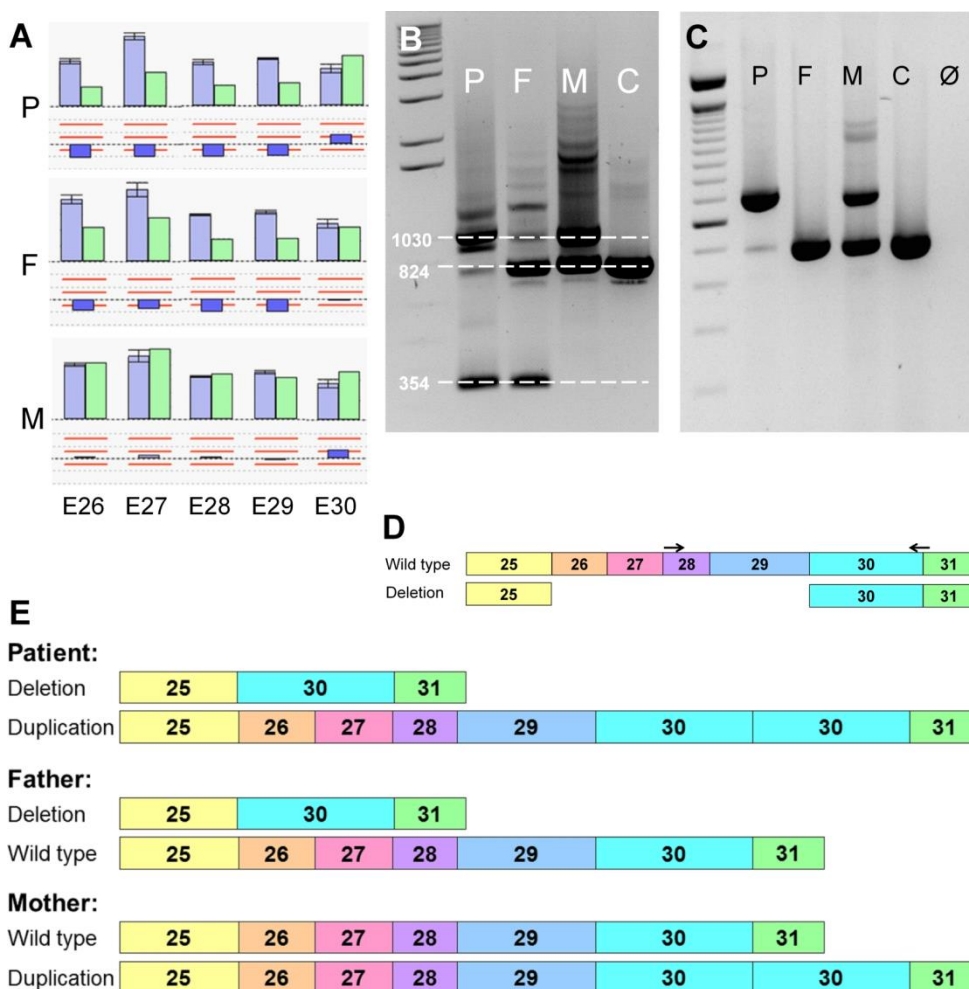


Figure 3.5: Analysis of family JBS-52.

(A) MLPA results for family JBS-52. The image combines results of interest from probemixes UBR1-B, -C, and -D. A customised probemix for this family could not be generated because the probes for the exons of interest have overlapping sizes. (B) PCR on cDNA with a primer combination (UBR1_e26_RTf and UBR1_RT_30R, see Table B.2.2) spanning exons 26-29. The small fragment at 354 bp represents the allele lacking four exons in the patient and his father. Wild type allele is seen in the father, mother and control at 824 bp. An additional band at 1030 bp representing the exon 30 duplication was visible in the samples derived from the patient and his mother. (C) Allele-specific PCR to generate a PCR product of the patient only containing the expanded allele. Forward primer UBR1_C28F and reverse primer UBR1_RT_30R were used. This product was then subjected to Sanger sequencing. (D) Position of primers in allele specific PCR indicated by arrows. (E) Visualisation of exon arrangement in family JBS-52. E, exon; P, patient; F, father; M, mother; C, control; Ø, blank.

In a patient who was previously detected to carry the missense mutation p.Ala563Asp on one allele of the *UBR1* gene (family JBS-24), no further mutation could be detected by MLPA analysis. This patient is described in detail in chapter 3.1.7. The index patient from family JBS-60, in whose DNA no mutation was detected at all, is also commented on below in the same chapter.

3.1.5 SNPs AND UNCLASSIFIED VARIANTS OF THE *UBR1* GENE

Besides the above mentioned mutations, further variants were detected in individuals with JBS and other phenotypes. Some of these could be classified as polymorphisms and other remained unclassified. All variants detected in the *UBR1* gene were checked regarding their frequency and homozygosity in ExAC (Table 3.4), and with various missense (Appendix C.1) and splice site (Appendix C.2) mutation prediction tools.

Unclassified variants with an allele frequency of 1% or higher at ExAC database were considered as benign, given a low overall frequency of JBS. Silent mutations were checked for any possible influence on splice sites (Table C.2.2) and found to have no significant impact on correct splicing. This is also true for the intronic variants listed below. After applying the mentioned exclusion criteria, five unclassified missense variants are remaining (highlighted in yellow in Table 3.4). The serine to glycine substitution p.Ser405Gly was found heterozygous in one patient with isolated EPI and his unaffected father and sister. In all three of them, the p.Gly1264Glu variant was also detected heterozygous, thus indicating that the two sequence alterations are located on the same allele. The online prediction tools PolyPhen-2 and SIFT (see Table C.1.2) predict both variants to be benign and tolerated, respectively.

The p.Ile778Thr missense variant was detected heterozygous in a patient with an unclassified syndromic disorder comprising suspected pancreatic insufficiency (marginal decreased elastase I values in faeces), CHD and cognitive impairment. No further sequence changes were detected when screening the *UBR1* gene. In silico prediction rated this variant as probably damaging (PolyPhen-2) and damaging (SIFT). Although the phenotype did not fulfil the criteria for a definite clinical diagnosis of JBS, we cannot exclude any contribution of this variant to the phenotype.

The p.Thr1097Met missense variant is predicted to be probably damaging (PolyPhen-2) or damaging (SIFT). It was detected heterozygous in a patient in whom again no further mutations or unclassified variants of the *UBR1* gene were detected by Sanger sequencing. This patient was documented to have fat malabsorption, growth hormone deficiency, and extensive epiphyseal/metaphyseal dysplasia.

The arginine to glycine substitution p.Arg1612Gly was detected in three patients from our cohort. It was found heterozygous in a mother of a child with suspected JBS (of whom no DNA was available), in a patient with isolated EPI, and homozygous in a JBS

patient who additionally carries a homozygous frameshift mutation in the *UBR1* gene. Furthermore, this variant is rated as benign and tolerated, respectively, by the applied online prediction tools.

Table 3.4: SNPs and unclassified variants of the *UBR1* gene.

Location	Nucleotide alteration	Predicted effect	Frequency our cohort	Frequency ExAC	Homoz. ExAC	dbSNP
Exon 02	c.264G>A	p.E88E	0.34%	0.07909%	1	rs142558660
Exon 07	c.819G>A	p.A273A	0.33%	-	-	rs371383925
Intron 07	c.862-18C>T	-	83.01%	86.26%	45133	rs4924704
Intron 08	c.985+16G>A	-	0.65%	0.09754%	-	rs199817804
Exon 11	c.1213A>G	p.S405G	0.33%	0.3226%	3	rs77360687
Exon 21	c.2333T>C	p.I778T	0.33%	0.0008237%	-	-
Exon 25	c.2695A>G	p.I899V	2.92%	1.944%	32	rs35069201
Exon 30	c.3290C>T	p.T1097M	0.33%	0.06920%	1	rs142285781
Exon 34	c.3791G>A	p.G1264E	0.34%	0.3428%	1	rs139408969
Exon 35	c.3873G>A	p.K1291K	0.33%	0.1576%	-	rs149097306
Intron 36	c.4054-4C>G	-	0.34%	1.291%	23	rs138963231
Intron 38	c.4219-11T>G	-	0.66%	-	-	-
Exon 39	c.4242A>G	p.P1414P	0.33%	0.001693%	-	-
Exon 42	c.4642A>G	p.T1548A	9.43%	6.380%	328	rs3917223
Intron 42	c.4700+12A>G	-	83.65%	86.42%	45290	rs2054389
Exon 44	c.4834A>G	p.R1612G	1.32%	0.5484%	2	rs78948790
Exon 47	c.5205A>G	p.Q1735Q	4.87%	4.804%	217	rs16957277

Variants that are highlighted in yellow are commented on in detail in the text above. Homoz., homozygous appearance.

3.1.6 DISTRIBUTION OF MUTATIONS ALONG THE *UBR1* PROTEIN

Distribution of all detected mutations in *UBR1* is illustrated in Figure 3.6. Non-truncating mutations are represented by green (missense mutations) and yellow (small in-frame deletions) circles. Some clustering of those mutations can be seen at the UBR box (green), a highly conserved substrate-binding domain; the missense mutations p.Val122Leu, p.Cys127Phe, and p.His136Arg are located within this domain. In the other domains that are known today, no clustering of non-truncating mutations was seen. Notably, a 107 amino acid residues spanning part of the protein that is not denoted as a specific functional domain, so far, comprises five non-truncating mutations (p.Val660del, p.Ser700Pro, p.Arg754Cys, p.Arg754His, p.Glu766del). Also three further missense mutations p.Pro1426Leu, p.Ser1427Phe, and p.Ser1431Pro are located very close to each other and might indicate an unknown functionally relevant domain of the *UBR1* protein.

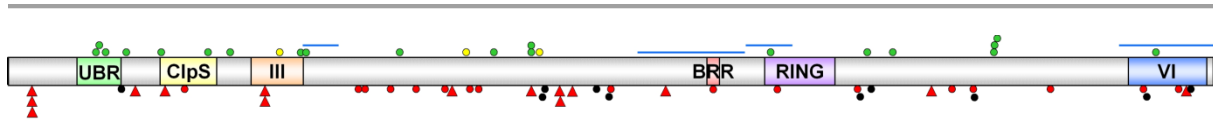


Figure 3.6: UBR1 protein with its conserved domains and distribution of mutations.

Functional domains and conserved regions of the UBR1 protein are highlighted according to Figure 1.2. Mutations are presented as circles, triangles, and bars. Green circles, missense mutations (20); yellow circles, small in-frame deletions (3); red circles, nonsense mutations (17); black circles, frameshift mutations (10); red triangles, splice site mutations (15); blue bars, whole exon deletions/duplications (4). A total of 69 mutations are shown in this figure. Several of the missense mutations are clustered at the UBR box and in a region between RING and region VI that has not been described as a functional domain so far. Figure adapted from [Sukalo et al., 2014a]. *For explanation of domains see chapter 1.2.1.*

3.1.7 JBS PATIENTS LACKING *UBR1* MUTATIONS

The study cohort subjected to *UBR1* analysis was clinically heterogeneous and included patients with a clear diagnosis of JBS, as well as patients with nosologically undefined phenotypes only partially overlapping with JBS and patients with isolated EPI. In the patients belonging to the latter two categories none could be clearly explained by disease-causing *UBR1*-mutations. In contrast, only in two cases with a convincing clinical JBS phenotype we were not able to detect biallelic mutations with the combined approach of Sanger sequencing and MLPA analysis. One patient had only one heterozygous mutation (family JBS-24), and in another patient we were not able to detect any mutation on the *UBR1* gene (family JBS-60).

The patient from family **JBS-24** was a woman aged 37 years with a mild manifestation of JBS. She had hypoplastic alae nasi, EPI treated with enzyme supplements, and oligodontia of permanent teeth. Additionally, prenatal growth deficiency and short stature were documented. She had progressive hearing loss and was supplied with hearing aids. At the age of 18 years, diabetes mellitus was diagnosed. Her IQ was not formally assessed, but according to her attending physician she had a mild-to-moderate cognitive impairment with delay of speech and motor skills in early childhood. At the age of 36 years, after two previous miscarriages, she gave birth to a healthy boy. Sanger sequencing detected a heterozygous missense mutation (p.Ala563Asp) in the patient's *UBR1* gene, but no mutation of the second allele was detected by applying MLPA analysis. Notably, by investigating the point mutation in her cDNA, significant underrepresentation of the second allele (wild-type for the mutation) was demonstrated (Figure 3.7). This suggests that a reduced expression or increased degradation of the *UBR1* allele that does not carry the known mutation, probably due to a mutation that could not be detected so far. These findings indicate an unidentified

genetic mechanism leading to defective *UBR1* expression from this allele. A mutation in the promoter or intronic regions as well as larger genomic deletions/duplications or rearrangements could be the explanation. Reduction of the UBR1 protein in this patient was proven by immunoblotting (Figure 3.8, lane 2). Taken together, these data suggest that the disease in this patient was indeed caused by UBR1 deficiency.

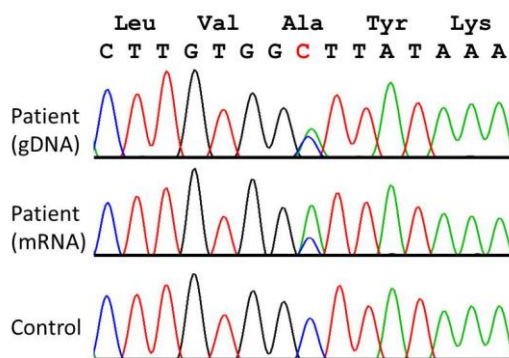


Figure 3.7: Electropherograms showing the mutation c.1688C>A (p.Ala563Asp).

Sequence traces obtained from the analysis of genomic DNA (gDNA) derived from lymphocytes of a patient from family JBS-24 are compared with mRNA derived from a LCL from this patient and a normal genomic control. Mutation c.1688C>A (p.Ala563Asp) was detected heterozygous in this patient; on the second allele no mutation could be detected. In the mRNA sample the wild type allele at position c.1688 is significantly underrepresented. Reproduced from [Sukalo et al., 2014a] with permission from John Wiley and Sons.

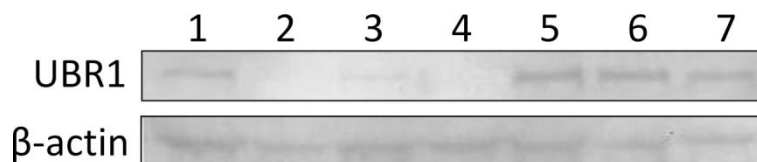


Figure 3.8: UBR1 immunoblotting (1).

Total proteins were extracted from LCLs, equal amounts verified by β -actin staining. SDS-PAGE was followed by immunoblotting with an antibody to human UBR1 (210 kDa) [Kwon et al., 2001]. β -actin (41 kDa) immunoblotting served as a loading control. (1) JBS-60, patient with JBS phenotype, no *UBR1* mutation detected. (2) JBS-24, [p.Ala563Asp] + [?]. (3) JBS-27, [p.Leu1232Trpfs*17] + [p.Ser1427Phe]. (4) JBS-28, [p.Ser629*] + [c.5109-3A>G]. (5) Family JBS-29, patient 1, [p.Ser1431Pro] + [p.Ser1431Pro]. (6) Family JBS-29, patient 2, [p.Ser1431Pro] + [p.Ser1431Pro]. (7) Control sample with normal amount of UBR1.

In family **JBS-60** a patient with a phenotype strongly similar to JBS was clinically described by Takahashi et al. [2004]. This 5.5-year-old Japanese boy born to consanguineous parents had all typical JBS symptoms: hypoplasia of alae nasi, low pancreatic enzymes (trypsin and elastase) indicating EPI, and total absence of permanent teeth. Hypoplasia of the pancreas and replacement with fatty tissue were detected in magnetic resonance imaging (MRI) analysis. Additional symptoms linked to JBS were a parietal scalp defect, hearing impairment, hypothyroidism, and cognitive impairment with speech delay. He had short stature in association with growth hormone deficiency; glucagon deficiency was also detected. Further features compatible with a diagnosis of JBS included an abnormal hair pattern with frontal upsweep and abnormal lacrimal canals. Tests for diabetes and cardiac involvement were negative. Sequencing of the patient's *UBR1* gene did not reveal any mutations, and MLPA analysis was also unremarkable. Also immunoblotting revealed normal *UBR1* level (Figure 3.8, lane 1). This is the only patient from the entire cohort who is clinically convincing but did not show any mutation in the *UBR1* gene or lack of the protein in all applied experiments. A SNP array and microsatellite analyses were also performed, but no homozygosity at the *UBR1* locus was detected. Thus, for this patient, we found no evidence for an underlying *UBR1* defect. The next step will be exome sequencing of this patient.

3.1.8 FUNCTIONAL ANALYSIS OF SELECTED *UBR1* MISSENSE MUTATIONS

In collaboration with the group of Alexander Varshavsky (Pasadena, United States of America) we studied the functional consequences of selected *UBR1* missense mutations and their correlation with phenotypic expression. Three missense mutations observed in patients with different degrees of clinical severity (Table 3.5) were studied in yeast counterparts.

Table 3.5: Phenotypic spectrum in JBS with different missense mutations.

Adapted from [Hwang et al., 2011].

			
Family	JBS-6	JBS-15	JBS-18
Facial phenotype	severe	moderate	mild
Oligodontia	+	+	+
Pancreatic insufficiency	+	+	+
Hearing impairment	+	+	-
Short stature	+	-	-
Scalp defect	+	+	+
Cognitive impairment	+	-	-
Hypothyroidism	+	-	+
Microcephaly	-	na	-
Congenital heart defect	-	-	-
Intrauterine growth restriction	-	-	-
Imperforate anus	+	-	-
Genital malformation	+	-	-
Renal anomalies	+	-	-
Diabetes	-	-	-
Genotype	[p.H136R] [c.2254+2T>C]	[p.R503*] [p.Q1102E]	[p.V122L] [p.H774Sfs*6]
Yeast counterpart	p.H160R	p.Q1224E	p.V146L

These three missense mutations (p.Val122Leu, p.His136Arg, p.Gln1102Glu) affect positions in the UBR box that are conserved among eukaryotes (Table C.1.1) and were therefore eligible for functional analysis in a yeast model. The *Saccharomyces cerevisiae* Ubr1 counterparts were p.Val146Leu, p.His160Arg, and p.Gln1224Glu, respectively. Low copy plasmids that expressed either the wild-type yeast Ubr1 or one of the three mutants from the native *PUBR1* promoter, were transformed into *ubr1Δ* cells that lacked Ubr1. These cells also carried plasmids that expressed a tyrosine-β-galactosidase (Tyr-βgal) N-end rule reporter [Varshavsky, 2005] which serves as an Ubr1 substrate

through its N-terminal tyrosine residue. Results of the protein degradation assay are displayed in Figure 3.9. The yeast experiments were carried out by Cheol-Sang Hwang in the California Institute of Technology (Pasadena, United States of America).

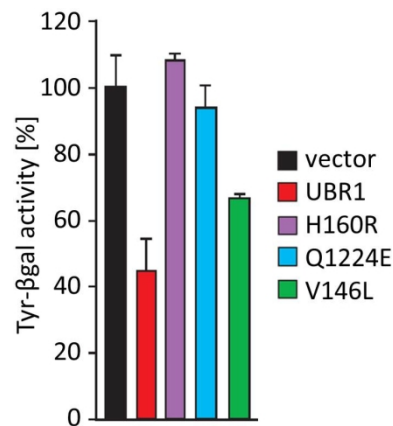


Figure 3.9: Protein degradation assay.

The β -galactosidase activity was measured in yeast expressing either wild type or mutant Ubr1 together with the Ubr1 substrate Tyr- β gal. β -galactosidase activity is thus inversely related to Ubr1 and N-end rule pathway function. Tyr- β gal degradation by wild type Ubr1 (red column) reduces its activity to less than half of the level in the Ubr1-deficient state (empty vector; black column). The yeast Ubr1 mutant p.His160Arg (purple column) appears to be inactive, while p.Gln1224Glu (blue) and p.Val146Leu (green) have marginal and intermediate capacities to degrade Tyr- β gal, respectively. Tyr- β gal, tyrosine- β -galactosidase. Adapted from [Hwang et al., 2011].

Additionally, UBR1 protein amounts were tested in LCLs from those three patients and compared to cell lines from healthy controls as well as JBS patients carrying mutations presumably leading to a complete lack of the UBR1 protein (Figure 3.10). In lane 3 a very faint band represents an almost complete loss of the gene product for the patient with a heterozygous missense mutation and severe phenotype (family JBS-6). Lane 4 represents the moderately reduced UBR1 amount for the patient with p.Gln1102Glu mutation and moderate phenotype (family JBS-15). Of the patient with mild manifestation of the syndrome (family JBS-18) no appropriate material was available.

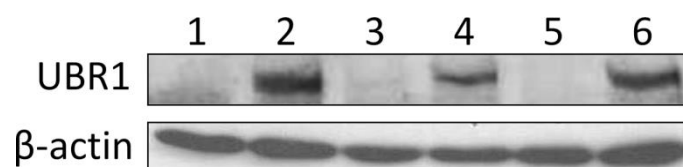


Figure 3.10: UBR1 immunoblotting (2).

Total proteins were extracted from LCLs, equal amounts verified by β -actin staining. SDS-PAGE was followed by immunoblotting with an antibody to human UBR1 (210 kDa) [Kwon et al., 2001]. β -actin (41 kDa) immunoblotting served as a loading control. (1) JBS-4, [p.Gln587*] + [p.Gln587*]. (2) Control with normal amount of UBR1. (3) JBS-6, [p.His136Arg] + [c.2254+2T>C]. (4) JBS-15, [p.Arg503*] + [p.Gln1102Glu]. (5) JBS-16, [c.3998-1G>C] + [p.Glu1648Lysfs*21]. (6) Control with normal amount of UBR1. Adapted from [Hwang et al., 2011].

3.1.9 PHENOTYPIC SPECTRUM ASSOCIATED WITH **UBR1** DEFICIENCY

All patients identified with *UBR1* mutations in this study and previously published work displayed a phenotype typical or at least suggestive of JBS, but individual expression of the phenotype was variable. Table 3.6 summarises genotype and phenotype data of the entire cohort of patients with *UBR1* mutations ascertained in the Zenker lab since 2005, including previously published and/or analysed cases (families JBS-1 to JBS-35) as well as newly recruited subjects investigated in the context of this thesis work (families JBS-36 to JBS-59). The genotype and phenotype findings in families JBS-1 to JBS-49 were reviewed by Sukalo et al. in 2014 [Sukalo et al., 2014a], while families JBS-50 to JBS-59 have been recruited subsequently. Several patients from this study cohort were also published as case reports to describe the clinical and mutational spectrum of this entity:

Patient **JBS-38.1** was born to consanguineous parents and the first patient described in literature with a homozygous missense mutation, namely p.Pro700Ser [Almashraki et al., 2011]. He presented with the typical JBS symptoms plus anemia requiring frequent blood transfusions and mild to moderate thrombocytopenia. Later, the same homozygous missense mutation was detected in the newly born sister of the index patient, who also exhibited the typical JBS symptoms (Table 3.6, patient JBS-38.2). This family was remarkable because of the association of JBS with haematological abnormalities and the detection of a new disease-causing missense mutation.

Another case report is about a baby girl from India (**JBS-47.1**) with congenital cardiac defect, secondary apnoea, and feeding difficulties with poor weight gain [Godbole et al., 2013], all being symptoms within the JBS spectrum. When the girl was about 7 months of age, *UBR1* sequencing that was performed within this study detected the homozygous splice mutation c.529-13G>A. RNA analysis of this intronic variant demonstrated that this alteration creates an ectopic splice site resulting in an inclusion of 11 nucleotides from intron 4 into the coding sequence; those additional base pairs cause a frameshift that leads to a premature stop codon (see above, Table 3.2). Nomenclature designates this mutation as p.Asn177Leufs*10. No evidence of a normally spliced transcript could be found by RNA analysis. We therefore presume that this mutation leads to a complete or near complete loss of function which is in line with the classical JBS phenotype seen in this girl.

Our patient **JBS-46.1** was reported by Singh et al. [2014] with emphasis on his hepatic and hematologic features. Hepatic involvement presented with direct hyperbilirubinemia and elevated hepatic enzyme levels, whereas hematologic involvement was represented by severe anemia with the requirement of blood transfusions. Another homozygous missense mutation (p.Gly1661Arg) of the *UBR1* gene was detected in this patient.

The patients **JBS-30.1** and **JBS-30.2** were gender-discordant twins with the novel *UBR1* stop mutation p.Gln1228* [Quaio et al., 2014]. The female twin (JBS-30.2) died at the age of 3 months due to refractory severe diarrhea, and no further detailed clinical data was available. The male twin (JBS-30.1) also developed severe diarrhea but was rescued by treatment with pancreatic enzyme supplements. His last documented medical check-up was at 13 years of age. The *UBR1* mutation discovered as part of this study was a c.3682C>T nucleotide substitution that causes a premature stop codon (p.Gln1228*).

Another JBS patient belonging to our study cohort (**JBS-54.1**) was reported to have two novel mutations of the *UBR1* gene [Atik et al., 2015]. The girl presented with a mild phenotype and did not show any signs of cognitive impairment. Molecular analysis revealed compound heterozygosity for the missense mutation p.Leu427Arg and a splice site mutation at position c.2432+5G>C.

Table 3.6 summarises the genotype and phenotype data of all JBS patients whose *UBR1* mutations were molecularly verified in our group. The cohort comprises a total of 59 molecularly proven JBS families including 73 affected individuals. Twenty-four families were ascertained and molecularly confirmed within this doctoral thesis. In the entire cohort, the gender ratio is nearly balanced (33 males, 40 females). The mean age of all patients is 7.5 years, the median age 4.5 years. Of the 72 JBS patients that were born alive, 10 were recorded to have deceased from complications that were supposed to be related to the syndrome. Death frequently occurred during the first months of life, most commonly secondary to EPI when enzyme supplementation was lacking or inadequate. All patients present with aplasia or hypoplasia of the alae nasi. In some cases, facial clefting occurs as the severe end of this congenital anomaly. Oligodontia of permanent teeth has been observed in all patients who could be investigated regarding this symptom and a high proportion even suffers from complete anodontia of permanent

teeth. EPI with onset at birth or in early infancy was another consistent symptom. Of the 70 patients that could be investigated regarding EPI, all were found to have this symptom. Hearing impairment was detected in 78% of all patients and 63% presented with scalp defects. Short stature (below 3rd percentile, according to growth charts from World Health Organisation and Robert Koch Institut) was documented in 62%. Cognitive impairment ranged from borderline to severe retardation and was found in 61% of the patients. For classification of intellectual disability we used a system introduced by Zhang et al. [2005], as displayed in Table D.2, because formal IQ measurements were only available from very few individuals. Hypothyroidism and microcephaly (occipital frontal circumference below 3rd percentile, according to growth charts from World Health Organisation and Robert Koch Institut) were apparent in 40% and 38% of the patients. Less frequent symptoms were CHD (27%), intrauterine growth restriction (IUGR, 25%), imperforate anus (23%), genital malformations (19%), and renal anomalies (13%). Diabetes was diagnosed in only 9% of the patients but the lifetime risk is probably higher because the patients can develop this symptom secondary to EPI during their teenage years.

Several concomitant symptoms have been frequently documented in JBS patients but were not included in this statistical analysis, as they are either secondary effects or cannot be objectively classified. Edemas, typically of the lower extremities, are a secondary effect due to malnutrition caused by EPI. As part of the facial dysmorphism in JBS patients, anomalies of the hairline were seen frequently. Here, the major observation is a frontal upsweep of the hair, called “cow-lick”, and a less frequently observed pattern is an extension of the lateral hairline onto the forehead. Additionally, many patients were noticed to have abnormal lacrimal canals, such as cutaneolacrimal fistulae.

In a recently published article by Corona-Rivera et al. [2016], we reported four cases with JBS and oblique facial clefting that have not been described in detail before (**JBS-1.1, -36.1, -43.1, -58.1**, Figure 3.11), and compare them to three cases from literature (JBS-2.1, -2.2, -10.1, previously reported by [Cheung et al., 2009; Guzman and Carranza, 1997; Jones et al., 1994; Sukalo et al., 2014a; Timoney et al., 2004; Zenker et al., 2005]).



Figure 3.11: Oblique facial clefts in patients with JBS.

(A) Patient JBS-58.1 was born to non-consanguineous Mexican parents and subsequently presented with compound-heterozygosity for mutations in the *UBR1* gene, namely c.81+1G>A and p.Arg1019*. He had severe facial clefting, classified as Tessier clefts types 3 and 4. (B) Patient JBS-43.1 from Costa Rica was found to harbour the p.Gln513* homozygously. The facial clefts were classified as types 4 and 5. (C) Another patient from Costa Rica (JBS-1.1) with the same homozygous nonsense mutation (p.Gln513*) had bilateral severe oblique facial clefts that were classified as Tessier type 4. (D) A patient of Russian origin (JBS-36.1) at the age of 12 years. He had incomplete oro-facial clefting on the left side classified as Tessier types 1 and 2 that were surgically corrected during childhood. Mutation analysis of the *UBR1* gene revealed compound-heterozygosity for a deletion of four amino acid residues, namely p.Ala389_Phe392, and the missense mutation p.Arg754Cys. Reproduced from [Corona-Rivera et al., 2016] with permission from John Wiley and Sons.

Legend to Table 3.6: Overview of mutations and clinical data of all JBS patients. Pages 64-66.

M, male; F, female; y, year(s); m, month(s); w, week(s); d, day(s), †, deceased; TOP, termination of pregnancy; na, no data available; H, hypoplasia; A, aplasia; C, facial clefting; NS, present but not specified; +, present; -, not present; ID, moderate to severe intellectual disability; MID, mild intellectual disability; BL, borderline intellectual disability; HCM, hypertrophic cardiomyopathy; TOF, tetralogy of Fallot; VSD, ventricular septal defect; O, other anomalies; ASD, atrial septal defect; DCM, dilated cardiomyopathy; PDA, patent ductus arteriosus; #, twins; HY, hypospadias; CR, cryptorchidism; MI, micropenis; CL, clitoral hypertrophy / clitoromegaly; EP, epispadias; P<3, percentile below 3rd (according to growth charts from World Health Organisation and Robert Koch Institut). References: (1) Zenker et al., 2005; (2) Guzman and Carranza, 1997; (3) Schoner et al., 2012; (4) Rudnik-Schöneborn et al., 1991; (5) Hwang et al., 2011; (6) Vanlieferinghen et al., 2001; (7) Vanlieferinghen et al., 2003; (8) Zerres and Holtgrave, 1986; (9) Swanenburg de Veye et al., 1991; (10) Jones et al., 1994; (11) Timoney et al., 2004; (12) Cheung et al., 2009; (13) Vieira et al., 2002; (14) McHeik et al., 2002; (15) Elting et al., 2008; (16) Reichart et al., 1979; (17) Alkhouri et al., 2008; (18) Quaio et al., 2014; (19) Liu et al., 2011; (20) Fallahi et al., 2011; (21) Almashraki et al., 2011; (22) Singh et al., 2014; (23) Godbole et al., 2013; (24) Atik et al., 2015; (25) Corona-Rivera et al., 2015. ^aGenotypes and tabulated clinical data of families JBS-1 to JBS-49 were published in Sukalo et al., [2014a].

Table 3.6: Overview of mutations and clinical data of all JBS patients.

Family (JBS-)	Patient (JBS-)	Mutations	Gender	Age	Exocrine pancreatic insufficiency	Nasal wings gestalt	Oligodontia of permanent teeth	Hearing impairment	Scalp defect	Short stature (P<3)	Cognitive impairment	Hypothyroidism	Microcephaly (P<3)	Congenital heart defect	Intrauterine growth restriction (P<3)	Imperforate anus	Genital malformation	Renal anomalies	Diabetes (age of onset/diagnosis)	Parental consanguinity	Reference ^a
1	1.1	[p.Q513*] + [p.Q513*]	M	11.8y	+	A,C	na	+	-	+	NS	na	-	-	-	-	-	-	na	-	1,25
	2.1	[p.Q513*] + [p.Q513*]	F	8y	+	A,C	na	+	+	+	ID	-	-	-	-	-	-	-	na	-	1,2,25
2	2.2	[p.Q513*] + [p.Q513*]	M	9m†	+	A,C	na	na	+	+	na	-	+	-	-	-	-	-	na	-	1,2,25
	3.1	[p.Q550*] + [p.Q550*]	F	10y	+	A	+	+	+	-	ID	+	-	-	-	+	-	-	-	+	1
4	4.1	[p.Q587*] + [p.Q587*]	M	7y	+	A	+	+	+	+	ID	+	-	-	-	+	HY,CR	na	na	+	1,3
	4.2	[p.Q587*] + [p.Q587*]	M	1d†	+	A	na	na	+	na	na	na	-	HCM	+	-	MI,O	+	na	+	1,3
5	5.1	[c.2379+1G>C] + [c.2379+1G>C]	M	14.8y	+	A	+	+	+	+	ID	+	+	-	-	-	O	na	na	+	1,4
	5.2	[c.2379+1G>C] + [c.2379+1G>C]	M	3w†	+	A	na	na	+	na	na	na	na	na	TOF	na	-	-	na	+	1,4
6	5.3	[c.2379+1G>C] + [c.2379+1G>C]	F	4m	+	H	na	+	+	+	na	na	+	-	-	-	CL	na	na	-	-
	6.1	[p.H136R] + [c.2254+2T>C]	F	13.5y	+	A	+	+	+	+	MID	+	-	-	-	+	NS	+	-	-	1,5
7	7.1	[p.E1643*] + [p.E1643*]	M	14d†	+	A	na	+	+	na	na	-	-	VSD,O	+	+	MI	na	na	+	1,6
	7.2	[p.E1643*] + [p.E1643*]	M	TOP	na	A	na	na	+	na	na	na	-	-	-	+	-	-	na	+	7
8	8.1	[c.660-2_660-1delAG] + [p.G1279S]	F	11y	+	H	+	-	-	-	-	-	na	-	-	-	-	-	na	-	1,8
	9.1	[c.1911+14C>G] + [p.M849fs*13]	M	25y	+	H	+	+	-	+	-	-	-	-	+	-	-	-	-	-	1,4,9
10	10.1	[p.G160Afs*5] + [p.G160Afs*5]	F	12y	+	A,C	+	+	+	-	ID	+	-	ASD	-	+	-	+	(12)	-	1,10-12,25
	11.1	[p.C251*] + [p.C251*]	M	13y	+	A	+	+	+	+	NS	+	+	VSD	+	-	-	-	-	+	1,10-12
12	12.1	[p.P867Hfs*12] + [p.P867Hfs*12]	M	4.5y	+	NS	+	+	-	+	NS	-	-	-	-	-	-	-	na	+	1
	13.1	[c.1094-12A>G] + [c.1094-12A>G]	F	1.1y	+	A	na	+	+	-	na	-	-	-	-	-	-	-	na	+	1,13
14	14.1	[c.1094-13A>G] + [c.1094-13A>G]	M	3y	+	A	na	+	+	+	NS	+	na	VSD	-	-	HY	na	na	+	-
	15.1	[p.R503*] + [p.Q1102E]	F	15.3y	+	H	+	+	+	-	-	-	na	-	-	-	-	-	-	-	5
16	16.1	[c.3998-1G>C] + [p.E1648Kfs*21]	M	11.9y	+	H	+	-	+	+	MID	-	-	-	-	+	-	-	-	-	14
	17.1	[p.I286R] + [p.R665*]	M	19y	+	H	+	+	-	+	BL	+	-	-	-	-	-	-	-	-	-
18	18.1	[p.V122L] + [p.H774Sfs*6]	F	20y	+	H	+	-	+	-	-	+	-	-	-	-	-	-	-	-	5
	19.1	[c.2839+5G>A] + [c.2839+5G>A]	F	7.1y	+	H	+	+	+	-	-	+	-	DCM	-	-	-	-	-	+	15
19	19.2	[c.2839+5G>A] + [c.2839+5G>A]	F	22y	+	H	+	-	-	-	-	-	-	-	+	-	-	-	-	-	15
	20.1	[c.529-13G>A] + [c.529-13G>A]	F	5m	+	A	na	+	+	-	NS	-	+	PDA	-	-	-	-	-	+	-

Family (IBS-)	Patient (IBS-)	Mutations	Gender	Age	Exocrine pancreatic insufficiency	Nasal wings gestalt	Oligodontia of permanent teeth	Hearing impairment	Scalp defect	Short stature (P<3)	Cognitive impairment	Hypothyroidism	Microcephaly (P<3)	Congenital heart defect	Intrauterine growth restriction (P<3)	Imperforate anus	Genital malformation	Renal anomalies	Diabetes (age of onset/diagnosis)	Parental consanguinity	Reference ^a
21	21.1	[p.E766del] + [p.R1242G]	M	12.1y	+	H	+	-	-	-	-	-	na	-	-	-	-	-	-	-	-
22	22.1	[p.A563D] + [p.A563D]	F	12y	+	H	+	-	+	-	-	-	na	-	na	-	-	-	-	-	16
22	22.2	[p.A563D] + [p.A563D]	F	7y	+	H	+	+	+	-	BL	-	na	-	na	-	-	-	-	-	16
23	23.1	[c.81+5G>C] + [p.V660del]	F	12.3y	+	H	+	+	-	-	-	-	-	-	-	-	-	-	-	-	17
24	24.1	[p.A563D] + [?]	F	37y	+	H	+	+	-	+	BL	-	na	-	+	-	-	-	-	-	-
25	25.1	[c.2839+5G>A] + [c.2839+5G>A]	F	5.5y	+	H	na	+	+	+	NS	+	+	ASD	+	-	-	-	-	+	15
25	25.2	[c.2839+5G>A] + [c.2839+5G>A]	F	3m†	+	H	na	na	+	na	na	na	+	-	+	-	-	na	-	-	15
26	26.1	[p.Y1508*] + [c.4836-?_5250+?del]	F	5.6y	+	A	+	+	+	-	NS	+	-	-	-	-	-	-	-	-	-
27	27.1	[p.L1232Wfs*17] + [p.S1427F]	M	8.9y	+	H	+	na	-	+	-	-	na	-	na	-	na	na	-	-	-
28	28.1	[p.S629*] + [c.5109-3A>G]	F	18y	+	H	+	+	-	+	-	-	-	-	-	-	-	+	-	-	-
29	29.1	[p.S1431P] + [p.S1431P]	M	12.2y	+	H	+	-	-	-	-	-	-	-	-	-	-	-	-	-	-
29	29.2	[p.S1431P] + [p.S1431P]	F	9.8y	+	H	+	-	-	-	-	-	-	-	-	-	-	-	-	-	-
30	30.1	[p.Q1228*] + [p.Q1228*]	M	13y	+	H	+	+	+	+	ID	-	+	-	#	-	CR	-	-	-	18
30	30.2	[p.Q1228*] + [p.Q1228*]	F	3m†	+	H	na	na	na	na	na	na	na	na	#	na	na	na	na	-	18
31	31.1	[p.H166R] + [p.Y678*]	F	15y	+	H	+	-	+	-	-	-	-	-	-	-	-	-	-	-	-
32	32.1	[p.R503*] + [p.R503*]	F	23y	+	H	na	+	-	+	na	-	na	-	na	-	-	-	-	-	-
32	32.2	[p.R503*] + [p.R503*]	M	20y	+	H	na	+	-	+	na	-	na	-	na	-	-	-	-	na	-
32	32.3	[p.R503*] + [p.R503*]	F	17y	+	H	na	+	-	+	na	-	na	-	na	-	-	-	-	-	-
33	33.1	[p.L317P] + [p.P1426L]	F	1.8y	+	H	+	-	+	+	ID	-	na	-	na	+	-	-	-	-	19
34	34.1	[c.81+2dupT] + [p.E1694*]	M	7.7y	+	H	+	+	-	-	na	-	+	-	-	-	-	+	-	-	-
35	35.1	[p.C1396*] + [p.C1396*]	M	3.5y	+	H	+	+	+	+	BL	+	-	PDA,O	-	-	HY	-	+	-	20
36	36.1	[p.A389_F392del] + [p.R754C]	M	17y	+	A,C	+	+	+	-	-	-	-	-	na	-	-	-	-	-	25
37	37.1	[p.R1712Lfs*14] + [p.R1712Lfs*14]	M	8m	+	A	na	+	-	+	na	-	+	ASD	na	+	-	na	-	+	-
37	37.2	[p.R1712Lfs*14] + [p.R1712Lfs*14]	M	1w	+	A	na	na	+	na	na	na	+	-	+	+	EP	+	-	-	-
38	38.1	[p.S700P] + [p.S700P]	M	3y	+	A	na	-	+	+	na	+	+	ASD	+	-	HY	-	-	-	21
38	38.2	[p.S700P] + [p.S700P]	F	1.5m	+	H	na	na	+	na	na	+	+	ASD	-	-	-	-	+	-	-

Family (IBS-)	Patient (IBS-)	Mutations	Gender	Age	Exocrine pancreatic insufficiency	Nasal wings gestalt	Oligodontia of permanent teeth	Hearing impairment	Scalp defect	Short stature (P<3)	Cognitive impairment	Hypothyroidism	Microcephaly (P<3)	Congenital heart defect	Intrauterine growth restriction (P<3)	Imperforate anus	Genital malformation	Renal anomalies	Diabetes (age of onset/diagnosis)	Parental consanguinity	Reference ^a
39	39.1	[p.L217R] + [p.Q1365*]	M	22y	+	H	+	+	+	+	ID	+	na	-	-	-	-	+	-	-	-
40	40.1	[p.C127F] + [p.C127F]	F	2.3y	+	A	+	+	+	+	NS	+	-	-	+	-	-	-	+	-	-
41	41.1	[c.660-2_660-1delAG] + [p.E870*]	F	13.6y	+	A	+	+	+	-	na	+	-	-	-	+	CL,O	-	-	-	-
42	42.1	[p.L1398Rfs*3] + [p.L1398Rfs*3]	F	1.7y	+	H	+	+	-	+	NS	-	-	-	-	-	-	-	+	-	-
43	43.1	[p.Q513*] + [p.Q513*]	F	4m [†]	+	A,C	+	na	-	na	na	-	na	-	+	-	-	-	+	-	25
44	44.1	[c.2380-1G>A] + [c.2380-1G>A]	M	1.3y	+	A	na	+	+	-	NS	+	-	-	-	-	HY	-	+	-	-
45	45.1	[p.R754H] + [p.R754H]	F	4m [†]	+	A	na	na	+	+	na	-	+	ASD	+	-	-	-	+	+	-
46	46.1	[p.G1661R] + [p.G1661R]	M	2.5m	+	H	na	na	+	+	na	na	+	-	-	-	-	-	+	+	22
47	47.1	[c.529-13G>A] + [c.529-13G>A]	F	10m	+	H	na	+	-	+	na	+	-	ASD,PDA	-	-	-	-	+	+	23
48	48.1	[p.R1249Kfs*4] + [p.R1249Kfs*4]	F	1.2y	+	A	na	+	+	+	na	-	+	-	-	-	-	-	+	+	-
49	49.1	[p.E1110*] + [p.E1110*]	F	2.5m [†]	+	A	na	na	-	na	na	+	-	ASD	-	-	-	-	+	+	-
50	50.1	[c.1282-?_1439+?del] + [c.1282-?_1439+?del]	F	2.5m	+	A	na	+	-	na	na	+	na	ASD	-	-	-	-	+	+	-
51	51.1	[p.Q420K] + [p.Q420K]	M	4.3y	na	na	na	na	na	na	na	na	na	na	na	na	na	na	+	+	-
52	52.1	[c.2740-?_3209+?del] + [c.3210-?_3415+?dup]	M	8m	+	A	na	+	+	+	na	-	na	ASD	-	-	-	-	-	-	-
53	53.1	[p.H166R] + [p.H166R]	M	2y	+	H	na	na	-	+	na	+	+	-	na	+	-	-	+	+	-
54	54.1	[p.L427R] + [c.2432+5G>C]	F	3y	+	H	na	-	-	-	-	-	-	-	-	-	-	-	-	-	24
55	55.1	[c.2839+5G>A] + [c.2839+5G>A]	F	1y	+	H	na	na	+	na	na	na	na	-	-	+	-	-	+	+	-
56	56.1	[p.R1019*] + [p.R1019*]	F	5m	+	A	na	+	+	+	na	na	+	-	-	-	-	na	+	+	-
57	57.1	[p.E771Nfs*8] + [p.E771Nfs*8]	F	1w	+	H	na	na	na	na	na	na	na	na	na	+	-	na	+	+	-
58	58.1	[c.81+1G>A] + [p.R1019*]	M	2m [†]	na	A,C	na	na	+	na	MID	+	-	-	-	+	-	+	-	-	25
59	59.1	[p.R1019*] + [p.R1019*]	M	5m	+	H	na	na	-	+	na	-	+	DCM	+	-	-	-	+	+	-
		%			100	100	100	78	63	62	61	40	38	27	25	23	19	13	9		-

For legend see page 63.

3.2 ADAMS-OLIVER SYNDROME

Sequencing of AOS and isolated ACC patients was mainly carried out within this thesis work, but some genetic investigations on patients from our study cohort was also performed in London, United Kingdom (collaboration partner: Laura Southgate) and Antwerp, Belgium (collaboration partner: Wim Wuyts) within our collaboration in this study (AOS CONSORTIUM). As a member of this consortium, our group focused on families with apparent autosomal recessive inheritance of AOS, specifically on *DOCK6*, the first gene for autosomal recessive AOS, that was discovered in 2012 [Shaheen et al., 2011]. We also sequenced this gene in a considerable number of DNAs from patients with autosomal recessive and sporadic AOS from the patient cohorts of our collaboration partners. *NOTCH1* was in turn preferentially investigated in London and the majority of *RBPJ*, *EOGT* and *DLL4* sequencing was performed in Antwerp, but we also analysed some patients in our lab and verified the mutations that were detected in London and Antwerp, respectively.

At the beginning of this project an MD student (Felix Tilsen) who was instructed by me performed parts of the lab work (most of the *ARHGAP31* approaches and nearly half of the *DOCK6* sequencing).

Pathogenicity of all variants was checked according to the guidelines established in chapter 2.3.19. Evaluation of missense mutations, splice site mutations and variants of unknown significance is shown in Appendix C.

3.2.1 *DOCK6*

A major focus of our efforts was directed towards *DOCK6* after its discovery as the gene responsible for AOS (AOS2; MIM #614219) in two consanguineous Arab families [Shaheen et al., 2011]. Due to its autosomal recessive way of inheritance, only patients with a suspected autosomal recessive family background or sporadic patients were included. Parental consanguinity and/or the presence of multiple affected children of clinically unaffected parents were regarded as possible indicators of autosomal recessive inheritance. Families with parent-child transmission of the phenotype suggesting autosomal dominant inheritance were excluded from *DOCK6* analysis. Thirteen index patients with autosomal recessive pattern of inheritance or consanguineous parents, and 26 sporadic cases from our Magdeburg cohort were

analysed (at the time of the below mentioned publication, 10 autosomal recessive families and 18 sporadic cases were analysed). Additionally, 30 cases with a clinical diagnosis of AOS from a cohort collected in London were included to this study. The London cohort comprised nine autosomal recessive cases (including four patients that had been pre-analysed by exome sequencing in London) and 21 sporadic cases. For the data analysis and publication, the results of *DOCK6* sequencing performed by our collaborator in Antwerp in his own cohort (20 cases: 12 autosomal recessive families and eight sporadic patients) were also included. This brought the total of unrelated patients investigated within this joint study to 78 and resulted in the publication of the original article “*DOCK6* Mutations Are Responsible for a Distinct Autosomal-Recessive Variant of Adams-Oliver Syndrome Associated with Brain and Eye Anomalies” in the *Journal Human Mutation* [2015].

The 13 mutations detected in our patients, plus four previously published ones [Lehman et al., 2014; Shaheen et al., 2011; Shaheen et al., 2013], and 20 variants of unknown significance, were collected at an online database (<http://databases.lovd.nl/shared/variants/DOCK6>). Furthermore, an overview of the clinical data of the *DOCK6* mutation positive patients from our cohort (n=12) and those from literature (n=6) [Lehman et al., 2014; Shaheen et al., 2011; Shaheen et al., 2013], plus the data of patients with unclassified *DOCK6* variants (n=18) were added to LOVD (<http://databases.lovd.nl/shared/individuals/DOCK6>). Figure 3.12 exemplarily shows *DOCK6* variant entries.

Effect	Reported	Exon	DNA change (cDNA)	RNA change	Protein
?/.	1	2	c.100C>G	r.(?)	p.(His34Asp)
+?/.	1	5	c.484G>T	r.(?)	p.(Glu162*)
+?/.	2	7	c.788T>A	r.(?)	p.(Val263Asp)
-?/.	2	9	c.885C>T	r.(=)	p.(=)
+?/.	1	11	c.1245dupT	r.(?)	p.(Asp416*)
?/.	1	12	c.1289G>A	r.(?)	p.(Arg430His)
+?/.	1	12	c.1296_1297delinsT	r.(?)	p.(Gln434Argfs*21)
+?/.	1	12	c.1358C>T	r.(?)	p.(Thr453Met)

Figure 3.12: LOVD entries for *DOCK6* variants.

MUTATIONS OF THE *DOCK6* GENE

Among 78 unrelated families selected for *DOCK6* analysis, a total of 10 families were molecularly confirmed with AOS2. The mutations observed in these 10 families included nonsense (n=1), missense (n=4), frameshift (n=4), and splice site mutations (n=3), as well as one larger intragenic deletion-insertion resulting in deletion of exons 42 to 47. The latter was identified through the failure to amplify the terminal exons by PCR and confirmed by focused MLPA and breakpoint sequencing (analysis performed in Antwerp, data not shown). Eleven of these 13 mutations were novel and two have been previously described [Shaheen et al., 2011; Shaheen et al., 2013] (Table 3.7). Seven index patients had homozygous mutations consistent with known parental consanguinity in these families, while the remaining three had compound heterozygous changes.

Table 3.7 summarises all mutations detected in the patients from Magdeburg, London, and Antwerp.

Table 3.7: Mutations in the *DOCK6* gene that are related to AOS.

Location	Nucleotide alteration	Predicted effect ^a	Family (AOS-)	References
Exon 05	c.484G>T	p.E162*	8	[Sukalo et al., 2015]
Exon 07	c.788T>A	p.V263D	6	[Sukalo et al., 2015]
Exon 12	c.1296_1297delinsT	p.Q434Rfs*21	3	[Sukalo et al., 2015]
Exon 12	c.1362_1365del	p.T455Sfs*24	2	[Sukalo et al., 2015] [Shaheen et al., 2011]
Exon 17	c.1902_1905del	p.F635Pfs*32	7	[Sukalo et al., 2015]
Exon 21	c.2520dupT	p.R841Sfs*6	10	[Sukalo et al., 2015] [Shaheen et al., 2013]
Exon 25	c.3047T>C	p.L1016P	1	[Sukalo et al., 2015]
Exon 26	c.3154G>A	p.E1052K	5	[Sukalo et al., 2015]
Intron 32	c.4106+5G>T	r.spl.? p.?	7	[Sukalo et al., 2015]
Intron 35	c.4491+1G>A	<i>p.F1447_H1497del</i>	2	[Sukalo et al., 2015]
Exon 38	c.4786C>T	p.R1596W	4	[Sukalo et al., 2015]
Intron 41 – Intron 47	c.5235+205_6102-15 delinsCATGGGGCTG	p.? ^b	9	[Sukalo et al., 2015]
Intron 46	c.5939+2T>C ^c	r.spl.? p.?	6	[Sukalo et al., 2015]

^aItalic letters indicate that the effect of splicing mutations was demonstrated on the mRNA level. ^bMLPA analysis revealed deletion of exons 42 to 47. ^cThis alteration is also listed in dbSNP (rs201387914) with unknown pathogenicity and frequency. Online tools predict destruction of the donor splice site (see Table C.2.3). Mutation nomenclature refers to GenBank reference sequence NM_020812.3. Nucleotide numbering reflects cDNA numbering with +1 corresponding to the A of the ATG translation initiation codon in the reference sequence, according to mutation nomenclature guidelines (www.hgvs.org/mutnomen). The initiation codon is codon 1.

Of the 14 *DOCK6* mutations detected in our AOS cohort (Table 3.7), only two have been published previously. The frameshift mutation p.Thr455Serfs*24 was initially reported in the homozygous state in a patient of Arab origin [Shaheen et al., 2011]. In our sporadic AOS cohort, a patient (AOS-2) from Germany was found to carry the same mutation in compound-heterozygosity with a splice site mutation. The second recurrent mutation, also a frameshift mutation (p.Arg841Serfs*6) was detected in two unrelated AOS families, each with homozygosity in the affected individuals. It was initially published by Shaheen et al. [2013] in a family of Arab background. We detected this mutation in a patient from family AOS-10. Unfortunately, no ethnic background is known for this patient. The ethnical background provides no indication for a common ancestral allele in these families.

Of the four missense mutations observed in this cohort, three were homozygous in affected children from consanguineous families (p.Leu1016Pro, p.Glu1052Lys, p.Arg1596Trp) and one (p.Val263Asp) occurred in compound heterozygosity with a splice site mutation on the second allele. All four missense variations were classified as likely causative mutations, as assessed by various online prediction tools (Table C.1.1). Notably, in the consanguineous family harbouring the missense mutation p.Leu1016Pro (family AOS-1), previous homozygosity mapping using a SNP array had demonstrated a 22 Mb stretch of autozygosity on chromosome 19 in the index patient (data not shown), consistent with linkage to the *DOCK6* locus. In one pedigree (family AOS-6), segregation of compound heterozygosity for the missense mutation p.Val263Asp and a splice site mutation on the second allele (c.5939+2T>C) was confirmed in the two affected siblings from family AOS-6. None of the four missense mutations detected in the *DOCK6* gene was listed at dbSNP or detected in a homozygous state, according to the ExAC Genome Browser. The mutations p.Glu1052Lys and p.Arg1596Trp were both detected once in a heterozygous state in ExAC, equalling an allele frequency of <0.02%.

Of the three splice site mutations observed in this study, one (c.4106+5G>T) is outside of the canonical splice site dinucleotide. Unfortunately, no appropriate material could be obtained to prove the splicing effect on the mRNA level. However, compound heterozygosity for this change and a frameshift mutation on the other allele was found to segregate with the phenotype in family AOS-7. Furthermore, splice prediction tools consistently calculated that this change presumably abrogated splice donor function at this site (Table C.2.3), thus supporting the likely pathogenic role of this variation. The

c.4491+1G>A splice site mutation in intron 35 causes skipping of exon 34 in the mRNA. As displayed in Figure 3.13, the second allele carrying a frameshift mutation is significantly underrepresented; presumably this mRNA is rapidly degraded by nonsense mediated decay due to its anomaly. No further analyses of other patients' cDNA could be performed due to the lack of appropriate material.

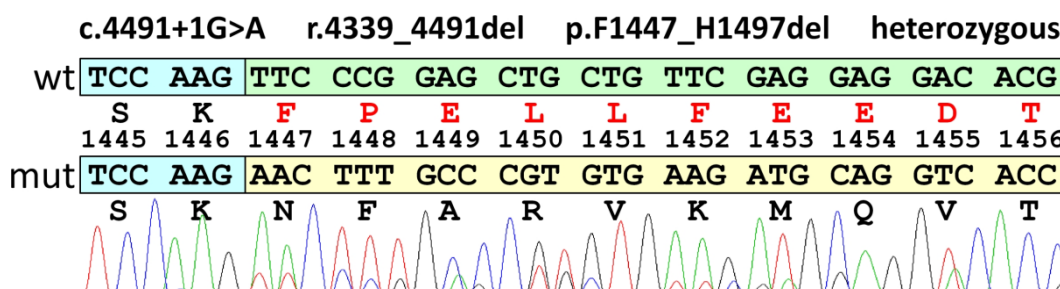


Figure 3.13: Electropherogram of a *DOCK6* splice site mutation.

Wild type cDNA sequence (wt) and amino acid residues are compared to the mutated cDNA sequence (mut) and subsequent amino acid residues. Wild type shows correct junction of exon 34 (blue box) and 35 (green box). In the cDNA of patient AOS-2.1, the splice site mutation c.4491+1G>A destroys the donor splice site which subsequently causes deletion of the whole exon 35 (r.4339_4491del). No frameshift is generated, but 51 amino acid residues are predicted to be missing in the translated protein. The yellow box represents exon 36. This alteration was detected in compound-heterozygosity in the patient, together with the p.Thr455Serfs*24 frameshift mutation on the other allele.

DOCK6 mutations are distributed over the entire gene with no obvious clustering to certain domains of the encoded protein (Figure 3.14). A deleterious effect on the gene product is plausible for most of these changes, as they are predicted to lead to either a truncated protein or nonsense-mediated mRNA decay. However, the precise functional consequences of the novel missense mutations presented here remain to be explored.

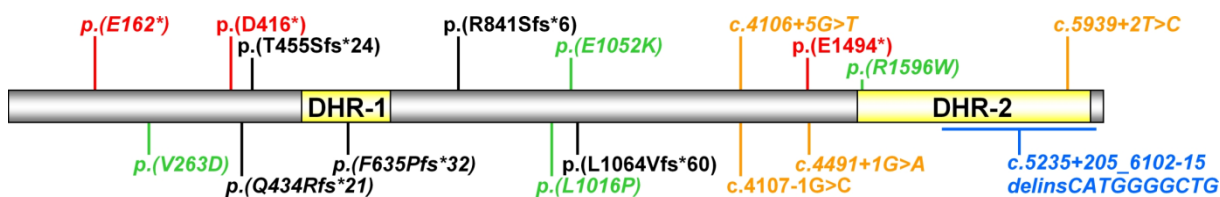


Figure 3.14: *DOCK6* protein with known functional domains and distribution of mutations.

The protein contains two DOCK homology regions, DHR-1 and DHR-2. DHR-1 spans about 200 amino acids at the N-terminal end of the protein, whereas DHR-2 is located towards the C-terminus and has an approximate length of 500 amino acids [Cote and Vuori, 2002]. All currently known mutations are displayed according to their location in the *DOCK6* protein. Red represents nonsense mutations (3), black indicates frameshift mutations (5), missense mutations are shown in green (4), splice-site mutations are coloured in orange (4), and the blue line represents one large deletion insertion at the C-terminal end of the *DOCK6* protein-spanning exons 42–47. Novel mutations are written in italics, others were previously published by Shaheen et al., [2011] and [2013] and by Lehman et al., [2014]. Reprinted from [Sukalo et al., 2015] with the permission of John Wiley and Sons.

SNPs AND UNCLASSIFIED VARIANTS OF THE *DOCK6* GENE

In addition to the pathogenic mutations described above, we also identified 16 heterozygous *DOCK6* sequence variations in our cohort, which remained as unclassified due to either uncertain clinical significance or annotation in dbSNP (build 139) as rare variants (minor allele frequency (MAF) <0.01 in TGP) (Table 3.8). These variants included predicted amino acid substitutions (n=8), synonymous alterations in the coding sequence (n=5), and intronic substitutions within 20 bp of the splice site (n=3). None of these variations were consistently classified as disease-causing by prediction tools. Thirteen unrelated sporadic AOS patients harboured a single heterozygous unclassified *DOCK6* variant, while two patients were found to have two or more variants. Of these, one case had inherited both variants (p.Asn295Asn and p.Gly702Ser) from the mother on the same allele (data not shown). Another patient was found to carry three unclassified variants (p.Asn295Asn, p.Arg430His, c.1833-19C>G), the segregation of which could not be studied. Notably, this patient was previously reported in the literature as a variant subtype of AOS associated with cerebral anomalies, seizures and severe cognitive impairment, but without ACC of the scalp [Brancati et al., 2008]. While most of these variations are more likely to be non-pathogenic (Table C.1.4 and Table C.2.4), we cannot fully exclude any contribution to the observed phenotype. Our mutation screening strategy did not assess mutations of the promoter and intronic changes. We also did not systematically screen for larger genomic deletions/duplications. Therefore, it remains possible that additional pathogenic variants may have been missed in this cohort and that the given figure of the contribution of *DOCK6*-related disease is somewhat underestimated. However, for the *DOCK6* mutation-negative patients originating from consanguineous families, we can state that five of them had a previous SNP array analysis showing no suggestive stretch of homozygosity at the *DOCK6* locus (data not shown). In two out of four further subjects who had no previous homozygosity mapping, *DOCK6* sequencing revealed at least one heterozygous SNP, whilst for two cases, sequencing results were uninformative to exclude homozygosity at the *DOCK6* locus. Thus, at least for our consanguineous families we can conclude that genes other than *DOCK6* are very likely involved in the pathogenesis of AOS.

Table 3.8: Unclassified variants of the *DOCK6* gene.

Location	Nucleotide alteration	Predicted effect	Frequency our cohort	Frequency ExAC	Homoz. ExAC	dbSNP
Exon 02	c.100C>G	p.H34D	0.76%	0.1247%	-	rs201065561
Exon 09	c.885C>T	p.N295N	1.54%	0.8338%	8	rs146599144
Exon 12	c.1289G>A	p.R430H	0.78%	0.3896%	1	rs143655255
Exon 12	c.1358C>T	p.T453M	0.78%	0.003601%	-	-
Exon 13	c.1445C>T	p.P482L	0.77%	0.002489%	-	rs557547319
Intron 16	c.1833-19C>G	r.spl.? p.?	0.78%	0.3405%	-	rs188183013
Exon 19	c.2104G>A	p.G702S	0.74%	0.6156%	2	rs199838752
Exon 23	c.2767G>A	p.V923I	0.78%	0.02354%	-	rs143194982
Exon 30	c.3873C>T	p.C1291C	0.78%	0.04477%	-	rs200843111
Exon 31	c.3913C>T	p.R1305C	0.78%	0.8342%	9	rs112911897
Exon 37	c.4732C>T	p.L1578F	0.78%	0.02393%	-	-
Exon 38	c.4899G>A	p.L1633L	0.78%	0.2561%	-	rs72985308
Exon 41	c.5229C>A	p.G1743G	0.76%	0.1046%	-	rs56243833
Exon 44	c.5640C>T	p.H1880H	0.78%	0.1167%	-	rs200959822
Intron 44	c.5688+9G>A	r.spl.? p.?	0.78%	-	-	-
Intron 45	c.5833-16C>G	r.spl.? p.?	1.54%	0.06603%	-	rs199764395

Only variants within 20 bp of the exons and MAF ≤ 0.01 (in TGP) were included.
Homoz., homozygous appearance.

PHENOTYPIC SPECTRUM ASSOCIATED WITH *DOCK6* MUTATIONS

The main clinical findings of all 12 patients with *DOCK6* mutations are summarised in Table 3.9. Detailed clinical data could be obtained from 10 patients originating from eight families. The patients' ages ranged between one week and 20 years (median 4.3 years). All except one affected individual from these families had ACC of the scalp and TTLD of variable expression; a patient from family AOS-7 presented only with mild hypoplasia of toenails along with a CHD, impaired vision and mild cognitive impairment, whereas his sister presented with classic AOS features including ACC and TTLD. Across our *DOCK6*-positive cohort, the limb defects ranged from minimal hypoplasia of terminal phalanges to severe transverse reduction defects (Figure 3.15). Hypoplasia of finger and toe nails, cutaneous syndactyly, brachydactyly, amputation defects at the level of the proximal phalanges, or absence of all fingers or toes were described in *DOCK6* mutation positive patients from our cohort. Notably, aside from ACC typically located on the scalp vertex, four patients had additional areas of ACC on the abdomen.



Figure 3.15: ACC of the scalp and TTLD of the hands.

Clinical photographs of three *DOCK6*-positive individuals with AOS from the Magdeburg cohort showing areas of alopecia on the vertex resulting from aplasia cutis congenita and terminal defects of the digits of varying severity. (A) Patient AOS-1.1. (B) Patient AOS-2.1. (C) Patient AOS-3.1. Reprinted from [Sukalo et al., 2015] with the permission of John Wiley and Sons.

Further associated anomalies, primarily related to the nervous system, were present in all individuals carrying homozygous or compound-heterozygous *DOCK6* mutations. Specifically, all patients from whom sufficient data could be obtained were reported with developmental delay or mental retardation, ranging from mild to severe (Table 3.9). A broad range of additional neurological abnormalities were reported in most cases, including cerebral palsy, spasticity, contractures, and epilepsy. Only one patient out of seven aged ≥ 5 years had achieved the ability to walk without support. Behavioural abnormalities including autistic behaviour or temper tantrums were reported in two patients. Brain MRI or CT (computed tomography) scan had been performed for seven patients and was abnormal in all of them. The most frequent changes observed on brain imaging included ventriculomegaly, periventricular leukomalacia/calcifications, and hypoplasia/atrophy of the corpus callosum (Table 3.9). Images from the two affected individuals AOS-2.1 and AOS-3.1 from our Magdeburg cohort are exemplarily shown in Figure 3.16. Patient AOS-4.1 underwent cerebral ultrasonography at 3 months of age, which also showed ventriculomegaly. Another patient (AOS-6.2) had previously been

reported with ventricular dilatation, partial agenesis of the corpus callosum, and periventricular leukomalacia on autopsy [Orstavik et al., 1995]. Where available, measurements of head circumference were in the microcephalic range for all eight patients. Ocular anomalies including microphthalmia, retinal detachment, and visual impairment were reported in all patients for whom clinical information could be obtained (exemplarily shown in Figure 3.16B3). In contrast, cardiac anomalies were observed in only three cases (Table 3.9).

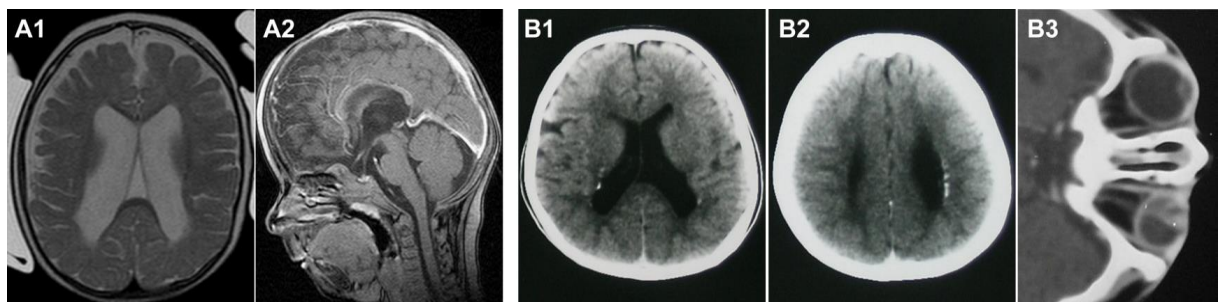


Figure 3.16: Brain imaging of AOS patients with *DOCK6* mutations.

(A) Cranial MRI of patient AOS-2.1 at age 1 year: (A1) T2-weighted axial section showing enlarged lateral ventricles and cerebral atrophy particularly affecting the frontal lobe. (A2) Contrast enhanced T1-weighted median sagittal section illustrating thin corpus callosum and enlarged basal subarachnoid spaces. (B) CT scan of patient AOS-3.1 at age 6 years: (B1 and B2) Axial sections showing ventriculomegaly and periventricular calcifications. (B3) Orbital section showing right microphthalmia with interocular hyperdensities representing retinal detachment and cystic malformation of the anterior chamber. Reprinted from [Sukalo et al., 2015] with the permission of John Wiley and Sons.

Table 3.9: AOS patients with *DOCK6* mutations.

Family (AOS-)	Patient (AOS-)	Mutations	Gender	Age	Parental consanguinity	Intra uterine growth restriction (P<3)	Scalp defect	TTLD [hands/feet]	Congenital heart defect	Brain anomalies	Microcephaly	Ocular anomalies	Cognitive impairment	Neurology	Additional features	Reference
1	1.1	[p.L1016P] + [p.L1016P]	F	5y	+	na	+	+/+	na	na	+	MO,RD,VO,ACA	DD	SE	high palate	-
2	2.1	[p.T455Sfs*24] + [c.4491+1G>A]	M	10y	-	-	+	+/+	na	VD/BA,CCH	+	NS	sev ID	SE, CP	CMTC, single umbilical artery, cryptorchidism	-
3	3.1	[p.Q434Rfs*21] + [p.Q434Rfs*21]	M	20y	+	+	+	+/+	-	VD/BA,PVL	+	MO,RD,ACA	sev ID	SE, CP	CMTC, abdominal skin defect	-
4	4.1	[p.R1596W] + [p.R1596W]	F	3m	+	-	+	+/+	PDA	VD/BA	+	MO	na	-	knee dislocation	-
5	5.1	[p.E1052K] + [p.E1052K]	M	9y	+	+	+	+/+	-	VD/BA,CCH,PVL	+	MO,RD	mod ID	SE	cryptorchidism	1
6	6.1	[p.V263D] + [c.5939+2T>C]	F	na	-	-	+	+/+	VSD	VD/BA,PVL	+	MO,RD,VO	sev ID	SE, CP	abdominal skin defects, absence of right patella	2
	6.2	[p.V263D] + [c.5939+2T>C] ^a	M	1w [†]	-	+	+	+/+	na	VD/BA,CCH	na	RD	na	na	abdominal skin defect, patella fixed to skin	2
7	7.1	[p.F635Pfs*32] + [c.4106+5G>T]	F	7y	-	-	+	+/+	-	NS	+	NS	sev ID	SE	abdominal skin defect	-
	7.2	[p.F635Pfs*32] + [c.4106+5G>T]	M	8y	-	+	-	-/+	TAPVD	na	na	NS	mild ID	-	hypothyroidism	-
8	8.1	[p.E162*] + [p.E162*]	F	na	+	na	+	+/+	na	na	na	na	na	na	-	-
9	9.1	[c.5235+205_6102-15delins10] + [c.5235+205_6102-15delins10]	F	7y	+	-	+	+/+	na	PVL	na	na	na	na	-	-
10	10.1	[p.R841Sfs*6] + [p.R841Sfs*6]	F	na	+	-	+	+/+	na	VD/BA,CCH,PVL	+	na	na	SE	-	-

^aGenotype was not directly confirmed as patient is deceased but is assumed to be the same as in affected sibling.

F, female; M, male; y, year(s); m, month(s); w, weeks(s); †, deceased; na, no data available; +, present; -, not present; TTLD, terminal transverse limb defects; PDA, patent ductus arteriosus; VSD, ventricular septal defect; TAPVD, total anomalous pulmonary venous connection; VD/BA, ventricular dilatation / brain atrophy; CCH, corpus callosum hypoplasia/atrophy; PVL, periventricular lesions (calcification, gliosis); NS, abnormality present; not further specified; MO, microphthalmia; RD, retinal detachment; VO, vitreous opacities/membranes; ACA, anterior chamber abnormality; DD, developmental delay; ID, intellectual disability; sev, severe; mod, moderate; SE, seizures/epilepsy; CP, cerebral palsy / spasticity; CMTC, cutis marmorata telangiectatica congenita.

References: (1) Prothero et al., 2007; (2) Orstavik et al., 1995. Families 1-4: Magdeburg; 5-7: London; 8-10: Antwerp. Adapted from [Sukalo et al., 2015].

3.2.2 *ARHGAP31*

The *ARHGAP31* gene was the first gene to be published in association with AOS [Southgate et al., 2011]. *ARHGAP31* mutations are responsible for a very rare autosomal dominant form of AOS (AOS1, MIM #100300). This gene was studied in a collective of four autosomal dominant families with AOS or isolated ACC and 24 sporadic cases. No clear mutations were detected, but some known SNPs and unclassified variants. Table 3.10 summarises the three unclassified variants (two silent changes and a missense mutation) with a MAF <0.01 in TGP that were detected heterozygous in one patient each. Variants were again analysed applying the algorithms described in chapter 2.3.19. The results are tabulated in Appendix C (Table C.1.5 and Table C.2.5). When using *in silico* prediction for the missense variant p.Thr727Ile, it was rated non-pathogenic by all employed online tools, PolyPhen-2, SIFT, MutPred, and GERP (Table C.1.5). Additionally, this position is not even conserved in *Mus musculus* and it was detected in two control DNAs by our partners in London. All three variants are predicted to not affect splicing of the exon, according to BDGP and NetGene2 (Table C.2.5).

Table 3.10: Unclassified variants in *ARHGAP31*.

Location	Nucleotide alteration	Predicted effect	Frequency our cohort	Frequency ExAC	dbSNP
Exon 04	c.384G>C	p.L128L	1.72%	0.1764%	rs150339878
Exon 12	c.2180C>T	p.T727I	1.72%	0.06215%	rs539048828
Exon 12	c.2901C>T	p.L967L	1.72%	0.001659%	-

Only variants within 20 bp of the exons and MAF ≤ 0.01 (in TGP) were included.

3.2.3 *RBPJ*

During the course of this study, *RBPJ* was published as a further gene associated to autosomal dominant AOS (AOS3, MIM #614814) [Hassed et al., 2012]. This gene was screened in 24 sporadic cases and four autosomal dominant families from our cohort with clinically diagnosed AOS or isolated ACC or TTLD. No mutations of this gene were identified in our cohort. The majority of the *RBPJ* mutational screening in our patients was performed in the lab of our collaboration partner in Antwerp, but nine cases were sequenced in our lab. All variants detected in this gene were classified as benign.

3.2.4 *EOGT*

The gene *EOGT* was published in 2013 as the second gene for an autosomal recessive form of AOS (AOS4, MIM #615297) [Shaheen et al., 2013]. Autosomal recessive families (n=13) and sporadic cases (n=16) from our AOS cohort were screened for mutations in the *EOGT* gene. Sanger sequencing in this cohort was performed in Magdeburg (n=12) and Antwerp (n=17). We detected a homozygous splice site mutation in one of our AOS patients (AOS-11.1) which we confirmed in both parental DNA samples in the heterozygous state. This c.311+1G>T splice donor mutation in intron 5 is listed in dbSNP (rs369583084) and was detected four times heterozygous in 60,706 unrelated individuals (0.003301%; ExAC Browser). This sequence alteration is predicted to abrogate the splice donor site of exon 5 as predicted by the splice site prediction tools BDGP and NetGene2 (Table C.2.6).

The parents of the index patient had had a stillbirth prior to the index patient. This male stillborn was documented to have a large scalp defect with underlying skull defect and TTLD affecting all four limbs. Otherwise, the development was appropriate for gestational age (31 weeks); intrauterine death was attributed to placental insufficiency. The index patient is aged 25 years and presented with a large scalp defect and underlying bony defect, but only very subtle limb defects were noticed (Figure 3.17). The skull defect closed spontaneously around the age of 18 years, the scalp defect is still visible as a large bald area on the vertex. Livedo of the hand was documented and can be interpreted as a form of CMTC. Cognitive function appears to be normal, and a cranial CT scan and cardiac examination did not reveal any anomalies.

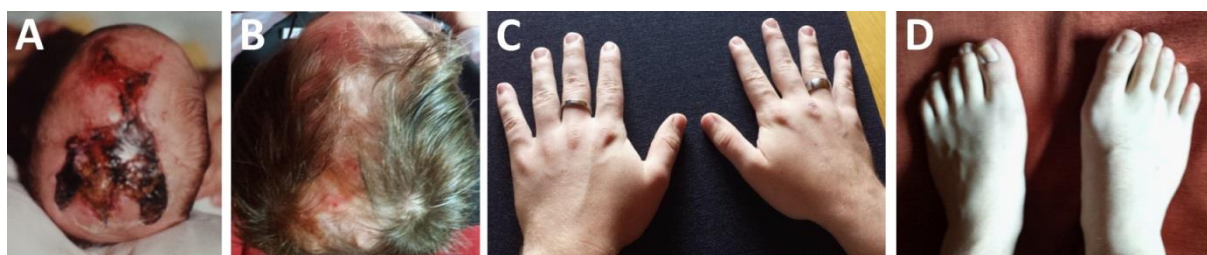


Figure 3.17: Clinical pictures of a patient with *EOGT*-associated AOS.

(A) Baby boy with large scalp defect and underlying bony defect spanning from parietal to vertex region. (B) Same patient with a large hairless scar on his scalp at the age of 25 years. (C) Slightly hypoplastic terminal phalanges of fingers. (D) Feet without visible limb defects.

3.2.5 *NOTCH1*

Mutations in the gene *NOTCH1* were first published to cause another autosomal dominant type of AOS (AOS5, MIM #616028) in 2014 [Stittrich et al., 2014]. Independently, *NOTCH1* mutations were detected in two AOS patients by exome sequencing performed in the lab of our collaboration partner in London. Subsequently, the patient cohorts from Magdeburg, London, and Antwerp were screened for further mutations in the *NOTCH1* gene. Patients with AOS and also patients with ACC were screened for mutations within this gene. Sequencing of 17 patients from our cohort was performed in London in the lab of our collaborator Laura Southgate, while nine patients were screened for *NOTCH1* mutations in our lab (all sporadic cases). Among the index patients from 22 families with sporadic occurrence of AOS or ACC and four autosomal dominant families with AOS or ACC from the Magdeburg cohort, 10 mutations were detected (Table 3.11). Eight of the 10 mutations and the respective families were included in the publication by Southgate et al. [2015] and two families were ascertained since then. Missense mutations were the major type (70%). In the 10 *NOTCH1* mutation positive families from our cohort, only one splice site mutation, one nonsense mutation and one frameshift mutation were detected. *In silico* prediction of the missense mutations was performed using the above mentioned online prediction tools (chapter 2.3.19); the resulting scores and protein alignments are summarised in Table C.1.6. Splice site prediction can be found in Table C.2.7. None of the detected mutations was recurrent within our Magdeburg cohort, but the p.Arg448Gln missense mutation was – besides from our patient of Greek origin (family AOS-23) – also reported in a patient from the London cohort, originating from the United Kingdom [Southgate et al., 2015]. Also, none of the detected mutations was annotated in the dbSNP or TGP databases. In ExAC, the variants p.Ala1740Ser (allele frequency 0.008402%) and c.1669+5G>A (0.0008530%) were the only listed variants. Parents were analysed when appropriate material was available (families AOS-12, -13, -14, -15, -18, -21).

Table 3.11: Mutations in the *NOTCH1* gene that are related to AOS.

Location	Nucleotide alteration	Predicted effect ^a	Family (AOS-)	Reference
Exon 07	c.1220C>G	p.P407R	15	[Southgate et al., 2015]
Exon 08	c.1343G>A	p.R448Q	19	[Southgate et al., 2015]
Exon 08	c.1345T>C	p.C449R	14	[Southgate et al., 2015]
Exon 08	c.1367G>A	p.C456Y	18	[Southgate et al., 2015]
Exon 08	c.1393G>A	p.A465T	20	-
Intron 10	c.1669+5G>A	<i>p.F520_G557del</i>	21	-
Exon 25	c.4120T>C	p.C1374R	12	[Southgate et al., 2015]
Exon 26	c.4663G>T	p.E1555*	13	[Southgate et al., 2015]
Exon 26	c.4739dupT	p.M1580Ifs*30	16	[Southgate et al., 2015]
Exon 28	c.5218G>T	p.A1740S	17	[Southgate et al., 2015]

^aItalic letters indicate that the effect of splicing mutation was demonstrated on the mRNA level.

Figure 3.18 illustrates the location of observed mutations relative to functional domains of the NOTCH1 protein. Six missense mutations and one donor splice site mutation are located within the extracellular domain composed of 36 EGF-like repeats. The missense mutations p.Pro407Arg, p.Arg448Gln, p.Cys449Arg, p.Cys456Tyr, and p.Ala465Thr are clustered in EGF-like repeats 10 to 12. The splice site mutation c.1669+5G>A affects an exon located in EGF-like repeats 13 and 14. Furthermore, the missense mutation p.Cys1374Arg is located more C-terminally in the EGF-like repeats domain. The only observed missense mutation localised outside of the EGF-like repeats is p.Ala1740Ser; this amino acid substitution affects the transmembrane domain of the NOTCH1 protein and has a less clear effect on the structural integrity of the receptor, when compared to the other missense mutations [Southgate et al., 2015]. The nonsense mutations p.Glu1555* and p.Met1580Ilefs*30 are located at the C-terminal end of the extracellular domain. These mutations either lead to degradation of the mutant mRNA through nonsense mediated mRNA decay, which is more likely, or result in a truncated protein where the intracellular domain is missing.

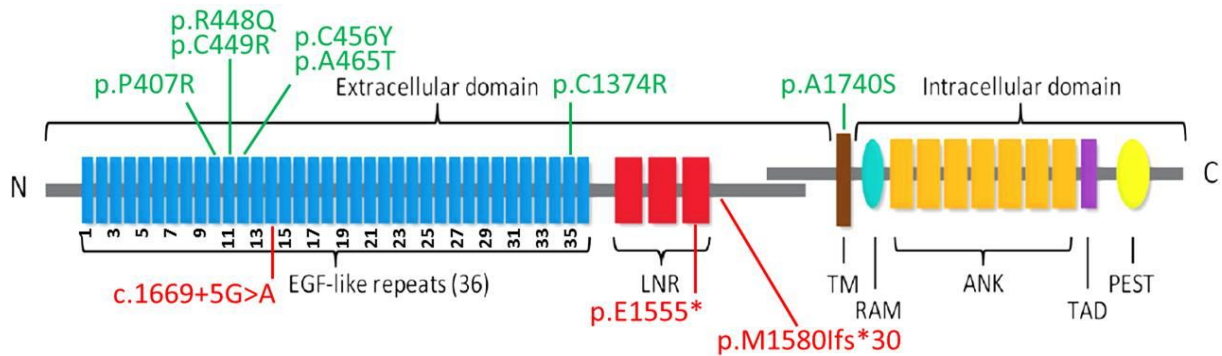


Figure 3.18: NOTCH1 protein with functional domains and distribution of mutations.

Schematic of the NOTCH1 protein highlighting the critical functional domains. Missense mutations are written in green, truncating and splice site mutations are written in red type. EGF, epidermal growth factor; LNR, Lin-12/Notch repeats; TM, transmembrane domain; RAM, RBP-J κ -associated molecule; ANK, ankyrin repeats; TAD, transactivation domain; PEST, peptide sequence that is rich in proline, glutamic acid, serine, and threonine. Adapted from [Southgate et al., 2015].

The unpublished splice site mutation c.1669+5G>A that was detected in family AOS-21 was evaluated in detail as shown in Figure 3.19. Sequencing of both parents revealed that the mutation was inherited from the father (Figure 3.19A). In silico prediction was ambiguous; BDGP predicted total loss of the donor splice site, whereas in NetGene2 no difference was seen when comparing wild type and mutated allele. The father was, so far, not diagnosed to have AOS. Detailed re-evaluation did not detect a scalp or limb defect, but CMTC had been recorded at birth; echocardiography did not reveal any anomalies. To prove a possible effect on mRNA splicing, RT-PCR experiments were performed on paternal material. Gel electrophoresis of the PCR-amplified cDNA fragment showed two bands representing the normal product and an abnormal fragment shortened by approximately 100 bp (Figure 3.19B). Sequencing confirmed skipping of exon 10 (Figure 3.19D). As both bands are nearly equal in intensity, we suggest that the mutated splice site is not working and therefore the majority of mRNA produced from this allele is missing exon 10. This assumption is supported by the electropherograms shown in Figure 3.19D where the overlying peaks (caused by the heterozygous deletion of exon 10) have nearly the same height (Figure 3.19D).

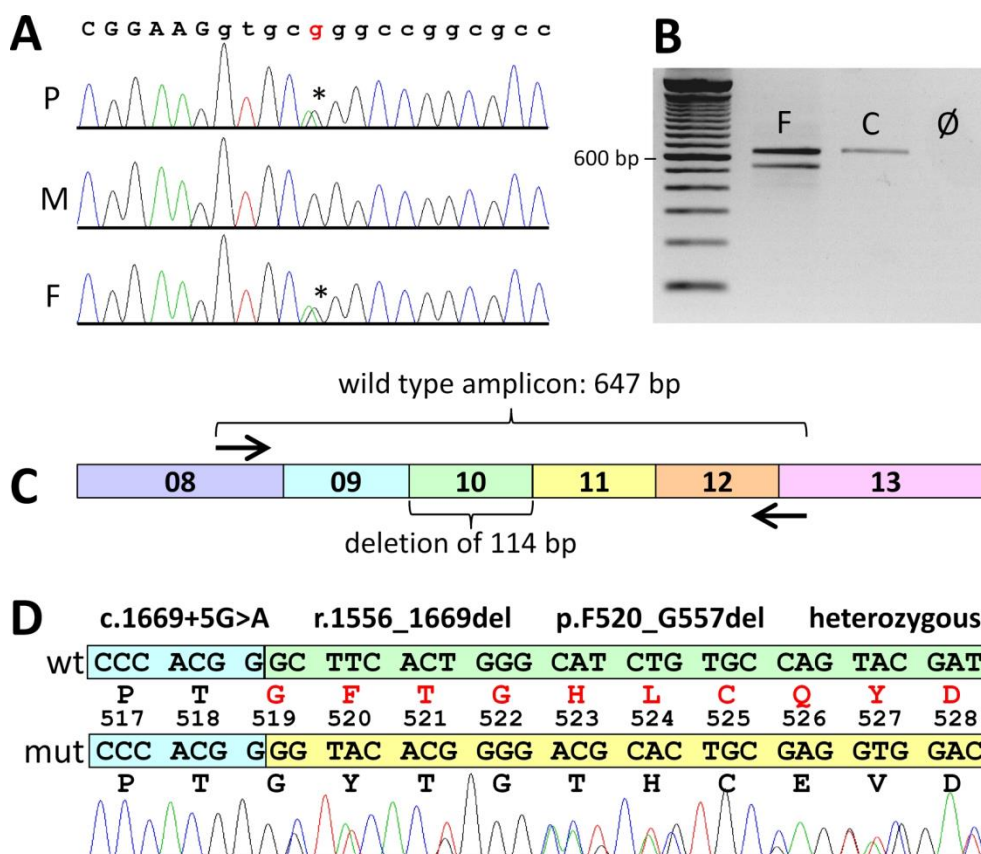


Figure 3.19: Analysis of a splice site mutation in *NOTCH1*.

(A) Electropherograms of family AOS-21 showing the splice site mutation c.1669+5G>A on genomic DNA level. In the shown sequence, capital letters indicate exonic regions, intronic regions are written in lower case letters. (B) Gel electrophoresis of paternal cDNA gained from RT-PCR that was performed with RNA extracted from blood with the help of the PAXgene system. The two bands represent a wild type allele (same as in the control) and a shorter fragment missing approximately 100. (C) Position of RT primers (NOTCH1_C08F and NOTCH1_C12-13R), relative exon sizes and location of the deletion. (D) Wild type cDNA sequence (wt) and amino acid residues are compared to the mutated cDNA sequences (mut) and subsequent amino acid residues. Wild type shows correct junction of exon 9 (blue box) and 10 (green box). In the cDNA of patient AOS-21.2, the splice site mutation c.1669+5G>A completely destroys the donor splice site which subsequently causes deletion of the whole exon 10 (r.1556_1669del). No frameshift is generated, but 38 amino acid residues are predicted to be missing in the translated protein. The yellow box represents exon 11. P, patient; M, mother; F, father; C, control.

A total of 16 individuals from 10 families were identified with *NOTCH1* mutations. Ten out of 16 were found to have a scalp defect (63%), including five individuals with an underlying bony defect (31%). Twelve had TTLD (75%), including one patient (6%) with TTLD restricted to the hands and five patients (31%) with TTLD restricted to the feet. Thirteen patients had a cardiac examination, of which six (46%) showed a CHD. Those defects included VSD, ASD, aortic stenosis, and other. CMTC was documented in 39% of the patients (6/16). Additional features were epilepsy, hepatosplenomegaly and portal hypertension, missing portal vein, bilateral cryptorchidism, and other. Figure 3.20 exemplarily shows scalp defects and TTLD of *NOTCH1*-mutated patients AOS-12.1, AOS-14.1, and AOS-16.1.



Figure 3.20: Clinical features of AOS patients with *NOTCH1* mutations.

(A) Patient AOS-12.1 at age 2.8 years. (A1) Residual skin defect after multiple operations of a large scalp ACC. (A2) Minor hypoplasia of terminal phalanges of toes. (A3) Normal fingers. (B) Patient AOS-14.1 as a newborn. (B1) Large scalp defect involving the underlying bone. (B2) Hypoplasia of terminal phalanges of both feet. (C) Patient AOS-16.1 at age 14.7 years. (C1) Small area of alopecia marking a healed skin defect. (C2) Hypoplasia of terminal phalanges and nails of the left foot. (C3) Normal fingers. Adapted from [Southgate et al., 2015].

Table 3.12 summarises genotype and phenotype of all 16 individuals from 10 families with a *NOTCH1* mutation from our cohort. No gender preference can be seen. Scalp and limb defects seem to be the most frequent symptoms, but one has to keep in mind that these anomalies were the inclusion criteria for this study.

Table 3.12: AOS patients from the Magdeburg cohort with *NOTCH1* mutations.

Family (AOS-)	Patient (AOS-)	Pedigree ID	Mutation	Gender	Age	Scalp defect	TTLD [hands/feet]	Congenital heart defect	CMTC	Additional features	Reference(s)
12	12.1	III-2	p.C1374R	M	8y	++	-/+	-	+		1
	12.2	II-4	p.C1374R	M	40y	-	-	-	-		1
	12.3	II-3	p.C1374R	M	35y	-	-/+	-	-		1
	12.4	I-1	p.C1374R	M	65y	-	-	-	-		1
13	13.1	II-1	p.E1555*	F	25y	+	+/+	AS, CoA, PMV, VSD	-		1
	13.2	I-2	p.E1555*	F	47y	-	-/-	AR, AS	-		1
	14.1	II-1	p.C449R ^a	F	1y [†]	++	-/+	VSD	-		1
15	15.1	II-1	p.P407R	M	8y	+	+/-	-	-	bilateral cryptorchidism, bilateral abdominal wall hernia, hypertelorism, down-slanting palpebral fissures, lacrimal duct anomaly, cow-lick	1
	15.2	I-2	p.P407R	F	na	-	-	na	-		1
16	16.1	II-1	p.M1580Ifs*30	M	15y	+	-/+	-	+	epilepsy, dyslexia, abnormal behaviour	1
	17.1	II-1	p.A1740S	F	33y	+	+/+	na	-		1
18	18.1	II-2	p.C456Y ^a	F	16y	++	+/+	ASD, EHPVT, hepatopetal and hepatofugal collateral veins	+	hepatosplenomegaly and portal hypertension with gastrointestinal bleeding	1, 2, 3
19	19.1	II-2	p.R448Q	M	19y	++	+/+	EPVO, large hepatofugal coronary vein, tiny hepatopetal cavernoma	-	hepatosplenomegaly and portal hypertension	1, 2, 3
20	20.1	II-2	p.A465T	F	6.5m [†]	++	+/+	-	+	anemia, missing portal vein	-
	21.1	II-1	c.1669+5G>A	F	5m	+	-/+	VSD	+		-
21	21.2	I-1	c.1669+5G>A	M	30y	-	-	na	+		-

^a*de novo* mutations. ID, identifier; F, female; M, male; y, year(s); m, month(s); †, deceased; na, no data available; +, present; -, not present; ++, with underlying osseous skull defect; TTLD, terminal transverse limb defects; AS, aortic stenosis; CoA, coarctation of the aorta; PMV, parachute mitral valve; VSD, ventral septal defect; AR, aortic regurgitation; ASD, atrial septal defect; EHPVT, extra-hepatic portal vein thrombosis; EPVO, extra-hepatic portal vein obstruction; CMTC, cutis marmorata telangiectatica congenita. No brain anomalies, microcephaly, ocular anomalies, cognitive impairment, or neurological anomalies were reported in these individuals. Index patients are listed first in every family. (1) Southgate et al., 2015; (2) Girard et al., 2005; (3) Franchi-Abella et al., 2014.

The mutations p.Cys449Arg (family AOS-14) and p.Cys456Tyr (family AOS-18) were not detected in the parental DNA samples. The indicated relationships were confirmed by genotyping of 16 highly polymorphic microsatellites (AmpF ℓ STR Identifiler Plus PCR Amplification Kit), thus attesting these mutations to be *de novo*. In four families (AOS-12, -13, -15, -21) inheritance from one of the parents was demonstrated, and in another four families (AOS-16, -17, -19, -20) analysis of inheritance was not possible due to a lack of appropriate material.

The pedigrees of all 10 families from our cohort that were found to have a *NOTCH1* mutation are shown on the following page in Figure 3.21. In family AOS-12 investigation of relatives of the index patients revealed several instances familial transmission of the mutation by individuals showing only minor or no symptoms of AOS. The index patient (III-2) presented with a large scalp defect and underlying skull defect, mild TTLD of the toes, and was reported with marbled skin at birth, representing a full-blown picture of AOS. No CHDs were detected in this family. The father (II-4) is an apparently unaffected carrier of the p.Cys1374Arg mutation, just like the paternal grandfather (I-1). Thorough clinical investigation showed mildly shortened toes in the index patient's uncle (II-3) with small nails, what can be considered as a minimal sign of AOS. Hence, family AOS-12 exemplarily represents intrafamilial variability and reduced penetrance of the phenotype.

In family AOS-13, the index patient had ACC, TTLD, and CHD, whereas the mother who was also found to harbour the familial p.E1555* *NOTCH1* mutation was only reported to have aortic regurgitation and AOS. The index patient from family AOS-21 presented with AOS including ACC, TTLD, CHD and CMTC; the father, also carrying the familial splice site mutation c.1669+5G>A, was thoroughly investigated, but no AOS-associated symptoms were detected, besides a CMTC that had been reported at birth. The missense mutation p.P407R was detected in a mother and son in family AOS-15. The child had ACC and TCC, but the mother appeared to be an unaffected carrier of this mutation (Figure 3.21).

The genotypes and clinical data of families AOS-12 to AOS-19 were published together with three further families with *NOTCH1* mutations in the original article "Haploinsufficiency of the NOTCH1 Receptor as a Cause of Adams-Oliver Syndrome With Variable Cardiac Anomalies" [Southgate et al., 2015].

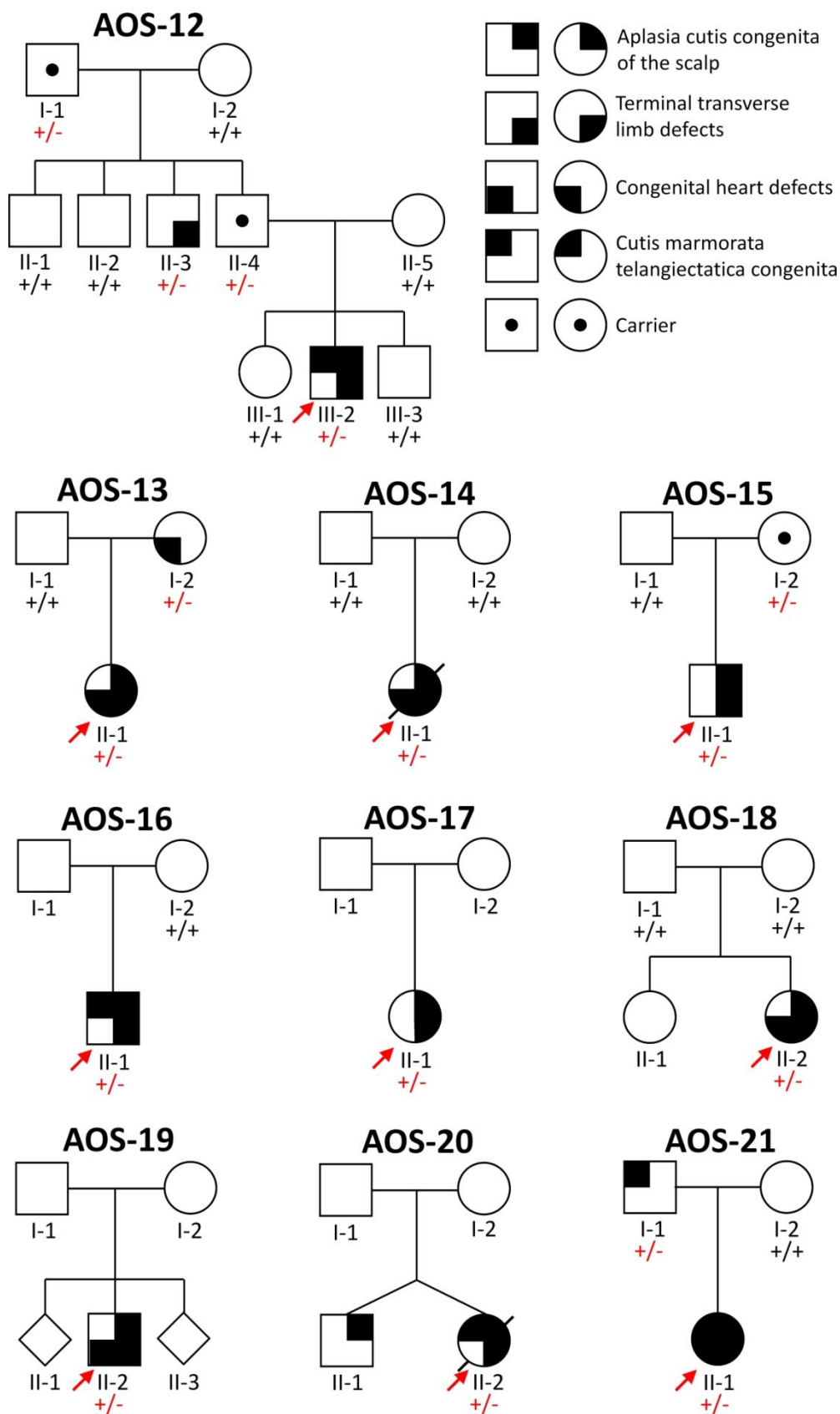


Figure 3.21: Pedigrees of AOS families with *NOTCH1* mutations.

All 10 families with *NOTCH1* mutations are displayed. Reduced penetrance and variable expression can be seen, especially in the pedigree AOS-12. +, wild type allele; -, mutated allele. Index patients are marked by red arrows.

3.2.6 *DLL4*

The latest gene that was published as responsible for AOS was *DLL4* (AOS6, MIM #616589) [Meester et al., 2015]. By whole exome analysis, our collaboration group from Antwerp identified *DLL4* as a new candidate gene for autosomal dominant AOS. Two families with suspected autosomal dominant inheritance of AOS or isolated ACC and two sporadic cases were Sanger sequenced at our lab; another index from a family with suspected autosomal dominant inheritance plus six sporadic cases from our Magdeburg cohort were analysed in Antwerp by Sanger sequencing or next generation sequencing of a custom-made AOS panel; no mutations were detected in our patients. Meester et al. [2015] screened a total of 91 families affected with AOS or isolated ACC, and identified nine heterozygous variants in the *DLL4* gene.

4 DISCUSSION

4.1 JOHANSON-BLIZZARD SYNDROME

Within this study, a broad range of *UBR1* mutations was detected in JBS patients. In the complete cohort of 60 families with JBS that were genetically analysed during and prior to my thesis work, 117 mutations were detected on 120 *UBR1* alleles, which equals a mutation detection rate of 97.5%. By applying conventional Sanger sequencing, 112 mutations (93.3%) were detected; MLPA analysis added another five mutated alleles (4.2%). Mutation types and their frequencies are displayed in the pie chart in Figure 4.1. This mutational spectrum is typical of autosomal recessively inherited diseases with loss of function mutations. Overall, many truncating mutations were detected (42.5%), and these were distributed across the whole gene. The missense mutations (25%) were clustered in known functional domains (UBR box) but apparent clustering was seen also in domains of hitherto unknown functional relevance. The broad mutational spectrum includes mostly private mutations; only eight recurrent mutations were detected in the *UBR1* gene, with the minority of them being assigned to common ancestor alleles.

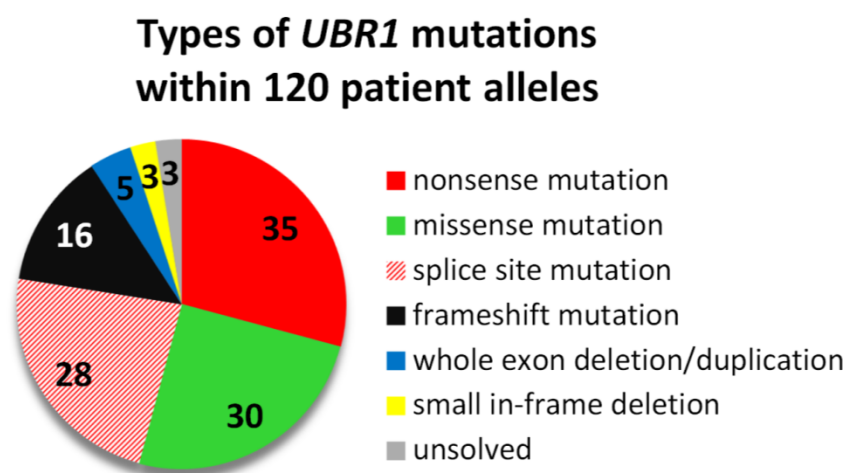


Figure 4.1: Mutational spectrum in the *UBR1* gene.

Comparison of the 13 JBS families (JBS-1 to JBS-13) described by Zenker et al. [2005] with those identified during my thesis work (JBS-36 to JBS-59) reveals significant differences in the mutational spectrum. The major types of mutations seen in the 26 alleles of families JBS-1 to JBS-13 are nonsense (46%) and splice site (27%) mutations.

These mutation types were only seen in 23% and 19% of the 48 alleles of families JBS-36 to JBS-59. On the other hand, missense mutations accounted for 31% of the mutated alleles in JBS-36 to JBS-59, whereas only 8% of the alleles from families JBS-1 to JBS-13 harboured a missense mutation of the *UBR1* gene. These discrepancies can be explained by the different inclusion criteria applied when recruiting the patients. Identification of the *UBR1* gene in 2005 was accomplished in patients with a severe manifestation and full-blown spectrum of JBS symptoms, whereas the inclusion criteria for retrospectively recruited patients were softened to possibly discover *UBR1*-related phenotypes beyond the previously known phenotypic spectrum of JBS and/or delineate new clinical entities or subtypes. These differences in the clinical manifestation and mutational spectrum are consistent with the identified genotype-phenotype correlation which is described in detail in chapter 4.1.2.

The results gained prior to and during my thesis work suggest, that JBS is a genetically homogeneous disease only caused by mutations of the *UBR1* gene. This could still be true considering the mutation detection rate of 97.5%. The few unsolved alleles may carry mutations located in intronic or promoter regions, or larger deletions or duplications that were not detected with the available methods. In fact, in patients with a clear JBS phenotype, only three alleles remained without a *UBR1* mutation after sequencing and MLPA. This included one patient where a mutation could be identified on only one allele (JBS-24.1) and another one with completely normal sequencing and MLPA results (JBS-60.1):

In patient JBS-24.1 a missense mutation was detected on one allele; the second allele remained unsolved in sequencing and MLPA approaches. Presumably this individual harbours a mutation on the second allele that could not be identified due to methodological limitations. Overrepresentation of the allele carrying the p.Ala563Asp mutation was demonstrated on mRNA-level, thus suggesting instability of the mRNA produced from the allele assumed to harbour the unidentified mutation. Additionally, immunoblotting revealed clearly decreased expression of the *UBR1* protein.

On the other hand, patient JBS-60.1 [Takahashi et al., 2004], who definitely displayed all major and additionally some minor JBS symptoms, raises doubts regarding the hypothesis of genetic homogeneity in JBS. Extensive experiments, including Sanger sequencing, MLPA analysis, linkage analysis, and immunoblotting of the *UBR1* protein did not reveal any hints to a mutation of the *UBR1* gene or deficiency of the protein

product. Exome or genome sequencing in this patient may reveal a new candidate gene for JBS. However, we currently do not have any additional JBS patients with unsolved genetic etiology to confirm a new candidate.

4.1.1 PHENOTYPE ASSOCIATED WITH *UBR1* DEFICIENCY

Phenotype data from 73 affected individuals with a confirmed *UBR1* defect could be reviewed and analysed in this study. All individuals carrying homozygous or compound heterozygous *UBR1* mutations as well as the individual in whom the mutation could only be identified on one allele had a clear clinical diagnosis of JBS. We did not find any evidence for a contribution of mutations in this gene to other phenotypes partially overlapping with JBS such as isolated EPI in children or other types of syndromic scalp defects. However, the clinical expression of the syndrome and of individual manifestations showed wide variation. This variability appeared to be more pronounced between than within families. All 70 patients with a proven *UBR1* defect and of whom the data was available were affected by clinically apparent EPI leading to failure to thrive. Manifestation of this symptom was documented within the first year of life, in the vast majority shortly after birth. All patients who were followed up for long term had a need of permanent pancreatic enzyme supplementation. As a second highly consistent anomaly, all patients displayed anomalies of the nasal wings that ranged from quite subtle hypoplasia to complete aplasia of the nasal wings (Figure 4.2).

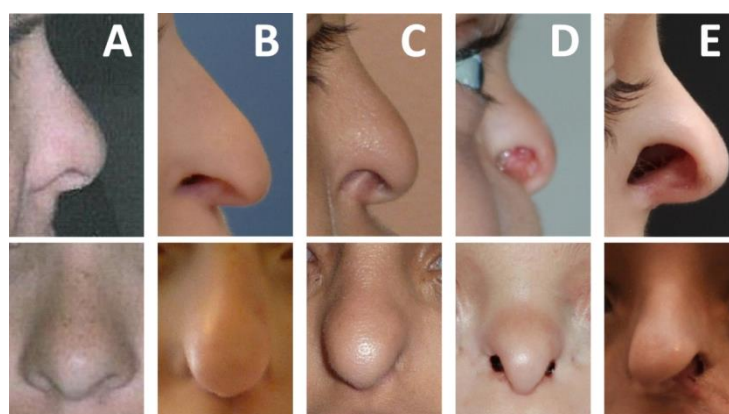


Figure 4.2: Broad range of underdeveloped alae nasi in JBS patients.

These patients are from our JBS cohort and were tested positively for *UBR1* mutations. (A) Subtle hypoplasia. (B) Hypoplasia. (C) Severe hypoplasia. (D) Aplasia. (E) Aplasia with facial clefting, surgically corrected.

In some cases the nasal wing defects were associated with more severe lateral facial clefting. A recent publication has been dedicated to this aspect [Corona-Rivera et al., 2016]. In the reported patients, the facial clefts vary in the clefting lines from types 2 to 6 of Tessier's classification [Tessier, 1976], but in all cases the nasal wings are involved. Remarkably, out of the seven JBS patients with facial clefting, four had the same homozygous nonsense mutation (p.Gln513*) and were of Latin-American descent. Oblique facial clefting mostly occurs as rare sporadic cases and has an incidence ranging from 0.75 to 5.4 per 1,000 common clefts [van der Meulen, 1985]. Carefully reviewing all previously published cases – with and without molecular confirmation – a total of approximately 100 JBS patients have been published so far (see also discussion, chapter 4.1.5). Subsequently the frequency of oblique facial clefts in JBS is estimated to 5-10%. Our observations and review published by Corona-Rivera et al. [2016] emphasises that extensive facial clefting might be the severe end of the spectrum of facial malformations occurring in JBS. Although four out of seven patients originate from Costa Rica and share the same nonsense mutation (p.Gln513*), no obvious genotype-phenotype correlation could be identified, because the other patients have another genetic and ethnic background. Anomalies of secondary dentition (anodontia, oligodontia) were also present in all patients on whom appropriate information of the dental status was available (36 out of 73 patients).

Based on these data gained from our cohort of 73 JBS patients with *UBR1* mutations we propose the following clinical criteria for the diagnosis of JBS:

1. EPI with onset in infancy (by the end of the first year of life)
2. Nasal wing hypoplasia/aplasia
3. At least one of the following: sensorineural deafness, scalp defect, hypothyroidism, or imperforate anus.
4. Hypodontia of permanent teeth

For clinical diagnosis of JBS criterion 1 (EPI) plus two out of the three other criteria (2-4) are required. When applying these criteria to the cohort we oversee, 99% of patients with a confirmed *UBR1* defect would have been classified as having JBS. The only exception is patient JBS-54.1 who has a very mild manifestation of symptoms [Atik et al., 2015]. The girl aged 3 years was documented to have EPI and hypoplastic alae nasi, but the permanent teeth were not erupted so far and no roentgenographic imaging

was performed. She was documented to have no further symptoms that have been associated to JBS so far.

Vice versa, only one patient (JBS-60.1) fulfils those clinical criteria but was not found to harbour a *UBR1* mutation (by Sanger sequencing and MLPA) or *UBR1* deficiency (by immunoblotting).

4.1.2 GENOTYPE-PHENOTYPE CORRELATIONS

In order to determine to what extent the *UBR1* genotype may contribute to the variability of the clinical expression, we compared the group of patients with biallelic *truncating* (nonsense, frameshift) mutations (group 1; n=26) to those with a *non-truncating* mutation (missense or small in-frame deletion) on at least one allele (group 2; n=23), assuming that truncating mutations most likely lead to complete lack of a functional *UBR1* protein, while non-truncating mutations may in some cases retain some residual protein function. Biallelic splice site mutations were excluded from this evaluation because we cannot predict the exact impacts of those pathogenic variants. Besides the highly consistent symptoms of EPI and hypodontia, this comparison revealed gradual differences in other aspects of the disease (Figure 4.3). Regarding the facial phenotype, it was observed that milder expression of nasal wing hypoplasia was significantly associated with the presence of at least one non-truncating allele, whereas facial clefting and complete aplasia of the alae nasi were typically found in patients with biallelic truncating alleles. Patients with two biallelic truncating mutations constantly presented with hearing impairment (100%) and cognitive impairment (100%), and frequently with short stature (88%), whereas individuals of the group with non-truncating mutations showed these features in a significantly lower frequency: 44%, 39% and 50%, respectively (Figure 4.3). Several other symptoms were also seen at a higher frequency in group 1, although the differences did not reach statistical significance due to a lower overall prevalence. Those included microcephaly (45% in group 1 vs. 33% in group 2), heart defects (33% vs. 13%), imperforate anus (32% vs. 13%), genital malformations (24% vs. 9%) and diabetes (14% vs. 5%). The clinical data collected for the study does not allow to exclude that some of the observed differences (e.g. in stature, head growth) might at least in part be secondary to nutritional aspects related to the severity of pancreatic dysfunction. Scalp defects, hypothyroidism, IUGR

and renal anomalies had an almost equal distribution in both groups. The most evident difference was related to the mental status of the patients. In group 1, all patients had some degree of cognitive impairment, with half of them classified as having moderate to severe intellectual disability, whereas in group 2 more than half of the individuals were reported to have intellectual abilities within the normal range. Together, these findings suggest that at least some of the non-truncating mutations might represent hypomorphic alleles. Different levels of residual function have indeed been demonstrated for three missense mutations examined in a yeast model [Hwang et al., 2011]. However, there is currently no method available to easily assess the function of mutant UBR1 proteins. The data also suggest that the minimal requirements for UBR1 function vary between different cells/tissues. While some residual UBR1 protein function seems to be sufficient for rescuing the brain function, it is insufficient to prevent pancreatic insufficiency, oligodontia and nasal wing hypo-/aplasia.

Although this analysis provides evidence for a significant impact of the genotype on phenotypic expression of JBS, intrafamilial clinical variability between siblings carrying the same mutations can be observed. For example, patient JBS-19.1 was reported to have – besides the obligate JBS symptoms – diabetes, hearing impairment and a serious congestive cardiomyopathy whereas her older sister (JBS-19.2) did not exhibit any of these symptoms [Elting et al., 2008]. Patients JBS-22.1 and -22.2 [Reichart et al., 1979] were sisters with the same homozygous missense mutation. Both were reported to have a relatively mild phenotype, but there were differences in mental and hearing abilities. In another family (JBS-4) one affected child had severe lethal urogenital malformations while the older brother had no such anomalies [Schoner et al., 2012]. Taking this into account, it is obvious that the *UBR1* genotype alone cannot explain all the phenotypic variability. The existence of unlinked genetic or non-genetic modifiers or stochastic factors has to be assumed, but their nature as well as their possible impact on the phenotype is currently unknown.

On the severe end of the spectrum of facial malformations, lateral facial clefting was observed in several individuals, notably in four patients from three Costa Rican families (JBS-1, -2, -43) with the same homozygous nonsense mutation p.Arg513*. It was speculated that this may rather be an effect of genetic background than directly correlated with this specific *UBR1* genotype, giving the possibility of an unidentified genetic modifier in JBS [Corona-Rivera et al., 2016; Sukalo et al., 2014a].

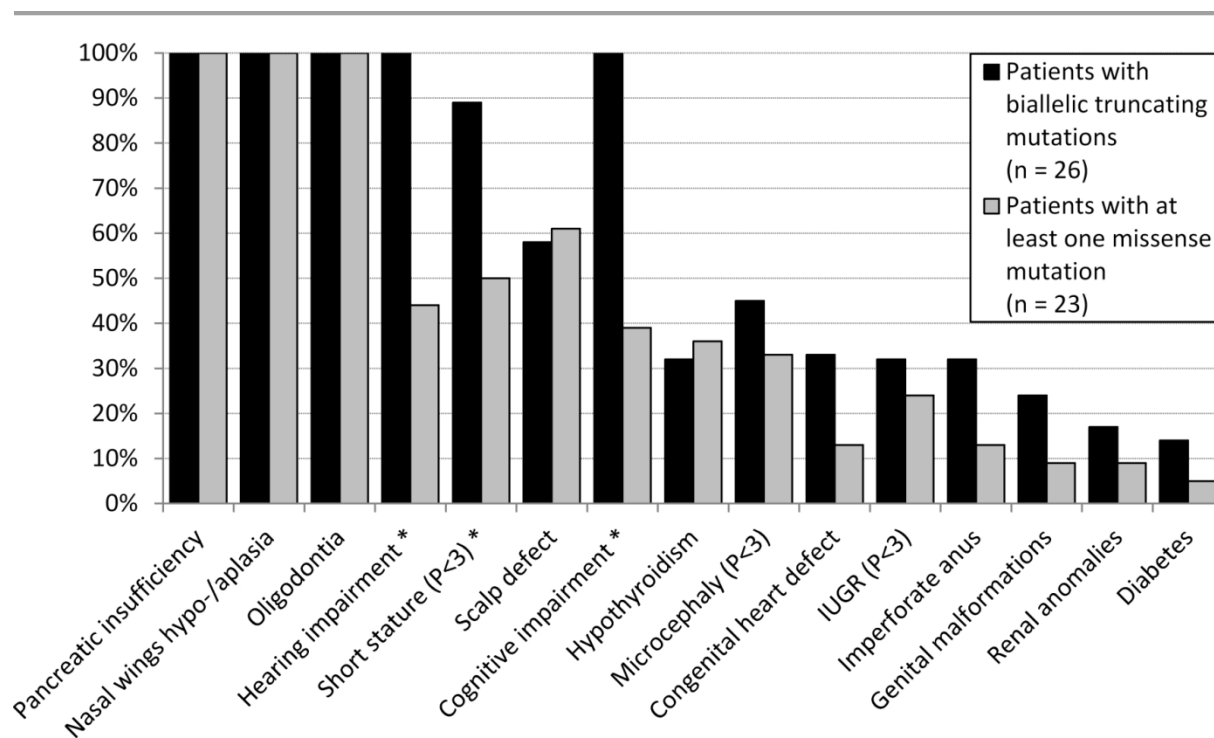


Figure 4.3: Genotype-phenotype correlation in JBS patients.

Comparison of clinical data derived from 26 JBS patients with biallelic truncating mutations (black bars) and 23 patients with at least one non-truncating mutation (grey bars). Symptoms showing significant differences ($P < 0.05$ in Fisher's exact test) between those two groups are marked with asterisks. $P < 3$, percentile below 3rd (according to growth charts from World Health Organisation and Robert Koch Institut); IUGR, intrauterine growth restriction.

Additionally, it is reasonable that microcephaly and hypothyroidism are correlated with cognitive abilities of the JBS patients. Of the patients with data for head circumference and cognitive abilities, all six patients with microcephaly were also found to have impaired intellectual functioning; vice versa, all 11 patients with normal intellectual abilities did not have a head circumference in microcephalic range (Table 3.6). Fifteen out of 17 patients with documented hypothyroidism were reported to have intellectual disability of varying degree, which equals 88%. On the other hand, only two out of 16 patients (12.5%) with cognitive abilities within the normal range were reported to have hypothyroidism. It is well known that hypothyroidism occurring in infancy has a negative impact on brain development, and only immediate and efficient treatment is able to prevent severe intellectual deficits.

4.1.3 PATHOPHYSIOLOGY OF JBS

So far, the pathophysiology of JBS has not been studied sufficiently. The biological mechanism affected in JBS, namely the N-end rule pathway, regulates degradation of intracellular proteins and subsequently their half-life [Varshavsky, 1996]. Therefore, the JBS-associated UBR1 defect is supposed to lead to an inadequate overexpression of several proteins, which probably causes pathogenetic effects in particular cells [Zenker, 2008]. It is possible that different proteins that are involved in the pathogenesis of specific tissues and organs might be affected, having in common only that they are targets of the N-end rule pathway [Zenker, 2008]. Therefore, the analysis of pathophysiological mechanisms is challenging and requires appropriate cell or tissue models.

Some of the symptoms commonly seen in JBS seem to result from early defects of organ development; this type of development anomalies includes defects of nasal wings and scalp, imperforate anus, genitourinary and heart anomalies and defects of dental anlages. However, there is also evidence that other organ manifestations do not result from disturbed primary development, but instead are the consequence of destructive and potentially progressive processes occurring beyond organogenesis, including EPI, hearing loss, and hypothyroidism. Autopsy findings in pancreatic tissues of JBS fetuses suggested that the EPI in JBS is caused by an early-onset destruction of the exocrine part of the pancreas [Zenker et al., 2005; Zenker et al., 2006]. Observation of a very young patient with seemingly intact pancreatic function [Al-Dosari et al., 2008] further supports the hypothesis of a progressive decay of acinar tissue as the cause of impaired exocrine pancreatic function. Additional evidence for an ongoing destruction of the pancreas is given by the late onset of diabetes [Zenker et al., 2006] which has been documented during the teenage years in four JBS patients from our cohort (JBS-10.1, -24.1, -28.1, -32.2). Zenker et al. [2006] postulated that UBR1 plays a critical role in maintaining the integrity of acinar cells and that the destruction of pancreatic tissue in JBS is caused by necrotic acinar cell loss [Zenker et al., 2006]. Identification of the underlying molecular mechanisms has to play a role in future research on JBS and UBR1.

4.1.4 MOLECULAR GENETIC ANALYSIS OF THE *UBR1* GENE IN DIAGNOSTICS

The implications of the experience gathered within this study for the application of *UBR1* analysis in a clinical diagnostic setting have been summarized in the *Clinical Utility Gene Card* by Sukalo et al. to help clinicians with the diagnosis and to discuss the relevance of mutation testing in the *UBR1* gene [Sukalo et al., 2014b]. Sequencing of coding exons of the *UBR1* gene and adjacent intronic sections (splice sites) and – if necessary – complemented by MLPA analysis for exon deletions/duplications, is useful to confirm a clinical diagnosis of JBS. Families with proven *UBR1* mutations can be offered prenatal and carrier testing. As clinical signs of JBS are usually present from birth, the genetic test, even in young children, is to be considered diagnostic and not predictive.

The clinical specificity (proportion of negative tests if the disease is not present) of *UBR1* testing is 100%. On the basis of current experience gathered in this project, it can be excluded that a healthy individual carries disease-causing *UBR1* mutations on both alleles. The positive clinical predictive value (life-time risk of developing the disease if the test is positive) of *UBR1* testing is also 100%, because penetrance of the disease is complete, and in all known cases symptoms had been present from birth. There is, however, considerable variability in the clinical expression with a larger interfamilial than intrafamilial variability. Because genotype-phenotype correlations are only tentative, genotype-based predictions regarding severity of the disease are very limited.

In the vast majority of patients, the clinical picture is very clear and distinctive. Stool tests (fat excretion and fecal elastase determination) and imaging by ultrasound/CT may be required to substantiate EPI. Furthermore, audiometry, blood tests of thyroid hormones and dental x-rays are helpful to corroborate the diagnosis. Genetic testing, however, is the only diagnostic tool that provides a definite diagnosis, and thus cannot be replaced by alternative methods in cases where some uncertainty remains about the clinical diagnosis (especially in patients with mild symptoms). Moreover, identification of the causative mutations in a family is the precondition for carrier identification or early prenatal testing.

As treatment of JBS is purely symptomatic, all therapeutic measures mainly depend on the individual clinical problems and not on the genetic test result. Treatment should include pancreatic enzyme replacement and dental surgery. Further therapeutic treatment includes – in necessary – hearing aids, surgery for correction of congenital

malformations, thyroid hormone substitution, special education, and controls/regulation of the blood sugar level. Multidisciplinary follow-up covering all the health issues known in JBS has to be recommended. Since known genotype-phenotype correlations are only tentative, results of genetic testing are unlikely to modify the prognosis. However, the molecular test is essential to confirm the clinical diagnosis and for accurate genetic counselling of the families concerned. The possibility of molecular carrier enables more precise genetic risk assessment in family members.

The result of the molecular genetic test may have no immediate medical consequences for the affected individuals and their families, but having a positive molecular genetic diagnosis will influence genetic counselling and may influence reproductive decisions. It is likely that relatives will consider genetic counselling and carrier testing to assess their own risks. Patients themselves may benefit from the confirmation of a diagnosis that is not certain on a clinical basis alone in that unnecessary additional diagnostic tests can be saved. Moreover, possible symptoms that might occur during the course of the disease, such as oligodontia of permanent teeth, hypothyroidism, hearing impairment or diabetes are more likely to be detected early, if the diagnosis is clear.

4.1.5 CRITICAL REAPPRAISAL OF THE LITERATURE

In the light of the experience gathered within this project, a critical review of the literature on JBS and JBS-like phenotypes was performed. Obviously, there are published cases that are erroneously classified as JBS but they are cited in the literature again and again, leading to blurring of the characteristic JBS phenotype. This critical review includes case reports of patients suggested to have JBS without a molecular confirmation, as well as earlier reported patients that were retrospectively classified as probable JBS cases and cited as such in the literature.

Retrospectively, a case reported by Morris and Fisher in 1967 seems to be the first article to describe this entity. The reported patient presented with symptoms that are indicative of JBS, namely trypsinogen deficiency, imperforate anus, poor weight gain, delayed motor development, and a “beak-like”, small nose. The published facial photographs are typical for JBS. There are some earlier reports that have frequently been cited in reviews on JBS, including the description of individuals with fatty

replacement of the pancreas [Lumb and Beautyman, 1952], “somewhat depressed” nasal bridge [Berger and Klempman, 1965], trypsinogen deficiency disease [Townes, 1965], or pancreatic insufficiency [Grand et al., 1966], but the data provided in these reports are insufficient to clearly support the diagnosis of JBS in the described individuals. Table D.3 sums up all published cases that were available for literature review.

A total of 91 cases primarily or retrospectively classified as JBS were extracted from 78 articles published by April 2016 (for references see Table D.3; the large cohort published by Sukalo et al. [2014a] was not included), some of the individuals being described in more than one article and some articles describing more than one case. Of those 91 patients published as JBS or cited in the literature as probable JBS cases, 60 cases have sufficient documentation of the phenotype and fulfil the clinical criteria of JBS (as defined above), 31 of them having also a molecular confirmation. In 13 individuals the classification remained ambiguous due to a lack of important clinical details. Eighteen patients published as probable JBS do not meet our clinical criteria of JBS and most likely have a different diagnosis. Within this study, there was an opportunity to perform *UBR1* testing in four of those patients, confirming the absence of *UBR1* mutations. A summary with all references to those data is provided in Appendix D, Table D.3.

Interestingly, even in the last 10 years, when *UBR1* testing was already available, six publications can be found presenting five patients that, in my experienced opinion, do definitely not have JBS [Barroso et al., 2010; Ellery and Erdman, 2014; Kaba et al., 2013; Ramos et al., 2010; Santhosh and Jethmalani, 2013; Sudarshan et al., 2010]. I contacted most of them and offered a *UBR1* molecular testing on a research basis, but none of the authors was interested. The clinically atypical patient published by Kaba et al. [2013] had even been investigated in our lab before and was molecularly confirmed to have no detectable *UBR1* mutation. Nevertheless, this patient was published as a case of JBS in a Turkish journal. In general, this careful review demonstrates that many of the literature reports claiming an “expansion of the JBS spectrum” are describing cases in which the diagnosis JBS has to be challenged. This in turn underlines the hypothesis that JBS (I) is a molecularly homogenous disease, (II) is clinically variable but only within a certain spectrum, and (III) additional symptoms occur rarely and may not directly be linked to the disease. Consequently, individuals with atypical JBS and/or a novel symptom that has not been described previously should undergo analysis of the *UBR1* gene.

4.2 ADAMS-OLIVER SYNDROME

4.2.1 GENETIC BASIS OF AOS

At the beginning of this study, no genes were associated to this disease. As a member of the collaborative AOS CONSORTIUM that includes partners in Magdeburg, London, and Antwerp, we could contribute to the identification of two new genes that are associated to autosomal dominant inherited AOS [Meester et al., 2015; Southgate et al., 2015]. Furthermore, the phenotype associated to mutations in the *DOCK6* gene was delineated and the mutational spectrum was extended as part of the research that was done for this doctoral thesis [Sukalo et al., 2015].

Since 2011, six genes were published in association with AOS. Recessive types of this syndrome can result from mutations in the genes *DOCK6* (MIM *614194; AOS2, MIM #614219 [Shaheen et al., 2011]) or *EOGT* (MIM *614789; AOS4, MIM #615297 [Shaheen et al., 2013]), whereas autosomal dominant types can be caused by mutations in *ARHGAP31* (MIM *610911; AOS1, MIM #100300 [Southgate et al., 2011]), *RBPJ* (MIM *147183; AOS3, MIM #614814 [Hassed et al., 2012]), *NOTCH1* (MIM *190198; AOS5, MIM #616028 [Stittrich et al., 2014]), or *DLL4* (MIM *605185; AOS6, MIM #616589 [Meester et al., 2015]). Figure 4.4 tabulates the chronology of publications about genes associated with AOS.

2011	➤ <i>ARHGAP31</i> mutations cause autosomal dominant AOS [Southgate et al., 2011]
	➤ <i>DOCK6</i> mutations cause autosomal recessive AOS [Shaheen et al., 2011]
2012	➤ <i>RBPJ</i> mutations cause autosomal dominant AOS [Hassed et al., 2012]
2013	➤ <i>EOGT</i> mutations cause autosomal recessive AOS, new mutations in <i>DOCK6</i> [Shaheen et al., 2013]
2014	➤ New mutations in <i>EOGT</i> [Cohen et al., 2014]
	➤ New mutations in <i>ARHGAP31</i> [Isrie et al., 2014]
	➤ <i>NOTCH1</i> mutations cause autosomal dominant AOS [Stittrich et al., 2014]
	➤ New mutations in <i>DOCK6</i> [Lehman et al., 2014]
2015	➤ New mutations in <i>DOCK6</i> [Sukalo et al., 2015]
	➤ <i>NOTCH1</i> mutations cause autosomal dominant AOS [Southgate et al., 2015]
	➤ <i>DLL4</i> mutations cause autosomal dominant AOS [Meester et al., 2015]

Figure 4.4: Timeline of publications of genes associated with AOS.

4.2.2 AOS MUTATION DETECTION FREQUENCY

The Magdeburg cohort comprised 33 AOS index cases, including 10 families with suggested autosomal recessive inheritance (for criteria see chapter 2.1), 21 sporadic cases, and two families with an autosomal dominant inheritance pattern. Moreover, isolated ACC was seen in three families with suggestive autosomal recessive inheritance, in four sporadic cases, and in two families with parent-child-transmission of the phenotype, suggesting autosomal dominant inheritance. Additionally, a single sporadic case with TTLD but without ACC was analysed (Table D.1). In the 10 families with presumed autosomal recessive inheritance of AOS, we found three index patients to carry biallelic *DOCK6* mutations and one patient with a homozygous splice site mutation of the *EOGT* gene. Among the sporadic AOS cases, nine *NOTCH1* mutations were detected, and one patient turned out to have autosomal recessive, *DOCK6*-related AOS. One patient that was initially classified as a case of sporadic ACC had a *NOTCH1* mutation; clinical re-evaluation revealed subtle limb anomalies, and therefore this patient was reclassified to have AOS. Also some of the cases that were initially classified as sporadic AOS cases were reclassified as familial AOS with autosomal dominant inheritance, because relatives also carrying the familial mutation were subsequently found to have subtle signs of AOS. When including all cases of AOS, isolated ACC, and isolated TTLD, 15 out of 43 cases (35%) were explained by mutations in four of the six known AOS genes. When restricting the calculation to the 33 AOS cases (including the reclassified ACC case), we were able to detect AOS-associated mutations in 45% of the index patients (Figure 4.5). Due to our focus on *DOCK6* analysis within the AOS CONSORTIUM, the Magdeburg cohort has a bias towards autosomal recessive AOS families and thus does not represent a random AOS cohort. However, the overall mutation detection rate of less than 50% points towards additional genetic heterogeneity of this syndrome.

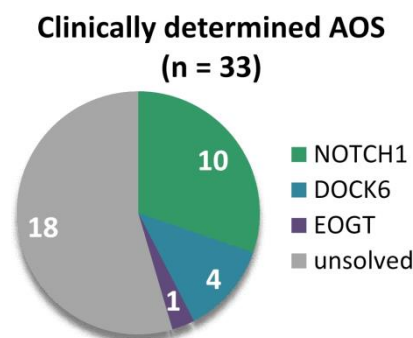


Figure 4.5: AOS mutation detection frequency in our Magdeburg cohort.

4.2.3 MUTATION SPECTRUM AND GENOTYPE-PHENOTYPE CORRELATIONS

ARHGAP31

Table 4.1 summarises the major symptoms as seen in AOS of six different genetic etiologies. Patients with *ARHGAP31* mutations appear to be quite mildly affected, compared to others AOS types, but only three families have been published, so far [Isrie et al., 2014; Southgate et al., 2011]. *ARHGAP31* mutation carriers show a significant variability and reduced penetrance of ACC and TTLD [Southgate et al., 2011]. Scalp defects were reported in less than 50% of the patients and limb defects were seen in a large variety ranging from unaffected mutations carriers to adactyly [Isrie et al., 2014; Southgate et al., 2011].

DOCK6

Studies performed within this PhD thesis focused particularly on genotype-phenotype correlations in *DOCK6*-associated AOS (AOS2). After the initial identification of *DOCK6* mutations in two families with autosomal recessive inheritance of AOS [Shaheen et al., 2011] and subsequent description of three additional families [Lehman et al., 2014; Shaheen et al., 2013], we could identify *DOCK6* as the responsible gene in 10 new families from a study cohort consisting of 78 unrelated index patients (47 sporadic cases and 31 cases with a pedigree constellation suggestive of autosomal recessive disease transmission). *DOCK6* mutations included nonsense, frameshift, missense, splice site changes, as well as one larger intragenic deletion-insertion resulting in deletion of exons 42 to 47, and are likely to confer loss of function of the gene product. Taking together mutations from previous reports and the newly identified ones from this study, it can be shown that *DOCK6* mutations are distributed over the entire gene with no obvious clustering to certain domains of the encoded protein.

The most striking phenotypic attribute of *DOCK6*-related AOS in our cohort is the strong association with important neurodevelopmental and ocular anomalies. The pattern of neurological impairment and most of the reported morphological changes (microcephaly, ventricular dilatation, periventricular calcifications, cortical changes) [Lehman et al., 2014; Shaheen et al., 2011; Shaheen et al., 2013; Sukalo et al., 2015] are suggestive of a disruptive vascular pathogenesis rather than a primary maldevelopment of the brain. Lesions classified as calcifications according to density analysis of MRI and CT images, may represent primary calcifications but can in fact also have resulted from

previous microbleeds. Likewise, the main ocular anomalies observed in our *DOCK6*-positive patients (microphthalmia and retinal detachment) are compatible with a disruptive vasculogenesis. The high prevalence of brain and eye abnormalities as well as the pattern of cerebral and ocular involvement is in line with previous case reports [Lehman et al., 2014; Shaheen et al., 2011; Shaheen et al., 2013]. However the data on the previously reported patients do not provide specific details to definitely state that brain involvement is a constant feature in AOS type 2. While *DOCK6* mutations are generally a rare cause of AOS, in our cohort they accounted for 8/25 (32%) cases presenting with major neurodevelopmental defects and for 9/19 (47%) cases with documented brain abnormalities. Taken together, these data suggest that *DOCK6* mutations are particularly responsible for a variant of AOS characterized by ACC, TTLD plus cerebral and ocular abnormalities. The existence of such a variant was postulated nearly 20 years ago on the basis of an observation of recurrence of AOS symptoms and brain defects in two siblings [Orstavik et al., 1995]. Our study could confirm that *DOCK6* is indeed the gene responsible for the disease in this family (AOS-6). The strong association of *DOCK6* mutations with anomalies of the brain and eye implies that deleterious effects on vasculature caused by *DOCK6* deficiency also affect these particular structures. In their clinical review on AOS, Snape et al. concluded that abnormal brain and ocular findings are more common in autosomal recessive AOS [Snape et al., 2009]. It is becoming clear that the individuals with *DOCK6* mutations account for a substantial part for this observation.

EOGT

By contrast, among 20 patients with *EOGT* mutations that were reported in literature, only two were reported to have brain anomalies and no abnormal ocular findings were reported in any subject [Cohen et al., 2014; Shaheen et al., 2013]. A total of 11 families (at least three of them being related) have been diagnosed with *EOGT*-associated AOS, so far, but only three different mutations were detected in this gene [Cohen et al., 2014; Shaheen et al., 2013]. The patients with the major p.Gly359Aspfs*28 mutation were found to exhibit scalp defects of variable extend, sometimes with underlying skull defects, and minor limb defects (nail deformities, syndactyly), whereas the limb defects in patients with other *EOGT* mutations also included absent phalanges. A minority of those patients (n=3) was reported to have a CHD. We could ascertain *EOGT* mutation-associated AOS4 only in a single family from our cohort. The affected

individual had a large scalp defect with underlying bony defect, mild CMTc, but only subtle limb defects were detected. Cognitive functions were classified within the normal range, and cranial CT and cardiac examination showed no anomalies. These clinical findings are in line with those described in the literature [Cohen et al., 2014; Shaheen et al., 2013] and corroborate the significant phenotypic differences between the two known recessive types of AOS.

RBPJ

The lack of a mutation in the *RBPJ* gene in our cohort is consistent with a suspected low frequency; only two families have been described to have *RBPJ* mutations until now [Hassed et al., 2012]. The limited dataset does not allow to establish genotype-phenotype correlations. The intelligence may sometimes be affected (3 out of 6 reported cases with clinical data), while structural brain anomalies and heart defects were not reported.

NOTCH1

While this PhD thesis study was in progress, mutations in *NOTCH1* were discovered to cause autosomal dominant AOS. This was first published by a competing group [Stittrich et al., 2014] who reported five families with five different *NOTCH1* mutations. *NOTCH1* was independently identified through exome sequencing by our collaboration partner in London, and our patients were subsequently studied as a replication cohort by targeted sequencing. The resulting joint publication by Southgate et al. [2015] added another 11 independent families (including eight families from our Magdeburg cohort) with nine different mutations of the *NOTCH1* gene, all of them not described before. Again – like already described for the *DOCK6* gene – we were able to confirm and delineated the genotype-phenotype correlations in *NOTCH1*-associated AOS, namely its particular association with cardiovascular anomalies. The most frequent cardiovascular defects observed in our *NOTCH1*-positive cohort were aortic regurgitation, aortic valve stenosis, coarctation of the aorta, parachute mitral valve, and VSD. Noteworthy, two patients that have previously been reported clinically [Franchi-Abella et al., 2014; Girard et al., 2005] showed unusual vascular anomalies of the portal vein with hepatosplenomegaly and portal hypertension. The mutations detected in these patients (p.Cys456Tyr and p.Arg448Gln) are located close to the missense mutations p.Cys449Gln (AOS-14.1) and p.Ala465Thr (AOS-20.1), all within the EGF-like repeats 11

and 12 of the NOTCH1 protein. Interestingly, also the other two patients carrying mutations at this particular site showed major vascular defects. Patient AOS-14.1 had truncus arteriosus; she died early in life and no autopsy was performed. Patient AOS-20.1 was reported to have a missing portal vein. Moreover, another patient from our partner's cohort (patient 5-II:1 in Southgate et al. [2015]) who also carried the p.Arg448Gln missense mutation was operated for Fallot tetralogy in infancy and at 5 years of age portal vein thrombosis and portal hypertension were documented. These observations suggest the EGF-like repeats to play an essential role in NOTCH1 functioning, especially regarding vasculogenesis. They expand the spectrum of *NOTCH1* mutation-associated vascular defects and point at portal vein anomalies as another hotspot of *NOTCH1*-related disturbance of vasculogenesis. Already in 2005, Garg et al. had identified two mutations of the *NOTCH1* gene in two families with aortic valve disease. Isolated cardiac valve anomalies as reported in these families may represent the mild end of the spectrum caused by *NOTCH1* mutations, whereas the *NOTCH1*-associated AOS is a more severe and complex phenotype with heart defects, ACC, and TTLD. Incomplete penetrance of the phenotype and intra- and interfamilial variability of the symptoms seems to be characteristic for *NOTCH1*-related (cardio)vascular disease. Interestingly, based on the similarity of cardiovascular abnormalities, *NOTCH1* had already been proposed as a candidate gene for dominant AOS with heart defects in 2008 [Digilio et al., 2008], but could not be verified on molecular level by that time. Taken together, *NOTCH1* mutation-associated AOS5 can be clinically distinguished from the other types by frequent cardiovascular involvement in addition to scalp defects and mild to moderate limb defects [Southgate et al., 2015]. Cognitive impairment has not been described for patients with *NOTCH1* mutations.

DLL4

The most recently published gene for an autosomal dominant form of AOS, namely AOS6, is the *DLL4* gene. Meester et al. [2015] report nine patients that either have isolated ACC or AOS including ACC, mild TTLD, and sometimes heart defects. Patients with suggested autosomal dominant inheritance of AOS and ACC, and sporadic cases from our Magdeburg cohort were also screened for mutations in the *DLL4* gene within the frame of this publication, but no mutations were detected.

In summary, the phenotype associations commented on above indicate that particular AOS-associated symptoms (such as involvement of central nervous system, ocular anomalies, CHD) can give a hint to the underlying gene (see also Table 4.1). However, the clinical variability within the genetic subtypes of AOS is considerable and their phenotypic spectra are grossly overlapping. Confirmation of the underlying gene can only be achieved by genetic testing. Adams-Oliver syndrome has emerged as an exceedingly heterogeneous disease where many cases still remain unsolved (55% in our Magdeburg AOS cohort), thus suggesting the existence of additional causative genes that may be disclosed in the near future.

Table 4.1: Appearance of typical symptoms in AOS subtypes.

Gene	OMIM	Inh.	ACC	TTLD	CHD	CNS	OC	Reference
<i>ARHGAP31</i>	AOS1	AD	○	○	-	-	-	[Southgate et al., 2011]
<i>DOCK6</i>	AOS2	AR	+	+	-	+	+	[Shaheen et al., 2011]
<i>RBPJ</i>	AOS3	AD	○	○	-	○	-	[Hassed et al., 2012]
<i>EOGT</i>	AOS4	AR	+	○	○	-	-	[Shaheen et al., 2013]
<i>NOTCH1</i>	AOS5	AD	+	○	+	-	-	[Stittrich et al., 2014]
<i>DLL4</i>	AOS6	AD	+	○	○	-	-	[Meester et al., 2015]

OMIM, Online Mendelian Inheritance in Man; Inh., mode of inheritance; ACC, aplasia cutis congenita; TTLD, terminal transverse limb defects; CHD, congenital heart defects; CNS, central nervous system involvement; OC, ocular anomalies; +, frequent; ○, occasional; -, no association assumed.

4.2.4 AOS PATHWAYS

The so far known six genes for AOS point towards two major functional pathways involved in the molecular pathogenesis of AOS: the ARHGAP31/DOCK6 regulatory circle and the NOTCH1 signalling pathway; the latter one also including the proteins RBPJ, EOGT and DLL4.

THE ARHGAP31/DOCK6 REGULATORY CIRCLE

The proteins DOCK6 and ARHGAP31 are linked via the Rho GTPases CDC42 and RAC1. DOCK6 (dedicator of cytokinesis 6) functions as a guanine nucleotide exchange factor for the small G proteins RAC1 and CDC42. DOCK6 can activate these by catalysing an exchange of bound GDP by GTP (Figure 4.6). Rho GTPases like Rac1 and Cdc42 are involved in the regulation of cell division, survival, and migration, and are known to be of critical importance in regulation of the actin cytoskeleton [Etienne-Manneville and Hall, 2002; Vega and Ridley, 2008]. This links DOCK6 to a role in reorganisation of the actin cytoskeleton. A siRNA induced Dock6 knockdown in N1E-155 cells (murine neuroblastoma cell line) results in a decrease of active Rac1 and Cdc42 [Miyamoto et al., 2007]. The *DOCK6* mutations detected in autosomal recessive AOS cases probably cause a *loss of function* and are therefore supposed to diminish the activation of RAC1 and CDC42.

ARHGAP31 (Rho GTPase activating protein 31) is a GAP (GTPase activating protein) for the Rho GTPases CDC42 and RAC1 [Tcherkezian et al., 2006]. Mutations in *ARHGAP31* have been proposed to cause a *gain of function*, based on the finding that mutant transcripts are stable and increase the ARHGAP31 activity *in vitro* [Southgate et al., 2011]. Just like DOCK6, ARHGAP31 regulates the Rho GTPases RAC1 and CDC42 (Figure 4.6). It acts as a GTPase-activation protein for small GTPases. Thus, its normal function is to reset activated RAC1 and CDC42 into the inactivated state. Accordingly, gain-of-function mutations in ARHGAP31 reduce the availability of active CDC42 and is assumed to have similar consequences on actin cytoskeleton regulation as loss of DOCK6 function [Southgate et al., 2011].

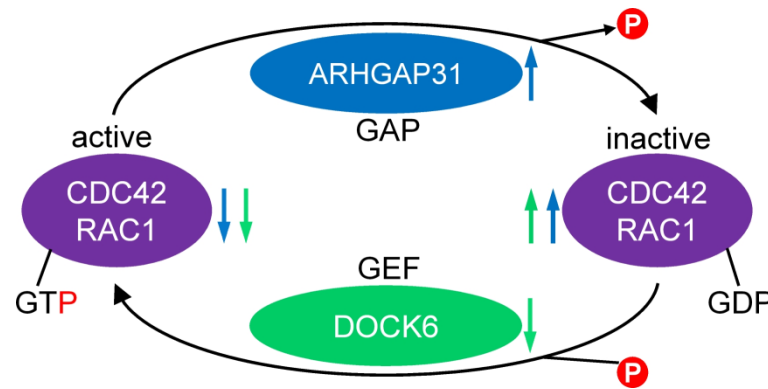


Figure 4.6: Regulatory circle of ARHGAP31 and DOCK6.

Interaction of the proteins ARHGAP31 and DOCK6 with the Rho GTPases CDC42 and RAC1. By cleavage of a phosphate residue from bound GTP, ARHGAP31 inactivates CDC42 and RAC1. Gain-of-function mutations in ARHGAP31 result in a decrease of active Rho GTPases and accumulation of inactive forms. DOCK6 catalyses an exchange of CDC42/RAC1-bound GDP by GTP and subsequently transfers the Rho GTPases into an active state. Loss-of-function mutations in DOCK6 (green arrows) have the same effect as the above mentioned gain-of-function mutations in ARHGAP31 (blue arrows). GTP, guanosine triphosphate; GDP, guanoside diphosphate; GAP, GTPase activating protein; GEF, guanine nucleotide exchange factor.

THE NOTCH1 SIGNALING PATHWAY

All the other four genes that were associated to AOS so far (*DLL4*, *EOGT*, *NOTCH1*, *RBPJ*) are part of the canonical Notch pathway (Figure 4.7). This pathway is involved in many different cellular processes, including cell-fate determination and neural and hematopoietic stem cell differentiation [Chillakuri et al., 2012; Luca et al., 2015]. Notch pathway members, particularly Notch1, also have an established role in the development of the cardiovascular system [High and Epstein, 2008]. In mammals, canonical signalling through the Notch family is stimulated by ligand binding at the cell surface. After stimulation of the Notch pathway by extracellular ligand binding, which initiates cleavage of the intracellular NOTCH1 component NICD (Notch intracellular domain), the NICD is released into the signal-receiving cell, where it complexes with RBPJ and further proteins. This complex binds to the promoter and significantly increases the transcriptional rate of the target genes *HEY1* and *HES1*. *NOTCH1* mutations are predominantly missense mutations located within EGF domains of the receptor; the majority of them is supposed to potentially perturb function by disrupting the tertiary structure and affecting Ca^{2+} -binding (which is essential for the maintenance of NOTCH1 function) and ligand interaction [Southgate et al., 2015].

Mutations in the *DLL4* gene were just recently associated with an autosomal dominant form of AOS [Meester et al., 2015]. *DLL4* is one of the canonical ligands of NOTCH1. The corresponding protein was linked to vasculo- and angiogenesis before [Liu

et al., 2003]. Expression of *DLL4* is limited to endothelial cells, particularly arteries and capillaries [Suchting et al., 2007]. Glycosylation of NOTCH1 by EOGT is an essential posttranslational modification for executing its function in the signalling pathway. EOGT glycosylates NOTCH1 by binding O-GlcNAc (O-linked N-acetylglucosamine) to serine and threonine residues. Homozygous or compound-heterozygous mutations of the *EOGT* gene are supposed to impair correct glycosylation of NOTCH1 and therefore also impair signalling of the Notch pathway. RBPJ is the principal DNA-binding partner of the NOTCH1-NICD and coordinates transcription of target genes through the assembly of protein complexes containing coactivators [Hassed et al., 2012]. Mutations in RBPJ may decrease the binding affinity to the promoters of the target genes, which presumably results in a disturbed regulation of the genes that are located downstream of this complex [Hassed et al., 2012].

Based on these functional interconnections, it is assumed that mutations in all of these four genes perturb NOTCH1 signalling; this assumption was substantiated by the demonstration of decreased *HEY1* and *HES1* gene expression in cells expressing mutant *NOTCH1* [Southgate et al., 2015].

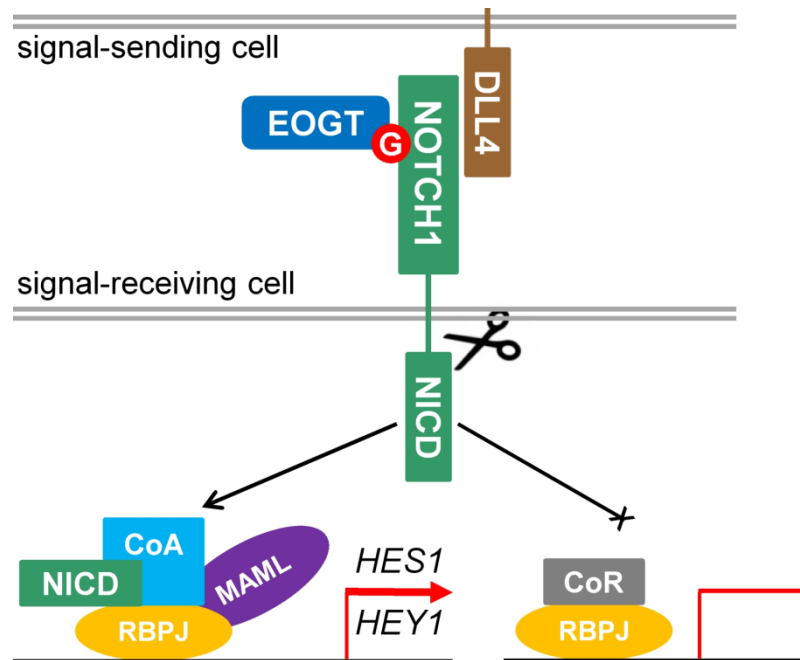


Figure 4.7: Simplified schematic of the canonical Notch signalling pathway.

The EGF (epidermal growth factor) domain of NOTCH1 is glycosylated (G) by EOGT. Activation of the Notch signalling cascade is initiated by the binding of a ligands (here DLL4) through direct contact of adjacent cells. This ligand activation leads to cleavage and release of NICD (Notch intracellular domain), which translocates to the nucleus to form an active transcriptional complex with RBPJ, mastermind (MAML) and transcriptional coactivators (CoA) to initiate transcription of the downstream genes *HEY1* and *HES1*. In the absence of Notch activation, RBPJ complexes with co-repressor proteins (CoR) to repress transcription of downstream genes. Adapted from [Southgate et al., 2015].

The regulatory circle of ARHGAP31 and DOCK6 has not been directly linked to the NOTCH1 signalling pathway, so far. A connection between the Notch signalling pathway and the small Rho GTPases Rac1 and Cdc42, that are affected by the ARHGAP31/DOCK6 regulatory circle, was demonstrated in the control of dendritic development in *Drosophila* [Redmond and Ghosh, 2001]. Furthermore, Rac1 is suggested to be the main regulator of genes that are associated to radiation-resistant head and neck squamous cell carcinoma cell lines, also including Notch1.

Summarising, a considerable genetic heterogeneity is seen in AOS; thus, this syndrome may represent a cluster of disorders of phenotypes with a related cause [Southgate et al., 2015]. Shaheen et al. [2013] propose to classify AOS as an actin cytoskeletopathy. Furthermore, the term “NOTCH1 signalopathy” seems appropriate for patients with mutations in the four genes that are involved in the canonical Notch signalling pathway.

4.2.5 COMMON MECHANISMS UNDERLYING SYNDROMIC SCALP DEFECTS

We could show that JBS is genetically homogeneous, and its clinical manifestations are probably caused by pleiotropic effects of impaired intracellular protein degradation due to a defective N-end rule pathway. AOS instead, can be related to dysfunctional actin cytoskeleton regulation and impaired NOTCH1 signalling. Possible interconnections between the molecular pathogenesis underlying these two disorders could open up a more comprehensive view on the pathophysiology of congenital scalp defects, the shared clinical feature of AOS and JBS, and thereby could provide new insights into the physiology of vasculogenesis. A hypothetical connection between NOTCH1 and the N-end rule pathway is shown in Figure 4.8. For the cleavage of the NICD from the NOTCH1 receptor into the signal-receiving cell, there are four known possible cleavage sites at four consecutive peptide bonds, thus generating four NICD isoforms that differ just in the most N-terminal amino acids (Table 4.2).

Table 4.2: List of NICD Δ C species generated in the cell-free assay.
[Tagami et al., 2008]

NICD type	Protein sequence	Molecular mass
NICD-V(Δ C)	V ¹⁷⁴⁴ LLSRKRRRQHGQLWFPEGFKVSEAEQKLISEEDL	4210 Da
NICD-L(+1)(Δ C)	LLSRKRRRQHGQLWFPEGFKVSEAEQKLISEEDL	4111 Da
NICD-L(+2)(Δ C)	LSRKRRRQHGQLWFPEGFKVSEAEQKLISEEDL	3998 Da
NICD-S(+3)(Δ C)	SRKRRRQHGQLWFPEGFKVSEAEQKLISEEDL	3885 Da

NICD-V(Δ C) with a valine residue at the N-terminus is the most stable variant with a half-life period of 100 hours. The smaller cleavage isoforms NICD-L(+1)(Δ C), NICD-L(+2)(Δ C), and NICD-S(+3)(Δ C) with N-terminal leucine or serine have significantly shorter half-life periods, namely 5.5 hours (+1, +2) and 1.9 hours (+3), consistent with the N-end rule [Gonda et al., 1989; Tagami et al., 2008]. The specific NICD types are known to have different efficiencies regarding transcriptional activation and may compete among each other for binding to the transcriptional complex with RBPJ, mastermind (MAML), and coactivators. When attached to this complex and bound to the specific promoter, the NICD-V(Δ C) type generates the highest transcription rate of the downstream genes (especially *HES1* and *HEY1*), compared to the other NICD species (Figure 4.8) [Tagami et al., 2008].

UBR1, the JBS-associated gene, plays an important role in the N-end rule pathway, by recognising the N-terminal amino acid of a protein, and affecting their degradation efficiency [Varshavsky, 1996, 2012]; thereby, the half-life period of a protein is determined. If it is true that the N-end rule pathway is regulating the half-life of NICD isoforms carrying N-degrons via *UBR1*, a defect of *UBR1* could in turn lead to shifted proportions of NICD types. NICD isoforms with destabilising N-degrons (L and S) could achieve significantly increased half-lives under conditions of an impaired N-end rule pathway. Overrepresentation of these NICDs, which have been reported to induce much weaker intracellular Notch signal transmission than NICD-V [Tagami et al., 2008], may cause competition with the physiologically more stable NICD-V for binding to the transcriptional complex. The resulting competitive inhibition of NOTCH1 signalling might have similar effects as heterozygous loss-of-function mutations in the genes *NOTCH1* or *DLL4*, eventually causing decreased transcription of target genes such as *HES1* and *HEY1*, which has already been experimentally verified for AOS-associated *NOTCH1* mutations [Southgate et al., 2015]. Proving this connection in functional experiments will be the subject of future research.

Through the identification a common mechanism underlying AOS and JBS, further candidate genes for syndromic or isolated scalp defects could also emerge.

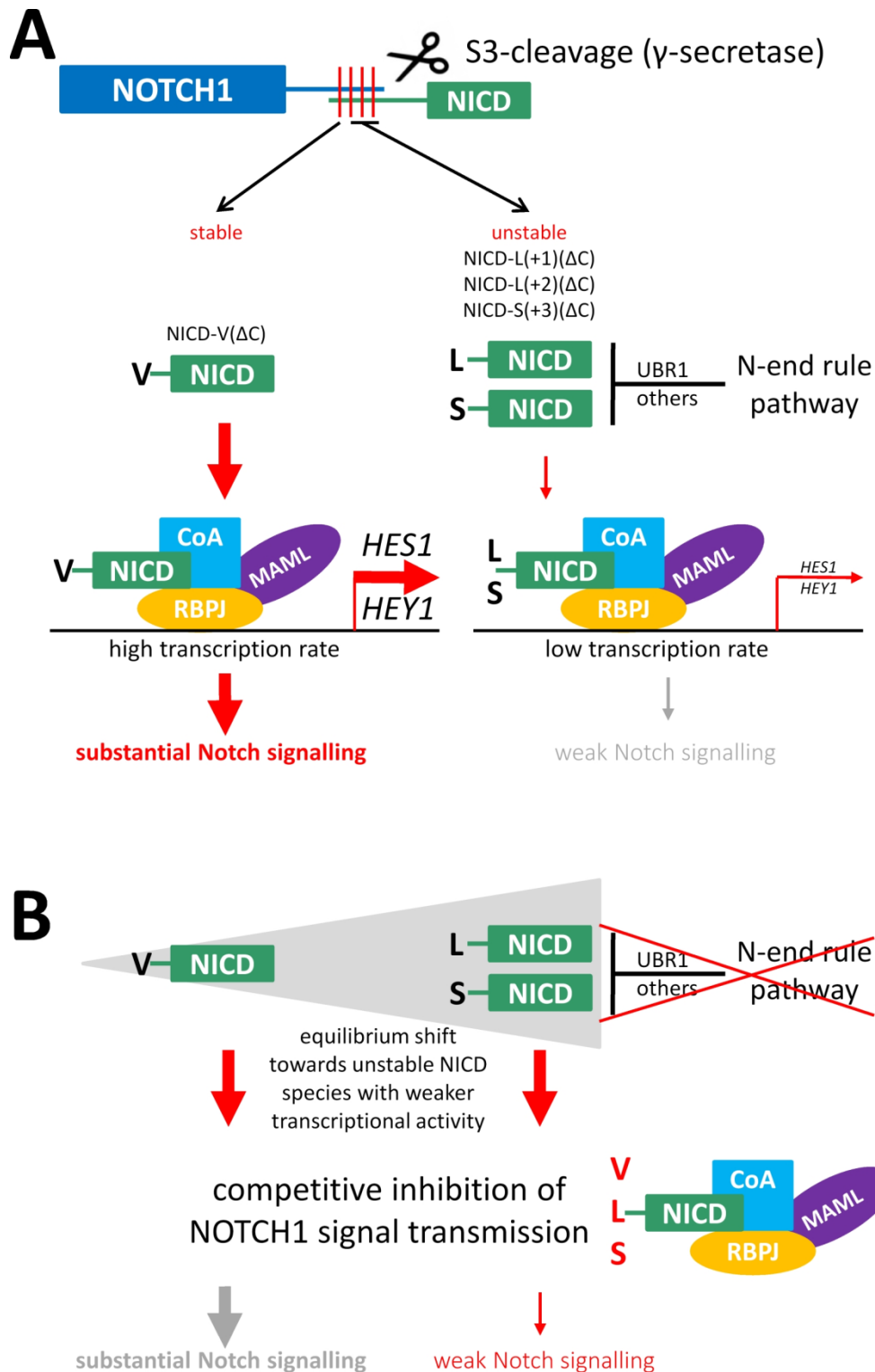


Figure 4.8: Hypothetical connection between Notch signalling and the N-end rule pathway.

(A) S3-cleavage of the NICD (Notch intracellular domain) from the NOTCH1 receptor at four possible cleavage sites generates four NICD isoforms with different N-terminal amino acids. When stable NICD-V binds to the transcriptional complex with RBPJ, MAML (mastermind), and CoA (transcriptional coactivators), the highest transcription rate of downstream genes (*HES1* and *HEY1*) is generated, leading to a substantial Notch signalling. The unstable isoforms NICD-L and NICD-S have a low transcription rate and only generate a weak Notch signal when bound to the transcriptional complex. The unstable isoforms are degraded via the N-end rule pathway. (B) An impaired N-end rule pathway (due to defective UBR1, for example) results in an equilibrium shift towards abundance of NICD isoforms with weaker transcriptional activity (NICD-L and NICD-S) which then compete with the NICD-V for binding to the transcriptional complex. This competitive inhibition of NOTCH1 signal transmission leads to weak Notch signalling.

5 CONCLUSIONS

This PhD thesis work has significantly contributed to the understanding of the genetic and molecular basis of two syndromic conditions, JBS and AOS, which are linked by the occurrence of scalp defects as part of both syndromes. JBS was further delineated as a genetic homogeneous disease. EPI, hypo-/aplasia of alae nasi, and oligodontia of permanent teeth were determined as the major clinical criteria for this syndrome. Genotype-phenotype correlations were demonstrated by comparing the clinical data of parents with biallelic truncating mutations to those with at least one non-truncating mutation.

In patients with AOS, a wide genetic heterogeneity was assumed, detected, and verified. Resequencing of the *DOCK6* gene yielded to extension of the mutational spectrum and to further delineation of the phenotype associated to this gene. Novel genes were assigned to autosomal dominant AOS, namely *NOTCH1* and *DLL4*. For the *NOTCH1* gene we could also expand the mutational spectrum and delineate the phenotype. Nevertheless, 55% of the patients from our cohort were not found to harbour a mutation in the six AOS-associated genes, underlining the genetic heterogeneity of the disease and giving the necessity for further research towards new candidate genes for this syndrome.

The results of this study support the growing evidence of disturbed angiogenesis being the underlying mechanism in the pathogenesis of AOS. The scalp defects seen in JBS are also supposed to emerge from a defect in vasculogenesis, giving a hint to a possible common mechanism for the development of scalp defects in both syndromes. A hypothetical pathogenetic link between JBS and AOS has to be evaluated in future research.

REFERENCES

- Abecasis GR, Auton A, Brooks LD, DePristo MA, Durbin RM, Handsaker RE, Kang HM, Marth GT, McVean GA. 2012. An integrated map of genetic variation from 1,092 human genomes. *Nature* 491:56-65.
- Adams FH, Oliver CP. 1945. Hereditary deformities in man due to arrested development. *J Hered* 36:3-7.
- Adzhubei IA, Schmidt S, Peshkin L, Ramensky VE, Gerasimova A, Bork P, Kondrashov AS, Sunyaev SR. 2010. A method and server for predicting damaging missense mutations. *Nat Methods* 7:248-9.
- Al-Dosari MS, Al-Muhsen S, Al-Jazaeri A, Mayerle J, Zenker M, Alkuraya FS. 2008. Johanson-Blizzard syndrome: report of a novel mutation and severe liver involvement. *Am J Med Genet A* 146A:1875-9.
- Alkhouri N, Kaplan B, Kay M, Shealy A, Crowe C, Bauhuber S, Zenker M. 2008. Johanson-Blizzard syndrome with mild phenotypic features confirmed by UBR1 gene testing. *World J Gastroenterol* 14:6863-6.
- Almashraki N, Abdunabee MZ, Sukalo M, Alrajoudi A, Sharafadeen I, Zenker M. 2011. Johanson-Blizzard syndrome. *World J Gastroenterol* 17:4247-50.
- Alpay F, Gul D, Lenk MK, Ogur G. 2000. Severe intrauterine growth retardation, aged facial appearance, and congenital heart disease in a newborn with Johanson-Blizzard syndrome. *Pediatr Cardiol* 21:389-90.
- Altschul SF, Gish W, Miller W, Myers EW, Lipman DJ. 1990. Basic local alignment search tool. *J Mol Biol* 215:403-10.
- Atik T, Karakoyun M, Sukalo M, Zenker M, Ozkinay F, Aydogdu S. 2015. Two novel UBR1 gene mutations in a patient with Johanson Blizzard Syndrome: A mild phenotype without mental retardation. *Gene* 570:153-5.
- Auslander R, Nevo O, Diukman R, Morrad E, Bardicof M, Abramovici H. 1999. Johanson-Blizzard syndrome: a prenatal ultrasonographic diagnosis. *Ultrasound Obstet Gynecol* 13:450-2.
- Bachmair A, Finley D, Varshavsky A. 1986. In vivo half-life of a protein is a function of its amino-terminal residue. *Science* 234:179-86.
- Baillie EE. 1983. Lipoprotein abnormalities and viral infections. *Jama* 249:474-5.
- Baraitser M, Hodgson SV. 1982. The Johanson-Blizzard syndrome. *J Med Genet* 19:302-3.
- Barroso KMA, Leite DFB, Alves PM, de Medeiros PFV, Godoy GP. 2010. Johanson-Blizzard syndrome—A case study of oral and systemic manifestations. *International Journal of Pediatric Otorhinolaryngology Extra* 5:180-182.
- Berger GM, Klempman S. 1965. A case of female hermaphroditism with associated congenital defects: Review of some aetiologic problems. *S Afr Med J* 39:23-6.
- Bohring A, Stamm T, Spaich C, Haase C, Spree K, Hehr U, Hoffmann M, Ledig S, Sel S, Wieacker P, Ropke A. 2009. WNT10A mutations are a frequent cause of a broad spectrum of ectodermal dysplasias with sex-biased manifestation pattern in heterozygotes. *Am J Hum Genet* 85:97-105.
- Brancati F, Garaci FG, Mingarelli R, Dallapiccola B. 2008. Abnormal neuronal migration defect in the severe variant subtype of Adams-Oliver syndrome. *Am J Med Genet A* 146A:1622-3.
- Braun J, Lerner A, Gershoni-Baruch R. 1991. The temporal bone in the Johanson-Blizzard syndrome. A CT study. *Pediatr Radiol* 21:580-3.
- Bresson JL, Schmitz J, Saudubray JM, Lesec G, Hummel JA, Rey J. 1980. [Johanson-Blizzard's syndrome: another cause of pancreatic lipomatosis (author's transl)]. *Arch Fr Pediatr* 37:21-4.
- Brunak S, Engelbrecht J, Knudsen S. 1991. Prediction of human mRNA donor and acceptor sites from the DNA sequence. *J Mol Biol* 220:49-65.
- Castillo M. 1994. Congenital abnormalities of the nose: CT and MR findings. *AJR Am J Roentgenol* 162:1211-7.
- Cheung JC, Thomson H, Buncic JR, Heon E, Levin AV. 2009. Ocular manifestations of the Johanson-Blizzard syndrome. *J Aapos* 13:512-4.
- Chillakuri CR, Sheppard D, Lea SM, Handford PA. 2012. Notch receptor-ligand binding and activation: insights from molecular studies. *Semin Cell Dev Biol* 23:421-8.
- Cluzeau C, Hadj-Rabia S, Jambou M, Mansour S, Guigue P, Masmoudi S, Bal E, Chassaing N, Vincent MC, Viot G, Clauss F, Maniere MC, Toupenay S, Le Merrer M, Lyonnet S, Cormier-Daire V, Amiel J, Faivre L, de Prost Y, Munnich A, Bonnefont JP, Bodemer C, Smahi A. 2011. Only four genes (EDA1, EDAR, EDARADD, and WNT10A) account for 90% of hypohidrotic/anhidrotic ectodermal dysplasia cases. *Hum Mutat* 32:70-2.
- Cohen I, Silberstein E, Perez Y, Landau D, Elbedour K, Langer Y, Kadir R, Volodarsky M, Sivan S, Narkis G, Birk OS. 2014. Autosomal recessive Adams-Oliver syndrome caused by homozygous mutation in EOGT, encoding an EGF domain-specific O-GlcNAc transferase. *Eur J Hum Genet* 22:374-8.

- Cooper GM, Stone EA, Asimenos G, Green ED, Batzoglou S, Sidow A. 2005. Distribution and intensity of constraint in mammalian genomic sequence. *Genome Res* 15:901-13.
- Corona-Rivera JR, Zapata-Aldana E, Bobadilla-Morales L, Corona-Rivera A, Pena-Padilla C, Solis-Hernandez E, Guzman C, Richmond E, Zahl C, Zenker M, Sukalo M. 2016. Oblique facial clefts in Johanson-Blizzard syndrome. *Am J Med Genet A* 170:1495-501.
- Cote JF, Vuori K. 2002. Identification of an evolutionarily conserved superfamily of DOCK180-related proteins with guanine nucleotide exchange activity. *J Cell Sci* 115:4901-13.
- da-Silva EO. 1991. Waardenburg I syndrome: a clinical and genetic study of two large Brazilian kindreds, and literature review. *Am J Med Genet* 40:65-74.
- Daentl DL, Frias JL, Gilbert EF, Opitz JM. 1979. The Johanson-Blizzard syndrome: case report and autopsy findings. *Am J Med Genet* 3:129-35.
- Davidai G, Zakaria T, Goldstein R, Gilai A, Freier S. 1986. Hypovitaminosis E induced neuropathy in exocrine pancreatic failure. *Arch Dis Child* 61:901-3.
- Day DW, Israel JN. 1978. Johanson-Blizzard syndrome. *Birth Defects Orig Artic Ser* 14:275-87.
- Demmel U. 1975. Clinical aspects of congenital skin defects. I. Congenital skin defects on the head of the newborn. *Eur J Pediatr* 121:21-50.
- den Dunnen JT, Antonarakis SE. 2000. Mutation nomenclature extensions and suggestions to describe complex mutations: a discussion. *Hum Mutat* 15:7-12.
- Deutsch CK, Hreczko T, Holmes LB. 2013. Quantitative assessment of craniofacial morphology in Johanson-Blizzard syndrome. *Birth Defects Res A Clin Mol Teratol* 97:166-9.
- Devillers AC, de Waard-van der Spek FB, Oranje AP. 1999. Cutis marmorata telangiectatica congenita: clinical features in 35 cases. *Arch Dermatol* 135:34-8.
- Digilio MC, Marino B, Dallapiccola B. 2008. Autosomal dominant inheritance of aplasia cutis congenita and congenital heart defect: a possible link to the Adams-Oliver syndrome. *Am J Med Genet A* 146A:2842-4.
- Donlan MA. 1977. Growth failure, cleft palate, ectodermal dysplasia and apparent pancreatic insufficiency - a new syndrome? *Birth defects. Original Article Series XIII*. p 3B:230-1.
- Dror Y, Freedman MH. 2002. Shwachman-diamond syndrome. *Br J Haematol* 118:701-13.
- Dumic M, Ille J, Bobonj G, Kordic R, Batinica S. 1998. [The Johanson-Blizzard syndrome]. *Lijec Vjesn* 120:114-6.
- Durie PR. 1997. Inherited causes of exocrine pancreatic dysfunction. *Can J Gastroenterol* 11:145-52.
- Dutertre JP, Jonville AP, Moraine C, Autret E. 1991. [Aplasia cutis after exposure to carbimazole in utero]. *J Gynecol Obstet Biol Reprod (Paris)* 20:575-6.
- Ellery KM, Erdman SH. 2014. Johanson-Blizzard syndrome: expanding the phenotype of exocrine pancreatic insufficiency. *Jop* 15:388-90.
- Elting M, Kariminejad A, de Sonnaville ML, Ottenkamp J, Bauhuber S, Bozorgmehr B, Zenker M, Cobben JM. 2008. Johanson-Blizzard syndrome caused by identical UBR1 mutations in two unrelated girls, one with a cardiomyopathy. *Am J Med Genet A* 146A:3058-61.
- Ermito S, Dinatale A, Carrara S, Cavaliere A, Imbruglia L, Recupero S. 2009. Prenatal diagnosis of limb abnormalities: role of fetal ultrasonography. *J Prenat Med* 3:18-22.
- Etienne-Manneville S, Hall A. 2002. Rho GTPases in cell biology. *Nature* 420:629-35.
- EUROCAT. 2004. EUROCAT Guide 3: For the description and classification of congenital limb defects (2nd Ed). University of Ulster: EUROCAT Central Registry.
- Fallahi GH, Sabbaghian M, Khalili M, Parvaneh N, Zenker M, Rezaei N. 2011. Novel UBR1 gene mutation in a patient with typical phenotype of Johanson-Blizzard syndrome. *Eur J Pediatr* 170:233-5.
- Fichter CR, Johnson GA, Braddock SR, Tobias JD. 2003. Perioperative care of the child with the Johanson-Blizzard syndrome. *Paediatr Anaesth* 13:72-5.
- Fokkema IF, den Dunnen JT, Taschner PE. 2005. LOVD: easy creation of a locus-specific sequence variation database using an "LSDB-in-a-box" approach. *Hum Mutat* 26:63-8.
- Fokkema IF, Taschner PE, Schaafsma GC, Celli J, Laros JF, den Dunnen JT. 2011. LOVD v.2.0: the next generation in gene variant databases. *Hum Mutat* 32:557-63.
- Franchi-Abella S, Fabre M, Mselati E, De Marsillac ME, Bayari M, Pariente D, Jacquemin E, Bernard O. 2014. Obliterative portal venopathy: a study of 48 children. *J Pediatr* 165:190-193 e2.
- Frieden IJ. 1986. Aplasia cutis congenita: a clinical review and proposal for classification. *J Am Acad Dermatol* 14:646-60.
- Froster-Iskenius UG, Baird PA. 1989. Limb reduction defects in over one million consecutive livebirths. *Teratology* 39:127-35.
- Gershoni-Baruch R, Lerner A, Braun J, Katzir Y, Iancu TC, Benderly A. 1990. Johanson-Blizzard syndrome: clinical spectrum and further delineation of the syndrome. *Am J Med Genet* 35:546-51.
- Giedion A. 1966. [Tricho-rhino-phalangeal syndrome]. *Helv Paediatr Acta* 21:475-85.

- Ginzberg H, Shin J, Ellis L, Morrison J, Ip W, Dror Y, Freedman M, Heitlinger LA, Belt MA, Corey M, Rommens JM, Durie PR. 1999. Shwachman syndrome: phenotypic manifestations of sibling sets and isolated cases in a large patient cohort are similar. *J Pediatr* 135:81-8.
- Girard M, Amiel J, Fabre M, Pariente D, Lyonnet S, Jacquemin E. 2005. Adams-Oliver syndrome and hepatoportal sclerosis: occasional association or common mechanism? *Am J Med Genet A* 135:186-9.
- Godbole K, Maja S, Leena H, Martin Z. 2013. Johanson-blizzard syndrome. *Indian Pediatr* 50:510-2.
- Gonda DK, Bachmair A, Wunning I, Tobias JW, Lane WS, Varshavsky A. 1989. Universality and structure of the N-end rule. *J Biol Chem* 264:16700-12.
- Gould NS, Paton JB, Bennett AR. 1989. Johanson-Blizzard syndrome: clinical and pathological findings in 2 sibs. *Am J Med Genet* 33:194-9.
- Grand RJ, Rosen SW, Di Sant'Agnese PA, Kirkham WR. 1966. Unusual case of XXY Klinefelter's syndrome with pancreatic insufficiency, hypothyroidism, deafness, chronic lung disease, dwarfism and microcephaly. *Am J Med* 41:478-85.
- Gray KA, Seal RL, Tweedie S, Wright MW, Bruford EA. 2016. A review of the new HGNC gene family resource. *Hum Genomics* 10:6.
- Gülaşı S, Turhan AH, Çelik Y. 2011. Johanson Blizzard sendromu. *J Child* 11:86-89.
- Guzman C, Carranza A. 1997. Two siblings with exocrine pancreatic hypoplasia and orofacial malformations (Donlan syndrome and Johanson-Blizzard syndrome). *J Pediatr Gastroenterol Nutr* 25:350-3.
- Harris HH, Foucar E, Andersen RD, Ray TL. 1986. Intrauterine herpes simplex infection resembling mechanobullous disease in a newborn infant. *J Am Acad Dermatol* 15:1148-55.
- Hassed SJ, Wiley GB, Wang S, Lee JY, Li S, Xu W, Zhao ZJ, Mulvihill JJ, Robertson J, Warner J, Gaffney PM. 2012. RBPJ mutations identified in two families affected by Adams-Oliver syndrome. *Am J Hum Genet* 91:391-5.
- Helin I, Jodal U. 1981. A syndrome of congenital hypoplasia of the alae nasi, situs inversus, and severe hypoproteinemia in two siblings. *J Pediatr* 99:932-4.
- Higginbottom MC, Jones KL, Hall BD, Smith DW. 1979. The amniotic band disruption complex: timing of amniotic rupture and variable spectra of consequent defects. *J Pediatr* 95:544-9.
- High FA, Epstein JA. 2008. The multifaceted role of Notch in cardiac development and disease. *Nat Rev Genet* 9:49-61.
- Hoffman WH, Lee JR, Kovacs K, Chen H, Yaghmai F. 2007. Johanson-Blizzard syndrome: autopsy findings with special emphasis on hypopituitarism and review of the literature. *Pediatr Dev Pathol* 10:55-60.
- Hurst JA, Baraitser M. 1989. Johanson-Blizzard syndrome. *J Med Genet* 26:45-8.
- Hwang CS, Sukalo M, Batygin O, Addor MC, Brunner H, Aytes AP, Mayerle J, Song HK, Varshavsky A, Zenker M. 2011. Ubiquitin ligases of the N-end rule pathway: assessment of mutations in UBR1 that cause the Johanson-Blizzard syndrome. *PLoS One* 6:e24925.
- Ibrahim A. 2014. Bilateral congenital absence of the alae nasi with bilateral auricular sinuses in an albino child. *Saudi Journal of Medicine & Medical Sciences* 2:43-45.
- Iso T, Kedes L, Hamamori Y. 2003. HES and HERP families: multiple effectors of the Notch signaling pathway. *J Cell Physiol* 194:237-55.
- Isrie M, Wuyts W, Van Esch H, Devriendt K. 2014. Isolated terminal limb reduction defects: extending the clinical spectrum of Adams-Oliver syndrome and ARHGAP31 mutations. *Am J Med Genet A* 164A:1576-9.
- Johanson A, Blizzard R. 1971. A syndrome of congenital aplasia of the alae nasi, deafness, hypothyroidism, dwarfism, absent permanent teeth, and malabsorption. *J Pediatr* 79:982-7.
- Jones NL, Hofley PM, Durie PR. 1994. Pathophysiology of the pancreatic defect in Johanson-Blizzard syndrome: a disorder of acinar development. *J Pediatr* 125:406-8.
- Kaba S, Doğan M, Bulan K, Doğan SZ, Demir N, Üstüol L. 2013. Johanson Blizzard sendromlu bir vaka sunumu. *Tıp Araştırmaları Dergisi* 11:15-17.
- Kerem BS, Buchanan JA, Durie P, Corey ML, Levison H, Rommens JM, Buchwald M, Tsui LC. 1989. DNA marker haplotype association with pancreatic sufficiency in cystic fibrosis. *Am J Hum Genet* 44:827-34.
- Kishino T, Lalonde M, Wagstaff J. 1997. UBE3A/E6-AP mutations cause Angelman syndrome. *Nat Genet* 15:70-3.
- Kobayashi S, Ohmori K, Sekiguchi J. 1995. Johanson-Blizzard syndrome facial anomaly and its correction using a microsurgical bone graft and tripartite osteotomy. *J Craniofac Surg* 6:382-5.
- Kovall RA, Hendrickson WA. 2004. Crystal structure of the nuclear effector of Notch signaling, CSL, bound to DNA. *Embo J* 23:3441-51.

- Kristjansson K, Hoffman WH, Flannery DB, Cohen MJ. 1988. Johanson-Blizzard syndrome and hypopituitarism. *J Pediatr* 113:851-3.
- Kulkarni ML, Shetty SK, Kallambella KS, Kulkarni PM. 2004. Johanson-Blizzard syndrome. *Indian J Pediatr* 71:1127-9.
- Kumar P, Henikoff S, Ng PC. 2009. Predicting the effects of coding non-synonymous variants on protein function using the SIFT algorithm. *Nat Protoc* 4:1073-81.
- Kuster W, Lenz W, Kaariainen H, Majewski F. 1988. Congenital scalp defects with distal limb anomalies (Adams-Oliver syndrome): report of ten cases and review of the literature. *Am J Med Genet* 31:99-115.
- Kwak KS, Zhou X, Solomon V, Baracos VE, Davis J, Bannon AW, Boyle WJ, Lacey DL, Han HQ. 2004. Regulation of protein catabolism by muscle-specific and cytokine-inducible ubiquitin ligase E3alpha-II during cancer cachexia. *Cancer Res* 64:8193-8.
- Kwon YT, Reiss Y, Fried VA, Hershko A, Yoon JK, Gonda DK, Sangan P, Copeland NG, Jenkins NA, Varshavsky A. 1998. The mouse and human genes encoding the recognition component of the N-end rule pathway. *Proc Natl Acad Sci U S A* 95:7898-903.
- Kwon YT, Xia Z, Davydov IV, Lecker SH, Varshavsky A. 2001. Construction and analysis of mouse strains lacking the ubiquitin ligase UBR1 (E3alpha) of the N-end rule pathway. *Mol Cell Biol* 21:8007-21.
- Kwon YT, Xia Z, An JY, Tasaki T, Davydov IV, Seo JW, Sheng J, Xie Y, Varshavsky A. 2003. Female lethality and apoptosis of spermatocytes in mice lacking the UBR2 ubiquitin ligase of the N-end rule pathway. *Mol Cell Biol* 23:8255-71.
- Lango Allen H, Flanagan SE, Shaw-Smith C, De Franco E, Akerman I, Caswell R, Ferrer J, Hattersley AT, Ellard S. 2012. GATA6 haploinsufficiency causes pancreatic agenesis in humans. *Nat Genet* 44:20-2.
- Larkin MA, Blackshields G, Brown NP, Chenna R, McGettigan PA, McWilliam H, Valentin F, Wallace IM, Wilm A, Lopez R, Thompson JD, Gibson TJ, Higgins DG. 2007. Clustal W and Clustal X version 2.0. *Bioinformatics* 23:2947-8.
- Lehman A, Stittrich AB, Glusman G, Zong Z, Li H, Eydoux P, Senger C, Lyons C, Roach JC, Patel M. 2014. Diffuse angiopathy in Adams-Oliver syndrome associated with truncating DOCK6 mutations. *Am J Med Genet A* 164A:2656-62.
- Lek M, Karczewski KJ, Minikel EV, Samocha KE, Banks E, Fennell T, O'Donnell-Luria AH, Ware JS, Hill AJ, Cummings BB, Tukiainen T, Birnbaum DP, Kosmicki JA, Duncan LE, Estrada K, Zhao F, Zou J, Pierce-Hoffman E, Berghout J, Cooper DN, Deflaux N, DePristo M, Do R, Flannick J, Fromer M, Gauthier L, Goldstein J, Gupta N, Howrigan D, Kiezun A, Kurki MI, Moonshine AL, Natarajan P, Orozco L, Peloso GM, Poplin R, Rivas MA, Ruano-Rubio V, Rose SA, Ruderfer DM, Shakir K, Stenson PD, Stevens C, Thomas BP, Tiao G, Tusie-Luna MT, Weisburd B, Won HH, Yu D, Altshuler DM, Ardissino D, Boehnke M, Danesh J, Donnelly S, Elosua R, Florez JC, Gabriel SB, Getz G, Glatt SJ, Hultman CM, Kathiresan S, Laakso M, McCarroll S, McCarthy MI, McGovern D, McPherson R, Neale BM, Palotie A, Purcell SM, Saleheen D, Scharf JM, Sklar P, Sullivan PF, Tuomilehto J, Tsuang MT, Watkins HC, Wilson JG, Daly MJ, MacArthur DG; Exome Aggregation Consortium. 2016. Analysis of protein-coding genetic variation in 60,706 humans. *Nature* 536:285-91.
- Lemke RP, Machin G, Muttitt S, Bamforth F, Rao S, Welch R. 1993. A case of aplasia cutis congenita in dizygotic twins. *J Perinatol* 13:22-7.
- Levin DL, Nolan KS, Esterly NB. 1980. Congenital absence of skin. *J Am Acad Dermatol* 2:203-6.
- Li B, Krishnan VG, Mort ME, Xin F, Kamati KK, Cooper DN, Mooney SD, Radivojac P. 2009. Automated inference of molecular mechanisms of disease from amino acid substitutions. *Bioinformatics* 25:2744-50.
- Lin AE, Westgate MN, van der Velde ME, Lacro RV, Holmes LB. 1998. Adams-Oliver syndrome associated with cardiovascular malformations. *Clin Dysmorphol* 7:235-41.
- Liu ZF, Zhang ZH, Li M, Jin Y, Lian M, Tang WW. 2011. [Report of a case with Johanson-Blizzard syndrome and literatures review]. *Zhonghua Er Ke Za Zhi* 49:66-9.
- Liu ZJ, Shirakawa T, Li Y, Soma A, Oka M, Dotto GP, Fairman RM, Velazquez OC, Herlyn M. 2003. Regulation of Notch1 and Dll4 by vascular endothelial growth factor in arterial endothelial cells: implications for modulating arteriogenesis and angiogenesis. *Mol Cell Biol* 23:14-25.
- Luca VC, Jude KM, Pierce NW, Nachury MV, Fischer S, Garcia KC. 2015. Structural biology. Structural basis for Notch1 engagement of Delta-like 4. *Science* 347:847-53.
- Lumb G, Beautyman W. 1952. Hypoplasia of the exocrine tissue of the pancreas. *J Pathol Bacteriol* 64:679-86.
- Maniscalco M, Zedda A, Faraone S, de Laurentiis G, Verde R, Molese V, Lapicciarella G, Sofia M. 2005. Association of Adams-Oliver syndrome with pulmonary arterio-venous malformation in the same family: a further support to the vascular hypothesis. *Am J Med Genet A* 136:269-74.

- Mardini MK, Ghandour M, Sakati NA, Nyhan WL. 1978. Johanson-Blizzard syndrome in a large inbred kindred with three involved members. *Clin Genet* 14:247-50.
- Maunoury V, Nieuwarts S, Ferri J, Ernst O. 1999. [Pancreatic lipomatosis revealing Johanson-Blizzard syndrome]. *Gastroenterol Clin Biol* 23:1099-101.
- McGoey RR, Lacassie Y. 2008. Adams-Oliver syndrome in siblings with central nervous system findings, epilepsy, and developmental delay: refining the features of a severe autosomal recessive variant. *Am J Med Genet A* 146A:488-91.
- McHeik JN, Hendiri L, Vabres P, Berthier M, Cardona J, Bonneau D, Levard G. 2002. [Johanson-Blizzard syndrome: a case report]. *Arch Pediatr* 9:1163-5.
- Meester JA, Southgate L, Stittrich AB, Venselaar H, Beekmans SJ, den Hollander N, Bijlsma EK, Helderman-van den Enden A, Verheij JB, Glusman G, Roach JC, Lehman A, Patel MS, de Vries BB, Ruivenkamp C, Itin P, Prescott K, Clarke S, Trembath R, Zenker M, Sukalo M, Van Laer L, Loeys B, Wuyts W. 2015. Heterozygous loss-of-function mutations in *DLL4* cause Adams-Oliver syndrome. *Am J Hum Genet* 97:475-82.
- Miki Y, Swensen J, Shattuck-Eidens D, Futreal PA, Harshman K, Tavtigian S, Liu Q, Cochran C, Bennett LM, Ding W, et al. 1994. A strong candidate for the breast and ovarian cancer susceptibility gene *BRCA1*. *Science* 266:66-71.
- Miyamoto Y, Yamauchi J, Sanbe A, Tanoue A. 2007. Dock6, a Dock-C subfamily guanine nucleotide exchanger, has the dual specificity for Rac1 and Cdc42 and regulates neurite outgrowth. *Experimental cell research* 313:791-804.
- Moeschler JB, Lubinsky MS. 1985. Johanson-Blizzard syndrome with normal intelligence. *Am J Med Genet* 22:69-73.
- Moeschler JB, Polak MJ, Jenkins JJ, 3rd, Amato RS. 1987. The Johanson-Blizzard syndrome: a second report of full autopsy findings. *Am J Med Genet* 26:133-8.
- Morris MD, Fisher DA. 1967. Trypsinogen deficiency disease. *Am J Dis Child* 114:203-8.
- Motohashi N, Pruzansky S, Day D. 1981. Roentgencephalometric analysis of craniofacial growth in the Johanson-Blizzard syndrome. *J Craniofac Genet Dev Biol* 1:57-72.
- Nagashima K, Yagi H, Kuroume T. 1993. A case of Johanson-Blizzard syndrome complicated by diabetes mellitus. *Clin Genet* 43:98-100.
- Neitzel H. 1986. A routine method for the establishment of permanent growing lymphoblastoid cell lines. *Hum Genet* 73:320-6.
- Nieminen P, Kotilainen J, Aalto Y, Knuutila S, Pirinen S, Thesleff I. 2003. *MSX1* gene is deleted in Wolf-Hirschhorn syndrome patients with oligodontia. *J Dent Res* 82:1013-7.
- Nordstrom-O'Brien M, van der Luijt RB, van Rooijen E, van den Ouweland AM, Majoor-Krakauer DF, Lolkema MP, van Brussel A, Voest EE, Giles RH. 2010. Genetic analysis of von Hippel-Lindau disease. *Hum Mutat* 31:521-37.
- Ogawa M, Sawaguchi S, Kawai T, Nadano D, Matsuda T, Yagi H, Kato K, Furukawa K, Okajima T. 2015. Impaired O-linked N-acetylglucosaminylation in the endoplasmic reticulum by mutated epidermal growth factor (EGF) domain-specific O-linked N-acetylglucosamine transferase found in Adams-Oliver syndrome. *J Biol Chem* 290:2137-49.
- Ono K, Ogawa T, Matsuda N. 1987. Oral findings in Johanson-Blizzard syndrome. *J Oral Med* 42:14-6, 66.
- Orstavik KH, Stromme P, Spetalen S, Flage T, Westvik J, Vesterhus P, Skjeldal O. 1995. Aplasia cutis congenita associated with limb, eye, and brain anomalies in sibs: a variant of the Adams-Oliver syndrome? *Am J Med Genet* 59:92-5.
- Park IJ, Johanson A, Jones HW, Jr., Blizzard R. 1972. Special female hermaphroditism associated with multiple disorders. *Obstet Gynecol* 39:100-6.
- Patel MS, Taylor GP, Bharya S, Al-Sanna'a N, Adatia I, Chitayat D, Suzanne Lewis ME, Human DG. 2004. Abnormal pericyte recruitment as a cause for pulmonary hypertension in Adams-Oliver syndrome. *Am J Med Genet A* 129A:294-9.
- Pirinen S, Kentala A, Nieminen P, Varilo T, Thesleff I, Arte S. 2001. Recessively inherited lower incisor hypodontia. *J Med Genet* 38:551-6.
- Prater JF, D'Addio K. 2002. Johanson-Blizzard syndrome--a case study, behavioral manifestations, and successful treatment strategies. *Biol Psychiatry* 51:515-7.
- Prothero J, Nicholl R, Wilson J, Wakeling EL. 2007. Aplasia cutis congenita, terminal limb defects and falciform retinal folds: confirmation of a distinct syndrome of vascular disruption. *Clin Dysmorphol* 16:39-41.
- Quaio CR, Koda YK, Bertola DR, Sukalo M, Zenker M, Kim CA. 2014. Case report. Johanson-Blizzard syndrome: a report of gender-discordant twins with a novel *UBR1* mutation. *Genet Mol Res* 13:4159-64.

- Ramos S, Ramos HF, Ramos RF, Peixoto CA, Ramos BF. 2010. Johanson-Blizzard syndrome. *Braz J Otorhinolaryngol* 76:794.
- Redmond L, Ghosh A. 2001. The role of Notch and Rho GTPase signaling in the control of dendritic development. *Curr Opin Neurobiol* 11:111-7.
- Reese MG, Eeckman FH, Kulp D, Haussler D. 1997. Improved splice site detection in Genie. *J Comput Biol* 4:311-23.
- Reichart P, Flatz S, Burdelski M. 1979. [Ectodermal dysplasia and exocrine pancreatic insufficiency--a familial syndrome]. *Dtsch Zahnarztl Z* 34:263-5.
- Rosanowski F, Hoppe U, Hies T, Eysholdt U. 1998. [Johanson-Blizzard syndrome. A complex dysplasia syndrome with aplasia of the nasal alae and inner ear deafness]. *Hno* 46:876-8.
- Rudnik-Schoneborn S, Keller B, Beemer FA, Pistor K, Swanenburg de Veye HF, Zerres K. 1991. [Johanson-Blizzard syndrome]. *Klin Padiatr* 203:33-8.
- Saeed M, Rana MN, Ahmad TM. 2010. Johanson-Blizzard syndrome with Diamond-Blackfan anemia. *J Coll Physicians Surg Pak* 20:627-8.
- Sakaidani Y, Ichihayashi N, Saito C, Nomura T, Ito M, Nishio Y, Nadano D, Matsuda T, Furukawa K, Okajima T. 2012. O-linked-N-acetylglucosamine modification of mammalian Notch receptors by an atypical O-GlcNAc transferase Eogt1. *Biochem Biophys Res Commun* 419:14-9.
- Sandhu BK, Brueton MJ. 1989. Concurrent pancreatic and growth hormone insufficiency in Johanson-Blizzard syndrome. *J Pediatr Gastroenterol Nutr* 9:535-8.
- Santhosh BP, Jethmalani P. 2013. Johanson-Blizzard syndrome: dental findings and management. *J Contemp Dent Pract* 14:544-7.
- Schoner K, Fritz B, Huelskamp G, Louwen F, Zenker M, Moll R, Rehder H. 2012. Recurrent Johanson-Blizzard syndrome in a triplet pregnancy complicated by urethral obstruction sequence: a clinical, molecular, and immunohistochemical approach. *Pediatr Dev Pathol* 15:50-7.
- Schouten JP, McElgunn CJ, Waaijer R, Zwijnenburg D, Diepvens F, Pals G. 2002. Relative quantification of 40 nucleic acid sequences by multiplex ligation-dependent probe amplification. *Nucleic Acids Res* 30:e57.
- Schussheim A, Choi SJ, Silverberg M. 1976. Exocrine pancreatic insufficiency with congenital anomalies. *J Pediatr* 89:782-4.
- Schwitzgebel VM, Mamin A, Brun T, Ritz-Laser B, Zaiko M, Maret A, Jornayvaz FR, Theintz GE, Michielin O, Melloul D, Philippe J. 2003. Agenesis of human pancreas due to decreased half-life of insulin promoter factor 1. *J Clin Endocrinol Metab* 88:4398-406.
- Shaheen R, Faqeih E, Sunker A, Morsy H, Al-Sheddi T, Shamseldin HE, Adly N, Hashem M, Alkuraya FS. 2011. Recessive mutations in DOCK6, encoding the guanidine nucleotide exchange factor DOCK6, lead to abnormal actin cytoskeleton organization and Adams-Oliver syndrome. *Am J Hum Genet* 89:328-33.
- Shaheen R, Aglan M, Keppler-Noreuil K, Faqeih E, Ansari S, Horton K, Ashour A, Zaki MS, Al-Zahrani F, Cueto-Gonzalez AM, Abdel-Salam G, Temtamy S, Alkuraya FS. 2013. Mutations in EOGT confirm the genetic heterogeneity of autosomal-recessive Adams-Oliver syndrome. *Am J Hum Genet* 92:598-604.
- Sherry ST, Ward MH, Kholodov M, Baker J, Phan L, Smigielski EM, Sirotkin K. 2001. dbSNP: the NCBI database of genetic variation. *Nucleic Acids Res* 29:308-11.
- Silberstein E, Pagkalos VA, Landau D, Berezovsky AB, Krieger Y, Shoham Y, Levy A, Rosenberg L, Silberstein T. 2014. Aplasia cutis congenita: clinical management and a new classification system. *Plast Reconstr Surg* 134:766e-774e.
- Singh A, Chaudhary N, Dhingra D, Sukalo M, Zenker M, Kapoor S. 2014. Johanson-Blizzard syndrome: Hepatic and hematological features with novel genotype. *Indian J Gastroenterol* 33:82-4.
- Sismanis A, Polisar IA, Ruffy ML, Lambert JC. 1979. Rare congenital syndrome associated with profound hearing loss. *Arch Otolaryngol* 105:222-4.
- Snape KM, Ruddy D, Zenker M, Wuyts W, Whiteford M, Johnson D, Lam W, Trembath RC. 2009. The spectra of clinical phenotypes in aplasia cutis congenita and terminal transverse limb defects. *Am J Med Genet A* 149A:1860-81.
- Southgate L, Machado RD, Snape KM, Primeau M, Dafou D, Ruddy DM, Branney PA, Fisher M, Lee GJ, Simpson MA, He Y, Bradshaw TY, Blaumeiser B, Winship WS, Reardon W, Maher ER, FitzPatrick DR, Wuyts W, Zenker M, Lamarche-Vane N, Trembath RC. 2011. Gain-of-function mutations of ARHGAP31, a Cdc42/Rac1 GTPase regulator, cause syndromic cutis aplasia and limb anomalies. *Am J Hum Genet* 88:574-85.

- Southgate L, Sukalo M, Karountzos AS, Taylor EJ, Collinson CS, Ruddy D, Snape KM, Dallapiccola B, Tolmie JL, Joss S, Brancati F, Digilio MC, Graul-Neumann LM, Salviati L, Coerdts W, Jacquemin E, Wuyts W, Zenker M, Machado RD, Trembath RC. 2015. Haploinsufficiency of the NOTCH1 Receptor as a Cause of Adams-Oliver Syndrome With Variable Cardiac Anomalies. *Circ Cardiovasc Genet* 8:572-81.
- Steinbach WJ, Hintz RL. 2000. Diabetes mellitus and profound insulin resistance in Johanson-Blizzard syndrome. *J Pediatr Endocrinol Metab* 13:1633-6.
- Stittrich AB, Lehman A, Bodian DL, Ashworth J, Zong Z, Li H, Lam P, Khromykh A, Iyer RK, Vockley JG, Baveja R, Silva ES, Dixon J, Leon EL, Solomon BD, Glusman G, Niederhuber JE, Roach JC, Patel MS. 2014. Mutations in NOTCH1 cause Adams-Oliver syndrome. *Am J Hum Genet* 95:275-84.
- Suchting S, Freitas C, le Noble F, Benedito R, Breant C, Duarte A, Eichmann A. 2007. The Notch ligand Delta-like 4 negatively regulates endothelial tip cell formation and vessel branching. *Proc Natl Acad Sci U S A* 104:3225-30.
- Sudarshan R, Annigeri RG, Shettar SS. 2010. Johanson-Blizzard syndrome: A rare case report. *JIAOMR* 22:225-228.
- Sukalo M, Fiedler A, Guzman C, Spranger S, Addor MC, McHeik JN, Oltra Benavent M, Cobben JM, Gillis LA, Shealy AG, Deshpande C, Bozorgmehr B, Everman DB, Stattin EL, Liebelt J, Keller KM, Bertola DR, van Karnebeek CD, Bergmann C, Liu Z, Duker G, Rezaei N, Alkuraya FS, Ogur G, Alrajoudi A, Venegas-Vega CA, Verbeek NE, Richmond EJ, Kirbiyik O, Ranganath P, Singh A, Godbole K, Ali FA, Alves C, Mayerle J, Lerch MM, Witt H, Zenker M. 2014a. Mutations in the human UBR1 gene and the associated phenotypic spectrum. *Hum Mutat* 35:521-31.
- Sukalo M, Mayerle J, Zenker M. 2014b. Clinical utility gene card for: Johanson-Blizzard syndrome. *Eur J Hum Genet* 22 doi:10.1038/ejhg.2013.65.
- Sukalo M, Tilsen F, Kayserili H, Muller D, Tuysuz B, Ruddy DM, Wakeling E, Orstavik KH, Snape KM, Trembath R, De Smedt M, van der Aa N, Skalej M, Mundlos S, Wuyts W, Southgate L, Zenker M. 2015. DOCK6 mutations are responsible for a distinct autosomal-recessive variant of Adams-Oliver syndrome associated with brain and eye anomalies. *Hum Mutat* 36:593-8. *Erratum in: Hum Mutat* 36:1112.
- Swanenburg de Veye HF, Heineman-de-Boer JA, Beemer FA. 1991. A child of high intelligence with the Johanson-Blizzard syndrome. *Genet Couns* 2:21-5.
- Swartz EN, Sanatani S, Sandor GG, Schreiber RA. 1999. Vascular abnormalities in Adams-Oliver syndrome: cause or effect? *Am J Med Genet* 82:49-52.
- Szilagyi PG, Corsetti J, Callahan CM, McCormick K, Metlay LA. 1987. Pancreatic exocrine aplasia, clinical features of leprechaunism, and abnormal gonadotropin regulation. *Pediatr Pathol* 7:51-61.
- Tagami S, Okochi M, Yanagida K, Ikuta A, Fukumori A, Matsumoto N, Ishizuka-Katsura Y, Nakayama T, Itoh N, Jiang J, Nishitomi K, Kamino K, Morihara T, Hashimoto R, Tanaka T, Kudo T, Chiba S, Takeda M. 2008. Regulation of Notch signaling by dynamic changes in the precision of S3 cleavage of Notch-1. *Mol Cell Biol* 28:165-76.
- Takahashi T, Fujishima M, Tsuchida S, Enoki M, Takada G. 2004. Johanson-Blizzard syndrome: loss of glucagon secretion response to insulin-induced hypoglycemia. *J Pediatr Endocrinol Metab* 17:1141-4.
- Tasaki T, Mulder LC, Iwamatsu A, Lee MJ, Davydov IV, Varshavsky A, Muesing M, Kwon YT. 2005. A family of mammalian E3 ubiquitin ligases that contain the UBR box motif and recognize N-degrons. *Mol Cell Biol* 25:7120-36.
- Tasaki T, Sriram SM, Park KS, Kwon YT. 2012. The N-end rule pathway. *Annu Rev Biochem* 81:261-89.
- Tcherkezian J, Triki I, Stenne R, Danek EI, Lamarche-Vane N. 2006. The human orthologue of CdGAP is a phosphoprotein and a GTPase-activating protein for Cdc42 and Rac1 but not RhoA. *Biology of the cell / under the auspices of the European Cell Biology Organization* 98:445-56.
- Tessier P. 1976. Anatomical classification facial, cranio-facial and latero-facial clefts. *J Maxillofac Surg* 4:69-92.
- Timoney N, Weinberg MJ, Ross DA, Thomson HG. 2004. Johanson-Blizzard syndrome: A challenge in nasal reconstruction. *The Canadian Journal of Plastic Surgery* 12:81-85.
- Townes PL. 1965. Trypsinogen deficiency disease. *J Pediatr* 66:275-85.
- Townes PL. 1969. Proteolytic and lipolytic deficiency of the exocrine pancreas. *J Pediatr* 75:221-8.
- Townes PL, White MR. 1981. Identity of two syndromes. Proteolytic, lipolytic, and amylolytic deficiency of the exocrine pancreas with congenital anomalies. *Am J Dis Child* 135:248-50.
- Trellis DR, Clouse RE. 1991. Johanson-Blizzard syndrome. Progression of pancreatic involvement in adulthood. *Dig Dis Sci* 36:365-9.
- van der Meulen JC. 1985. Oblique facial clefts: pathology, etiology, and reconstruction. *Plast Reconstr Surg* 76:212-24.

- Vanlieferinghen P, Gallot D, Francannet C, Meyer F, Dechelotte P. 2003. Prenatal ultrasonographic diagnosis of a recurrent case of Johanson-Blizzard syndrome. *Genet Couns* 14:105-7.
- Vanlieferinghen PH, Borderon C, Francannet CH, Gembara P, Dechelotte P. 2001. Johanson-Blizzard syndrome. a new case with autopsy findings. *Genet Couns* 12:245-50.
- Varshavsky A. 1996. The N-end rule: functions, mysteries, uses. *Proc Natl Acad Sci U S A* 93:12142-9.
- Varshavsky A. 2005. Regulated protein degradation. *Trends Biochem Sci* 30:283-6.
- Varshavsky A. 2011. The N-end rule pathway and regulation by proteolysis. *Protein Sci* 20:1298-345.
- Varshavsky A. 2012. Three decades of studies to understand the functions of the ubiquitin family. *Methods Mol Biol* 832:1-11.
- Vega FM, Ridley AJ. 2008. Rho GTPases in cancer cell biology. *FEBS Lett* 582:2093-101.
- Verdyck P, Holder-Espinasse M, Hul WV, Wuyts W. 2003. Clinical and molecular analysis of nine families with Adams-Oliver syndrome. *Eur J Hum Genet* 11:457-63.
- Vieira MW, Lopes VL, Teruya H, Guimaraes-Lamonato L, Oliveira LC, Costa CD. 2002. [Johanson-Blizzard syndrome: the importance of differential diagnostic in pediatrics]. *J Pediatr (Rio J)* 78:433-6.
- Wildeman M, van Ophuizen E, den Dunnen JT, Taschner PE. 2008. Improving sequence variant descriptions in mutation databases and literature using the Mutalyzer sequence variation nomenclature checker. *Hum Mutat* 29:6-13.
- Winter WE, Maclaren NK, Riley WJ, Toskes PP, Andres J, Rosenbloom AL. 1986. Congenital pancreatic hypoplasia: a syndrome of exocrine and endocrine pancreatic insufficiency. *J Pediatr* 109:465-8.
- Xie Y, Varshavsky A. 1999. The E2-E3 interaction in the N-end rule pathway: the RING-H2 finger of E3 is required for the synthesis of multiubiquitin chain. *Embo J* 18:6832-44.
- Yoshii SR, Kishi C, Ishihara N, Mizushima N. 2011. Parkin mediates proteasome-dependent protein degradation and rupture of the outer mitochondrial membrane. *J Biol Chem* 286:19630-40.
- Zenker M, Mayerle J, Lerch MM, Tagariello A, Zerres K, Durie PR, Beier M, Hulskamp G, Guzman C, Rehder H, Beemer FA, Hamel B, Vanlieferinghen P, Gershoni-Baruch R, Vieira MW, Dumic M, Auslender R, Gil-da-Silva-Lopes VL, Steinlicht S, Rauh M, Shalev SA, Thiel C, Ekici AB, Winterpacht A, Kwon YT, Varshavsky A, Reis A. 2005. Deficiency of UBR1, a ubiquitin ligase of the N-end rule pathway, causes pancreatic dysfunction, malformations and mental retardation (Johanson-Blizzard syndrome). *Nat Genet* 37:1345-50.
- Zenker M, Mayerle J, Reis A, Lerch MM. 2006. Genetic basis and pancreatic biology of Johanson-Blizzard syndrome. *Endocrinol Metab Clin North Am* 35:243-53, vii-viii.
- Zenker M. 2008. *UBR1* and the N-end rule pathway and the Johanson-Blizzard syndrome. In: Epstein CJ, Erickson RP, Wynshaw-Boris A, editors. *Inborn Errors of Development*: Oxford University Press. p 1190-4.
- Zerres K, Holtgrave EA. 1986. The Johanson-Blizzard syndrome: report of a new case with special reference to the dentition and review of the literature. *Clin Genet* 30:177-83.
- Zeth K, Ravelli RB, Paal K, Cusack S, Bukau B, Dougan DA. 2002. Structural analysis of the adaptor protein ClpS in complex with the N-terminal domain of ClpA. *Nat Struct Biol* 9:906-11.
- Zhang X, Snijders A, Segraves R, Niebuhr A, Albertson D, Yang H, Gray J, Niebuhr E, Bolund L, Pinkel D. 2005. High-resolution mapping of genotype-phenotype relationships in cri du chat syndrome using array comparative genomic hybridization. *Am J Hum Genet* 76:312-26.

APPENDIX A: MATERIAL

Table A.1: Chemicals and reagents

Product	Company
1 Kb Plus DNA Ladder, invitrogen	Thermo Fisher Scientific Inc.; Waltham, MA, USA
100 bp DNA Ladder, invitrogen	Thermo Fisher Scientific Inc.; Waltham, MA, USA
Acrylamide (2x)	SERVA Electrophoresis GmbH; Heidelberg, Germany
Agencourt AMPure XP	Beckman Coulter; Brea, CA, USA
Agencourt CleanSEQ	Beckman Coulter; Brea, CA, USA
Ammonium persulfate (APS)	SERVA Electrophoresis GmbH; Heidelberg, Germany
β -mercaptoethanol $\geq 99.0\%$	Sigma-Aldrich Corporation; St. Louis, MO, USA
Betaine solution 5M, PCR reagent	Sigma-Aldrich Corporation; St. Louis, MO, USA
Boric acid $\geq 99.8\%$	Carl Roth GmbH + Co. KG; Karlsruhe, Germany
Blotting Grade Blocker Non-Fat Dry Milk	Bio-Rad Laboratories Inc.; Hercules, CA, USA
Bradford reagent	Sigma-Aldrich Corporation; St. Louis, MO, USA
CompleteMini Protease Inhibitor Cocktail	F. Hoffmann-La Roche AG; Basel, Switzerland
Conditioning Reagent, 3500 Series, Applied Biosystems	Thermo Fisher Scientific Inc.; Waltham, MA, USA
Descosept AF	Dr. Schumacher GmbH; Melsungen, Germany
Dimethyl Sulfoxide (DMSO)	Merck KGaA; Darmstadt, Germany
DNA-ExitusPlus IF	AppliChem GmbH; Darmstadt, Germany
Ethylenediaminetetraacetic acid (EDTA) $\geq 99\%$	Carl Roth GmbH + Co. KG; Karlsruhe, Germany
Ethanol 70%, 85%, 100%	Zentralapotheke Universitätsklinikum Magdeburg; Germany
Ethidium bromide 1%, in H ₂ O	Carl Roth GmbH + Co. KG; Karlsruhe, Germany
Ficoll 400	Pharmacia Fine Chemicals; Uppsala, Sweden
GeneScan 500 LIZ dye Size Standard, Applied Biosystems	Thermo Fisher Scientific Inc.; Waltham, MA, USA
GeneScan 600 LIZ dye Size Standard v2.0, Applied Biosystems	Thermo Fisher Scientific Inc.; Waltham, MA, USA
Hi-Di Formamide, Applied Biosystems	Thermo Fisher Scientific Inc.; Waltham, MA, USA
Hydrochloric acid (HCl) 5M	Sigma-Aldrich Corporation; St. Louis, MO, USA
Incidin Foam	Ecolab Inc.; Saint Paul, MN, USA
Orange G	Chemapol; Prague, Czech Republic
POP-7 Performance Optimized Polymer, 3500 Series, Applied Biosystems	Thermo Fisher Scientific Inc.; Waltham, MA, USA
ProSieve QuadColor Protein Marker (4.6-300 kDa)	Lonza Group AG; Basel, Switzerland
Protein Standard I Bovine Plasma Gamma Globulin, Lyophilized	Bio-Rad Laboratories Inc.; Hercules, CA, USA
RNase free H ₂ O	QIAGEN; Hilden, Germany
RNaseOUT, invitrogen	Thermo Fisher Scientific Inc.; Waltham, MA, USA
SALSA MLPA reagents	MRC-Holland; Amsterdam, The Netherlands
Sodium chloride (NaCl) $> 99.8\%$	Carl Roth GmbH + Co. KG; Karlsruhe, Germany
Sodium dodecyl sulphate (SDS)	Carl Roth GmbH + Co. KG; Karlsruhe, Germany
Tetramethylethylenediamine (TEMED)	SERVA Electrophoresis GmbH; Heidelberg, Germany
Tris(hydroxymethyl)aminomethane	Carl Roth GmbH + Co. KG; Karlsruhe, Germany
Tween20	USB Corporation; Cleveland, OH, USA
UltraPure Agarose, invitrogen	Thermo Fisher Scientific Inc.; Waltham, MA, USA

Table A.2: Antibodies

Antibody	Specificity	Company
Anti-UBR1-1	rabbit polyclonal antibody to mouse Ubr1	[Kwon et al., 2001]
Anti-rabbit	goat anti-rabbit IgG, HRP conjugate	Merck KGaA; Darmstadt, Germany
Anti- β -actin	mouse monoclonal antibody to human β -actin	Sigma Aldrich, St. Louis, USA
Anti-mouse	goat anti-mouse IgG, HRP conjugate	Merck KGaA; Darmstadt, Germany

Table A.3: Kits

Product	Company
AmpF ℓ STR [®] Identifiler Plus PCR Amplification Kit, Applied Biosystems	Thermo Fisher Scientific Inc.; Waltham, MA, USA
BigDye Terminator v3.1 Cycle Sequencing Kit, Applied Biosystems	Thermo Fisher Scientific Inc.; Waltham, MA, USA
chemagic DNA Blood Kit special	PerkinElmer chemagen; Baesweiler, Germany
DNA Gel Extraction Kit	Merck Millipore Corporation; Darmstadt, Germany
dNTP Set (100 mM), invitrogen	Thermo Fisher Scientific Inc.; Waltham, MA, USA
Expand Long Range dNTPack	F. Hoffmann-La Roche AG; Basel, Switzerland
GC-RICH PCR System	F. Hoffmann-La Roche AG; Basel, Switzerland
illustra GenomiPhi V2 DNA Amplification Kit	GE Healthcare Life Sciences; Little Chalfont, UK
MinElute Gel Extraction Kit	QIAGEN; Hilden, Germany
Multiplex PCR Kit	QIAGEN; Hilden, Germany
Oligo(dT) ₁₂₋₁₈ Primer, invitrogen	Thermo Fisher Scientific Inc.; Waltham, MA, USA
oragene·DNA collection kits	DNA Genotek Inc.; Kanata, ON, Canada
PAXgene Blood RNA Kit	PreAnalytiX GmbH; Hombrechtikon; Switzerland
pd(N) ₆ Sodium Salt	GE Healthcare Life Sciences; Little Chalfont, UK
Platinum Taq DNA Polymerase, invitrogen	Thermo Fisher Scientific Inc.; Waltham, MA, USA
prepIT·L2P	DNA Genotek Inc.; Kanata, ON, Canada
QIAamp DNA Blood mini Kit	QIAGEN; Hilden, Germany
QIAamp DNA mini Kit	QIAGEN; Hilden, Germany
RNeasy Mini Kit	QIAGEN; Hilden, Germany
SuperScript III Reverse Transcriptase, invitrogen	Thermo Fisher Scientific Inc.; Waltham, MA, USA
Taq DNA Polymerase, recombinant, invitrogen	Thermo Fisher Scientific Inc.; Waltham, MA, USA
Visualize Western Blot Detection Kit; rabbit/mouse	Merck KGaA; Darmstadt, Germany

Table A.4: Commercial buffers and solutions

Product	Company
Anode Buffer Container, 3500 Series, Applied Biosystems	Thermo Fisher Scientific Inc.; Waltham, MA, USA
Cathode Buffer Container, 3500 Series, Applied Biosystems	Thermo Fisher Scientific Inc.; Waltham, MA, USA
Developer G153	AGFA HealthCare; Mortsel, Belgium
Gibco PBS, 10x, pH 7.4	Thermo Fisher Scientific Inc.; Waltham, MA, USA
Low EDTA TE Buffer	Affymetrix; Santa Clara, CA, USA
Pierce LDS Sample Buffer, Non-Reducing (4X)	Thermo Fisher Scientific Inc.; Waltham, MA, USA
Pierce RIPA Buffer	Thermo Fisher Scientific Inc.; Waltham, MA, USA
Pierce Tris-HEPES-SDS Buffer (20x)	Thermo Fisher Scientific Inc.; Waltham, MA, USA
Pierce Western Blot Transfer Buffer, 10x	Thermo Fisher Scientific Inc.; Waltham, MA, USA
Rapid Fixer G354	AGFA HealthCare; Mortsel, Belgium

Table A.5: Preparation of customised buffers and solutions

Blocking buffer (4%)	
TBS buffer (1x)	10 ml
Non-fat dry milk	0.4 g
Tween20	10 μ l
Total volume	~ 10 ml
Developing solution	
H ₂ O, distilled	1250 ml
Solution A (Developer G153A)	1000 ml
Solution B (Developer G153B)	250 ml
Total volume	2500 ml
Fixing solution	
H ₂ O, distilled	2000 ml
Fixing Solution (Rapid Fixer G354)	500 ml
Total volume	2500 ml
Laemmli buffer (2x) with 10% β-mercaptoethanol	
Lithium dodecyl sulfate (LDS) sample buffer (4x)	50 μ l
β -mercaptoethanol	10 μ l
H ₂ O, distilled	40 μ l
Total volume	100 μ l
Loading dye	
Ficoll 400	7.5 g
EDTA	1 ml
fill up with ultra-pure H ₂ O	to 50 ml
add a very small amount of Orange G	
centrifuge 5 min at 3,000 rpm, use supernatant	
Running buffer (1x)	
Tris/HEPES/SDS Buffer (20x)	50 ml
H ₂ O, distilled	950 ml
Total volume	1000 ml
TBE buffer (5x)	
Tris base	54 g
Boric acid	27.5 g
EDTA (0.5 M)	20 ml
adjust pH with 5N hydrochloric acid HCl to 8.3	
fill up with distilled H ₂ O	to 1000 ml
TBS buffer (10x)	
Tris base (Formula weight 121.1 g)	24 g
Sodium chloride NaCl (Formula weight 58.4 g)	88 g
H ₂ O, distilled	900 ml
adjust pH with 5N hydrochloric acid HCl to 7.6	
fill up with distilled H ₂ O	to 1000 ml
Washing buffer (TBST 0.1%)	
TBS buffer (1x)	10 ml
Tween20	10 μ l
Total volume	~ 10 ml

Table A.6: Consumables

Product	Company
96-well flat bottom transparent microplate	Greiner Bio-One International GmbH; Kremsmünster, Austria
96 Well Multiply PCR plate, neutral	Sarstedt AG & Co; Nümbrecht, Germany
96-Well PCR Plate, non-skirted	4titude Limited; Wotton, UK
Acetate Foil for 96Well Plate	Sarstedt AG & Co; Nümbrecht, Germany
Biomek AP 96 P250 Tips	Beckman Coulter; Brea, CA, USA
Biopak Polisher	Merck Millipore Corporation; Darmstadt, Germany
CELLSTAR Standard Suspensionskulturflaschen	Greiner Bio-One International GmbH; Kremsmünster, Austria
CL-XPosure Film, 5 x 7 inches	Thermo Fisher Scientific Inc.; Waltham, MA, USA
Cling film	Carl Roth GmbH + Co. KG; Karlsruhe, Germany
Combitips advanced, 0.1 ml, 0.2 ml	eppendorf AG; Hamburg, Germany
Combitips plus, 0.5 ml, 1.0 ml	eppendorf AG; Hamburg, Germany
Disposable Scalpel stainless steel 10	FEATHER Safety Razor Co., Ltd.; Osaka, Japan
Filter Tips and Filter Tips wide-bore; 200 µl, 1.000 µl	QIAGEN; Hilden, Germany
High Density Paper K65HM-CE	Mitsubishi Electric Corporation; Tokyo, Japan
Kimtech Science precision wipes	Kimberly-Clark Corporation; Inving, TX, USA
MaiMed solution PF, nitrile gloves	MaiMed GmbH; Neuenkirchen, Germany
MicroAmp 8-Cap Strip, Applied Biosystems	Thermo Fisher Scientific Inc.; Waltham, MA, USA
MicroAmp Fast 96-Well Reaction Plate (0.1 mL), Applied Biosystems	Thermo Fisher Scientific Inc.; Waltham, MA, USA
MicroAmp Fast Reaction Tubes (8 Tubes/Strip), Applied Biosystems	Thermo Fisher Scientific Inc.; Waltham, MA, USA
MicroAmp Optical 96-Well Reaction Plate, Applied Biosystems	Thermo Fisher Scientific Inc.; Waltham, MA, USA
Multiply-µStrip Pro 8-strip	Sarstedt AG & Co; Nümbrecht, Germany
Nitrocellulose Membrane	Amersham Pharmacia Biotech; Little Chalfont, UK
PAGEr Precast Gel 4-12%	Lonza Group AG; Basel, Switzerland
Parafilm "M"	Pechiney Plastic Packaging; Menasha, WI, USA
PAXgene Blood RNA Tubes	PreAnalytiX GmbH; Hombrechtikon; Switzerland
PCR SingleCap, 8er-SoftStrips, 0.2 ml, domed cap	Biozym Scientific GmbH; Hessisch Oldendorf, Germany
PCR SoftTubes, 0.2 ml, domed cap	Biozym Scientific GmbH; Hessisch Oldendorf, Germany
Pipette tips 0.1-10 µl, 0.1-20 µl long, 1-200 µl, 2-200 µl, 50-1000 µl, 200-1000 µl	eppendorf AG; Hamburg, Germany Sarstedt AG & Co; Nümbrecht, Germany Gilson Inc.; Middleton, WI, USA
Reaction tubes with lids (1.5 ml, 2.0 ml)	eppendorf AG; Hamburg, Germany Sarstedt AG & Co; Nümbrecht, Germany
Reagent and centrifuge tubes (15 ml, 50 ml)	Sarstedt AG & Co; Nümbrecht, Germany
Sekuroka disposable bags, autoclavable	Carl Roth GmbH + Co. KG; Karlsruhe, Germany
Serological pipettes, plugged 5 ml, 10 ml, 25 ml	Sarstedt AG & Co; Nümbrecht, Germany
TGX Precast Gel 4-15%	Lonza Group AG; Basel, Switzerland
Thermowell Sealing Mats, 96 well	Corning Inc; Corning, NY, USA
Tube with screw cap (2 ml)	Sarstedt AG & Co; Nümbrecht, Germany

Table A.7: Laboratory equipment

Product	Company
8-channel pipet <i>m</i> 10, 0.5-10 µl	Biohit Oyj; Helsinki, Finland
2720 Thermal Cycler, Applied Biosystems	Thermo Fisher Scientific Inc.; Waltham, MA, USA
3500xL Genetic AnalyZer, Applied Biosystems	Thermo Fisher Scientific Inc.; Waltham, MA, USA
Agencourt SPRIPlate 96R ring magnetic plate	Beckman Coulter; Brea, CA, USA
Airstream PCR Cabinets	ESCO Technologies Inc.; St. Louis, MO, USA
Autoclave VX-150	Systec GmbH; Linden, Germany
Biomek NX ^P Laboratory Automation Workstation	Beckman Coulter; Brea, CA, USA
chemagic Magnetic Separation Module I	PerkinElmer chemagen; Baesweiler, Germany
Compressor 2x4-40	JUN-AIR; Benton Harbor, MI, USA
Cooling and heating block CHB-202	biostep; Jahnsdorf, Germany
Devision DBox	Decon Science Tec GmbH; Hohengandern, Germany
E143 Electrophoresis Power Supply	Consort bvba; Turnhout, Belgium
Electrophoresis accessories (gel trays, combs, casting chambers)	PeqLab; Erlangen, Germany
Erlenmeyer flask 500 ml, SIMAX	Kavalierglass Co.Ltd; Prague, Czech Republic
Freezer and fridges	Liebherr; Bulle, Switzerland Robert Bosch GmbH; Gerlingen, Germany
Heraeus Labofuge 400	Thermo Fisher Scientific Inc.; Waltham, MA, USA
Heraeus Pico 17 Centrifuge	Thermo Electron Corporation; Waltham, MA, USA
Heraeus Oven	Thermo Fisher Scientific Inc.; Waltham, MA, USA
Ice machine ZBE 30-10	Ziegra Eismaschinen GmbH; Isernhagen, Deutschland
iCycler	Bio-Rad Laboratories Inc.; Hercules, CA, USA
inoLab pH meter	WTW Wissenschaftlich-Technische Werkstätten GmbH; Weilheim, Germany
M200 microplate reader	Tecan Group Ltd.; Männedorf, Switzerland
Magnetic stirrer IKAMAG RCT	IKA Werke GmbH & Co. KG; Staufen, Germany
Masterflex Console Drive	Cole-Parmer; Vernon Hills, IL, USA
Masterflex Easy-Load II	Cole-Parmer; Vernon Hills, IL, USA
Masterflex PharMed Tubing 24/36	Cole-Parmer; Vernon Hills, IL, USA
Measuring cylinder 100 ml, plastic	VITLAB GmbH; Grossostheim, Germany
Measuring cup 2000 ml, plastic	VITLAB GmbH; Grossostheim, Germany
Microwave oven R-939 IN	Sharp K.K.; Osaka, Japan
Milli-Q Reference Water Purification System	Merck Millipore Corporation; Darmstadt, Germany
Mini-PROTEAN Tetra Cell	Bio-Rad Laboratories Inc.; Hercules, CA, USA
Mini-PROTEAN trans-blot cell	Bio-Rad Laboratories Inc.; Hercules, CA, USA
MiniSpin	Eppendorf; Hamburg, Germany
Multipette plus/stream	Eppendorf; Hamburg, Germany
NanoDrop 2000/2000c UV-Vis spectrophotometer	Thermo Fisher Scientific Inc.; Waltham, MA, USA
PerfectBlue Gel System Mini S/L	PeqLab; Erlangen, Germany
pipetus-akku	Hirschmann Laborgeräte GmbH & Co. KG; Eberstadt, Germany
PowerPac Basic Power Supply	Lonza Group AG; Basel, Switzerland
Precision scale PEJ 4200-2M	Kern & Sohn GmbH; Balingen, Germany
QIAcube robotic workstation	QIAGEN; Hilden, Germany
Reagent bottle with screw cap, SIMAX; 250 ml, 500 ml, 1000 ml	Kavalierglass Co.Ltd; Prague, Czech Republic
Refrigerated centrifuge 3K 12	Sigma Laborzentrifugen GmbH; Osterode am Harz, Germany
Roll mixer RM5	Karl Hecht Assistent GmbH; Altnau, Switzerland
Single channel pipets	Gilson Inc.; Middleton, WI, USA eppendorf AG; Hamburg, Germany
Spinbar Magnetic Stirring Bars	Sarstedt AG & Co; Nümbrecht, Germany
Swivel mixer DESAGA SM1	Sarstedt AG & Co; Nümbrecht, Germany
Thermal Printer P93D	Mitsubishi Electric Corporation; Tokyo, Japan

Product	Company
Thermomixer compact	eppendorf AG; Hamburg, Germany
UV Transilluminator	Decon Science Tec GmbH; Hohengandern, Germany
Veriti 96-Well Fast Thermal Cycler, Applied Biosystems	Thermo Fisher Scientific Inc.; Waltham, MA, USA
Vortex Genie 2	Scientific Industries, Inc.; Bohemia, NY, USA
VWR Duo Cycler	VWR International, Radnor, PA, USA
X-Ray Film Processor	AGFA HealthCare; Mortsel, Belgium

Table A.8: Software

Software	Company
3500 Data Collection Software	Applied Biosystems; Waltham, MA, USA
Biomek software	Beckman Coulter; Brea, CA, USA
chemagic MSM I V5106	PerkinElmer chemagen; Baesweiler, Germany
Chromas Lite	Technelysium Pty Ltd; South Brisbane, Australia
DeVision G	Decon Science Tec GmbH; Hohengandern, Germany
GeneMapper	Applied Biosystems; Waltham, MA, USA
GenLAB7	projodis medical; Butzbach, Germany
Microsoft Office	Microsoft Corporation; Redmond, WA, USA
NanoDrop 2000/2000c	Thermo Fisher Scientific Inc; Waltham, MA, USA
Raw probe	MRC Holland; Amsterdam, The Netherlands
Sequence Pilot	JSI medical systems GmbH; Ettenheim, Germany
Sequencing Analysis	Applied Biosystems; Waltham, MA, USA
TECAN Magelan Software	Tecan Group Ltd.; Männerdorf, Switzerland

Table A.9: Online tools

Online tool	Homepage
1000 Genomes Project	http://www.1000genomes.org
Berkeley Drosophila Genome Project	http://www.fruitfly.org
Clustal Omega	http://www.ebi.ac.uk/Tools/msa/clustalo
ClustalW2	http://www.ebi.ac.uk/Tools/msa/clustalw2
dbSNP	http://www.ncbi.nlm.nih.gov/SNP
Ensembl Genome Browser	http://www.ensembl.org/index.html
ExAC Browser	http://exac.broadinstitute.org
GeneCards	http://www.genecards.org
Genomic Evolutionary Rate Profiling	http://mendel.stanford.edu/SidowLab/downloads/gerp/index.html
HUGO Gene Nomenclature Committee	http://www.genenames.org/
Human Genome Variation Society	http://www.hgvs.org/mutnomen/
Leiden Open Variation Database 3.0	http://www.lovd.nl/3.0/home
Mutalyzer	https://mutalyzer.nl/
MutationTaster	http://www.mutationtaster.org
MutPred	http://mutpred.mutdb.org
NCBI	http://www.ncbi.nlm.nih.gov
NCBI BLAST	http://blast.ncbi.nlm.nih.gov/Blast.cgi
NCBI PubMed	http://www.ncbi.nlm.nih.gov/pubmed
NetGene2	http://www.cbs.dtu.dk/services/NetGene2
Online Mendelian Inheritance in Man	http://www.omim.org
Orphanet	http://www.orpha.net
PolyPhen-2	http://genetics.bwh.harvard.edu/pph2
Primer3web 4.0.0	http://primer3.ut.ee
SIFT (via PROVEAN)	http://provean.jcvi.org/index.php
STRING	http://string-db.org
UCSC Genome Browser	https://genome.ucsc.edu/index.html

APPENDIX B: OLIGONUCLEOTIDES

B.1 PCR AND SEQUENCING PRIMER

Table B.1.1: *UBR1* standard primer.

Exon	Name	Sequence (5'-3')	Amplicon
1	UBR1_E01F* UBR1_E01R	gaagccactcctcgagtctg agacttggctggcagaaatg	400 bp
2	UBR1_E02F* UBR1_E02R	ggtggtatgtgagcagttgc tgggtcacacagcaagactc	535 bp
3	UBR1_E03F* UBR1_E03R	ggtcaaggcccaaagtattg tttctgtaaagcaacacacatcc	510 bp
4	UBR1_E04F UBR1_E04R*	ttttcgcacactttgcaatc aaaacagcaggggttctaactgg	543 bp
5	UBR1_E04F UBR1_E05R*	ttcattcctggacgatgttg ggatgagaggctgctaggtc	550 bp
6	UBR1_E06F UBR1_E06R*	cccacaggttgaaactacacag gagaggatggtcagacctagcac	361 bp
7+8	UBR1_E07+08F* UBR1_E07+08R	gagctcattaagtctttgggctac gcaaccctgaaaattaatcaaag	645 bp
9	UBR1_E09F UBR1_E09R*	cactgtgagaggctgagggtg aaagacaacatccctgggttt	442 bp
10	UBR1_E10F* UBR1_E10R	ggaggggtgcagaaaaagag aggccaagaacaaacttttgac	433 bp
11	UBR1_E11F UBR1_E11R*	tttttgctgatcataatatcttgc tcatctgcattgacgaggac	446 bp
12	UBR1_E12F* UBR1_E12R	cctgtctaattgggcttgagag acgcgaggcagtaacagttc	547 bp
13	UBR1_E13F UBR1_E13R*	agttagctgtgacaggcttgg ggatctatcaaaacaggatgagtg	558 bp
14	UBR1_E14F* UBR1_E14R	ttgaaccatgcattctgac tttccaggaataaacgtgtg	532 bp
15	UBR1_E15F* UBR1_E15R	tgcagtgagctgtgattatgc tgggtgggagatgagttacc	582 bp
16+17	UBR1_E16+17F* UBR1_E16+17R	gccaaatcaaatcgcacaag cactcagtaaaatctaggaacacagg	655 bp
18	UBR1_E18F* UBR1_E18R	tcatcctcgctagtcccttt tgtaaagcctcggcaagt	562 bp
19	UBR1_E19F UBR1_E19R*	tttttgacagtcctacatgagaaa aaggaagggatccagaacaaa	544 bp
20	UBR1_E20F UBR1_E20R*	tgagggcggtgtagagaag tctgtgcttttgtgaagggtga	583 bp
21	UBR1_E21F UBR1_E21R*	cttttgcccctctctcacag tcccagatcccttaccattg	595 bp
22	UBR1_E22F UBR1_E22R*	cgaagttggtctcccaaac cccctcattctcaccctttc	381 bp
23	UBR1_E23F* UBR1_E23R	attgcaatggaattttcataag tgatgaagtccatgatgcttg	503 bp
24	UBR1_E24F UBR1_E24R*	ggtgatgtctggctttgtcc gttgccactctcaaaaacc	472 bp
25	UBR1_E25F* UBR1_E25R	ggtttttgagagtgggcaac gacctgagatcttccctagctc	539 bp
26	UBR1_E26F UBR1_E26R*	tggtcgtgtgcacctctagtc tttcaggattgacaaattaaaactcc	398 bp

Exon	Name	Sequence (5'-3')	Amplicon
27	UBR1_E27F UBR1_E27R*	cctgaaaccaattccctgag aacactggaggcaagcagag	248 bp
28	UBR1_E28F* UBR1_E28R	ggcgtttgtcacagtcagag tcccgacctcaagtgatcta	545 bp
29	UBR1_E29F* UBR1_E29R	tgtcatgcagcctgtaatgc tgagttggtaatTTTTGGTTTgc	380 bp
30	UBR1_E30F UBR1_E30R*	ccaaaatatgaagacaagtgacca cccttatttccaaatgTTTTTca	362 bp
31	UBR1_E31F UBR1_E31R*	tgcttggacattcctaagacag gcccggccaattattacttt	472 bp
32	UBR1_E32F* UBR1_E32R	ttattggggcaaaaattcca tcagccccctcaagtaactg	488 bp
33	UBR1_E33F* UBR1_E33R	ttccttcccccttccaaaag tcaagaaatctgtacttgcaaacc	383 bp
34	UBR1_E34F* UBR1_E34R	aaaactaggcaggcatgggtg gtagggccacagagaactgg	571 bp
35	UBR1_E35F* UBR1_E35R	aacccttcttagctgtgagc accagaccaaatggcatgag	600 bp
36	UBR1_E36F UBR1_E36R*	aagattgctgcaggtgcttt cgctgtaaagtgcacatgct	483 bp
37	UBR1_E37F* UBR1_E37R	ctgcagctaattccgacaaac gcatggcttctgtaggtgggt	359 bp
38	UBR1_E38F* UBR1_E38R	gcagccttttctcagttcag gaaaaggccagaagaggag	552 bp
39	UBR1_E39F* UBR1_E39R	ctgctgcccttcacatttag aagcaggtccaagtgggtctc	488 bp
40	UBR1_E40F UBR1_E40R*	ggcaacaagagcgaaactct aaaactgaaactacacccttcc	468 bp
41	UBR1_E41F UBR1_E41R*	tgcccggctaattcagtaga atggggagaggagaagtgggt	499 bp
42	UBR1_E42F* UBR1_E42R	tgccaccatggTTTTatag TTTgccccctTTaatcag	365 bp
43	UBR1_E43F UBR1_E43R*	tgaacctaggaggcagaagc aggaaaaggacagccactcc	420 bp
44	UBR1_E44F UBR1_E44R*	ttgggcagTTTTgatctgg aggagTTTgaggctgcagtg	364 bp
45	UBR1_E45F* UBR1_E45R	tgggcatgtcagatgaagac ccatagtgacccccagattg	571 bp
46	UBR1_E46F* UBR1_E46R	ccaccattttccaaggtgtc cggTgtctggcctcaattac	544 bp
47	UBR1_E47F* UBR1_E47R	ggctccaggaacatctcaag acctggacatggagcaaaag	363 bp

Asterisks indicate unidirectional sequencing primer. NCBI transcript number: NM_174916.2.

Table B.1.2: DOCK6 standard primer.

Exon	Name	Sequence (5'-3')	Amplicon
1	DOCK6_E01F* DOCK6_E01R	gcctcctctccctaacttcc cggaaaggggttgaattggg	473 bp
2	DOCK6_E02F DOCK6_E02R*	gccctcggectatTTatttc taggaccaggacaggcactc	368 bp
3	DOCK6_E03F* DOCK6_E03R	accgccctcctatTTgagtt gcctctgtgaatccttctgc	479 bp
4	DOCK6_E04F* DOCK6_E04R	ggcaggacagtgtacactt gggacaatgggcagatacac	249 bp
5	DOCK6_E05F* DOCK6_E05R	caaacttgtctggtggagca caaggctgTTTgggtcattt	354 bp

Exon	Name	Sequence (5'-3')	Amplicon
6	DOCK6_E06F* DOCK6_E06R	cccaggtgacccttagagtg tgcccaataaacactgatcg	493 bp
7	DOCK6_E07F* DOCK6_E07R*	caggggatggaaagacggtta tggcacttaaggattggaga	400 bp
8+9	DOCK6_E08+09F* DOCK6_E08+09R	ggcctcaagagggagtgg gccctgattacccttcttgg	497 bp
10	DOCK6_E10F* DOCK6_E10R	aggccaacactaacccttga gcgagcttctctagcttct	378 bp
11	DOCK6_E11F* DOCK6_E11R*	gaagtggacacagccaaggt acagttcggccagcagag	370 bp
12+13	DOCK6_E12+13F* DOCK6_E12+13R	ctctgctggccgaactgt cctggcacagtaggtgctct	494 bp
14	DOCK6_E14F* DOCK6_E14R	agtctgccctgactacacagc ccctttcatgcctacacacc	398 bp
15+16	DOCK6_E15+16F* DOCK6_E15+16R	cccagcctcatgacctactc catcgatgctgccttatgtg	474 bp
17+18	DOCK6_E17+18F* DOCK6_E17+18R*	caataagggcgtggcatgg ctcccaggattgacaggaag	497 bp
19	DOCK6_E19F* DOCK6_E19R*	tcattcaccctgtgtctcca ccatcggcaactgttactca	395 bp
20	DOCK6_E20F* DOCK6_E20R	ggaccagctttaaggaag gcaaagggtcacagaagac	490 bp
21	DOCK6_E21F* DOCK6_E21R*	tgatccctcaaactctgatg tggccaagttgatctcgaa	400 bp
22	DOCK6_E22F* DOCK6_E22R*	gctgagtaggaaggactgg actctgctgccagagtgc	374 bp
23	DOCK6_E23F* DOCK6_E23R	agggcacttccactcctctt ccaaagtgttgggattacagg	370 bp
24	DOCK6_E24F* DOCK6_E24R	aacctaccttcagcccacct cagcaaagtggattcctgggt	456 bp
25+26	DOCK6_E25+26F* DOCK6_E25+26R*	gatcttgggtgagagccaagc gaggaacctataggagatgga	522 bp
27	DOCK6_E27F* DOCK6_E27R*	actccgtgccctgttacatc gtgcaacaggaatgcctat	461 bp
28	DOCK6_E28F* DOCK6_E28R	tgagcagagctcctgtctagc tccattacaggggagaaacc	450 bp
29	DOCK6_E29F* DOCK6_E29R*	gccatgaggggaagacttctg tgagatgaatcctggccaat	337 bp
30	DOCK6_E30F* DOCK6_E30R*	tccactttgaatgagagaagtca cagagtcctctgcacaaagaca	400 bp
31	DOCK6_E31F* DOCK6_E31R*	gagcacaagaaagggatgg cgcatgtgtacggatgatgat	360 bp
32	DOCK6_E32F* DOCK6_E32R	ttcatgcctgtgcatttctc acaaggtttcaccgtagcc	419 bp
33	DOCK6_E33F* DOCK6_E33R	gagagagctcagccatggag gggtcagaaatccaggtggt	296 bp
34	DOCK6_E34F* DOCK6_E34R	gtgccctgtggtctctgact ctgggattagaggcatgagc	316 bp
35	DOCK6_E35F* DOCK6_E35R	acttggccaaagaggacaga cctcactccctgtatggttga	354 bp
36+37	DOCK6_E36+37F* DOCK6_E36+37R	cggcaggttgagcagact atccctgttctccctgcac	520 bp
38	DOCK6_E38F* DOCK6_E38R*	gaggagattggctggtcctt gacaggatgtcgtcggagat	451 bp
39	DOCK6_E39F* DOCK6_E39R	ccctcgtggctgagtacct gctggaagggtctaggaagc	378 bp
40+41	DOCK6_E40+41F* DOCK6_E40+41R	gctcacaagggagatgggta gtgttactgatggctgctg	408 bp

Exon	Name	Sequence (5'-3')	Amplicon
42+43	DOCK6_E42+43F DOCK6_E42+43R*	gtcctcacactcccacatcctg gtccccaggaaacagcact	486 bp
44	DOCK6_E44F* DOCK6_E44R	tgacaaagtccccagatccc gaggtcctggaaccacctt	442 bp
45+46	DOCK6_E45+46F DOCK6_E45+46R*	cgactggcttcgatcagg taatgggaatcgggcaga	511 bp
47	DOCK6_E47F DOCK6_E47R*	acctcctattgctgggtcttt tccaagctaccagcaaacat	400 bp
48	DOCK6_E48F* DOCK6_E48R	atgtgggctgggaggtctat atgtgtggatatggggcagt	397 bp

Asterisks indicate unidirectional sequencing primer. NCBI transcript number: NM_020812.3.

Table B.1.3: ARHGAP31 standard primer.

Exon	Name	Sequence (5'-3')	Amplicon
1	ARHGAP31_E01F* ARHGAP31_E01R	gttcttccatcttccgatgc gcacaggcctggaatacatta	347 bp
2	ARHGAP31_E02F* ARHGAP31_E02R	tgaaaggaacatcacctacca ctgccacacttccctcagtt	387 bp
3	ARHGAP31_E03F* ARHGAP31_E03R	ttcctagggcctggagtaga ttccctcaccacgctaagat	430 bp
4	ARHGAP31_E04F ARHGAP31_E04R*	gctggagatgagggccttga tgcagggtgatttgggagactg	398 bp
5	ARHGAP31_E05F* ARHGAP31_E05R	tcaatcttgacatctttccaatg aaatgaccacttaagccacaga	378 bp
6	ARHGAP31_E06F ARHGAP31_E06R*	tttaggagatgagccttgtgc cagcatacacacagccaaca	367 bp
7	ARHGAP31_E07F* ARHGAP31_E07R	aagaatggagggactgtgga actgccatcttggctcctgag	378 bp
8	ARHGAP31_E08F ARHGAP31_E08R*	tcagagccattcataactgagg aacattgggagaagctgcat	459 bp
9	ARHGAP31_E09F* ARHGAP31_E09R	tgggtacttaaacagcctgacc caggcatgacagcttataaagg	231 bp
10a	ARHGAP31_E10aF* ARHGAP31_E10aR	cgtgtgcctgccccttact caaagggctcggagatggt	482 bp
10b	ARHGAP31_E10bF* ARHGAP31_E10bR	accggaacagctgaagggttt accgcactatattgccttgc	451 bp
11	ARHGAP31_E11F* ARHGAP31_E11R	aaacagggccaggagacag gtccctttggcagaaactga	498 bp
12a	ARHGAP31_E12aF* ARHGAP31_E12aR	atltgctgaactggcacagg ttccactggttgccttgtggag	499 bp
12b	ARHGAP31_E12bF* ARHGAP31_E12bR	ccctctggaggtgtggacta acgatctcaacctccctggt	474 bp
12c	ARHGAP31_E12cF* ARHGAP31_E12cR	agctgaagtcccaagacagc agagggtcagaattcctctctg	499 bp
12d	ARHGAP31_E12dF* ARHGAP31_E12dR	ttcgccagagccattctcta agggccaagttgaggggaag	488 bp
12e	ARHGAP31_E12eF* ARHGAP31_E12eR	agagcagcaaggagagttca gctcctctccagaggctga	500 bp
12f	ARHGAP31_E12fF* ARHGAP31_E12fR	ccttcatgggtcaaaatgtgc ggggaaaggaggactgaataa	500 bp
12g	ARHGAP31_E12gF* ARHGAP31_E12gR	aagcgcagtgtcagagacaga aacgtgtgcctggaatatgg	499 bp

Asterisks indicate unidirectional sequencing primer. NCBI transcript number: NM_020754.2.

Table B.1.4: RBPJ standard primer.

Exon	Name	Sequence (5'-3')	Amplicon
01iso1	RBPJ_ex01iso1F RBPJ_ex01iso1R*	gctggcgaattccagttct tggtgagaccactactgcaca	291 bp
01iso2	RBPJ_ex01iso2F RBPJ_ex01iso2R*	cattcctcgtccccgtagta cagacgcccgcgaactttc	422 bp
01iso3	RBPJ_ex01iso3F RBPJ_ex01iso3R*	tgttacacagggtagcagcag ctaccataaatccataaccacatct	463 bp
02	RBPJ_ex02F RBPJ_ex02R*	aaaagagatTTTTatgatgcctga gggaggagagatgagggaaa	288 bp
03	RBPJ_ex03F RBPJ_ex03R*	aagcattcctctcattacagagc tgaaccagtaatagaagccatc	290 bp
04	RBPJ_ex04F RBPJ_ex04R*	tttcccctattattcttcaggTTTT tgcccctttctggtgaacta	221 bp
05	RBPJ_ex05F RBPJ_ex05R*	acatggccattctgagttt ggctattgaaaaggcaatTTTT	346 bp
06	RBPJ_ex06F RBPJ_ex06R*	cactgccaagcagaatttcc ggagtgccatgccagtaac	478 bp
07	RBPJ_ex07F* RBPJ_ex07R	ttttcatgccagttcacagc ccatttgaatggttgatTTTTcc	391 bp
08	RBPJ_ex08F* RBPJ_ex08R	ggcataggacaaataactgtgatg ccttgaggaaggattgcttg	455 bp
09	RBPJ_ex09F* RBPJ_ex09R	atgtagggattggcaaagca cccatgaaatgaaatgatgc	395 bp
10	RBPJ_ex10F* RBPJ_ex10R	aggagcgtacttgccagaaa cattacaatcagtgccagggaaa	387 bp
11	RBPJ_ex11F* RBPJ_ex11R	aggggtgtgggtacaggag gagacaacggggtTTTTgaa	588 bp

Asterisks indicate unidirectional sequencing primer. To cover all coding exons, the variants RBPJ-001, -002, and -003 (ENST00000345843, ENST00000361572, ENST00000342320), who have differences regarding the first exon, have to be analysed (Figure 1.11B). NCBI transcript number for RBPJ-001: NM_203283.2.

Table B.1.5: EOGT standard primer.

Exon	Name	Sequence (5'-3')	Amplicon
04	EOGT_E04F EOGT_E04R*	atacttagcccttgacccttt acaaccgaaaattagaattctgcc	444 bp
05	EOGT_E05F* EOGT_E05R	tgtaagaaccttgagactgct atggctcctggctgtttctcc	499 bp
06	EOGT_E06F* EOGT_E06R	tgtagtgaggcgtagttttgg gggcaatagacagaaactccg	348 bp
07	EOGT_E07F* EOGT_E07R	tgtgtggtttgaatgtgaggg acttgggtttgggaggtcac	369 bp
08	EOGT_E08F* EOGT_E08R	atcgcattgcaaagttgggt gcaactgagggattcactcg	473 bp
09	EOGT_E09F EOGT_E09R*	tccataggagtgtctgtacca tggaagtccaattagttcaact	399 bp
10	EOGT_E10F* EOGT_E10R	gatgggatagaataaaaacttgcttg tcacaacatcagagtcacaca	250 bp
11	EOGT_E11F* EOGT_E11R	tttaacacaggcaaatcagggt tcagaaatcagtggtaattggct	300 bp
12+13	EOGT_E12+13F EOGT_E12+13R*	tcaagcaatgcaaaatggaga acatggtctcctgattattttctgt	495 bp
14	EOGT_E14F* EOGT_E14R	cctgagagtgggtgaaggaa gcataggccatcaacttttctc	360 bp
15	EOGT_E15F* EOGT_E15R	tggggcctggatttgaactt ccttctgggcctacaaatgc	380 bp

Exon	Name	Sequence (5'-3')	Amplicon
16	EOGT_E16F* EOGT_E16R	ggaatgtggttttaaataatgggca agccttttgatgctcagaatga	329 bp
17	EOGT_E17F* EOGT_E17R	tcctcagtcttggtttacaaccttt tctttgcagcactgaagtca	331 bp
18	EOGT_E18F* EOGT_E18R	tggagtaactgtgactgagacc acaacacataacaatatcctgaagg	492 bp
18b	EOGT_E18bF* EOGT_E18bR*	cagcctgcaccaccacac gcttgggtactgagaatcacaact	589 bp

Asterisks indicate unidirectional sequencing primer. Exons 4-18 represent isoform EOGT-002 (ENST00000383701), exon 18b is an alternative last exon in isoform EOGT-203 (ENST00000615922). NCBI transcript number for EOGT-002: NM_001278689.

Table B.1.6: NOTCH1 standard primer.

Exon	Name	Sequence (5'-3')	Amplicon
01	NOTCH1_E01F NOTCH1_E01R	ctgagcctcactagtgcctc gatcccgggactccagaac	498 bp
02	NOTCH1_E02F NOTCH1_E02R	agagtgcgtccgggtag caatggcctagtgttctgtc	300 bp
03	NOTCH1_E03F NOTCH1_E03R	ctgtgcccatagacagggttc tccaataacttccgggtca	470 bp
04	NOTCH1_E04F NOTCH1_E04R	tgtggtccttcatctgcaa atcccgccttcccaactc	640 bp
05	NOTCH1_E05F NOTCH1_E05R	ctggagtgaggcagggga ctagtctgcctggcctgg	397 bp
06	NOTCH1_E06F NOTCH1_E06R	gaggagtccagcccaggaag ggcctcccctgaccagaaag	483 bp
07	NOTCH1_E07F NOTCH1_E07R	tccaagtgtcacgggatg acctcactgcacaccacc	441 bp
08	NOTCH1_E08F NOTCH1_E08R	atgagtgtctcgtgggtag aagcaaccacagatgttcc	486 bp
09	NOTCH1_E09F NOTCH1_E09R	ggttcgtttctgtccaagt tctgggaatctgaacaaa	592 bp
10	NOTCH1_E10F NOTCH1_E10R	ctcactgctggggctctgg agaccaagggtgtccatgacc	291 bp
11+12	NOTCH1_E11+12F NOTCH1_E11+12R	gggccgccagtcctaagt cctcaccacaaccctcag	567 bp
13	NOTCH1_E13F NOTCH1_E13R	tggaaggatgtggccagaag tttctggccatctcaagct	411 bp
14	NOTCH1_E14F NOTCH1_E14R	attgcagaccgggagtg cctcctcatctccaagagcc	383 bp
15	NOTCH1_E15F NOTCH1_E15R	ctggggagctggagacac tcccaggcatcctgtatctt	600 bp
16	NOTCH1_E16F NOTCH1_E16R	cactctgatggcgaaagac ggtgctcccagggtcaattcc	379 bp
17	NOTCH1_E17F NOTCH1_E17R	attaggggagaggggatgg cctccctgggtgcttatgg	398 bp
18	NOTCH1_E18F NOTCH1_E18R	ctgtcccagccatgcag aggacagggtcggtaaatg	480 bp
19	NOTCH1_E19F NOTCH1_E19R	ctaggggtgagcagaagggg tgctcagatcccagaaacc	453 bp
20+21	NOTCH1_E20+21F NOTCH1_E20+21R	gttggagtaggccccttgg cctatcagggttcagttttctcc	625 bp
22	NOTCH1_E22F NOTCH1_E22R	gtctgacaggagcgaggg tttctggctgggtcctggat	381 bp
23	NOTCH1_E23F NOTCH1_E23R	tgacagcccagacctgag gtaagagcagggcagtgaga	429 bp

Exon	Name	Sequence (5'-3')	Amplicon
24	NOTCH1_E24F NOTCH1_E24R	cctgtccaatccctgcca ggtgaggaggaggatgaagg	399 bp
25a	NOTCH1_E25aF NOTCH1_E25aR	caggttagaggagagcgggtg caggctgcagacctgtgtg	488 bp
25b	NOTCH1_E25bF NOTCH1_E25bR	catccgagagccccttctac ccctgagcagagccttagaa	471 bp
26	NOTCH1_E26F NOTCH1_E26R	ttctaaggctctgctcaggg taaagtggggagagtactgc	669 bp
27	NOTCH1_E27F NOTCH1_E27R	tctgactgtggcgtcatg ttccagaaaagccctacccc	400 bp
28	NOTCH1_E28F NOTCH1_E28R	tgatcgggtgcatgtgaagtg gtgaggatgctcggccag	638 bp
29+30	NOTCH1_E29+30F NOTCH1_E29+30R	gacctggccgagcatcct aggatgaaagctctcacccc	605 bp
31	NOTCH1_E31F NOTCH1_E31R	gtggccccttgagcttgg gctcccagggccacgtaa	480 bp
32+33	NOTCH1_E32+33F NOTCH1_E32+33R	atctcaggaggggtctcgtct caggcccttgtgtccctg	580 bp
34a	NOTCH1_E34aF NOTCH1_E34aR	aggttgactgctgcttctcct caggcaggtggttgaggg	621 bp
34b	NOTCH1_E34bF NOTCH1_E34bR	aaggcacggaggaagaagtc cctaccatgccatgctgc	515 bp
34c	NOTCH1_E34cF NOTCH1_E34cR	tgaatggtcaatgagagtggtg caggcagagtagctgtg	570 bp
34d	NOTCH1_E34dF NOTCH1_E34dR	cctggcgggtgcacactatt aaaaggctcctctggtcgg	413 bp

NCBI transcript number: NM_017617.3.

Table B.1.7: DLL4 standard primer.

Exon	Name	Sequence (5'-3')	Amplicon
01	DLL4_E01F DLL4_E01R	cagcgagaaggccaaagg cgctcgttgatgaactcctg	355 bp
02	DLL4_E02F DLL4_E02R	gcactttggcagcaggtaac acaaggaaatctggggaggg	485 bp
03	DLL4_E03F DLL4_E03R	ttaattaaacaggctgccgc ccccgcctagaacagattaac	220 bp
04	DLL4_E04F DLL4_E04R	ggctgattggttggctgatc tgaccaagaagctccactgt	450 bp
05+06	DLL4_E05-06F DLL4_E05-06R	gaggccaggagtaggaagag tccaggtgacgaatcggatt	476 bp
07	DLL4_E07F DLL4_E07R	gcaaacatggactgcaagga aatgcctgtccatggctgta	346 bp
08	DLL4_E08F DLL4_E08R	tacagccatggacaggcatt ccctccctcaccagaagtct	392 bp
09a	DLL4_E09aF DLL4_E09aR	aacgtgttcttggaatgggg gccagcagtagcagcag	483 bp
09b	DLL4_E09bF DLL4_E09bR	cccttatggcttctgtgggc tcccgcctggcctaagag	500 bp
10	DLL4_E10F DLL4_E10R	caagaaccacctgcagatg ggaccaagagtccactgaa	346 bp
11	DLL4_E11F DLL4_E11R	cccatgccttctcccag cacggatgccagtgagg	476 bp

NCBI transcript number: NM_019074.3.

B.2 RT-PCR AND OTHER PRIMER

Table B.2.1: *UBR1* primer for splice site analysis.

Range	Name	Sequence (5'-3')	Location	Amplicon
Ex2-Ex6	UBR1_e5_RTf	tggagcatttcagctttgtg	Ex2	526 bp
	UBR1_e5_RTr	acgaccctctttgtcaatgg	Ex6/Ex7	
Ex8-Ex12	UBR1_e10_RTf	aaatttgctttgcgtcttg	Ex8	478 bp
	UBR1_e10_RTr	ttccaatttgctcctggcta	Ex12	
Ex13-Ex17	UBR1_RNA_SeqF	gcaaaccacaatatggacag	Ex13	550 bp
	UBR1_RNA_SeqR	ccatttcttcgccacatctc	Ex17	
Ex16-Ex23	12614_IVS16f	ctctaggacccttgctggtctt	Ex15/Ex16	721 bp
	12614_wtr	ctgcatatggtcagccttgc	Ex23/Ex24	
Ex25-Ex28	UBR1_e26_RTf	gaattctgccctgctttcag	Ex25	405 bp
	UBR1_e26_RTr	agattccgatcctgatgtgg	Ex28	
Ex34-Ex38	UBR1_e35_RTf	ggagttccattccatcctga	Ex34	424 bp
	UBR1_e35_RTr	taacacagcaccacacaaa	Ex38/Ex39	
Ex45-Ex47	29339_F	gaaagcatcctgtcctctgc	Ex45	319 bp
	29339_R	atgcagtgttggtgccagac	Ex47	

Table B.2.2: *UBR1* primer for analysis of family JBS-52.

Name	Sequence (5'-3')	Location
UBR1_5'UTRF	gtttccgcttgccctctgg	5'UTR
UBR1_e26_RTf	gaattctgccctgctttcag	Ex25
UBR1_C25R	atcccttcgggtccacaagtt	Ex25
UBR1_C28F	tgtttgacacagtgaagcga	Ex28
UBR1_RNA-Seq_4F	accacatcaggatcgggaatc	Ex28
UBR1_e26_RTr	agattccgatcctgatgtgg	Ex28
UBR1_C30F	ggtattatcggcctgtgtcc	Ex30
UBR1_RT_30R	agtgggtctagggtcttctcc	Ex30/Ex31

UTR, untranslated region.

Table B.2.3: *DOCK6* RT-Primer.

Range	Name	Sequence (5'-3')	Location	Amplicon
Ex33-Ex37	DOCK6_RT_32-33F	ggacaagaccaaggatgaaatg	Ex32/Ex33	660 bp
	DOCK6_RT_37-38R	cgggcaattctgtacatgagg	Ex37/Ex38	

Table B.2.4: *NOTCH1* RT primer.

Range	Name	Sequence (5'-3')	Location	Amplicon
Ex8-Ex12	NOTCH1_C08F	ccagaacgacgccacctg	Ex08	647 bp
	NOTCH1_C12-13R	tgttacacatgctccctgtg	Ex12/13	

Table B.2.5: *GAPDH* RT primer.

Range	Name	Sequence (5'-3')	Amplicon
Ex06-Ex07	GAPDH_RT_E06F	tggtatcgtggactca	189 bp
	GAPDH_RT_E07R	atgccagtgaccctgtt	

B.3 MLPA PROBES

Table B.3.1: *UBR1* MLPA probes

Ex	Name	Sequence (5'-3') ^a	Length	Mix
1	UBR1_Ex1_LP UBR1_Ex1_RP	CGGACGAGGAGGCTGGAGGTACTGAGAGGATGGAAATC AGCGCGGAGTTACCCCAGACCCCTCAGCGTCT	112 nt	A
2	UBR1_Ex2_LP UBR1_Ex2_RP	ATTTGGAGAAGATCCAGATATTTGCTTAGAGAAATTG AAGCACAGTGGAGCATTTCAGCTTTGTGGGAGGGTTT	116 nt	A
3	UBR1_Ex3_LP UBR1_Ex3_RP	GGATTGTGCAATTGATCCAACATGTG TACTCTGTATGGACTGCTTCCAGGACAGTGTT	100 nt	A
4	UBR1_Ex4_LP UBR1_Ex4_RP	GTGACTGTGGAGACACAGAGGCATGGAAAACGGCCC TTTTTGTGTAAATCATGAACCTGGAAGAGCAGGTACTATAAAAGA	124 nt	A
5	UBR1_Ex5_LP UBR1_Ex5_RP	ctcggettthtttatagAATTCACGCTGTCCGTGAATG AAGAGGTAATTGTCCAAGCCAGGAAAATATTTCTT	116 nt	B
6	UBR1_Ex6_LP UBR1_Ex6_RP	CCACGTCATATCGTCATATACAGCCTACAAAGAGCTCTTGAC TGTGAGCTCGCAGAGGCCAGTTGCATACCCTGACC	120 nt	A
7	UBR1_Ex7_LP UBR1_Ex7_RP	GTCGTCGGGCTGTTAAAGCGGGAGCTTATG CTGCTTGCCAGGAAGCAAAGGAAGATATAAAG	104 nt	A
8	UBR1_Ex8_LP UBR1_Ex8_RP	CTCTCAACATCCACTTCATGTAGAAGTATTACACTCAG AGATTATGGCTCATCAGAAATTTGCTTTGCGTCTTGTTT	120 nt	B
9	UBR1_Ex9_LP UBR1_Ex9_RP	GAGAATCCCTGTCTCATAAGCAGGTTAATGCTTTGGGATG CAAAGCTTTATAAAGgtaagtagacatttgcttatgctgttt	124 nt	B
10	UBR1_Ex10_LP UBR1_Ex10_RP	GCCCGTAAGATCCTTCATGAATTG ATCTTCAGCAGTTTTTTTTATGGAGATGGAA	96 nt	A
11	UBR1_Ex11_LP UBR1_Ex11_RP	CAGTGATGATCATGACCAGAAGTATCTCTATAACTGCAC TTTCAGTTCAGATGTTTACTGTTCTACTCGgtatgtat	120 nt	C
12	UBR1_Ex12_LP UBR1_Ex12_RP	CTTATTGAAGAGCAGAATGTTATCTCTGTCATTACTGAAACTC TGCTAGAAGTTTTACCTGAGTACTTGGACAGGAACAATA	124 nt	C
13	UBR1_Ex13_LP UBR1_Ex13_RP	GCAAACCCACAATATGGACAGAAAGATTAAGAATGCAGTTC CTTGAAGTTTTTCGATCTTTTTGAAGATCTTACCTGTATGCAG	128 nt	A
14	UBR1_Ex14_LP UBR1_Ex14_RP	CAGGTTGGGCAACACATTGAAGTGGATCCTGATTGGGAGG CTGCCATTGCTATACAGATGCAATTGAAGAATATTTACTCA	124 nt	D
15	UBR1_In15_LP UBR1_In15_RP	ggtatatcttatgthttcctacaagthttgcagatcctgtggag gtagacttagtaatacatagaacaattttccactcatatttagt	128 nt	B
16	UBR1_Ex16_LP UBR1_Ex16_RP	GTCTTCATGTACGTTTAAAGCAGGCTGGGTG CTGTTTCAAGACTGCATGAATTTGTGTCTTTT	104 nt	B
17	UBR1_Ex17_LP UBR1_Ex17_RP	GGTACTAGTGAATATCCTTTACGTTGTCTGGTG TTGGTTGCCAGGTTGTTGCTGAGATGTGGCG	108 nt	A
18	UBR1_Ex18_LP UBR1_Ex18_RP	GTGCAGAGAAGAAATGTATGATAAAGATATCATCATGCTTCAG gtacctatthaaattgthttctgatattgtgtcttcatcttcc	128 nt	D
19	UBR1_Ex19_LP UBR1_Ex19_RP	CATCTTTAATGGATCCCAATAAGTCTTGTACTGG TACTTCAGAGGTATGAACTGCCGAGGCTTTAACAAG	116 nt	C
20	UBR1_Ex20_LP UBR1_Ex20_RP	ggttcagcgtacaggtgaCACTAATAGAAAGAAATGCTTCAGGT CCTCATCTATATTGTGGgtaagattggcgcactatattctatc	128 nt	E
21	UBR1_Ex21_LP UBR1_Ex21_RP	GAGAGAAATCATTCACTTGCTTTGCATTGAA CCCATGCCACACAGTGCCATTGCCAAA	100 nt	B
22	UBR1_In22_LP UBR1_In22_RP	gtactttggatactttgtagaagctctgaagttcttgcc tgaactccaagaataagagtgaatacagattag	116 nt	D
23	UBR1_Ex23_LP UBR1_Ex23_RP	GAAACCAGGTGTATCAGGC CATGGAGTTTATGAACTAAAAGATGAA	88 nt	C
24	UBR1_In24_LP UBR1_In24_RP	gactaagthtttgatcaggatattcctcatc tattttgcattagthttctctagaacacaa	104 nt	C
25	UBR1_Ex25_LP UBR1_Ex25_RP	ATTCTGCCCTGCTTTCAGCAAAGTGATTAAC CTTCTCACTGTGATATCATGATGTACATTCTCAG	108 nt	B
26	UBR1_Ex26_LP UBR1_Ex26_RP	GAAGAGAAGCAACAGCTTCAAAAAGCTCCTGAAG AAGAAGTAACATTTGACTTTTATCATAAGGCTTCAA	112 nt	B

Ex	Name	Sequence (5'-3') ^a	Length	Mix
27	UBR1_Ex27_LP UBR1_Ex27_RP	TGAATATACAAATGCTTTTGGAAAACTC AAAGGAATTCCCCAGTTAGAAGGCC	96 nt	B
28	UBR1_In28_LP UBR1_In28_RP	gtgacattcatctctgtctttgaactttactgg tataaggagctactgctttttgttaggagaaacct	112 nt	C
29	UBR1_Ex29_LP UBR1_Ex29_RP	GAAGCTGCTAGGCTACATCGCCAG AAGATCATGGCTCAGATGTCTGCCTTACAG	96 nt	C
30	UBR1_Ex30_LP UBR1_Ex30_RP	GGTCCTAAACGGGGTCCATCTGTTAC TGAAAAGGAGGTGCTGACGTGCATCCT	96 nt	D
31	UBR1_Ex31_LP UBR1_Ex31_RP	GCCCTAGACCCACTTTTCATGGATCC AGACTTGGCATATGGAAGTTATACAGGAAGCT	100 nt	C
32	UBR1_Ex32_LP UBR1_Ex32_RP	GGAGAAGAATATCTTTGCCCTCTTTGCAAATC TCTGTGCAATACTGTGATCCCCATTATTCCTTTG	108 nt	C
33	UBR1_Ex33_LP UBR1_Ex33_RP	GAGAATGCAGATGCTCTTGTCTCAACTTTTGAC CCTGGCACGGTGGATACAGACTGTTCTGGC	104 nt	D
34	UBR1_In34_LP UBR1_In34_RP	gggtttattctaacagtgcttgatg gaaacttcttaataaaatagggttaaagatgaaaact	104 nt	E
35	UBR1_Ex35_LP UBR1_Ex35_RP	TTGAAAGTGCCACCTGATGAAAGGGATCCTCGAGTC CCCATGCTGACCTGGAGCACCTGCGCTTCACTA	112 nt	D
36	UBR1_In36_LP UBR1_In36_RP	ccaacaaggtacatgtaactcatggc atgcctttttcccccccacagtttattatta	100 nt	D
37	UBR1_Ex37_LP UBR1_Ex37_RP	CATAATGGTCTGAAAGCATTAAATGCAGTTTGCAGTTGC ACAGAGGATTACCTGTCTCAGGTCTGATACAGAAACAT	120 nt	D
38	UBR1_Ex38_LP UBR1_Ex38_RP	GATACACCATGCCTTCTGTCTATAGATCTGTTTC ATGTTTTGgtaagtgttcagtaattttgtttaagtcactcatggtgataatt	128 nt	C
39	UBR1_Ex39_LP UBR1_Ex39_RP	GTGGGTGCTGTGTTAGCATTCC CATCCTTGATTGGGATGACCCTG	88 nt	D
40	UBR1_Ex40_LP UBR1_Ex40_RP	CTTCTTTGCAGAAATTTCTCAATATACAAGTG Ggtgagtaacaatccattagttcagttctattgt	108 nt	D
41	UBR1_Ex41_LP UBR1_Ex41_RP	GCATTGTTTTTCCACTATTACTTGGGGTAAC TCCGCCTGAGGAAGTGCATACC	96 nt	E
42	UBR1_Ex42_LP UBR1_Ex42_RP	GTTCTGCTCTTCCAGGAATATTGGGATAC TGTAAGGCCCTTGCTCCAGAGgtactat	100 nt	E
43	UBR1_Ex43_LP UBR1_Ex43_RP	CTGTTTGAAGCAAAAAACACCGTGGTC Aggttggttttactacttaatcctttctccctcatccacaag	112 nt	E
44	UBR1_Ex44_LP UBR1_Ex44_RP	TTCTGATGACTATAGTGCCTCCTGAATC AAGCTTCTCATTTTCAGgtaaggagagtggtatataatgtgtgtaat	120 nt	E
45	UBR1_Ex45_LP UBR1_Ex45_RP	GGGAAGAGGTTGGAGCTTGCATTTTTTCAGCACTTCCAC TGTGGAGCCGAGTCTGCATTTTCTAAAgtgagtagtgagtgt	124 nt	E
46	UBR1_Ex46_LP UBR1_Ex46_RP	CAGAGAATGCCGAGTGGTCTGGTTGAAGGTAAAGC CAGAGGCTGTGCCTATCCAGCTCCTTACTTGGATGAAT	116 nt	E
47	UBR1_Ex47_LP UBR1_Ex47_RP	CATTTATCTCGTGAGCGGTATCGGAAGCTCC ATTTGGTCTGGCAACAACACTGCATTATAGAAGAG	108 nt	E
		universal 5' primer binding sequence: GGGTTCCTAAGGGTTGGA		
		universal 3' primer binding sequence: TCTAGATTGGATCTTGCTGGCAC		

^aItalic letters indicate stuffer sequences. Ex, exon; nt, nucleotides.

APPENDIX C: MUTATION ANALYSIS

C.1 MISSENSE VARIANTS

Table C.1.1: UBR1 missense mutations.

In silico prediction of pathogenicity and conservation of UBR1 missense mutations.

Predicted effect	PolyPhen-2 HumVar	SIFT	Mut Pred	GERP	Clustal Omega alignment
p.V122L	B (0.223)	damaging	0.656	5.19	Hs 122 SCRDCAIDPTCVLCMDCFQDSVH Mm 122 SCRDCAIDPTCVLCMDCFQSSVH Gg 173 SCRDCAIDPTCVLCMDCFQNSIH Xt 117 SCRDCAIDPTCVLCMDCFQNSIH Dr 110 SCRDCAIDPTCVLCIECFQKSVH Dm 132 SCRECGVDPTCVLQVNCFKRSAH Sc 146 RCHECGDDPTCVLCIHCENPKDH UBR2 122 SCRDCAIDPTCVLCMECFLGSIH
	0.88 / 0.73	0.004 / 2.85			
p.C127F	PrD (0.998)	damaging	0.973	5.15	Hs 127 AIDPTCVLCMDCFQDSVHKNHRY Mm 127 AIDPTCVLCMDCFQSSVHKNHRY Gg 178 AIDPTCVLCMDCFQNSIHKNHRY Xt 122 AIDPTCVLCMDCFQNSIHKNHRY Dr 115 AIDPTCVLCIECFQKSVHSHRY Dm 137 GVDPTCVLCVNCFKRSAHRFHRY Sc 151 GCLDPTCVLCIHCENPKDHNHRY UBR2 127 AIDPTCVLCMECFLGSIHRDHR
	0.14 / 0.99	0.000 / 2.85			
p.H136R	B (0.031)	damaging	0.981	5.15	Hs 136 MDCFQDSVHKNHRYK--MHTSTGGG Mm 136 MDCFQSSVHKNHRYK--MHTSTGGG Gg 187 MDCFQNSIHKNHRYK--MHSSTGGG Xt 131 MDCFQNSIHKNHRYK--MHSSMGGG Dr 124 IECFQKSVHKSRYK--MHASSGGG Dm 146 VNCFKRSAHRFHRYK--MSTSGGGG Sc 160 IHCENPKDHNHRYVHVCTDICTEFTSG UBR2 136 MCFCLGSIHRDHRRYR--MTTSGGGG
	0.94 / 0.59	0.048 / 2.85			
p.H166R	PrD (0.988)	damaging	0.710	5.18	Hs 166 EAWKTGPFVCVNEPGRAGTIKEN Mm 166 EAWKTGPFVCDHEPGRAGTTKES Gg 217 EAWKAGPVCVKPEPGASGSPKEN Xt 161 EAWKTGPFYCKIPEPGASD---QN Dr 154 EAWKTGPFCCSQDPEGTEATMET Dm 176 EAWKQDQYCELELANRKNPLE-- Sc 192 EAWNSPLHCKAEQENDISEDPA UBR2 166 EAWKEGPFYCKKELNTSEIEEE
	0.53 / 0.95	0.002 / 2.85			
p.L217R	PrD (0.997)	damaging	0.450	5.59	Hs 217 IWEEEEKEL---PPELQIRE-KNERYYC Mm 217 IWEEEEKEL---PPELQIRE-KNERYYC Gg 268 IWEEEEKEL---PPELTIRE-KVDSYYC Xt 209 IWEEQKSL---PAYLDTGTVEVWQYYC Dr 204 IWEEENNDL---SEELKPKV-KEDSYFC Dm 227 ETEFNASLQCLDGNVEGGQVDGAYCT Sc 301 NQN[52]SNSPEASPSLAKIDPEINNTV UBR2 218 TWEKESEL---PADLEMVE-KSDTYYC
	0.27 / 0.98	0.000 / 2.85			
p.I286R	PrD (0.987)	damaging	0.801	5.79	Hs 286 AYAACQEAKEDEKSH---SENVSQHP Mm 286 VYATCQEAKEDEKSH---SENVSQHP Gg 337 HYASCQEAKEEIKRH---SENVSQRP Xt 279 TLEQCQEVTESEKANK---SENVSLKF Dr 273 TLRTCQQAQKDNERRN---SEHITCKE Dm 297 TFEENKLVKVENQ[8]STARNNQS Sc 399 Q[29]KYIILWTHC[12]RNMMGKT UBR2 287 DFQYCEQAQKSVTVRN---TS-RQTKF
	0.53 / 0.95	0.000 / 2.85			
p.L317P	PrD (0.997)	damaging	0.813	5.27	Hs 317 EIMAHQKFALRIGSWMNKIMSYS Mm 317 VVMAHQKFALRIGSWMNKIMSYS Gg 368 DVMAHQKFALRIGSWLNKIMSYS Xt 310 HVMAHQSFALCAIWLNLKLLAYS Dr 304 AVMAHQKFALRIGAWFQKTIIGYS Dm 336 GAVACQQFALQLGWFOQFLVRH Sc 439 -ATECRDMTPVVEKYFBNKFDKN UBR2 317 SIVAHQNFGLKLLSWLGSITIGYS
	0.27 / 0.98	0.002 / 2.85			

Predicted effect	PolyPhen-2 HumVar	SIFT	Mut Pred	GERP	Clustal Omega alignment
p.Q420K	PrD (0.980)	damaging	0.880	5.14	Hs 420 DR--SISITALSVQMFVPTLARHL Mm 420 ER--SISITALSVQMLTVPTLARHL Gg 471 DR--VLSVTALSVCIFFTVPTLARHL Xt 416 DR--NISVTAISVQVFTVPTLARLL Dr 407 QR--NISITALSVQIFFTVPTLARQL Dm 435 DH--AFSIVSLSVQLFTVPSIAHHL Sc 572 EPQLTARECVQLFTCPTNAKNI UBR2 420 ER--AVSVTALSVCFFTAPTLARML
	0.57 / 0.94	0.000 / 2.85			
p.L427R	PrD (0.998)	damaging	0.827	5.26	Hs 427 ALSVQMFVPTLARHLIEEQNVI Mm 427 ALSVQMFVPTLARHLIEEQNVI Gg 478 ALSVQIFVPTLARHLIEEQNVI Xt 423 AHSVQVFTVPTLARLLIEEQNVM Dr 414 ALSVQIFVPTLARQLIEEGTVI Dm 442 SLSVQVFTVPSIAHHLTAHEGIF Sc 579 ECVVQLFTCPTNAKNIENQSF UBR2 427 ALSVQVFTTAPTLARMLTTEENLM
	0.18 / 0.98	0.000 / 2.85			
p.A563D	PoD (0.587)	damaging	0.581	4.21	Hs 563 WCACDEELLVAYKECHKAVMRC Mm 563 WCACDEELLVAYKECHKAVMRC Gg 614 WCACDEELLRAYKECHKAVMRC Xt 559 WCATDDDLLKSYKECHLSLLOC Dr 550 WCSSDERVLLLAFOECHRALMSC Dm 580 WASGDVLLRKLKMTMRALVSN Sc 722 -DSIDSKLELNATR----IIS-- UBR2 565 WCASDEKVLIEAYKKCLAVLMQC
	0.81 / 0.83	0.001 / 2.84			
p.S700P	PoD (0.844)	damaging	0.674	5.20	Hs 700 DKDIIMLQIGAS--LMDPNKFLLLV Mm 700 DKDIIMLQIGAS--LMDPNKFLLLV Gg 751 DKDIIMLQIGAS--LMDPNHFLLLV Xt 696 DKDVVMLQIGAS--YLDPNSFLLV Dr 677 DKDVIMLQIAAS--KMDPNHFLMLV Dm 721 DRDIAQLQIGAS--LMESNEFLHVV Sc 845 SRDIHLNQLAILWERDLPRIIYNI UBR2 703 DKDVVMLQITGV--MMDPNHFLMIM
	0.73 / 0.88	0.002 / 2.84			
p.R754C	PrD (0.997)	damaging	0.853	5.26	Hs 754 MLQVLIYIVGER--YVPGVGNV--TKE Mm 754 MLQVLIYIVGER--YVPGVGNV--TRE Gg 805 MLQIIIIYVGER--YVPGVSNV--TKE Xt 751 MLHVLIYVIGER--YVPGISNV--TRE Dr 731 MLYLLIYIVGER--YVPGISNV--TKE Dm 780 FEELLIYVIGER--WMPGVSMV--TEE Sc 901 FTAFIYQLLTERQYFKTFSSLKDRRM UBR2 764 MLYLIIMLVGER--FSPGVGQV--NAT
	0.27 / 0.98	0.000 / 2.84			
p.R754H	PrD (0.997)	damaging	0.839	5.26	Hs 754 MLQVLIYIVGER--YVPGVGNV--TKE Mm 754 MLQVLIYIVGER--YVPGVGNV--TRE Gg 805 MLQIIIIYVGER--YVPGVSNV--TKE Xt 751 MLHVLIYVIGER--YVPGISNV--TRE Dr 731 MLYLLIYIVGER--YVPGISNV--TKE Dm 780 FEELLIYVIGER--WMPGVSMV--TEE Sc 901 FTAFIYQLLTERQYFKTFSSLKDRRM UBR2 764 MLYLIIMLVGER--FSPGVGQV--NAT
	0.27 / 0.98	0.000 / 2.84			
p.Q1102E	PrD (0.970)	damaging	0.561	4.86	Hs 1102 TEKEVLTCLCQEEQEVKIENNA Mm 1105 TEKEVLTCLCQEEQEVKIENNA Gg 1157 AEKEVLTCLCQEEQEVKLESAA Xt 1100 PSKDVLTCLCQEEQEVKLDKPT Dr 1075 LDWETLTCILCQEEQEVQAQAPA Dm 1131 GTDDTFKCLCQENCAISRGGRO Sc 1224 YSEDFTCALCQDSSSTD----F UBR2 1112 EQRFVTCILCQEEQEVKVESRA
	0.60 / 0.93	0.000 / 2.84			
p.R1242G	B (0.073)	tolerated	0.545	4.15	Hs 1242 TLARWI----QTVLARISGYNIRHAKG Mm 1245 TLARWI----QTVLARISGYNIRHAKG Gg 1298 SLARWL----ETLIVRISGYNVKNAKD Xt 1241 SLPHWL----DTVAARISGYNLTNTIKG Dr 1215 TLMRWI----QIMSSRLRGLKAMWTAD Dm 1258 PLDSFV----ETMSTLATELGN--NVKD Sc 1383 SEDTLS [18] SLMISQCQCFDKAVRKR UBR2 1253 NLTQWI----RLTSQQLKALQFLRKEE
	0.92 / 0.66	0.246 / 2.85			

Predicted effect	PolyPhen-2 HumVar	SIFT	Mut Pred	GERP	Clustal Omega alignment
p.G1279S	B (0.085)	tolerated	0.805	4.85	Hs 1279 STLEFHSILSFQVSS---IKYSNSI Mm 1283 STLEFHSILSFQVSS---VKYSNSI Gg 1335 SLEFHSILSFQVSS---AKYSSSI Xt 1278 QNYEERSILSFQVQAP---PRYPTCT Dr 1252 GQTEFRSILSFQVQEP---PKESRSI Dm 1299 GLAQEERSVQLIKNPPRLHADYLEGI Sc 1417 LSVHWANTISMLEIASRLEKPYISIF UBR2 1290 DELQLPEGFRPDRPK---IPYSESI
	0.91 / 0.67	0.169 / 2.85			
p.P1426L	PrD (0.997)	damaging	0.361	5.20	Hs 1426 SLYWDDF--VDLQFSSVSSSYNHLY Mm 1430 SLYWDDT--VDLQFSPSSSYNHLY Gg 1482 SLYWEDA--VDLQFSSISAYNHLY Xt 1425 SLYCEEN--VDLHPSSTLVSTYNNLY Dr 1399 SLYQEEA--VDLQPSAVSTAYNHLY Dm 1458 NLMVPEKGYKTIIPSG---SMDFDY Sc ---- KLYAKASKI-----GDVLKVSEQM UBR2 ---- ALQCQDF-----SGISLGTGDLHI
	0.27 / 0.98	0.013 / 2.83			
p.S1427F	PrD (0.997)	damaging	0.340	5.20	Hs 1427 LYWDDF--VDLQFSSVSSSYNHLY Mm 1431 LYWDDT--VDLQFSPSSSYNHLY Gg 1483 LYWEDA--VDLQFSSISAYNHLY Xt 1426 LYCEEN--VDLHPSSTLVSTYNNLY Dr 1400 LYQEEA--VDLQPSAVSTAYNHLY Dm 1459 LLMVPEKGYKTIIPSG---SMDFDY Sc ---- LLYAKASKI-----GDVLKVSEQML UBR2 1433 LQCQDF-----SGISLGTGDLHI
	0.27 / 0.98	0.001 / 2.89			
p.S1431P	PrD (0.963)	tolerated	0.278	2.66	Hs 1431 DF--VDLQFSSVSSSYNHLYLFLHLI Mm 1435 DT--VDLQFSPSSSYNHLYLFLHLI Gg 1487 DA--VDLQFSSISAYNHLYLFLHLI Xt 1450 EN--VDLHPSSTLVSTYNNLYLFLHLI Dr 1403 EA--VDLQPSAVSTAYNHLYLQLI Dm ---- EKGYKTIIPSG---SMDFDYIMQTM Sc 1537 ASKI-----GDVLKVSEQMLFALR UBR2 1437 DF-----SGISLGTGDLHLIFHLV
	0.62 / 0.92	0.304 / 2.85			
p.G1661R	PrD (0.999)	damaging	0.749	4.72	Hs 1661 VGACIFHALHCAGVCIFLKIRE Mm 1669 VGACVFHALHCAGVCIFLKIRE Gg 1717 LGACTSHALCCAGVCIFLKIRE Xt 1661 LGACTAHAMHCAGVCIFLSIRE Dr 1633 VGACTGHAACAGVGLFLRVRE Dm 1737 VGACTTHAHACAEVGLFLRIRD Sc 1728 HEMTKHLNKNCFKPFGAFILMPNS UBR2 1667 VGACTAHTYSCSGVGLFLRVRE
	0.09 / 0.99	0.000 / 2.85			

Various online prediction tools were used to evaluate mutation effects. **PolyPhen-2:** score >0.909, probably damaging (PrD); score 0.447 – 0.908, possibly damaging (PoD); score ≤0.446, benign (B). HumVar output was used for Mendelian inheritance. [sensitivity/specificity], sensitivity: True Positive Rate, the chance that the mutation is classified as damaging when it is indeed damaging; specificity: False Positive Rate, the chance that the benign mutation is correctly classified as benign [Adzhubei et al., 2013]. **SIFT:** [score/median info], score: normalised probability that the amino acid change is tolerated; ≤0.05, damaging; >0.05, tolerated; median information content: maximum 4.32, indicates complete conservation at this position; minimum 0.00, indicates a position where all 20 amino acids are tolerated; ideally between 2.75 and 3.5 [Ng and Henikoff, 2003]. **MutPred:** general score; ranges between 1.000 (deleterious mutation) and 0.000 (benign). **GERP:** ranges from 6.17 (highly conserved amino acid residue) to -12.3 (not conserved). **Clustal Omega Alignment:** multiple protein alignment of human UBR1 and its orthologues; numbers indicate position of affected amino acid residue. Black shading indicates identical amino acid residues; grey shading indicates similar residues (according to BLOSUM62 matrix). Hs, *Homo sapiens* (NP_777576.1); Mm, *Mus musculus* (NP_033487.2); Gg, *Gallus gallus* (XP_421165.3); Xt, *Xenopus tropicalis* (XP_002941132.2); Dr, *Danio rerio* (XP_009291507.1); Dm, *Drosophila melanogaster* (NP_573184.1); Sc, *Saccharomyces cerevisiae* (NP_011700.1); UBR2 (NP_056070.1).

Table C.1.2: UBR1 unclassified missense variants.*In silico* prediction of pathogenicity and conservation of UBR1 unclassified missense variants.

Predicted effect	PolyPhen-2 HumVar	SIFT	Mut Pred	GERP	Clustal Omega alignment
p.S405G	B (0.003)	tolerated	0.313	5.14	Hs 405 KYYKQLQKEYI SDDHDR-SISITA Mm 405 KYYKQLQKEYI SDDHDR-SISITA Gg 456 KYYKTLQKEYI SDDHDR-VLSVTA Xt 401 KHYKQLQKEYI NDDQDR-NISVTA Dr 392 EHYKQLQEDFI SDDHQR-NISITA Dm 420 RRYATI VEDFI SDDHDH-AFSIVS Sc 556 EIFNHITRSVAYMDREPQLTAIRE UBR2 405 KNYQQQLQRDFMDDHER-AVSVTA
	0.98 / 0.26	0.239 / 2.85			
p.I778T	PrD (0.994)	damaging	0.442	5.12	Hs 778 VTMREI IHLLC EPMPHSAIAKN Mm 778 VTMREI IHLLC EPMPHSAIARN Gg 829 VTMREI IHLLC EPMAHSAIAKA Xt 775 CTMREI IHLLC EPMAHSAIAKA Dr 755 VTMREI IHLLC EPMAHSTLIKS Dm 804 RLRKEI IQLLC KPYSHSELSRA Sc 928 QIKNSI IYNYLMKPLSYSKLLRS UBR2 788 EIKREI IHLIS KPMASHSELVKS
	0.46 / 0.96	0.000 / 2.84			
p.I899V	B (0.000)	tolerated	0.194	-2.07	Hs 899 MYILRTVFERA DTDSNLWTEGM Mm 899 MYILRTVFERA DMESNLWTEGM Gg 950 MHTLRTILQRAVELETHLWTEAM Xt 896 MHTLRTILKRAAEEDPTMWTEGM Dr 876 IHVLRLLQKAVEDRSNQTWTEPM Dm 928 LNTCSLIMERAALNAYSRSFTESH Sc 1055 AKVVYKLLQVCLDMEDSTFLNEL UBR2 909 LCI MGTLLQWAVEHNGYAWSESM
	1.00 / 0.00	1.000 / 2.85			
p.T1097M	PrD (0.998)	damaging	0.458	4.99	Hs 1097 RGPSVTEKEVL TCILCQEEQEVK Mm 1100 RGPVAVTEKEVL TCILCQEEQEVK Gg 1152 RGPSTAEKEVL TCILCQEEQEVK Xt 1095 RGFIVPSSKDVLT TCILCQEEQEVK Dr 1070 QGVMSLDWETLT TCILCQEEQEVQ Dm 1127 RKFYHGTD DDTFKCILCEFNCAIS Sc 1219 VGEKVVYSEDFTCALCQDSSSTD UBR2 1107 QTQVPEQRQFVTCILCQEEQEVK
	0.18 / 0.98	0.023 / 2.84			
p.G1264E	B (0.001)	tolerated	0.355	4.80	Hs 1264 GEN-P-LPIFFNQMGDSTLEFHSI Mm 1268 GEA-PAWPFVLENGMGDSTLEFHSI Gg 1320 DQQ--NAPAFVNRKLGNSALEFHSI Xt 1263 GTK-PITPEFC-KIYKQNYEERSI Dr 1237 DGS-D-AAEKAAAPFDEGQTEERSI Dm 1284 DHELTTLH [7] LSGVVGGLAQEERS Sc ---- RANFSH-KDVSLL----LSVHWANT UBR2 1276 EST-PNNASTKNSSEN-VDELQLPEG
	0.99 / 0.09	0.656 / 2.86			
p.T1548A	B (0.217)	tolerated	0.188	4.65	Hs 1548 YSALCSYLSLPTNLFLLFQEYWD Mm 1556 FSALCSYLSLPTNLFLLFQEYWD Gg 1604 FKALCSYLSLPTNLFLLFQEYWD Xt 1546 ISALCSYLSLPTNLFLLFQENWD Dr 1520 LPLLCYLSLPTNLFLLFQDHRD Dm 1617 FDLMCQYLGLDPM LGVYFD-MET Sc 1626 FEDTAEFVNKALK--MITEKES UBR2 1554 FEHLCSYLSLPTNLLICLFQENSE
	0.88 / 0.74	0.202 / 2.85			
p.R1612G	B (0.236)	tolerated	0.454	3.80	Hs 1612 YSCLLNQASHFRCPRSADDERKH Mm 1620 YSCLLNQASHFRCPRSADDERKH Gg 1668 YSCLLNQASQFRCPRSSDDEQKH Xt 1612 YSSLNQASQFRCPKSDAERKH Dr 1584 YSVLLNQASHFRCPNSSDDERKH Dm 1688 FSDLINSVSDIFCPNNEREEMKT Sc 1682 LNTYVTSKEIKLR [9] ADNRLD UBR2 1618 YSSLNQASNFSCPKSGGDKSRA
	0.88 / 0.75	0.107 / 2.85			

Various online prediction tools were used to evaluate mutation effects. For explanation of PolyPhen-2, SIFT, MutPred, and GERP see above (Table C.1.1). **Clustal Omega Alignment:** multiple protein alignment of human UBR1 and its orthologues; numbers indicate position of affected amino acid residue. Black shading indicates identical amino acid residues; grey shading indicates similar residues (according to BLOSUM62 matrix). Hs, *Homo sapiens* (NP_777576.1); Mm, *Mus musculus* (NP_033487.2); Gg, *Gallus gallus* (XP_421165.3); Xt, *Xenopus tropicalis* (XP_002941132.2); Dr, *Danio rerio* (XP_009291507.1); Dm, *Drosophila melanogaster* (NP_573184.1); Sc, *Saccharomyces cerevisiae* (NP_011700.1); UBR2 (NP_056070.1).

Table C.1.3: *DOCK6* missense mutations.*In silico* prediction of pathogenicity and conservation of *DOCK6* missense mutations.

Predicted effect	PolyPhen-2 HumVar	SIFT	Mut Pred	GERP	Clustal Omega alignment
p.V263D	PrD (0.998)	damaging	0.735	5.05	Hs 263 PPREHFGQRI L VKCLSLKFEI E I Mm 263 PPREHFGQRI L VKCLSLKFEI E I Gg7 307 VPKEHFGQRI L VKCLSLKFEI E I Xt 263 VPKEHFG F RL L VKFLSLKFEI E I Dr 263 VPKEH S GQRI M VKCLSLKFEI E I Dm 271 IPVEH M GHRIO N CL O LRLE L EV Ce 261 LPE Q EETPK L F V KEKAAAD P FF DOCK7 267 IPKEHFGQRI L VKCLSLKFEI E I
	0.18 / 0.98	0.000 / 2.85			
p.L1016P	PrD (0.977)	damaging	0.756	4.84	Hs 1016 LSLVDRGFV F LSVRAHYKQV A TR Mm 1080 L S IADRG I F S LVRAHYKQV A TR Gg7 1102 L S IMDRGFV F V L IKTCYKQV S SK Xt 829 LSLMDRGFV F N L IRSYKQV N NK Dr 1083 LSLMDRGFV F N L VRSY K Q I NNK Dm 1052 L S IMDRGFV E G L IKTY T K V LISK Ce 1027 F S IMDR T F V M K L V HKYLIA F AES DOCK7 1062 L S VMDRGFV F S L IK S CYKQV S SK
	0.58 / 0.94	0.000 / 2.85			
p.E1052K	PrD (0.999)	damaging	0.492	4.81	Hs 1052 RME F TRILCS H HYVTLN L PC P Mm 1116 RMD F TRILCS H HYVTLN L PC P Gg7 1138 R L D F LRI T CS H HYVTLN L PC S L Xt 865 RMD L IRIVCS O HYV V LN L PC T Dr 1119 RMD F IRI T CS H HYVTLN L PC A T Dm 1085 KID F LRI V CS H HE V ALN L PF G T Ce 1063 KID F VR V CS S Y H YLIV N IL S DL DOCK7 1098 R L D F LRI T CS H HYVTLN L PC S L
	0.09 / 0.99	0.000 / 2.85			
p.R1596W	PrD (0.999)	damaging	0.715	4.99	Hs 1596 IARGYQGS P DL R L T WLQ N MAG K H Mm 1660 IARGYQGS P DL R L T WLQ N MAG K H Gg7 1687 IAKGY O NS P DL R L T WLQ N MAG K H Xt 1406 IAKGY O NS P DL R L T WLQ N MA A KH Dr 1659 IAKGY O NS P DL R L T WLQ N MAG K H Dm 1618 IAKGY O NN P DL R L T WL E NNMA K H Ce 1560 LVEGY S NN P DL R L T WL N MA E RH DOCK7 1647 IAKGY O NS P DL R L T WLQ N MAG K H
	0.09 / 0.99	0.000 / 2.86			

Various online prediction tools were used to evaluate mutation effects. For explanation of PolyPhen-2, SIFT, MutPred, and GERP see above (Table C.1.1). **Clustal Omega Alignment:** multiple protein alignment of human *DOCK6* and its orthologues; numbers indicate position of affected amino acid residue. Black shading indicates identical amino acid residues; grey shading indicates similar residues (according to BLOSUM62 matrix). Hs, *Homo sapiens* (NP_065863.2); Mm, *Mus musculus* (NP_796004.2); Gg7, *Gallus gallus* DOCK7 (XP_422519.4); Xt, *Xenopus tropicalis* (XP_012808634.1); Dr, *Danio rerio* (ENSDART00000082944, Ensembl release 82); Dm, *Drosophila melanogaster* (FBpp0077762.3); Ce, *Caenorhabditis elegans* (F46H5.4, Ensembl release 82); DOCK7 (NP_001258929.1).

Table C.1.4: *DOCK6* unclassified missense variants.*In silico* prediction of pathogenicity and conservation of *DOCK6* unclassified missense variants.

Predicted effect	PolyPhen-2 HumVar	SIFT	Mut Pred	GERP	Clustal Omega alignment
p.H34D	B (0.017)	tolerated	0.155	1.86	Hs 34 KQVSRERSG S P H SSRR C SSSLG V Mm 34 KQVSRERSG S P H SSRR S SSSLG V Gg7 72 KQ I SG Q Y G GS P Q L L[9]SHHT T V Xt 34 KQVAREY G GS P Q L SKKRGGQ A SV Dr 36 KQV S REY G SP Q MS K K R AGAHQ P V Dm 33 K NVSG C HLS K AM D ----P S L C G Ce 35 K H V IS G L H PI H RL[10]SM M E K I DOCK7 32 KQ I SG Q Y S GS P Q L L[9]SHHT T V
	0.95 / 0.54	0.532 / 2.92			
p.R430H	PoD (0.512)	damaging	0.334	3.11	Hs 430 G E RR P AW T DR R R G P --- Q D RASS G D Mm 428 G E RR P W A ER R R G P --- Q D R G Y S G D Gg7 478 G E R K G S W S ER R N S S I [5]L E R T T S G D Xt 430 S E R K G T W N ER K K A F ----E R L S V G D Dr 431 T E R K G T W N ER K K K G F----E R M S V G E Dm 466 - D R[20]-L T R R G S [5]- K H R S W S P D Ce 470 - D R[23]-S R V T P[7]P V S N L P T S Q DOCK7 438 G E R K G S W S ER R N S S I [5]L E R T T S G D
	0.82 / 0.81	0.031 / 2.99			

Predicted effect	PolyPhen-2 HumVar	SIFT	Mut Pred	GERP	Clustal Omega alignment
p.T453M	PrD (0.974)	damaging	0.303	4.15	Hs 453 D-ACSFSGFRPATLTVTNFFKQEA Mm 451 D-ACSFSSFRPATLTVTNFFKQEA Gg7 506 E-ACNLTSFRPATLTVTNFFKQEG Xt 452 E-TCGLHTFRPATLTVTNFFKQEG Dr 453 D-MCNFTNFRPATLTVTNFFKQEG Dm 495 DFANVVENFRPTLTVPSEFFKQEA Ce 502 EVPNIEENMPSCNLIKFSSEIRQEG DOCK7 466 D-ACNLTSFRPATLTVTNFFKQEG
	0.59 / 0.93	0.001 / 2.92			
p.P482L	PrD (0.991)	damaging	0.416	4.42	Hs 482 DLFKFLADMRRFSSLLRRLRPVT Mm 480 DLFKFLADMRRFSSLLRRLRPVT Gg7 535 DLYKFLADMRRFSSVLRRLRPFT Xt 481 DLYKFLADMRRFSTALRRLRPVT Dr 482 DLYKFLADMRRFSSVLRRLRPVT Dm 524 DLYKFLPELKRFSVMKKYKCIPT Ce 531 DLYRICSEMRRFTNGKVHKKM-FN DOCK7 495 DLYKFLADMRRFSSVLRRLRPFT
	0.50 / 0.95	0.002 / 2.92			
p.G702S	B (0.211)	damaging	0.389	3.62	Hs 702 DVALPGRWVDCCHKGVFSVELTA Mm 700 DVALPGRWVDCCHKGVFSVELTA Gg7 755 EVPLPGMKWVNDHKGVENVEVVA Xt --- DQNVRSPT Dr 702 DVQLPGMKWVNDHKGVENVEVKA Dm 747 NVHLPGTKWLDNHRVAVFSINVEA Ce 743 NNALPNLKWVNDHKKPTFSCSTEV DOCK7 715 EVPLPGMKWVNDHKGVENVEVVA
	0.88 / 0.74	0.017 / 2.85			
p.V923I	B (0.029)	tolerated	0.327	3.53	Hs 923 LALQWVVSSAVREALQAWFF Mm 987 LALQWVVCSAVRELVLQAWFF Gg7 1009 LALQWVVCSGSVREALQAWFF Xt 736 LVLQWVVSSAVREALSQAWFF Dr 990 LALQWVVSTVREALQAWFF Dm 959 LALHWVVASGKAADLAMSNSWFL Ce 934 LLEVWLRARGSLRDVSLVHSWFL DOCK7 969 LALQWVVCSGSVRESALQAWFF
	0.94 / 0.59	0.094 / 2.91			
p.R1305C	B (0.259)	damaging	0.559	2.50	Hs 1305 AFQYKGGKAFERINSLTFK--KSLD Mm 1369 AFQYKGGKAFERINSLTFK--KSLD Gg7 1389 CFQYKGGKVFERMNSLTFK--KSKD Xt 1115 CFQYKGGKAFERINSLTFK--KSLD Dr 1368 CFQYKGGKAFERINSLTFK--KSD Dm 1329 TFEYTGQKN[5]ETNTQSERKTGSTD Ce --- SFEIKDDPA[5]-----PD DOCK7 1349 CFQYKGGKVFERMNSLTFK--KSKD
	0.87 / 0.75	0.001 / 2.91			
p.L1578F	PoD (0.453)	damaging	0.594	4.21	Hs 1578 KMKEHQEDPEMLIDLMYRIARGY Mm 1642 KMKEHQEDPEMLIDLMYRIARGY Gg7 1669 KMKEHQEDPEMLIDLMYRIARGY Xt 1388 KMKEHQEDPEMLIDLMYRIARGY Dr 1641 KMKEHQEDPEMLIDLMYRIARGY Dm 1600 KMKEHQEDPEMLIDLMYRIARGY Ce 1542 RMREHVNDYEMIDLMYQLVEGY DOCK7 1629 KMKEHQEDPEMLIDLMYRIARGY
	0.83 / 0.80	0.023 / 2.86			

Various online prediction tools were used to evaluate mutation effects. For explanation of PolyPhen-2, SIFT, MutPred, and GERP see above (Table C.1.1). **Clustal Omega Alignment:** multiple protein alignment of human DOCK6 and its orthologues; numbers indicate position of affected amino acid residue. Black shading indicates identical amino acid residues; grey shading indicates similar residues (according to BLOSUM62 matrix). Hs, *Homo sapiens* (NP_065863.2); Mm, *Mus musculus* (NP_796004.2); Gg7, *Gallus gallus* DOCK7 (XP_422519.4); Xt, *Xenopus tropicalis* (XP_012808634.1); Dr, *Danio rerio* (ENSDART00000082944, Ensembl release 82); Dm, *Drosophila melanogaster* (FBpp0077762.3); Ce, *Caenorhabditis elegans* (F46H5.4, Ensembl release 82); DOCK7 (NP_001258929.1).

Table C.1.5: ARHGAP31 unclassified missense variant.*In silico* prediction of pathogenicity and conservation of ARHGAP31 unclassified missense variant.

Predicted effect	PolyPhen-2 HumVar	SIFT	Mut Pred	GERP	Clustal Omega alignment
p.T727I	B (0.005)	tolerated	0.228	2.38	Hs 727 EVWTRDPANQS--I--QGASTAASREK Mm 705 EVWTRDANQS--I--QFAAILTIREK Gg 748 TPQIT---TQV--P-LFDGTSTERPD Xt ---VV-----NSLELEEPD Dr ---VMFDHPGATTF-----NSVMKHMPE Tr 701 VAFTRSDSVTHQFPDSNPAISLH-KD Dm ---RAATLPVKDQL--QAAAMCSPN AG32 1257 KIYPPSGSPEENTSTATMTYMTTPA
	0.97 / 0.44	0.42 / 2.87			

Various online prediction tools were used to evaluate mutation effects. For explanation of PolyPhen-2, SIFT, MutPred, and GERP see above (Table C.1.1). **Clustal Omega Alignment:** multiple protein alignment of human NOTCH1 and its orthologues; numbers indicate position of affected amino acid residue. Black shading indicates identical amino acid residues; grey shading indicates similar residues (according to BLOSUM62 matrix). Hs, *Homo sapiens* (NP_065805.2); Mm, *Mus musculus* (NP_064656.2); Gg, *Gallus gallus* (ENSGALP00000024275.4, Ensembl release 82); Xt, *Xenopus tropicalis* (XP_012813746.1); Dr, *Danio rerio* (XP_005165688.1); Tr, *Takifugu rubripes* (XP_011609886.1); Dm, *Drosophila melanogaster* (NP_610002.1); AG32, ARHGAP32 (NP_001136157.1).

Table C.1.6: NOTCH1 missense mutations.*In silico* prediction of pathogenicity and conservation of NOTCH1 missense mutations.

Predicted effect	PolyPhen-2 HumVar	SIFT	Mut Pred	GERP	Clustal Omega alignment
p.P407R	PrD (0.929)	tolerated	0.439	4.82	Hs 407 AICTCPSGYTG P ACSQDVDECSL Mm 407 AICTCPSGYTG P ACSQDVDECSL Gg 417 AICTCPSGY V GPACNQDVDECSL Xt 406 AICTCP P GYTG P ACNNDVDECSL Dr 427 AICTC L GY V GPACDQDVDECSL Tr 407 HICTC P TY T ASCNQDVDECSL Dm 444 YAC S CATGY K VD C SE D I D EC D Q NOTCH3 386 AICTCP P GF T GG A CDQDVDECSI
	0.67 / 0.91	0.326 / 2.87			
p.R448Q	PrD (0.917)	damaging	0.578	4.57	Hs 448 ECQCLQGYTG P RCEIDVNECVSN Mm 448 ECQCLQGYTG P RCEIDVNEC T SN Gg 458 QCQCLQGY S GP R CEIDVNEC L SN Xt 447 QC N C P QGYAG P RCEIDVNEC L SN Dr 468 QCKC L QGY V GA R CEIDVNEC L ST Tr 448 QCK C Q R GY M GP R CEIDVNEC L SN Dm 484 RC N S Q GF T GP R CE T NINEC S H NOTCH3 427 LC Q CG R GY T GP R CEIDVNEC L SG
	0.68 / 0.90	0.009 / 2.87			
p.C449R	PrD (1.000)	damaging	0.949	4.57	Hs 449 CQCLQGYTG P RCEIDVNECVSN P Mm 449 CQCLQGYTG P RCEIDVNEC L SN P Gg 459 CQCLQGY S GP R CEIDVNEC L SN P Xt 448 C N C P QGYAG P RCEIDVNEC L SN P Dr 469 CKC L QGY V GA R CEIDVNEC L ST P Tr 449 CK C Q R GY M GP R CEIDVNEC L SN P Dm 485 C N C S Q G F T GP R CE T NINEC S H P NOTCH3 428 C Q CG R GY T GP R CE T DVNEC L SG P
	0.00 / 1.00	0.001 / 2.87			
p.C456Y	PrD (1.000)	damaging	0.994	4.57	Hs 456 TGPRCEIDVNE C VSN P CQNDATC Mm 456 TGPRCEIDVNE C IS N PCQNDATC Gg 466 S G PRCEIDVNE C LS N PCQNDATC Xt 455 A G PRCEIDVNE C LS N PCQNDATC Dr 476 V G ARCEIDVNE C LS T PCQNDATC Tr 456 M G PRCEIDVNE C IS N PC M N E ATC Dm 492 T G PRCE T NINE C ES H PCQ N EG S C NOTCH3 435 T G PRCE T DVNE C LS G PC R N O ATC
	0.00 / 1.00	0.000 / 2.86			

Predicted effect	PolyPhen-2 HumVar	SIFT	Mut Pred	GERP	Clustal Omega alignment
p.A465T	PrD (0.907)	damaging	0.837	4.57	Hs 465 NECVSNPCQNDATCLDQIGEFQC
	0.69 / 0.90	0.004 / 2.86			Mm 465 NECLSNPCQNDATCLDQIGEFQC
p.C1374R	PrD (0.998)	damaging	0.888	4.73	Gg 475 NECLSNPCQNDATCLDQIGEFQC
	0.18 / 0.98	0.000 / 2.90			Xt 464 NECLSNPCQNDATCLDQIGEFQC
p.A1740S	B (0.093)	damaging	0.508	3.71	Dr 485 NECLSTPCQNDATCLDQIGEFHC
	0.91 / 0.68	0.027 / 2.88			Tr 465 NECLSNPCQNDATCLDKIGGFRC
					Dm 501 NECLSNPCQNEGSCLDPPGTFRC
					NOTCH3 444 NECLSGPCRNQATCLDRIGQETC
					Hs 1374 CISG-PRSPPTCLCLGPFPTGPECQF
					Mm 1374 CISG-PRSPPTCLCLGPFPTGPECQF
					Gg 1384 CISM-HKSSKQVCAAAFTGPECQY
					Xt 1373 CISV-LKSSKQVCEGEGYTCATCOY
					Dr 1351 CVSG-HKSPKCLCTPAFTGPECQD
					Tr 1374 CISG-SKSPKCLCPAFTGPECQY
					Dm 1401 VVADEGFGYRCECPRGTLGEHCEI
					NOTCH3 1315 CQQT-PRGERCACPPLSGESCRS
					Hs 1740 PF-PAQLHFMYVA ^A AAAFVLLFFVG
					Mm 1730 PL-PSQLHFM ^A MYVA ^A AAAFVLLFFVG
					Gg 1749 AR-NSQLYPMYV ^V VAAALVLLAF ^L IG
					Xt 1735 AKPEPPLYAM ^E SMLVIPL ^L IIFVI
					Dr 1717 S--PVELYPVYV ^V LAGLALLAF ^V VA
					Tr 1740 -QPQQLYPL ^P YLVL ^L AGIGMLAF ^L IG
					Dm 1748 GEPAN-VKYVI ^T GILV ^I I ^L ALAF
					NOTCH3 1647 PEPSVPL ^L PL ^L LV ^A GAVLL ^L VIL ^L -V

Various online prediction tools were used to evaluate mutation effects. For explanation of PolyPhen-2, SIFT, MutPred, and GERP see above (Table C.1.1). **Clustal Omega Alignment:** multiple protein alignment of human NOTCH1 and its orthologues; numbers indicate position of affected amino acid residue. Black shading indicates identical amino acid residues; grey shading indicates similar residues (according to BLOSUM62 matrix). Hs, *Homo sapiens* (NP_060087.3); Mm, *Mus musculus* (NP_032740.3); Gg, *Gallus gallus* (NP_001025466.1); Xt, *Xenopus tropicalis* (NP_001090757.1); Dr, *Danio rerio* (NP_571377.2); Tr, *Takifugu rubripes* (XP_003975158.1); Dm, *Drosophila melanogaster* (NP_001245510.1); NOTCH3 (NP_000426.2).

C.2 SPLICE SITE ANALYSIS

Table C.2.1: *UBR1* splice site mutation analysis.

Nucleotide alteration	Predicted effect ^a	Sequence (5'-3')	BDGP	Net Gene2
c.81+1G>A	r.spl.? p.?	WT CCCCTCAGCGTCTGGCATCTgtaagtcacctataggcaagtc MUT CCCCTCAGCGTCTGGCATCTataagtcacctataggcaagtc	0.96 -	0.987 -
c.81+2dupT	r.spl.? p.?	WT CCTCAGCGTCTGGCATCTgt-aagtcacctataggcaagtc MUT CCTCAGCGTCTGGCATCTgtt-aagtcacctataggcaagtc	0.96 -	0.987 -
c.81+5G>C	r.spl.? p.?	WT TCAGCGTCTGGCATCTgtaagtcacctataggcaagtcctctt MUT TCAGCGTCTGGCATCTgtaactccctataggcaagtcctctt	0.96 -	0.987 0.067
c.529-13G>A	<i>p.N177Lfs*10</i>	WT ttgactagtagtgtttttctcggcttttttatagAATTCAGG MUT ttgactagtagtgtttttctcagcttttttatagAATTCAGG	- -	0.302 0.611
c.660-2_660-1delAG	r.spl.? p.?	WT atatatgttttttttctaacaggGGAGAAAAATGAAAGATAC MUT atatatgttttttttctaac--GGAGAAAAATGAAAGATAC	0.97 -	0.989 -
c.1094-13A>G	<i>p.V365Efs*2</i>	WT tcattccccaccctccccaataaatctatagGTGCCCGT MUT tcattccccaccctccccaataaatctatagGTGCCCGT	- 0.85 -	- 0.190 0.020 0.001
c.1094-12A>G	r.spl.? p.?	WT cattccccaccctccccaataaatctatagGTGCCCGTA MUT cattccccaccctccccaagataaatctatagGTGCCCGTA	- 0.35 -	- 0.019 0.020 0.001
c.1911+14C>G	<i>p.G638Vfs*29</i>	WT GTCTTTTgtaagtgattctactaagattgatttgcttata MUT GTCTTTTgtaagtgattctagtaagattgatttgcttata	- 0.98 0.91 0.91	- 0.971 0.841 0.841
c.2254+2T>C	r.spl.? p.?	WT GTCCTCATCTATATGTGGgtaagattaaacacaatgttt MUT GTCCTCATCTATATGTGGcaagattaaacacaatgttt	0.86 -	0.959 0.009
c.2379+1G>C	r.spl.? p.?	WT CCAAAAATTACCTGAGAATgtaagtcctgattttggtttta MUT CCAAAAATTACCTGAGAATctaagtcctgattttggtttta	0.99 -	0.925 -
c.2380-1G>A	r.spl.? p.?	WT acaaaaatattgtttcaacaGAAAAATAATGAACTGGCTT MUT acaaaaatattgtttcaacaAAAAAATAATGAACTGGCTT	- -	0.077 -
c.2432+5G>C	r.spl.? p.?	WT AAGTGGCCACATTTAAgtaagtgtcttaattttatgcttat MUT AAGTGGCCACATTTAAgtaactgtcttaattttatgcttat	0.99 0.24	0.993 0.357
c.2839+5G>A	<i>p.R914Dfs*7</i>	WT TATCATAAGGCTTCAAgatggttgagatcactcttcaac MUT TATCATAAGGCTTCAAgatatttgagatcactcttcaac	0.88 -	0.775 0.062
c.3998-1G>C	<i>p.E1333_G1337del</i>	WT tatttttttttattctttgaGAAATCTATGGGAGATGAA MUT tatttttttttattctttgaCAAAATCTATGGGAGATGAA	0.34 -	0.246 -
c.5109-3A>G	<i>p.R1704Gfs*26</i>	WT tgtttttttctttttccctaagGAGGGGCAACCCCTTCA MUT tgtttttttctttttccctaGAGGGGCAACCCCTTCA	- - 0.99	0.801 0.516 0.607

^aItalic letters indicate that the effect of splicing mutations was demonstrated on mRNA level. Capital letters indicate exonic regions, intronic regions are written in lower case letters. Red letters indicate the altered position, blue letters denote an authentic splice site (when different from the altered position). BDGP, Berkeley Drosophila Genome Project.

Table C.2.2: *UBR1* splice site analysis of unclassified variants.

Nucleotide alteration	Predicted effect	Sequence (5'-3')	BDGP	Net Gene2
c.264G>A	p.E88E	WT GATCCAGATATTTGCTTAGAGAAATTGAAGCACAGTGGAGC MUT GATCCAGATATTTGCTTAGAAAAATTGAAGCACAGTGGAGC	- -	- -
c.819G>A	p.A273A	WT GGTTCGTCGGGCTGTTAAAGCGGAGCTTATGCTGCTTGCCA MUT GGTTCGTCGGGCTGTTAAAGCAAGGAGCTTATGCTGCTTGCCA	- -	- -
c.985+16G>A	r.spl.? p.?	WT TTCAAgtaagcataacctcctgtttttcttgtttctgataaa MUT TTCAAgtaagcataacctcctatttttcttgtttctgataaa	0.99 0.99	0.852 0.852
c.1213A>G	p.S405G	WT AACTGCAGAAAGAATATATCACTGATGATCATGACAGAAGT MUT AACTGCAGAAAGAATATATCGGTGATGATCATGACAGAAGT	- -	0.003 0.140
c.2333T>C	p.I778T	WT AATCATTCACCTTGCTTTGCACTGAACCCATGCCACACAGTG MUT AATCATTCACCTTGCTTTGCACTGAACCCATGCCACACAGTG	- -	- -
c.3290C>T	p.T1097M	WT TACTGAAAAGGAGGTGCTGACCTGCATCCTTTGCCAAGAAG MUT TACTGAAAAGGAGGTGCTGATGTGCATCCTTTGCCAAGAAG	- -	0.396 0.487
c.3791G>A	p.G1264E	WT TCCTATTTCTTTAATCAAGGAATGGGAGATTCTACTTTGG MUT TCCTATTTCTTTAATCAAGAATGGGAGATTCTACTTTGG	- -	0.164 0.024
c.3873G>A	p.K1291K	WT AAATATTCAAATAGCATCAAAGAAATGGTTATCTCTTTGC MUT AAATATTCAAATAGCATCAAAGAAATGGTTATCTCTTTGC	- -	- -
c.4219-11T>G	r.spl.? p.?	WT agccatattgatgtccatthttctctcatagGTGGGTGCTG MUT agccatattgatgtccatthttctctcatagGTGGGTGCTG	0.74 0.74	0.983 0.960
c.4242A>G	p.P1414P	WT GGTGCTGTGTTAGCATTCCCATCCTTGTATTGGGATGACCC MUT GGTGCTGTGTTAGCATTCCCCTCCTTGTATTGGGATGACCC	- -	- 0.005
c.4834A>G	p.R1612G	WT TGAATCAAGCTTCTCATTTCAGgtaaggagagtgtgtatat MUT TGAATCAAGCTTCTCATTTCGGgtaaggagagtgtgtatat	1.00 1.00	0.990 0.977

For key see Table C.2.1.

Table C.2.3: *DOCK6* splice site mutation analysis.

Nucleotide alteration	Predicted effect ^a	Sequence (5'-3')	BDGP	Net Gene2
c.4106+5G>T	r.spl.? p.?	WT CAGACCGCGTGGACAAgtaggtgtgggcaggagggtgtctg MUT CAGACCGCGTGGACAAgtagttgtgtgggcaggagggtgtctg	0.77 0.15	0.881 0.341
c.4107-1G>C	<i>p.T1370Mfs*19</i>	WT agacctcctttccccttccagGACCAAGGATGAAATGGAAC MUT agacctcctttccccttccacGACCAAGGATGAAATGGAAC	0.99 -	0.967 -
c.4491+1G>A	<i>p.F1447_H1497del</i>	WT AGAACTTCGAGATCGGCCACgtgagtggtgggctaggaggca MUT AGAACTTCGAGATCGGCCACatgagtggtgggctaggaggca	0.97 -	0.998 -
c.5939+2T>C	r.spl.? p.?	WT TCAAGGACTTCTGCAAGAAgtagggcgcaaaacccccagga MUT TCAAGGACTTCTGCAAGAAcagggcgcaaaacccccagga	0.14 -	0.734 0.004

^aItalic letters indicate that the effect of splicing mutations was demonstrated on mRNA level. For key see Table C.2.1.Table C.2.4: *DOCK6* splice site analysis of unclassified variants.

Nucleotide alteration	Predicted effect	Sequence (5'-3')	BDGP	Net Gene2
c.100C>G	p.H34D	WT GGGAAACGACAGTGGCTCCCCCACTCCAGCAGGCGCTGCAGC MUT GGGAAACGACAGTGGCTCCCCGACTCCAGCAGGCGCTGCAGC	- -	0.281 0.150
c.885C>T	p.N295N	WT tgtccccagATCTCGGAGAACTTCTACTTCGACCTGAACTC MUT tgtccccagATCTCGGAGAACTTCTACTTCGACCTGAACTC	0.70 0.68	0.512 0.405
c.1289G>A	p.R430H	WT AGCCTGGACAGACCCGCCCGTCGGGGGCCCCAGGACCGGG MUT AGCCTGGACAGACCCGCCATCGGGGGGCCCCAGGACCGGG	- -	0.011 -
c.1358C>T	p.T453M	WT CTCTGGCTTCCGTCCAAGCCACGCTAACTGTCACAAACTTCT MUT CTCTGGCTTCCGTCCAAGCCATGCTAACTGTCACAAACTTCT	0.14 0.13	0.135 0.184

Nucleotide alteration	Predicted effect	Sequence (5'-3')	BDGP	Net Gene2
c.1445C>T	p.P482L	WT CCTGGCTGACATGAGCGCCCGTCGTCCTGCTGCGGCGAC MUT CCTGGCTGACATGAGCGCCCTGTCGTCCTGCTGCGGCGAC	- -	- -
c.1833-19C>G	r.spl.? p.?	WT cccagccccagcagatcccagccccgattctgccagGT MUT cccagccccagcagatccgagccccgattctgccagGT	- -	- -
c.2104G>A	p.G702S	WT CGGGCATGCGCTGGGTGGACGGTCACAAGGGCGTGTTCAGT MUT CGGGCATGCGCTGGGTGGACAGTCACAAGGGCGTGTTCAGT	- -	0.040 0.001
c.2767G>A	p.V923I	WT GGGTGGTCAGCAGCAGTGCCGTACGCGAGGCCATCCTCCAG MUT GGGTGGTCAGCAGCAGTGCCATACGCGAGGCCATCCTCCAG	- -	0.373 -
c.3873C>T	p.C1291C	WT TTGGATTTGCTGTACCTTTGCTAGCTGCCTTTGAGTACAA MUT TTGGATTTGCTGTACCTTTGTCTAGCTGCCTTTGAGTACAA	- -	0.042 0.062
c.3913C>T	p.R1305C	WT agGGGAAAAAGGCCTTTGAACGCATCAACAGCCTCACATTC MUT agGGGAAAAAGGCCTTTGAATGCATCAACAGCCTCACATTC	0.64 0.62	0.727 0.700
c.4732C>T	p.L1578F	WT ACCAGGAGGACCTGAGATGCTCATCGACCTCATGTACAGg MUT ACCAGGAGGACCTGAGATGTCATCGACCTCATGTACAGg	- -	- -
c.4899G>A	p.L1633L	WT GTGGCTGAGTACCTCGCCCTGCTCGAGGACCACCGCCACCT MUT GTGGCTGAGTACCTCGCCCTACTCGAGGACCACCGCCACCT	- -	- -
c.5229C>A	p.G1743G	WT tcttccccacagAGTTCCGGCTGGGAGgtgagtcagccttg MUT tcttccccacagAGTTCCGGATGGGAGgtgagtcagccttg	- -	- -
c.5640C>T	p.H1880H	WT ACGCTGCTCAGCACCACCACCGCCTTCCCTACATCAAGAC MUT ACGCTGCTCAGCACCACCACCGCCTTCCCTACATCAAGAC	- -	0.024 0.004
c.5688+9G>C	r.spl.? p.?	WT CACCGGAGGAGgtgggtggggtacccctgggctggcggggg MUT CACCGGAGGAGgtgggtggcgatccctgggctggcggggg	0.62 0.62	0.918 0.918
c.5833-16C>G	r.spl.? p.?	WT atgcaggctggctcaccagtccctctacccccacagGGTCC MUT atgcaggctggctcaccagtgcctctacccccacagGGTCC	0.97 0.94	0.770 0.459

For key see Table C.2.1.

Table C.2.5: ARHGAP31 splice site analysis of unclassified variants.

Nucleotide alteration	Predicted effect	Sequence (5'-3')	BDGP	Net Gene2
c.384G>C	p.L128L	WT TGCCCTGAAGAAGGCCAACTGCCCCGAATCCAAAATGTTAT MUT TGCCCTGAAGAAGGCCAACTCGCCCCGAATCCAAAATGTTAT	- -	- -
c.2180C>T	p.T727I	WT GGATCCAGCCAATCAGAGCACACAGGGGCTTCCACAGCAG MUT GGATCCAGCCAATCAGAGCATACAGGGGCTTCCACAGCAG	- -	- -
c.2901C>T	p.L967L	WT GTTAAAAGCCAGTGGACTCTCGAGGTTCCCTCCTCCAGCAG MUT GTTAAAAGCCAGTGGACTCTTGAGGTTCCCTCCTCCAGCAG	- -	- -

For key see Table C.2.1.

Table C.2.6: EOGT splice site mutation analysis.

Nucleotide alteration	Predicted effect	Sequence (5'-3')	BDGP	Net Gene2
c.311+1G>T	r.spl.? p.?	WT AGCTATGTCGACATGGGATGgtaagtttccatatggaatac MUT AGCTATGTCGACATGGGATGttaagtttccatatggaatac	0.99 -	0.990 -

For key see Table C.2.1.

Table C.2.7: NOTCH1 splice site mutation analysis.

Nucleotide alteration	Predicted effect	Sequence (5'-3')	BDGP	Net Gene2
c.1669+5G>A	p.F520_G557del	WT TGTGTGTGCACGGAAGgtgcgggctggcgcccaccagcggg MUT TGTGTGTGCACGGAAGgtgcaaggctggcgcccaccagcggg	0.64 -	0.946 0.946

The effect of this splicing mutation was demonstrated on mRNA level. For key see Table C.2.1.

APPENDIX D: OTHER TABLES

Table D.1: Complete AOS cohort from Magdeburg.

		autosomal recessive	sporadic	autosomal dominant	Total
AOS	Families	10	21	2	33
	Patients	13	21	4	38
ACC	Families	3	4	2	9
	Patients	5	4	5	14
TTLD	Families	-	1	-	1
	Patients	-	1	-	1
Total	Families	13	26	4	43
	Patients	18	26	9	53

Table D.2: Classification of intellectual disability (ID).

Adapted from [Zhang et al., 2005].

	Range	Adult	Child
0	Normal IQ >80	No intellectual disability	No intellectual disability
1	Borderline IQ 70-80	Attends standard school; requires minor/major support; has simple reading, writing, and math ability	Normal developmental milestones; minor retardation obvious during the first school years
2	Mild ID IQ 50-70	Understands everything, including long sentences; has very simple reading, writing, and math ability	Developmental milestones delayed a few months; retardation obvious from 1-2 years
3	Moderate ID IQ 35-50	Understands almost everything; makes use of small sentences and lots of signs	Developmental milestones delayed several months; retardation obvious from age 1 year
4	Severe ID IQ <35	Understands simple, daily sentences and single words; uses sentences of 2-3 words, and many signs; walks (or less)	Developmental milestones delayed from several months to 1 year; retardation obvious before age 1 year (or less)

Table D.3: Critical review of 91 JBS literature cases from 78 publications.

Reference	Case	Remarks	JBS
[Lumb and Beautyman, 1952]	1	fatty replacement of pancreas, no further JBS symptoms	N
	2	fatty replacement of pancreas, no further JBS symptoms	N
[Berger and Klempman, 1965]	-	insufficient symptoms	N
[Townes, 1965]	1	trypsinogen deficiency disease	N
	2	trypsinogen deficiency disease	N
[Grand et al., 1966]	-	incompatible facial appearance, no oligodontia	N
[Morris and Fisher, 1967]	-	clinically confirmed	Y
[Townes, 1969]	-	clinically confirmed	Y
[Townes and White, 1981]	-	clinically confirmed	Y
[Johanson and Blizzard, 1971] [Park et al., 1972]	1	clinically confirmed	Y
[Johanson and Blizzard, 1971]	2	clinically confirmed	Y
	3	EPI unclear (20m)	?
[Schussheim et al., 1976]	-	clinically confirmed	Y
[Donlan, 1977]	1	EPI uncertain (4.5y), facial clefting, dental hypoplasia	?
	2	EPI uncertain (3m), facial clefting, dental hypoplasia	?
[Day and Israel, 1978]	7	clinically confirmed	Y
[Motohashi et al., 1981]	1	clinically confirmed	Y
[Day and Israel, 1978]	8	EPI uncertain	?
[Mardini et al., 1978]	-	clinically confirmed	Y
[Daentl et al., 1979]	-	clinically confirmed	Y
[Reichart et al., 1979]	1	[JBS-22.1]; clinically and genetically confirmed	Y
	2	[JBS-22.2]; clinically and genetically confirmed	Y
[Sismanis et al., 1979]	-	clinically confirmed	Y
[Bresson et al., 1980]	-	clinically confirmed	Y
[Helin and Jodal, 1981]	1	EPI uncertain (3m)	Y
	2	EPI uncertain (3m)	Y
[Motohashi et al., 1981]	2	clinically confirmed	Y
[Baraitser and Hodgson, 1982]	-	EPI uncertain	?
[Moeschler and Lubinsky, 1985] [Kobayashi et al., 1995]	1	at 12y: oligodontia uncertain	?
[Moeschler and Lubinsky, 1985]	2	clinically confirmed	Y
[Davidai et al., 1986]	-	insufficient symptoms	N
[Zerres and Holtgrave, 1986]	-	[JBS-8.1]; clinically and genetically confirmed	Y
[Moeschler et al., 1987]	-	clinically confirmed	Y
[Ono et al., 1987]	-	clinically confirmed	Y
[Szilagyi et al., 1987]	-	fatty replacement of acinar tissue; untypical facial appearance	N
[Kristjansson et al., 1988] [Hoffman et al., 2007]	-	no EPI at 4m (autopsy), negative <i>UBR1</i> test	N
[Gould et al., 1989]	1	clinically confirmed	Y
	2	clinically confirmed	Y
[Hurst and Baraitser, 1989]	-	clinically confirmed	Y
[Sandhu and Brueton, 1989]	-	EPI uncertain (14d), untypical facial appearance	?
[Gershoni-Baruch et al., 1990] [Braun et al., 1991]	1	clinically confirmed	Y
	2	clinically confirmed	Y
[Rudnik-Schoneborn et al., 1991]	1	clinically confirmed	Y
	2	[JBS-5.1]; clinically and genetically confirmed	Y
[Rudnik-Schoneborn et al., 1991] [Swanenburg de Veye et al., 1991]	3	[JBS-9.1]; clinically and genetically confirmed	Y
[Trellis and Clouse, 1991]	-	untypical facial appearance, oligodontia uncertain (19y)	?
[Nagashima et al., 1993]	-	clinically confirmed	Y
[Jones et al., 1994]	1	[JBS-10.1]; clinically and genetically confirmed	Y
[Timoney et al., 2004] [Cheung et al., 2009]	2	[JBS-11.1]; clinically and genetically confirmed	Y

Reference	Case	Remarks	JBS
[Guzman and Carranza, 1997]	1	[JBS-2.2]; clinically and genetically confirmed	Y
	2	[JBS-2.1]; clinically and genetically confirmed	Y
[Dumic et al., 1998]	-	EPI and oligodontia uncertain (18y), negative <i>UBR1</i> test	N
[Rosanowski et al., 1998]	-	clinically confirmed	Y
[Auslander et al., 1999]	1	EPI uncertain (termination of pregnancy)	Y
	2	EPI uncertain (termination of pregnancy)	Y
[Maunoury et al., 1999]	-	EPI and oligodontia uncertain (19y), facial dysmorphism untypical	N
[Alpay et al., 2000]	-	no EPI (10d), untypical facial dysmorphism	?
[Steinbach and Hintz, 2000]	-	no EPI, negative <i>UBR1</i> test	N
[Vanlieferinghen et al., 2001]	-	[JBS-7.1]; clinically and genetically confirmed	Y
[McHeik et al., 2002]	-	[JBS-16.1]; clinically and genetically confirmed	Y
[Prater and D'Addio, 2002]	-	no oligodontia documented (29y)	?
[Vieira et al., 2002]	-	[JBS-13.1]; clinically and genetically confirmed	Y
[Fichter et al., 2003]	-	isolated EPI	N
[Vanlieferinghen et al., 2003]	-	[JBS-7.2]; clinically and genetically confirmed	Y
[Kulkarni et al., 2004]	-	EPI uncertain (newborn)	?
[Takahashi et al., 2004]	-	[JBS-60.1]; clinically confirmed, but no <i>UBR1</i> -mutation detected	Y
[Al-Dosari et al., 2008]	-	no EPI (3m), but genetically confirmed	Y
[Alkhouri et al., 2008]	-	[JBS-23.1]; clinically and genetically confirmed	Y
[Elting et al., 2008]	1	[JBS-19.1]; clinically and genetically confirmed	Y
	2	[JBS-25.1]; clinically and genetically confirmed	Y
[Barroso et al., 2010]	-	no EPI (18y), untypical facial dysmorphism	N
[Ramos et al., 2010]	-	insufficient symptoms	N
[Saeed et al., 2010]	-	clinically confirmed	Y
[Sudarshan et al., 2010] [Santhosh and Jethmalani, 2013]	-	insufficient symptoms	N
[Almashraki et al., 2011]	-	[JBS-38.1]; clinically and genetically confirmed	Y
[Fallahi et al., 2011]	-	[JBS-35.1]; clinically and genetically confirmed	Y
[Liu et al., 2011]	-	[JBS-33.1]; clinically and genetically confirmed	Y
[Gülaşı et al., 2011]	-	EPI uncertain (4m), convincing symptoms	Y
[Schoner et al., 2012]	1	[JBS-4.2]; clinically and genetically confirmed	Y
	2	[JBS-4.1]; clinically and genetically confirmed	Y
[Deutsch et al., 2013]	-	EPI uncertain, untypical facial dysmorphism	?
[Godbole et al., 2013]	-	[JBS-47.1]; clinically and genetically confirmed	Y
[Kaba et al., 2013]	-	EPI uncertain (3.5y), negative <i>UBR1</i> test	N
[Singh et al., 2014]	-	[JBS-46.1]; clinically and genetically confirmed	Y
[Ibrahim, 2014]	-	no EPI detected (3m)	?
[Quaio et al., 2014]	1	[JBS-30.2]; clinically and genetically confirmed	Y
	2	[JBS-30.1]; clinically and genetically confirmed	Y
[Ellery and Erdman, 2014]	-	insufficient symptoms	N
[Atik et al., 2015]	-	[JBS-54.1]; clinically and genetically confirmed	Y
[Corona-Rivera et al., 2016]	1	[JBS-58.1]; clinically and genetically confirmed	Y
	2	[JBS-43.1]; clinically and genetically confirmed	Y
	3	[JBS-1.1]; clinically and genetically confirmed	Y
	4	[JBS-36.1]; clinically and genetically confirmed	Y

EPI, exocrine pancreatic insufficiency; y, year(s); m, month(s); d, day(s); N, no; Y, yes; ?, unsolved.

DANKSAGUNG

Der erste Dank gilt meinem Doktorvater Prof. Dr. med. Martin Zenker, der mir durch die Aufnahme am Institut für Humangenetik der Universität Magdeburg das Verfassen einer Dissertationsschrift ermöglicht hat. Mit seinem fachübergreifenden Wissen, welches von klinischer Pädiatrie über funktionelle Biologie und Biochemie bis hin zu umfangreichen Labortechniken geht, um nur einige Themen zu nennen, stand er mir beratend zur Seite. Außerdem bin ich dankbar, dass mein bisher erworbenes Fachwissen anerkannt wurde und ich dadurch viele wichtige Freiheiten in der Gestaltung und Auswertung meiner Experimente hatte.

Allen weiteren Mitarbeitern des Institutes gebührt mein Dank, da bei etwaigen Fragen jederzeit kompetente Hilfe zur Stelle war. Besonders hervorzuheben sind die Labormitarbeiter(innen), welche mit viel Erfahrung und Sachverstand bei kniffligen Experimenten mit Rat und Tat zur Seite standen. Auch aus dem Institut für Biochemie habe ich praktische und theoretische Unterstützung erhalten. Viele wichtige Gespräche, oft auch fachbezogen, gab es mit Christina Lißewski, Franziska Altmüller und Katharina Burkart; danke, dass ihr immer ein offenes Ohr für mich habt!

Ertragreiche Kollaborationen auf dem Gebiet des Adams-Oliver-Syndroms gab es vor allem mit Laura Southgate aus London; auch Wim Wuyts war maßgeblich an diesem Projekt beteiligt. Des Weiteren danke ich allen Ärzten die mir aus der ganzen Welt wertvolle Proben und detaillierte Fallberichte haben zukommen lassen. Ohne diese Vielzahl an Einsendungen wäre die gesamte Studie nicht möglich gewesen. Und natürlich auch nicht ohne die Bereitschaft der Patienten und deren Familien an dieser Studie teilzunehmen. Sie alle waren einverstanden ihre DNA und Krankheitsgeschichte mit der Forschung zu teilen um die Erbkrankheiten Johanson-Blizzard-Syndrom und Adams-Oliver-Syndrom besser erforschen und verstehen zu können.

Ohne die zur Verfügung gestellten Fördergelder der Deutschen Forschungsgemeinschaft (DFG) hätte es weder das Projekt noch meine Doktorandenstelle gegeben; deshalb ein Dankeschön dafür, dass es solch eine Einrichtung überhaupt gibt, sowie auch für die Genehmigungen dieser interessanten und ergiebigen Projekte.

Ein etwas ungewöhnlicher Dank geht an den Mensaclub Greifswald e. V. und an den Studentenclub Kiste e. V. aus Magdeburg, ohne deren Existenz die Verkettung glücklicher Umstände, die mich nach Magdeburg gebracht haben, nie in Gang gekommen wäre.

Auch wenn ich mich anfangs kopfüber in die Arbeit gestürzt und viele Wochenenden im Labor verbracht habe, musste ich einsehen, dass man auf Dauer nicht die gewünschten Leistungen bringen kann, wenn man seine Freizeit vernachlässigt. So habe ich Magdeburg lieben gelernt, aber auch in Magdeburg leben und lieben gelernt. Und egal wie weit man voneinander entfernt ist, einige wenige Freundschaften halten über viele Kilometer und Jahre hinweg.

Der letzte und wichtigste Dank gilt meiner Mutter, die mich immer unterstützt hat. Ohne die finanzielle Unterstützung wäre mein bisheriger Werdegang nur schwer möglich gewesen, aber ohne die mentale Unterstützung wäre es unmöglich gewesen. Ich danke dir für alles was du für mich getan hast!

CURRICULUM VITAE

PERSÖNLICHE DATEN

Name	Maja Sukalo
Geburtsdatum	13. Juli 1985
Geburtsort	Oldenburg (Oldb.)
Staatsangehörigkeit	deutsch

SCHULAUSSBILDUNG

1991-1994	Grundschule Wüstring, Niedersachsen
1994-1996	Orientierungsstufe Hude, Niedersachsen
1996-2003	Graf-Anton-Günther-Schule Oldenburg, Niedersachsen

HOCHSCHULAUSSBILDUNG

2003-2009	Studium der Biologie an der Ernst-Moritz-Arndt-Universität Greifswald, Mecklenburg-Vorpommern
2009	Abschluss als Diplom-Biologin

BERUFLICHER WERDEGANG

seit 2010	Wissenschaftliche Mitarbeiterin am Institut für Humangenetik der Otto-von-Guericke-Universität Magdeburg, Sachsen-Anhalt
-----------	--

PUBLICATIONS

Hwang CS, **Sukalo M**, Batygin O, Addor MC, Brunner H, Aytes AP, Mayerle J, Song HK, Varshavsky A, Zenker M. 2011. Ubiquitin ligases of the N-end rule pathway: assessment of mutations in UBR1 that cause the Johanson-Blizzard syndrome. *PLoS One* 6:e24925.

Almashraki N, Abdulnabee MZ, **Sukalo M**, Alrajoudi A, Sharafadeen I, Zenker M. 2011. Johanson-Blizzard syndrome. *World J Gastroenterol* 17:4247-50.

Godbole K, **Maja S**, Leena H, Martin Z. 2013. Johanson-Blizzard syndrome. *Indian Pediatr* 50:510-512. [No Erratum was made regarding the names]

Sukalo M, Mayerle J, Zenker M. 2014. Clinical utility gene card for: Johanson-Blizzard syndrome. *Eur J Hum Genet* 22. doi: 10.1038/ejhg.2013.65.

Singh A, Chaudhary N, Dhingra D, **Sukalo M**, Zenker M, Kapoor S. 2014. Johanson-Blizzard syndrome: hepatic and hematological features with novel genotype. *Indian J Gastroenterol* 33:82-4.

Sukalo M, Fiedler A, Guzmán C, Spranger S, Addor MC, McHeik JN, Oltra Benavent M, Cobben JM, Gillis LA, Shealy AG, Deshpande C, Bozorgmehr B, Everman DB, Stattin EL, Liebelt J, Keller KM, Bertola DR, van Karnebeek CD, Bergmann C, Liu Z, Düker G, Rezaei N, Alkuraya FS, Oğur G, Alrajoudi A, Venegas-Vega CA, Verbeek NE, Richmond EJ, Kirbiyik O, Ranganath P, Singh A, Godbole K, Ali FA, Alves C, Mayerle J, Lerch MM, Witt H, Zenker M. 2014. Mutations in the human UBR1 gene and the associated phenotypic spectrum. *Hum Mutat* 35:521-31.

Quaio CR, Koda YK, Bertola DR, **Sukalo M**, Zenker M, Kim CA. 2014. Case report. Johanson-Blizzard syndrome: a report of gender-discordant twins with a novel UBR1 mutation. *Genet Mol Res* 13:4159-64.

Sukalo M, Tilsen F, Kayserili H, Müller D, Tüysüz B, Ruddy DM, Wakeling E, Ørstavik KH, Snape KM, Trembath R, De Smedt M, van der Aa N, Skalej M, Mundlos S, Wuyts W, Southgate L, Zenker M. 2015. DOCK6 Mutations Are Responsible for a Distinct Autosomal-Recessive Variant of Adams-Oliver Syndrome Associated with Brain and Eye Anomalies. *Hum Mutat* 36:593-8. Erratum in: *Hum Mutat* 36:1112.

Southgate L, **Sukalo M**, Karountzos AS, Taylor EJ, Collinson CS, Ruddy D, Snape KM, Dallapiccola B, Tolmie JL, Joss S, Brancati F, Digilio MC, Graul-Neumann LM, Salviati L, Coerdt W, Jacquemin E, Wuyts W, Zenker M, Machado RD, Trembath RC. 2015. Haploinsufficiency of the NOTCH1 Receptor as a Cause of Adams-Oliver Syndrome with Variable Cardiac Anomalies. *Circ Cardiovasc Genet* 8:572-81.

Atik T, Karakoyun M, **Sukalo M**, Zenker M, Ozkinay F, Aydoğdu S. 2015. Two novel UBR1 gene mutations in a patient with Johanson Blizzard Syndrome: A mild phenotype without mental retardation. *Gene* 570:153-5.

Meester JA, Southgate L, Stittrich AB, Venselaar H, Beekmans SJ, den Hollander N, Bijlsma EK, Helderma-van den Enden H, Verheij JBG, Glusman G, Roach JC, Lehman A, Patel MS, de Vries BBA, Ruivenkamp C, Itin P, Prescott K, Clarke S, Trembath R, Zenker M, **Sukalo M**, Van Laer L, Loeys B, Wuyts W. 2015. Heterozygous loss-of-function mutations in SBDS cause Adams-Oliver Syndrome. *Am J Hum Genet* 97:475-82.

Corona-Rivera JR, Zapata-Aldana E, Bobadilla-Morales L, Corona-Rivera A, Pena-Padilla C, Solis-Hernandez E, Guzman C, Richmond E, Zahl C, Zenker M, **Sukalo M**. 2016. Oblique facial clefts in Johanson-Blizzard syndrome. *Am J Med Genet A* 170:1495-501.

ERKLÄRUNG

Hiermit erkläre ich, dass ich die von mir eingereichte Dissertation zu dem Thema "Syndromic scalp defects: Genotype-phenotype studies in Johanson-Blizzard syndrome and Adams-Oliver syndrome." selbständig verfasst, nicht schon als Dissertation verwendet habe und die benutzten Hilfsmittel und Quellen vollständig angegeben wurden.

Weiterhin erkläre ich, dass ich weder diese noch eine andere Arbeit zur Erlangung des akademischen Grades doctor rerum naturalium (Dr. rer. nat.) an anderen Einrichtungen eingereicht habe.

Magdeburg, den 22. April 2016

Maja Sukalo